

HENRY

Hydraulic Engineering Repository

Ein Service der Bundesanstalt für Wasserbau

Doctoral Thesis, Periodical Part,

Sorgatz, Julia

Towards reliability-based bank revetment design: Investigation of limit states and parameter uncertainty

BAWDissertationen

Verfügbar unter/Available at: <https://hdl.handle.net/20.500.11970/108341>

Vorgeschlagene Zitierweise/Suggested citation:

Sorgatz, Julia (2021): Towards reliability-based bank revetment design: Investigation of limit states and parameter uncertainty. (BAWDissertationen, 4)

Standardnutzungsbedingungen/Terms of Use:

Die Dokumente in HENRY stehen unter der Creative Commons Lizenz CC BY 4.0, sofern keine abweichenden Nutzungsbedingungen getroffen wurden. Damit ist sowohl die kommerzielle Nutzung als auch das Teilen, die Weiterbearbeitung und Speicherung erlaubt. Das Verwenden und das Bearbeiten stehen unter der Bedingung der Namensnennung. Im Einzelfall kann eine restriktivere Lizenz gelten; dann gelten abweichend von den obigen Nutzungsbedingungen die in der dort genannten Lizenz gewährten Nutzungsrechte.

Documents in HENRY are made available under the Creative Commons License CC BY 4.0, if no other license is applicable. Under CC BY 4.0 commercial use and sharing, remixing, transforming, and building upon the material of the work is permitted. In some cases a different, more restrictive license may apply; if applicable the terms of the restrictive license will be binding.



BAWDissertationen

Nr. 4

Towards reliability-based bank revetment design:
Investigation of limit states and parameter uncertainty

Julia Sorgatz



BAWDissertationen Nr. 4

Towards reliability-based bank revetment design:
Investigation of limit states and parameter uncertainty

Julia Sorgatz

Impressum

In der Reihe **BAW**Dissertationen werden Doktorarbeiten, die im Rahmen von wissenschaftlichen Kooperationen der BAW mit Universitäten entstanden sind, als Erst- oder Zweitveröffentlichung publiziert. Bei dieser Ausgabe handelt es sich um eine Zweitveröffentlichung.

Herausgeber (im Eigenverlag):
Bundesanstalt für Wasserbau (BAW)
Kußmaulstraße 17, 76187 Karlsruhe
Postfach 21 02 53, 76152 Karlsruhe
Telefon: +49 (0) 721 9726-0
Telefax: +49 (0) 721 9726-4540
E-Mail: info@baw.de, www.baw.de



Creative Commons BY 4.0

<https://creativecommons.org/licenses/by/4.0/>

Soweit nicht anders angegeben, liegen alle Bildrechte bei der BAW.

ISSN 2625-7777 (Print)
ISSN 2625-8072 (Online)

ISBN 978-3-939230-81-6 (Print)
ISBN 978-3-939230-82-3 (Online)

Karlsruhe · Dezember 2021

Towards reliability-based bank revetment design: Investigation of limit states and parameter uncertainty

Von der Fakultät für Bauingenieurwesen der Rheinisch-Westfälischen
Technischen Hochschule Aachen zur Erlangung des akademischen Grades
einer Doktorin der Ingenieurwissenschaften genehmigte Dissertation

vorgelegt von

Julia Sorgatz

Berichter: Univ.-Prof. Dr.-Ing. Holger Schüttrumpf
Univ.-Prof. Dr.-Ing. habil. Kerstin Lesny

Tag der mündlichen Prüfung: 14.12.2020

Diese Dissertation ist auf den Internetseiten der Universitätsbibliothek online
verfügbar.

ABSTRACT

To ensure safety and ease of navigation and to protect the adjacent terrain, sloped banks at inland waterways are commonly secured by bank protections, which safeguard slopes against erosion, e. g. caused by hydraulic loading from shipping and, if applicable, natural currents. Bank protection, which serve as superimposed load, reduce the risk of local slope sliding failure and liquefaction resulting from ship-induced rapid lowering of the water level.

In order to promote inland shipping as a sustainable transport mode, it is required to provide a sustainable waterway infrastructure, which, for instance, allows for a broad navigability of larger or more powerful vessels. As a result of high design standards which bank protections had and still have to meet, to date, the expansion of a waterway is required to allow for the passage of larger vessels, which, in turn, resulted in large construction and ecological costs. However, under increasing economic and ecological pressures, an increased utilisation of the existing infrastructure, possibly with a reduction of standards, attracts growing attention.

Current deterministic design approaches eschew any information on risks and lack a systematic basis for evaluating the degree of conservativeness inherent to design. They account for uncertainties arising from the definition of characteristic values of actions and material parameters as well as from the design model itself by conservative design assumptions and empirical knowledge. However, the development of a sustainable design and maintenance strategy involves meaningful key figures about the performance of a structure over lifetime, considering site-specific design conditions and with respect to risks associated with failure.

Using the example of loose armour stone revetments at German inland waterways, this thesis examines how probabilistic methods can be applied to revetment design. It is assumed that a reliability-based approach provides comparable key figures such as the reliability index or the probability of failure, which allow for a systematic evaluation of the degree of conservativeness inherent to design. Moreover, it is assumed that updated recommendations for the choice of characteristic values, the consideration of their probability of occurrence as well as the clarification of limit states will allow for a project-specific design that accounts for local traffic and safety requirements. Conservative design assumptions can be replaced by site-specific knowledge.

By means of expert interviews, the most significant causes of damage and damage types as well as current maintenance procedures are explored. Sensitivity analyses are performed to identify significant input parameters. Reliability analyses assist in investigating the most significant parameter uncertainties inherent to actions and material parameters. Within the scope of this thesis, statistical uncertainty is investigated by an extended bootstrapping approach; model factors are determined to account for transformation uncertainty, and a random field approach is used to quantify the effects of spatial variability of soil properties on revetment design.

As for the practitioner, the effect of parameter uncertainty on the resulting armour stone size and armour layer thickness is studied.

Based on the findings of this thesis, a probabilistic design concept for bank revetments is drafted and supplementary recommendations regarding selected aspects of such a probabilistic design concept are outlined.

ÜBERBLICK

Zur Gewährleistung der Sicherheit und Leichtigkeit der Schifffahrt und zum Schutz des angrenzenden Geländes werden geböschte Ufer an Binnenwasserstraßen durch Ufersicherungen geschützt. Diese sichern die Böschung vor Erosion, z. B. verursacht durch hydraulische Belastungen der Schifffahrt und gegebenenfalls natürliche Strömungen. Ufersicherungen, die als Auflast dienen, verringern das Risiko einer lokalen Böschungsrutschung und einer Verflüssigung des Bodens infolge einer schiffsinduzierten schnellen Wasserstandsänderung.

Um die Binnenschifffahrt als nachhaltigen Verkehrsträger zu fördern, bedarf es einer Wasserstraßeninfrastruktur, die z. B. eine weitgehende Befahrbarkeit durch größere oder leistungsfähigere Schiffe erlaubt. Aufgrund der hohen Bemessungsstandards, denen Ufersicherungen entsprachen und heute entsprechen müssen, ist bisher der Ausbau einer Wasserstraße erforderlich, um die Durchfahrt größerer Schiffe zu ermöglichen, was wiederum hohe bauliche und ökologische Kosten verursachte. Unter zunehmendem wirtschaftlichen und ökologischen Druck gewinnt eine Nutzung der bestehenden Infrastruktur, möglicherweise mit einer Reduzierung der Bemessungsstandards, an Aufmerksamkeit.

Derzeitigen deterministischen Bemessungsansätzen fehlt es an Information hinsichtlich Risiken und einer systematischen Grundlage für die Bewertung implizit im Bemessungsansatz enthaltener Sicherheiten. Deterministische Bemessungsansätze berücksichtigen die Unsicherheiten, die sich aus der Definition charakteristischer Einwirkungen und Widerstände sowie durch das Bemessungsmodell selbst ergeben, durch konservative Annahmen und empirisches Wissen. Die Entwicklung einer nachhaltigen Bemessungs- und Instandhaltungsstrategie beinhaltet jedoch aussagekräftige Kennzahlen zur Leistungsfähigkeit eines Bauwerks über seine Lebensdauer unter Berücksichtigung standortspezifischer Bemessungsbedingungen und im Hinblick auf die mit einem Versagen verbundenen Risiken.

In dieser Arbeit wird am Beispiel von losen Schüttsteindeckwerken an deutschen Binnenwasserstraßen untersucht, wie probabilistische Methoden auf die Deckwerksbemessung angewendet werden können. Es wird davon ausgegangen, dass ein zuverlässigkeitsbasierter Ansatz Kennzahlen wie den Zuverlässigkeitsindex oder die Versagenswahrscheinlichkeit liefert, die eine systematische Bewertung der systeminhärenten Sicherheiten einer Bemessung erlauben. Darüber hinaus wird angenommen, dass aktualisierte Empfehlungen für die Wahl charakteristischer Kennwerte, die Berücksichtigung ihrer Wahrscheinlichkeit sowie die Spezifizierung von Grenzzuständen eine projektspezifische Bemessung unter Berücksichtigung der örtlichen Verkehrs- und Sicherheitsanforderungen ermöglichen. Konservative Bemessungsannahmen können so durch standortspezifisches Wissen ersetzt werden.

Mit Hilfe von Experteninterviews werden die wichtigsten Schadensursachen und Schadensarten sowie aktuelle Instandhaltungsstrategien untersucht. Sensitivitätsanalysen dienen der Identifikation signifikanter Eingangsparameter. Zuverlässigkeitsanalysen helfen bei der Untersuchung der Parameterunsicherheiten verbunden mit Einwirkungen und Widerständen. Im Rahmen dieser Arbeit wird die statis-

tische Unsicherheit durch einen erweiterten Bootstrapping-Ansatz untersucht; Modellfaktoren werden bestimmt, um der Transformationsunsicherheit Rechnung zu tragen, und ein *random field* - Ansatz wird verwendet, um den Einfluss der räumlichen Variabilität der Bodeneigenschaften auf die Deckwerksbemessung zu quantifizieren. Was den Praktiker betrifft, so wird der Einfluss der Parameterunsicherheit auf die resultierenden Steindurchmesser und die Deckschichtdicke untersucht.

Basierend auf den Ergebnissen dieser Arbeit wird ein probabilistisches Bemessungskonzept für Deckwerke entworfen und ergänzende Empfehlungen zu ausgewählten Aspekten eines solchen probabilistischen Bemessungskonzeptes skizziert.

ACKNOWLEDGEMENTS

‘I can no other answer make but thanks, and thanks, and ever thanks.’

–William Shakespeare, English playwright, poet and actor

First and foremost, I would like to thank my supervisor Univ.-Prof. Dr.-Ing. Holger Schüttrumpf for guiding me through this thesis. His sharp remarks and subsequent discussions have provided me with new insights that assisted in completing this thesis. I also wish to show my gratitude to Univ.-Prof. Dr.-Ing. habil. Kerstin Lesny for her valuable comments on the present thesis as second referee.

I would like to thank the German Federal Ministry of Transport (BMVI) and the Federal Waterways Engineering and Research Institute (BAW) who initiated the research project ‘Reliability-based revetment design’ as part of the BMVI Network of Experts and gave access to funding as well as research facilities.

My sincere thanks goes to Dr.-Ing. Jan Kayser, Head of Department Geotechnical Engineering at BAW, for his insightful comments and encouragement throughout this thesis but, above all, for his patience with me and my thousand ideas.

I would like to pay my special regards to the Geo-Engineering Section at TU Delft, where I was welcomed warmly as visiting researcher for one month. Thanks to the excellent supervision of Prof. Dr. Michael Hicks and Dr. ir. A.P. Bram van den Eijnden during and beyond my stay, the random field analyses presented in this thesis could be realised. I am also indebted to Dr.-Ing. Héctor Montenegro who provided the FE model for the excess pore pressure calculations at rather short notice.

Furthermore, I would like to thank my colleagues at BAW and the Federal German Waterways and Shipping Administration (WSV). Without their expertise in the background, be it the expert interviews in the field departments, the countless literature orders in the library, the set-up of model and field tests with the colleagues from central service and geotechnical laboratory or the fruitful discussions in the sections Earthworks & Bank Protections and Geotechnical Engineering North, this thesis would not have been accomplished.

Special thanks go to Jeanne Ewers, Andreas Panenka and Dr. rer. nat. Wolf Pfeiffer for working through and commenting on my thesis but, even more, for the always enjoyable discussions which helped me to broaden my perspective. Moreover, I would like to thank my former student assistant Sonja Letzelter for taking the most tedious tasks off my hands.

I wish to acknowledge the support and great love of my parents, grandparents and my sister who motivated and encouraged me during this demanding journey. Finally, I would like to express my deepest gratitude to my husband Andreas for understanding, caring and enduring my stubbornness every day. Yet, I still believe that 05:30 AM in the morning is a perfect time to discuss research.

CONTENTS

List of Figures	v
List of Tables	vii
Conventions	ix
1 Introduction	1
1.1 Motivation	2
1.2 Addressing uncertainty	3
1.3 Objectives and methodologies	3
1.4 Outline and contents summary	5
2 Addressing uncertainty: Reliability-based revetment design	7
2.1 Introduction	9
2.2 Bank revetments at inland waterways	9
2.3 Deterministic revetment design	10
2.3.1 Design standards	10
2.3.2 Ship-induced loads	13
2.3.3 Hydraulic design	15
2.3.4 Geotechnical design	16
2.3.5 Summary and critical evaluation	19
2.4 Damage and failure	20
2.4.1 Damage and failure types	20
2.4.2 Causes of damage and failure	21
2.4.3 Damage development	22
2.4.4 Summary and critical evaluation	24
2.5 Methods of a probabilistic reliability assessment	24
2.5.1 Conceptual definitions	25
2.5.2 Probabilistic methods	26
2.5.3 Limit states and target reliabilities	30
2.5.4 Summary and critical evaluation	32
2.6 Revetment design under uncertainty	34
2.6.1 Reliability-based design of hydraulic structures	34
2.6.2 Definition and sources of uncertainty	35
2.6.3 Parameter uncertainty	37
2.6.4 Model uncertainty	40
2.6.5 Summary and critical evaluation	42
2.7 Specification of the research objective and methodology	43
2.7.1 Research objective	43
2.7.2 Methodology	44
3 Traffic and traffic loads: Field data collection	47
3.1 Introduction	48
3.2 Exemplary datasets	48
3.2.1 Waterway characteristics	48
3.2.2 Geometry and construction	49

3.3	Load parameters	50
3.3.1	Field measurements	50
3.3.2	Summary of data statistics	51
3.4	Material parameters	52
3.4.1	Soil characteristics	52
3.4.2	Armour stone characteristics	52
3.5	Quality assurance	55
3.5.1	Introduction of quality indicators for field observations	55
3.5.2	Discussion of quality indicators with respect to the data	57
3.6	Conclusions	60
4	Definition of limit states: Expert interviews	61
4.1	Introduction	62
4.2	Elicitation of expert knowledge	62
4.2.1	Definitions	62
4.2.2	Experimental set-up	63
4.3	Interview results	66
4.3.1	Questionnaires	66
4.3.2	On-site inspections	67
4.3.3	Interviews	70
4.4	Discussion	71
4.5	Summary	73
4.6	Conclusions	74
5	Identification of input parameters: Sensitivity analysis	77
5.1	Introduction	78
5.2	Basic formulation and methods	78
5.2.1	Problem definition and objectives	78
5.2.2	Model definition	79
5.2.3	Assessment procedure	80
5.3	Results of the sensitivity analyses	84
5.3.1	Hydraulic design	84
5.3.2	Geotechnical design	86
5.4	Discussion	90
5.5	Conclusions	91
6	Addressing statistical uncertainty: Distribution parameters	93
6.1	Introduction	94
6.2	Exploratory data analysis	94
6.2.1	Outliers	94
6.2.2	Distribution analysis	97
6.2.3	Correlation analysis	98
6.2.4	Summary of exploratory data analysis	100
6.3	Random sampling for sample size analysis	100
6.4	Uncertainty of load variables	103
6.4.1	Distribution type and parameters	103
6.4.2	Results of sample size analysis	103
6.5	Uncertainty of material parameters	107
6.5.1	Variation of distribution parameters for uncertainty analysis	107
6.5.2	Distribution type and parameters	107

6.5.3	Results of sample size analysis	108
6.6	Discussion	110
6.7	Conclusions	112
7	Addressing transformation uncertainty: Model factors for load parameters	115
7.1	Introduction	116
7.2	Basic formulation and methods	116
7.2.1	Load calculation from vessel passages	116
7.2.2	Determination of probabilistic model factors	117
7.2.3	Application of model factor calculations to ship-induced loads	118
7.2.4	Reliability assessment with model factors	118
7.3	Results of model factors for vessel-induced loads	120
7.3.1	Verification of randomness of model factors	120
7.3.2	Statistics of generalised model factors for vessel-induced loads	120
7.4	Probability of failure	122
7.5	Discussion	124
7.6	Conclusions	126
8	Addressing spatial variability: Geotechnical design	129
8.1	Introduction	130
8.2	Basic formulation and methods	130
8.2.1	Design equations of the infinite slope model	130
8.2.2	Determination of excess pore pressure profiles in response to drawdown	132
8.2.3	Generation of the random fields	133
8.2.4	Revetment design in presence of random fields	134
8.2.5	Parameter combinations	135
8.3	Results of the random field analysis	136
8.3.1	Influence of random fields on the embankment stability	136
8.3.2	Influence of a non-homogeneous friction angle	137
8.3.3	Influence of a non-homogeneous hydraulic conductivity	138
8.3.4	Influence of a non-homogeneous friction angle and hydraulic conductivity	139
8.4	Probability of slope failure	140
8.5	Discussion	141
8.6	Conclusions	142
9	Summary and conclusions	145
9.1	Introduction	146
9.2	Main findings	146
9.3	Usability of methods and results	148
9.4	Outlook and concluding remarks	150
	Bibliography	153

LIST OF FIGURES

1.1	Revetment in construction	2
1.2	Sources of aleatory and epistemic uncertainty associated with the revetment design	4
1.3	Thesis' outline	5
2.1	Overview of revetment types	9
2.2	Revetment in construction	10
2.3	Deterministic design model, input variables and uncertainties	11
2.4	Ship-induced loads at the waterway	13
2.5	Schematic illustration of ship-induced loads	14
2.6	Hydrostatic pore water pressure and excess pore pressure during rapid drawdown	17
2.8	Erosion of the cover layer	21
2.9	Scouring of the toe	21
2.10	Scouring of the bed	21
2.11	Sliding of the cover layer (local)	21
2.12	Liquefaction	21
2.13	Failure of the toe support	21
2.14	Shallow slope failure	21
2.15	Shallow slope failure	21
2.16	Fault tree for a bank protection	22
2.17	Damage development of rock slopes and gravel beaches	23
2.18	Probability of failure and reliability index	26
2.19	Representation of the Hasofer-Lind index in physical and standard space	27
2.20	Target reliabilities for risk-based analysis in geotechnical engineering	33
2.21	Visualisation of types of uncertainty	35
2.22	Sources of uncertainty contributing to the total uncertainty of revetment design	36
2.23	Random field model for natural soil variability	39
2.24	Methodology for the purpose of describing parameter uncertainties inherent to revetment design	45
3.1	Cross-section geometries used for analyses throughout this thesis	50
3.2	Current measurement set-up and post-processing of field observations	51
3.3	Statistics of passing distances and vessel velocities observed in the field	53
3.4	Relation between Poisson and Gaussian probability function	55
3.5	Dimensions of completeness	56
3.6	Vessel types derived from field measurements and lock statistics	58
4.1	Sampling methods employed in qualitative research	64
4.2	Essential elements of expert interviews from interview preparation to data evaluation	65
4.3	Damage classification for maintenance purposes	66
5.1	(Sampling-based) sensitivity analysis scheme	79
5.2	Workflow of a sensitivity analysis (I)	83
5.3	Workflow of a sensitivity analysis (II)	83
5.4	Results of sensitivity analysis of the hydraulic design using the Morris method	86

5.5	Results of sensitivity analysis of the hydraulic design using Sobol indices	87
5.6	Results of the sensitivity analysis of the geotechnical design using the Morris method	89
5.7	Results of sensitivity analysis of the geotechnical model using Sobol indices . . .	90
6.1	Boxplots of basic variables	95
6.2	Outliers of basic variables	96
6.3	Common methods of distribution fitting	98
6.4	Probability functions fitted to the basic variables	99
6.5	Correlation of basic variables	100
6.6	Proposed bootstrapping approach to assess distribution uncertainty	101
6.7	Calculation procedure to investigate the effects of statistical uncertainty	102
6.8	Uncertainty of distribution parameters of hydraulic loads as a function of the sample size	104
6.9	Effects of statistical uncertainty on the required armour stone diameter	105
6.10	Mean probability of failure as function of the required armour stone diameter . .	106
6.11	95 % quantile of the probability of failure as function of the required armour stone diameter	106
6.12	Effects of statistical uncertainty of the friction angle on the required armour layer thickness	108
6.13	Effects of statistical uncertainty of the hydraulic conductivity on the required armour layer thickness	109
6.14	Mean probability of failure as function of the required armour layer thickness . .	110
6.15	95 % quantile of the probability of failure as function of the required armour layer thickness	110
7.1	Correlation of passing distance and vessel velocity	119
7.2	Correlation between model factors of different vessel-induced loads and selected input parameters	121
7.3	Reliability assessment without and with application of model factors using MCS	123
7.4	Importance factors resulting from reliability assessment using hydraulic loads and vessel passages as input variables	124
7.5	Model bias and reliability prediction as components of model factors	126
8.1	Infinite slope subjected to rapid drawdown	130
8.2	Schematic diagram of the random field method applied to an infinite slope . . .	134
8.3	Limit state function with and without revetment	135
8.4	Parameter definition to compare the random field analyses to the benchmark solution	136
8.5	Stress, strength, excess pore pressure and limit state profiles with the corresponding random fields	136
8.6	Influence of a non-homogeneous effective friction angle on armour layer thickness	137
8.7	Influence of a non-homogeneous hydraulic conductivity on armour layer thickness	138
8.8	Influence of a non-homogeneous hydraulic conductivity and friction angle on armour layer thickness	140
8.9	Probability of failure for different materials and variability parameters	141
9.1	Probabilistic design model draft with input variables and uncertainties	150

LIST OF TABLES

2.1	International design guidelines for bottom and bank revetments and their main scope	12
2.2	Sources of equations for the calculation of hydraulic loads	15
2.3	Levels of reliability analysis	27
2.4	Indicative values of acceptable probabilities of failure within structure lifetime	32
2.5	Target reliability indices	32
3.1	Fact sheets characterising four waterways whose measurements are used throughout this thesis	49
3.2	Summary of statistical measures describing the four example datasets	54
3.3	Test statistics of armour stone diameters	55
4.1	Qualitative sampling scheme for the compilation of expert interviews	64
4.2	Answers to semi-quantitative questionnaire regarding damage patterns and failures at German inland waterways	67
4.3	Answers to semi-quantitative questionnaire regarding causes of damage at German inland waterways	67
4.4	Summary of waterway conditions at interview locations	68
4.5	Evaluation of expert interviews	70
5.1	Common methods of sensitivity analyses	80
5.2	Ranges of variables employed in the sensitivity analysis of the hydraulic design	84
5.3	Morris test statistics of hydraulic design	85
5.4	Ranges of variables employed in the sensitivity analysis of the geotechnical design	87
5.5	Morris test statistics of geotechnical design	88
6.1	Distributions and their parameters employed in the analysis of statistical uncertainty inherent to hydraulic revetment design	103
6.2	Additive factor relating statistical uncertainty to sample size derived from bootstrapping for different coefficients of variation and sample sizes	105
6.3	Combinations of actions and soil parameters employed in the analysis of statistical uncertainty inherent to geotechnical design	107
7.1	Generalised model factor statistics for H_{stern}	120
7.2	Generalised model factor statistics for v_{return}	120
7.3	Probability of failure and design points using MCS and FORM	122

CONVENTIONS

Acronyms and abbreviations

Parameter	Abbreviation
Abz	Field Department
AD	Anderson-Darling
ADCP	Acoustic Doppler Velocimeter
AIC	Akaike-Information-Criterion
AIS	Automatic Identification System
BAW	Federal Waterways Engineering and Research Institute
BIC	Bayesian-Information-Criterion
cdf	cumulative density function
cov	coefficient of variation
CPT	Cone Penetration Test
DEK	Dortmund-Ems Canal
DGSM	Derivative-based Global Sensitivity Measure
FLS	Limit State of Fatigue
FORM	First Order Reliability Method
FoS	factor of safety
FOSM	First Order Second Moment
GoF	Goodness-of-Fit
HOW	Oder-Havel Canal
IQR	Interquartile Range
jpgf	joint probability density function
jpmf	joint probability mass function
KS	Kolmogorov-Smirnov
KuK	Küsten Canal
MCS	Monte-Carlo simulations
MLE	Maximum Likelihood Estimate
MME	Method of Moments Estimate
NOK	Kiel Canal
pdf	probability density function
PCLS	Limit State of Progressive Failure
PEM	Point Estimate Method
pmf	probability mass function
SiK	Silo Canal
SKH	Junction Canal Hildesheim
SLS	Serviceability Limit State
SORM	Second Order Reliability Method
std	standard deviation
SPK	Sacrow-Panitzer Canal
SU	silty sand
SW	permeable sand
ULS	Ultimate Limit State

Parameter	Abbreviation
WDK	Wesel-Datteln Canal
WSV	Federal German Waterways and Shipping Administration

Notation

Although some symbols are used with multiple indexes, they are usually listed only once as examples. Exceptions are symbols whose meaning changes with the index. The dimensions are: length [L], mass [M] and time [T].

Greek letters

Parameter	Dimension	Definition
α_i	[1]	importance factor
β	[LL ⁻¹]	slope angle
β_0	[1]	regression parameter
β_1	[1]	regression parameter
β_C	[1]	Cornell reliability index
β_{HL}	[1]	Hasofer-Lind reliability index
β_w	[LL ⁻¹]	angle between wave crest of secondary diverging wave and the axis of the ship or the bank line
γ_B	[ML ⁻² T ⁻²]	unit weight of soil
γ'_B	[ML ⁻² T ⁻²]	buoyant unit weight of soil below the groundwater table
γ'_D	[ML ⁻² T ⁻²]	buoyant unit weight of the armour stones below the groundwater table
γ'_F	[ML ⁻² T ⁻²]	buoyant unit weight of the filter layer below the groundwater table
γ_S	[ML ⁻² T ⁻²]	unit weight of armour stones
$\gamma_{G,d}$	[1]	partial factor of resistances
γ_Q	[1]	partial factor of actions
Δp	[ML ⁻¹ T ⁻²]	excess pore pressure
ϵ	[1]	error
ζ	[1]	similarity parameter
θ	[L]	scale of fluctuation
μ	[1]	mean
ν_P	[1]	mean occurrence rate of Poisson distribution
ξ	[1]	standard deviation of ϵ
ρ	[1]	correlation coefficient
ρ_P	[1]	Pearson correlation coefficient
ρ_s	[ML ⁻³]	armour stone density
ρ_w	[ML ⁻³]	water density
σ	[1]	standard deviation
σ'_n	[ML ⁻¹ T ⁻²]	effective normal stress
σ'_v	[ML ⁻¹ T ⁻²]	effective vertical overburden stress
τ	[ML ⁻¹ T ⁻²]	shear stress
τ_A	[ML ⁻¹ T ⁻²]	additional stress from a revetment suspension
τ_F	[ML ⁻¹ T ⁻²]	additional stress from a toe support
$\bar{\tau}$	[ML ⁻¹ T ⁻²]	shear strength

Parameter	Dimension	Definition
Φ	[1]	standard density function of a Gaussian distribution
ϕ'	[LL ⁻¹]	effective friction angle of soil
$\phi'_{D,hydr}$	[LL ⁻¹]	angle of repose of the armour stones
ψ	[1]	Shield's parameter

Latin letters

Parameter	Dimension	Definition
a	[1]	pore pressure parameter
A	[L ²]	cross-section area
b	[1]	pore pressure parameter
b^*	[1]	pore pressure parameter at $t = 5$ s
b_{ws}	[L]	water surface width
B	[L]	vessel width
B^*	[1]	uniaxial loading efficiency parameter
B_B^*	[1]	empirical factor considering the frequency of occurrence
B'_B	[1]	empirical factor considering the revetment stability (stability coefficient)
b_{ws}	[L]	water surface width
c	[1]	consolidation coefficient
c'	[ML ⁻¹ T ⁻²]	effective cohesion of soil
$C_{B\ddot{o}}$	[1]	empirical factor considering the slope inclination
C_{Isb}	[1]	Izbash factor
cov	[1]	coefficient of variance
d_D	[L]	armour layer thickness
$d_{D, pres}$	[L]	in-situ armour layer thickness
$d_{D, req}$	[L]	required armour layer thickness
d_F	[L]	filter layer thickness
d_{crit}	[L]	critical depth of failure surface
d_{critB}	[L]	critical depth of failure surface to prevent soil liquefaction
d_{shore}	[L]	passing distance at the shore
D	[L]	sieve diameter
D_{50}	[L]	mean armour stone diameter
$D_{50, req}$	[L]	required mean armour stone diameter
$D_{50, pres}$	[L]	in-situ mean armour stone diameter
$D_{n, 50}$	[L]	nominal armour stone diameter
E	[¹]	expected value
E_{oed}	[ML ⁻¹ T ⁻²]	oedometric modulus
EE	[1]	elementary effects
f	[1]	density function
F	[1]	distribution function
FO	[1]	Sobol First Order index

Parameter	Dimension	Definition
g	[1]	limit state function
g_{geo}	[L]	limit state function of geotechnical design
g_{hydr}	[L]	limit state function of hydraulic design
g'	[ML ⁻² T ⁻²]	required unit weight under buoyancy
g_0	[LT ⁻²]	gravity
H_{design}	[L]	design wave height
H_{sec}	[L]	secondary wave height
$H_{\text{sec,div}}$	[L]	divergent secondary wave height
$H_{\text{sec,q}}$	[L]	secondary transversal stern wave height
$H_{\text{sec,trans}}$	[L]	transversal secondary wave height
H_{bow}	[L]	maximum bow wave height at the bank for an eccentric sailing line
H_{stern}	[L]	maximum stern wave height at the bank for an eccentric sailing line
$H_{\text{stern, design}}$	[L]	stern wave height relevant to the determine the armour stone size
I	[1]	indicator function
k	[LT ⁻¹]	hydraulic conductivity
k_1	[1]	stability criterion in Izbash (1935) equation
k_{eff}	[LT ⁻¹]	effective hydraulic conductivity
K_g	[ML ⁻¹ T ⁻²]	bulk modulus of the gas
K_s	[ML ⁻¹ T ⁻²]	bulk modulus of the solid
K_w	[ML ⁻¹ T ⁻²]	bulk modulus of water
K_{wg}	[ML ⁻¹ T ⁻²]	bulk modulus of the water-gas-mixture
L	[L]	vessel length
m	[LL ⁻¹]	slope inclination
M	[1]	model factor
N	[1]	number of simulations
N_s	[1]	stability number describing the stability of riprap against wave attack
\bar{n}	[1]	number of variables, layers, ...
n	[1]	porosity of soil
n_r	[1]	porosity of armour layer
O	[1]	origin
p_f	[1]	probability of failure
P^*	[1]	design point in standard space
Q_c	[MLT ⁻²]	calculated loads
Q_m	[MLT ⁻²]	measured loads
S	[L ³ L ⁻³]	degree of water saturation
S_d	[1]	cumulative damage
SF	[1]	shape factor
SO	[1]	Sobol Second Order index
ST	[1]	Sobol Total Order index
t_a	[T]	drawdown time
T	[L]	vessel draught
T_L	[L]	layer thickness
T_m	[T]	mean wave period

Parameter	Dimension	Definition
u^*	[1]	minimum distance between origin and P^* in U
u_c	[LT ⁻¹]	flow velocity
u_{\max}	[LT ⁻¹]	slope supply flow
u_z	[L]	vertical displacement
U	[1]	standard normal space
v_{crit}	[LT ⁻¹]	critical vessel velocity
v_{\max}	[LT ⁻¹]	maximum flow velocity
v_{perm}	[LT ⁻¹]	permitted speed according to BinSchStrO
v_{return}	[LT ⁻¹]	return current velocity
v_s	[LT ⁻¹]	vessel velocity
v_{za}	[LT ⁻¹]	drawdown rate
V	[¹]	variance
x	[¹]	values of random variable X
X	[¹]	random variable
X_c	[¹]	calculated response
X_m	[¹]	measured response
y	[L]	depth of plane in random field analysis
Y	[¹]	model output
z	[L]	depth in soil perpendicular to the slope
z_a	[L]	change in water level

¹Individually defined

1 | INTRODUCTION

'If I have a thousand ideas and only one turns out to be good, I am satisfied.'

–Alfred Nobel, Swedish chemist & creator of the Nobel prizes

Contents

1.1	Motivation	2
1.2	Addressing uncertainty	3
1.3	Objectives and methodologies	3
1.4	Outline and contents summary	5

1.1 Motivation

To ensure safety and ease of navigation and to protect the adjacent terrain, sloped banks at inland waterways are commonly secured by bank protections (see Figure 1.1), which safeguard a slope against erosion, e. g. caused by hydraulic loading from shipping and, if applicable, natural currents. Bank protections, which serve as overburden load, reduce the risk of a local slope sliding failure and liquefaction resulting from a ship-induced rapid lowering of the water level. Revetments are the most common bank protection type. Other means of bank protections are sheet pile walls or biological/biological-technical bank protections.



Figure 1.1: Common bank protections at inland waterways (Photos: BAWArchiv).

In order to promote inland shipping as a sustainable transport mode, it is required to provide a sustainable waterway infrastructure, which, for instance, allows for a broad navigability of larger or more powerful vessels. As a result of high design standards that bank protections had and still have to meet, to date, the expansion of a waterway is required to allow for the passage of larger vessels, which, in turn, resulted in large construction and ecological costs. However, under increasing economic and ecological pressures, the design of bank protections according to proven standards is more and more being questioned. This applies in particular to waterways where the volume of traffic is expected to remain low, while at the same time larger vessels may be expected. An increased utilisation of the existing infrastructure, possibly with a reduction of standards, attracts growing attention.

At present, design values of actions are obtained by empirical equations and worst-case “design vessel passages”. Following current standards, e. g. (DIN 4020:2010-12, 2010), characteristic material parameters are commonly defined on the basis of field and laboratory tests. Yet, the number of samples may not allow for statistical data evaluation. Thus, uncertainties arise with regard to characteristic action and material parameters, which design standards try to account for by presumably conservative design assumptions and empirical knowledge. While these approaches may be suitable, they eschew any information on risks and lack a systematic basis for evaluating the degree of (non-)conservativeness inherent to design.

Moreover, in contrast to Eurocode standards, current design standards for revetments do not clearly differentiate between different categories of limit states. Damage that endangers slope stability is not distinguished from damage that affects the serviceability. The formulation of the design equations only allows to determine minimum design specifications that ensure slope and revetment stability. Conclusively, they do not yield a comparable measure for the system performance, which relates to the stability of the revetment and embankment itself.

However, the development of a sustainable design and maintenance strategy involves meaningful key figures about the performance of a structure over lifetime, under consideration of site-specific design conditions and with respect to risks associated with failure. A reliability-based or a semi-probabilistic approach can assist in providing consistent information about the condition of the waterway while meeting the above discussed requirements. It allows to incorporate site-specific information like field observations while, at the same time, accounting for the uncertainties arising from the lack of knowledge inherent to data and design models. In the future, the generated key figures can assist in quantifying the effects of a reduction of standards on revetment conditions and necessary maintenance.

1.2 Addressing uncertainty

Although various classifications of uncertainties exist, the most common is the differentiation between *aleatory* and *epistemic* uncertainty. *Aleatory uncertainty* refers to an inherent uncertainty due to natural variability such as a variation of soil properties and load intensity, whereas the *epistemic uncertainty* describes a lack of knowledge caused by limited, insufficient or imprecise data or models.

In the case of revetment design, aleatory and epistemic uncertainty can be further divided into various uncertainties such as transformation uncertainty, statistical uncertainty or spatial variability contributing to the overall uncertainty of the design. Neither loads nor resistances can be characterised without uncertainty due to their random nature. For instance, there is an apparent intrinsic randomness of the characteristic soil properties, since the subsoil is not a standardised pre-fabricated material such as steel or concrete. The interaction of climate, relief, organisms and the initial rock material in combination with physical, chemical and biological processes over time lead to inhomogeneity and anisotropy of soil and, thus, the resulting soil properties. Characteristic actions, amongst others, may differ depending on the specific waterway and the characteristics of the selected observation location. In addition, the limited number of measurements contributes to the uncertainty of actions and material parameters. Finally, it is emphasised that the design models themselves comprise model uncertainties. The geotechnical and hydraulic design equations are a simplification of real-world problems and based on empirical and semi-empirical methods, which require conservative assumptions and physical simplifications. An illustration of uncertainties that are related to the design of bank revetments at inland waterways is given in Figure 1.2.

A precise assignment of uncertainties is difficult, as all types of uncertainty contribute to total uncertainty and depend on the context of application. Physical, financial and time constraints impede specification and evaluation of all of the above uncertainties. The so-called unknown unknowns (“black swans”) require alternative strategies such as robust or resilient design (Phoon, 2020).

1.3 Objectives and methodologies

Uncertainties are inherent to each design and construction in engineering. Various empirical and semi-empirical methods that commonly require conservative assumptions and physical simplifications have been proposed to deal with uncertainties. While these approaches may be suitable, they lack a systematic evaluation of uncertainty. As stated by ISO 2394:2015-03 (2015,

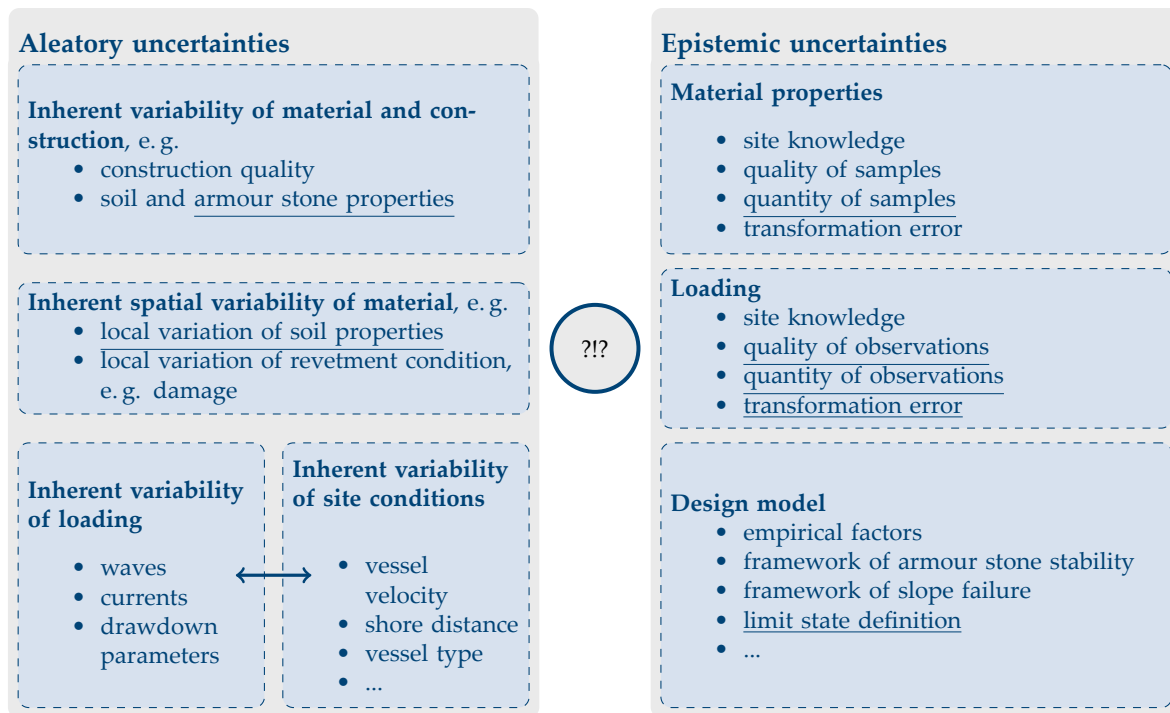


Figure 1.2: Sources of aleatory and epistemic uncertainty associated with the revetment design along inland waterways. The blue circle in the centre represents the “unknown unknowns”. The underlined sources of uncertainty are accounted for in this thesis.

p. 17), however, “uncertainties shall be represented in the decision process through probabilistic models such as random variables, stochastic processes and/or random fields.”

This thesis aims at complementing the revetment design by introducing reliability-based methods. It is assumed that a reliability-based approach provides comparable key figures such as the reliability index or the probability of failure, which allow for a systematic evaluation of the degree of (non-)conservativeness inherent to a design. Moreover, it is assumed that updated recommendations for the choice of characteristic values, the consideration of their probability of occurrence as well as the clarification of limit states will allow for a project-specific design that accounts for local traffic and safety requirements. Presumably conservative assumptions are replaced by site-specific knowledge.

Main objectives of the investigations are:

- to adapt the concept of a reliability-based design for revetments and to evaluate its applicability by comparing results of deterministic and reliability-based design
- to understand how parameter uncertainty affects revetment design

Based on these objectives, the procedures pursued within this thesis are described as follows:

Using the example of loose armour stone revetments at German inland waterways, it is examined how probabilistic methods can be applied to revetment design. Qualitative and quantitative methods of data collection and evaluation are combined. Sources of uncertainty and common ways to deal with them are identified by means of a literature review. Expert interviews are employed to explore the most significant causes of damage and damage types as well as current maintenance procedures. Sensitivity analyses are performed to identify significant

input parameters. By means of reliability analyses, the most significant parameter uncertainties inherent to basic variables such as actions and material strength are investigated. As for the practitioner, the effect of parameter uncertainty on the resulting armour stone size and armour layer thickness is studied.

1.4 Outline and contents summary

Figure 1.3 shows the general outline of this thesis. The outline reflects the two main aspects of the methods outlined above; that is data collection and uncertainty analysis of actions and soil parameters. A literature review and seven additional appendices provide supplementary information. The chapters of the thesis are summarised as follows:

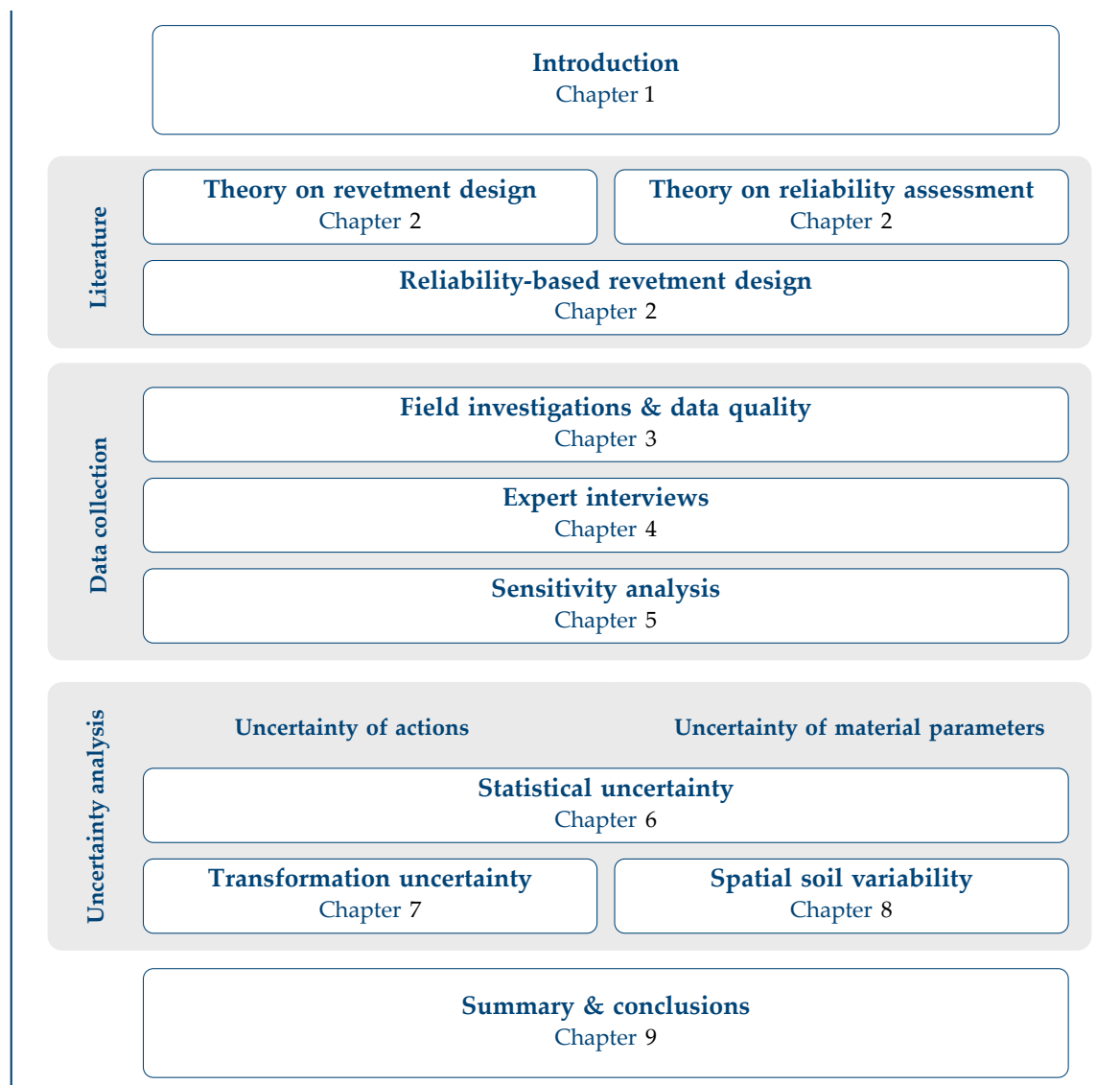


Figure 1.3: Outline of the thesis.

In **Chapter 2**, the theoretical background of revetment design and probability theory are introduced. Common methods of a reliability-based design are briefly summarised. Current research regarding a reliability-based revetment design is outlined. Knowledge gaps are identified and, thereby, the research questions specified.

In **Chapter 3**, four field campaigns are introduced as exemplary datasets, which illustrate the proposed approaches throughout this thesis. Data quality measures are discussed and applied to the evaluation of the four exemplary datasets.

Chapter 4 investigates which limit states apply to the geotechnical and hydraulic revetment design. By means of expert interviews, significant damage causes and modes of failure are identified. Based on these results, applicable limit states are specified. Furthermore, it is examined how maintenance is currently conducted.

Chapter 5 elaborates the design models with respect to the required design parameters. Sensitivity analyses allow, amongst others, to gain insight into the relative importance of the various input parameters of design models and assist in identifying limitations of employed models.

From the Bayesian point of view, statistical uncertainty is a result of limited information such as a limited number of field observations. When fitting a parametric distribution to limited data, the parameters of the distribution are of random nature. Based on the exemplary datasets, **Chapter 6** quantifies the uncertainty that results from the limited number of samples by means of bootstrapping.

Transformation uncertainties inherent to the calculation of characteristic values of actions are investigated in **Chapter 7**. Each campaign contains information on vessel passages such as velocity, bank distance and vessel geometry and on the majority of resulting hydraulic loads. Measured loads are compared to calculated loads aiming for a characterisation of transformation uncertainty. A model factor approach which may simplify the collection of field data is introduced. Transformation uncertainty of material parameters is not confined to revetment design, as it affects all forms of geotechnical constructions. It is therefore not considered in this thesis.

Inhomogeneous soil parameters such as a locally variable shear strength and hydraulic conductivity may affect the level of safety obtained with deterministic design approaches. **Chapter 8** elaborates the safety margins inherent to the geotechnical design and provides guidance regarding the choice of characteristic soil parameters required in revetment design.

Finally, based on the main findings of the previous chapters, **Chapter 9** offers a draft of a probabilistic design concept for bank revetments. For this purpose, the main findings from this work are summarised. Recommendations regarding specific aspects of a probabilistic design concept are outlined. Potentials for future research and development are discussed.

2 | ADDRESSING UNCERTAINTY: RELIABILITY-BASED REVETMENT DESIGN

‘Traditionally, engineering and civil engineering are very deterministic in their teaching and in the attitude of their practitioners. When something goes wrong, it takes them by surprise. And yet, all things they are handling, the raw materials, the input and the output, are random processes. If that can be taken seriously, the method of design can be improved considerably.’

–Peter Lumb, Professor of Civil Engineering at the University of Hong Kong

Contents

2.1	Introduction	9
2.2	Bank revetments at inland waterways	9
2.3	Deterministic revetment design	10
2.3.1	Design standards	10
2.3.2	Ship-induced loads	13
2.3.3	Hydraulic design	15
2.3.4	Geotechnical design	16
2.3.5	Summary and critical evaluation	19
2.4	Damage and failure	20
2.4.1	Damage and failure types	20
2.4.2	Causes of damage and failure	21
2.4.3	Damage development	22
2.4.4	Summary and critical evaluation	24
2.5	Methods of a probabilistic reliability assessment	24
2.5.1	Conceptual definitions	25
2.5.2	Probabilistic methods	26
2.5.3	Limit states and target reliabilities	30
2.5.4	Summary and critical evaluation	32

2.6	Revetment design under uncertainty	34
2.6.1	Reliability-based design of hydraulic structures	34
2.6.2	Definition and sources of uncertainty	35
2.6.3	Parameter uncertainty	37
2.6.4	Model uncertainty	40
2.6.5	Summary and critical evaluation	42
2.7	Specification of the research objective and methodology	43
2.7.1	Research objective	43
2.7.2	Methodology	44

2.1 Introduction

In order to enable operators of waterways to make optimal use of their resources, future revetment design should aim for a project-specific design targeting local traffic and safety requirements. Since the use of site-specific information may reduce or increase safety margins included in present design standards, uncertainties inherent to input variables and design models must be considered. Limit states must be defined with respect to risk.

This chapter introduces the theoretical background of revetment design and probability theory in detail. Section 2.2 outlines typical constructions of revetments at inland waterways. Secondly, current deterministic design approaches for revetments (Section 2.3) are presented and typical damage and failure types as well as their causes are summarised (Section 2.4). Subsequently, methods applied in probabilistic engineering are briefly introduced (Section 2.5). This is followed by a review of different types of uncertainty which apply in particular to revetment design (Section 2.6). Finally, after a summary and critical evaluation of the present state of knowledge, the objectives and further procedure of this thesis are specified (Section 2.7).

2.2 Bank revetments at inland waterways

Banks at inland waterways mostly exhibit inclinations of 1:3 (height:length), in rare cases up to 1:2. Most frequently, technical bank revetments are installed, which secure the bank from the bottom of the river or canal to the highest possible wave emergence (MAR, 2008). Revetments are built of an erosion-resistant cover layer, a filter layer and, if necessary, a sealing layer below. There are various types of cover layers, the installation of which depends in particular on the expected hydraulic loads. The different types of cover layer are summarised in Figure 2.1. This thesis uses the example of loose rip-rap revetments as a common revetment type at German inland waterways.

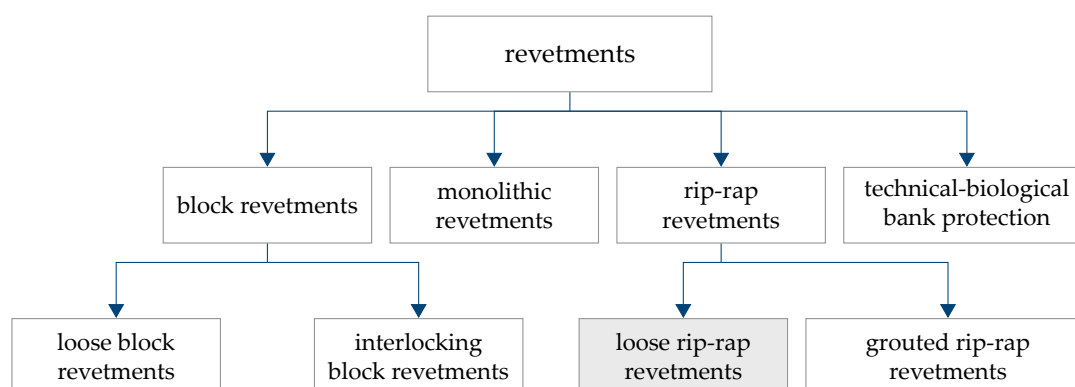


Figure 2.1: Overview of revetment types. Adopted from (Gier, 2017) and supplemented. Subject of this thesis are loose rip-rap revetments as indicated by the grey shaded rectangle.

For rip-rap revetments, the erosion-resistant cover layer is typically made up of armour stones. The weight of the cover layer ensures the local stability of the bank against slope sliding and liquefaction. The filter layer ensures the stability of the base soils by preventing the erosion of finer material below the filter layer (MAR, 2008; PIANC, 1987a). An important element for a revetment is the toe protection. Using an embedded toe where the revetment is placed 1.0 m to 1.5 m below the river or canal bed is common practice today. Further design types are toe

blankets and sheet pile walls. By providing additional shear strength, the toe support allows for lower layer thicknesses and prevents the revetment from being destroyed at the toe by hydraulic attack, especially when ships navigate close to the bank. Figure 2.2 shows a standard revetment design built in Germany.

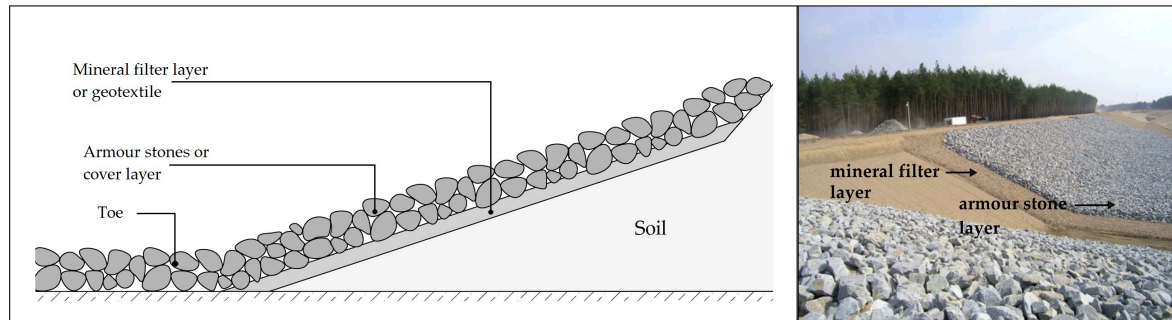


Figure 2.2: Revetment in construction. Visualisation of revetment elements (Photo: BAWArchiv).

2.3 Deterministic revetment design

2.3.1 Design standards

The design of revetments is distinguished into a hydraulic and a geotechnical design. The hydraulic design specifies the minimum armour stone diameter necessary to withstand ship-induced and natural waves and currents. The geotechnical design evaluates the required weight of the cover layer which ensures local embankment stability (GBB, 2010; PIANC, 1987a, 1989; Rock Manual, 2007). In the case of loose armour stone revetments, the required weight of the cover layer is transferred into a layer thickness.

Figure 2.3 shows a graphical representation of the current model for revetment design. As commonly accepted in slope stability analyses, input variables, which are subsequently also referred to as basic variables, are differentiated in actions and material parameters. Actions include waves, currents and drawdown. In the context of this thesis, they are also called hydraulic loads. On the resistance side, the material parameters, e. g. friction angle and hydraulic conductivity, of armour stones and soil are considered in this thesis. This corresponds to the partial factor approach of DIN EN 1997-1:2014-03 (2010), where, in the case of slope stability, actions and material strength are compared with regard to predefined limit states. Parameter and model uncertainties are accounted for by selecting characteristic values, locally non-specific partial and empirical factors (GBB, 2010; Rock Manual, 2007; USACE, 1997).

On an international level a number of design standards exists of which an overview is given in Table 2.1 with brief reference to their main scope of application.

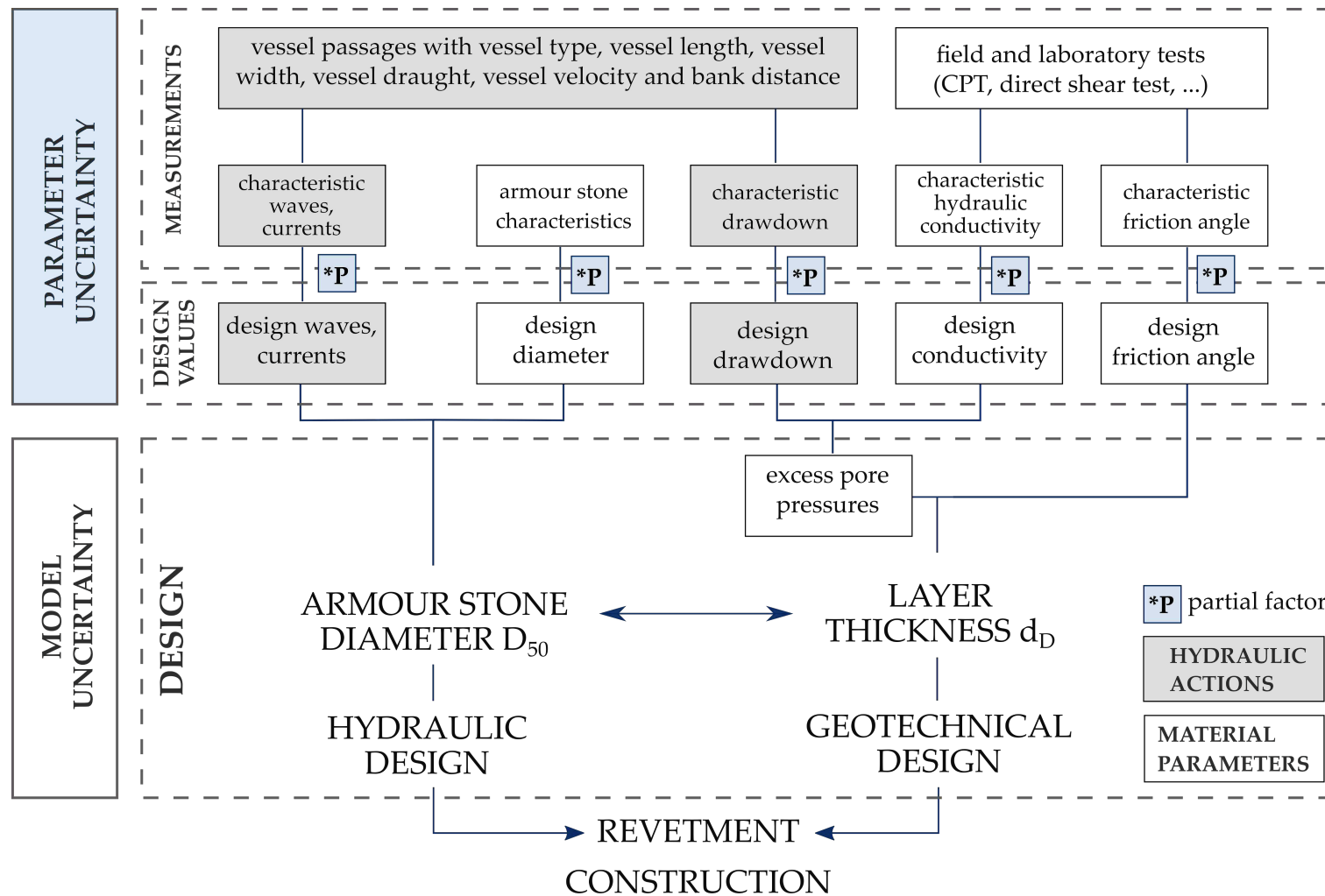


Figure 2.3: Deterministic design model, input variables and uncertainties. The grey highlighted boxes indicate hydraulic loads; white boxes indicate material parameters.

Table 2.1: Summary of international (English) design guidelines for bottom and bank revetments and their main scope.

Design code	Editor	Year	Country	Scope	Source
BAW Code of Practice: Principles for the Design of Bank and Bottom Protection for Inland Waterways (GBB)	Bundesanstalt für Wasserbau (BAW)	2010	Germany	Design of rip-rap revetments for inland waterways	GBB (2010)
BAW Code of Practice: Use of Standard Construction Methods for Bank and Bottom Protection on Inland Waterways (MAR)	Bundesanstalt für Wasserbau (BAW)	2008	Germany	Design of rip-rap revetments for inland waterways for standard canal geometries	MAR (2008)
The Rock Manual. The use of rock in hydraulic engineering	CIRIA, CUR, CETMEF	2007	UK, France, Netherlands	Design and construction of coastal, inland waterway and closure structures made of rock	Rock Manual (2007)
Coastal Engineering Manual	US Army Corps of Engineers	2002	USA	Design and expected performance of a broad variety of coastal projects such as harbours, flood protection or beach erosion control	US Army Corps of Engineers (2002)
Design of Coastal Revetments, Seawalls, and Bulkheads	US Army Corps of Engineers	1997	USA	Design of coastal revetments, seawalls, and bulkheads	USACE (1997)
Report of Working Group II-21: Guidelines for the design and construction of flexible revetments incorporating geotextiles in marine environment	Permanent International Association of Navigation Congresses (PIANC)	1992	International	Design and construction of flexible revetments for a maritime environment with an emphasis on geotextile as filter layer	PIANC (1992b)
Design of Riprap Revetments	U.S. Department of Transportation	1989	USA	Design of revetments for canals and rivers with emphasis on rip-rap revetments	PIANC (1989)
Risk consideration when determining bank protection requirements	Permanent International Association of Navigation Congresses (PIANC)	1987	International	Application of risk analysis for the design of bottom and bank revetments of inland waterways	PIANC (1987b)
Report of Working Group I-4: Guidelines for the design and construction of flexible revetments incorporating geotextiles for inland waterways	Permanent International Association of Navigation Congresses (PIANC)	1987	International	Design and construction of flexible revetments for inland waterways with an emphasis on geotextile as filter layer	PIANC (1987a)
Shore Protection Manual. Volume I and II	US Army Corps of Engineers	1984	USA	Design and construction of coastal structures, small section on design of canals revetments	USACE (1984a,b)

2.3.2 Ship-induced loads

Ship-induced loads in a limited cross-section comprise waves, currents and a rapid lowering of the water level, which is subsequently referred to as drawdown, see Figure 2.4. During manoeuvring, propulsion caused by the propeller jet may act on the bank (GBB, 2010). The magnitude of the hydraulic effects depends, among other things, on the vessel velocity, the distance from the shore and the ratio of waterway to submerged ship area (n -ratio).

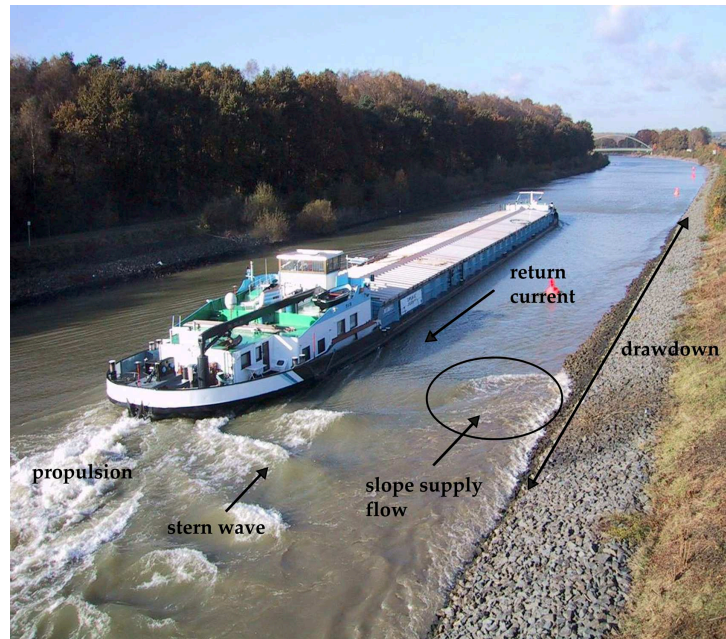


Figure 2.4: Ship-induced loads at the waterway (Photo: BAWArchiv).

When a vessel passes through the water, a few centimetres of water accumulate in front of the vessel causing bow waves. The discharge conditions trigger a flow around the vessel from the bow to the stern, the return current. The acceleration of the water flow velocity causes a lowering of the water level next to the vessel which is subsequently referred to as drawdown. The drawdown causes pressure fluctuations and transient currents, since it is replenished by a current in the opposite direction to that of the vessel called the slope supply flow. Starting from the vessel's stern, the lowered water level is re-balanced by the transversal stern wave. The described sequence of bow wave, drawdown and wave is called primary wave system. The secondary wave system consists of short period oblique and transverse waves. In contrast to the primary waves, the wave height of secondary waves remains approximately constant as the distance to the vessel increases (Gesing, 2010). Figure 2.5 illustrates the described system of hydraulic loads.

A major advancement in the field of revetment design along inland waterways is certainly the ability to separate the design into two steps: firstly, the calculation of hydraulic loads and secondly, the calculation of resulting revetment dimensions. In contrast to coastal engineering, the design therefore no longer depends on measurements of hydraulic loads. Instead, with assumptions on vessel geometry, vessel velocity and shore distance, hydraulic wave heights and currents are calculated for "design vessel passages", which are derived from worst-case scenarios and empirical knowledge (GBB, 2010; PIANC, 1987a; Rock Manual, 2007). Subsequently, drawdown height and drawdown time are derived from the wave heights. To study

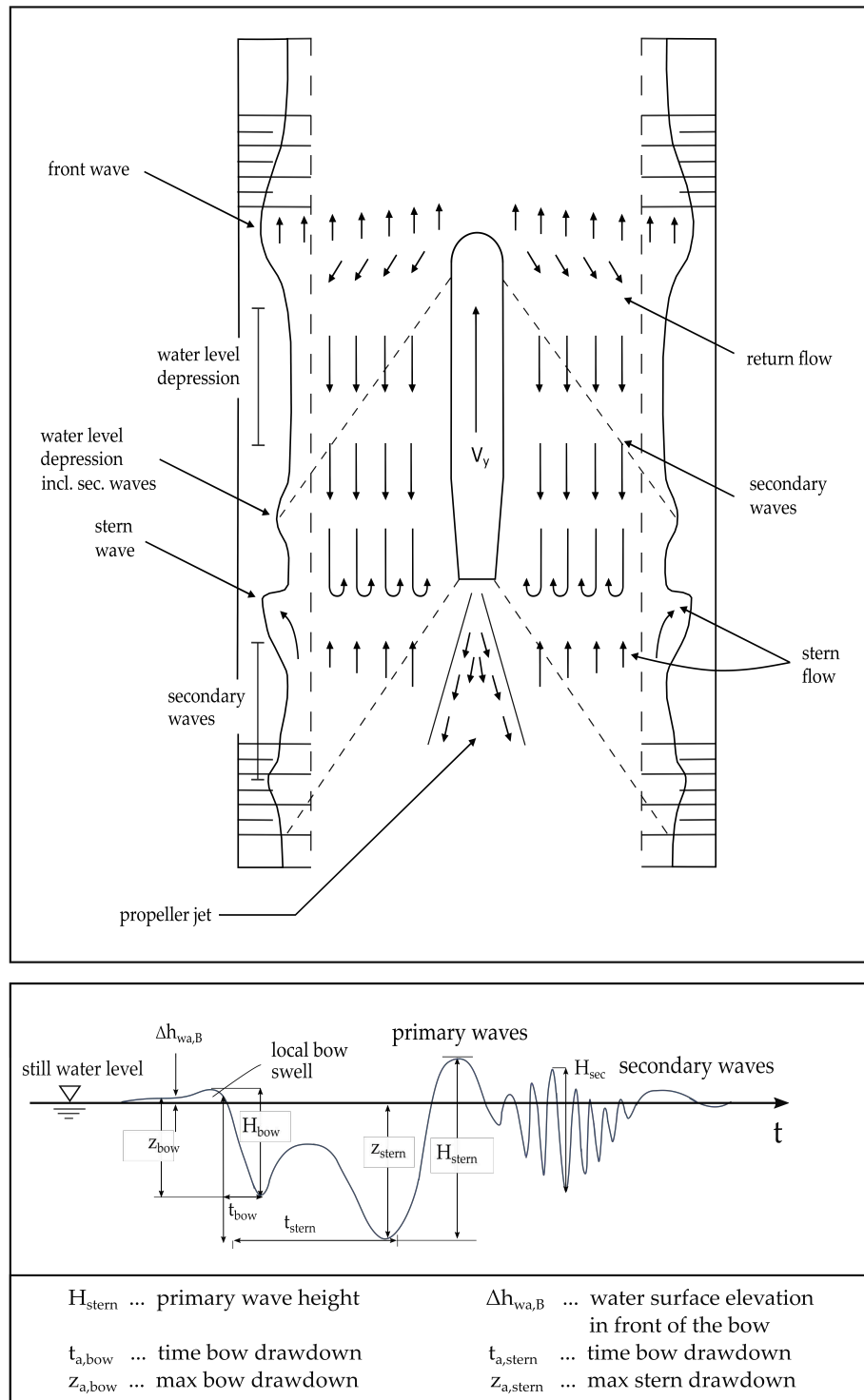


Figure 2.5: Schematic illustration of ship-induced loads in plain view (Rock Manual, 2007, cf. p. 435) and over time (GBB, 2010, cf. p. 62).

the equations that allow to compute hydraulic loads, please see the literature summarised in Table 2.2.

Table 2.2: Sources of equations for the calculation of hydraulic loads grouped by origin.

Parameter	Literature
Stern wave height H_{stern}	Przedwojski et al. (1995) and van Hijum and Pilarczyk (1982)
Bow wave height H_{bow}	Przedwojski et al. (1995) and van Hijum and Pilarczyk (1982)
Secondary wave height H_{sec}	Blaauw et al. (1984), Gates and Herbich (1977), Maynord (2005), Söhngen, Pohl et al. (2010) and van Hijum and Pilarczyk (1982)
Return current velocity v_{return}	Bouwmeester et al. (1977), GBB (2010), Maynord (1990) and Schijf and Jansen (1953)
Slope supply flow u_{max}	BAW (2009), Söhngen, Pohl et al. (2010) and Verheij and Bogaerts (1989)

2.3.3 Hydraulic design

Required stone diameter to resist currents

In contrast to coastal structures, the revetment design for rivers and canals must not only consider waves but also ship-induced and natural currents parallel to the embankment. The foundation for present design equations against currents was particularly laid by Hjulström (1935) and Izbash (1935) with a purely empirical approach based on critical flow velocity and Shields (1936) outlining a semi-empirical relation between critical shear stress and bottom roughness (Rock Manual, 2007). Both approaches deal with the beginning of sediment transport and apply to uniform material with grain sizes $D_{50} < 100$ mm.

Shield's equation (Shields, 1936) is given in eq. (2.1). It allows to calculate the required grain diameter D_{50} with shear stress parameter ψ (Shield's parameter) and shear stress τ . In addition, the gravity g_0 , water density ρ_w and armour stone density ρ_s are required.

$$\psi = \frac{\tau}{(\rho_s - \rho_w)g_0D_{50}} \quad (2.1)$$

The Izbash equation as outlined by Blaauw et al. (1984) determines the required grain diameter D_{50} with the flow velocity u_c and a stability criterion k_1 . It is defined as follows:

$$k_1 = \frac{u_c}{g_0 \frac{\rho_s - \rho_w}{\rho_w} D_{50}} \quad (2.2)$$

Based on model and field measurements, the equations by Izbash (1935) and Shields (1936) were modified to account for larger particles, e. g. Dorer (1986), Izbash and Khaldre (1970), Meyer-Peter and Müller (1949), Pilarczyk (1985), Stevens et al. (1984) and van Rijn (1993). Froehlich and Benson (1996) describes a design approach for loose armour stones against currents based on the probabilistic description of critical shear stress. PIANC (1987b) outlines general recommendations regarding a probabilistic revetment design against currents but stresses the importance of choosing a limit state function which accounts for the nature and duration of loading. Results of Rock Manual (2007) suggest that different equations may yield different results, e. g. depending on the level of turbulence.

The design of bank revetments is commonly conducted with a modified formula of Izbash and Khaldre (1970). According to DVWK (1997), the formula of Izbash and Khaldre (1970) yields the most conservative design. For near-bed structures, the equations of Shields (1936) or a combination of Izbash/ Shields formulae are equally suitable depending on the limitations of each equation specifically. A summary of commonly used design equations is given in Appendix A.1.

Required stone diameter to resist wave attack

Before the stability of revetments on inland waterways was investigated, there already had been numerous publications on the stability of coastal protection structures. The work of Hudson (1959) and Iribarren and Nogales (1952) certainly influences the design of revetments and breakwaters up until this day. The equation of Hudson (1959) as given in eq. (2.3) describes the required armour stone size by the armour stone mass M_{50} at 50 % throughput of the cumulative line. It is a function of armour stone density ρ_s , gravity g_0 , design wave height H , stability coefficient K_D , water density ρ_w and slope inclination $\cot \beta$

$$M_{50} = \frac{\rho_s g_0 H^3}{K_D \left(\frac{\rho_s - \rho_w}{\rho_w} \right)^3 \cot \beta} \quad (2.3)$$

With the help of a large number of model experiments, various authors improved the empirical coefficient K_D of the Hudson (1959) equation for different boundary conditions, e.g. BAW (2009), Carver and Davidson (1977), Font (1970), Jackson (1968) and van de Kreeke (1969). In the late 1980s, van der Meer (1987, 1988b) introduced new design equations, which consider random wave attack mainly for deep but also for shallow foreshores. In detail, the influence of shallow shores on the wave height was included in a set of equations presented by van Gent et al. (2003). In 1989, Verheij and Bogaerts (1989) modified the equation of Hudson (1959) in order to account for ship-induced secondary waves in the revetment design. Boeters et al. (1993) primarily deal with damage prediction adapting the equations of van der Meer (1988b). In particular for fairways confined both laterally and in depth, GBB (2010) provides equations for the positional stability of armour stones which account for the superimposition of the primary and secondary wave system.

The number of available stability equations against wave attack is manifold (see Appendix A.1). As outlined by Rock Manual (2007), engineers must thus ensure that the formulae are valid for the desired application. Moreover, Rock Manual (2007) recommends to conduct sensitivity analyses and to use probabilistic methods to account for the uncertainty inherent to the design equations.

2.3.4 Geotechnical design

Experience shows that in the river and canal beds, especially in areas of shallow water depths or in water exchange zones, gaseous components in the pore water occur. The gas entrapped in the fluid can lead to the build-up of excess pore pressure. The three-phase system 'soil' consisting of grain matrix, pore water and gas phase can be modelled as a two-phase system with grain matrix and compressible fluid phase.

The presence of even small volumes of entrapped gas in the voids, for example as a result of natural water level fluctuations and/or biogenic gas generation, in combination with ‘rapid’ external hydraulic or static load changes can lead to the build-up of excess pore pressure. The reason for such a response is primarily a consequence of the compressibility of the gaseous phase in the pore fluid. The expression ‘rapid loading’ must be considered with respect to the soil’s hydraulic conductivity and therefore involves a wide range of time scales. The excess pore pressures lead to reduced effective stress, which lowers the shear strength of the soil. This may result in local slope sliding along a failure surface in the ground or in liquefaction of soil directly below the revetment.

In simplified terms, the depths of sliding surface and liquefaction area are determined by the ratio of overburden load and excess pore pressure, which commonly reaches a minimum at 1 m below surface to surface. Both failure mechanisms thus describe failures near the surface. Local slope sliding refers to failures in which the sliding surface of the sliding wedge is relatively close to the surface. Soil liquefaction refers to a process where soil near the surface starts behaving like a liquid since the grains of soil lose their contacts due to the exceedance of their contact forces by excess pore pressure.

Drawdown and, thus, the development of excess pore pressure in the embankment is a time-dependent process. Various authors, e. g. Madsen (1978), Okusa (1985) and Yamamoto et al. (1978), have developed analytical methods to account for harmonic changes in pore water pressures and effective stresses induced by wave loading using Biot’s equations (Biot, 1941). Starting from the mid-1980s, Köhler (1985, 1989, 1993, 1997a,b) conducted a number of physical model tests and numerical studies to assess the pore water pressure distribution caused by ship-induced rapid drawdown. Based on the investigations of Köhler (1985), vessel wave induced drawdowns can be simplified by a uniformly decreasing water level characterised by a constant drawdown rate (change in water level z_a during the drawdown time t_a). It can be shown that the excess pore pressure attains a maximum at the end of the drawdown which allows to assess the acting forces as a steady-state problem as shown in Figure 2.6.

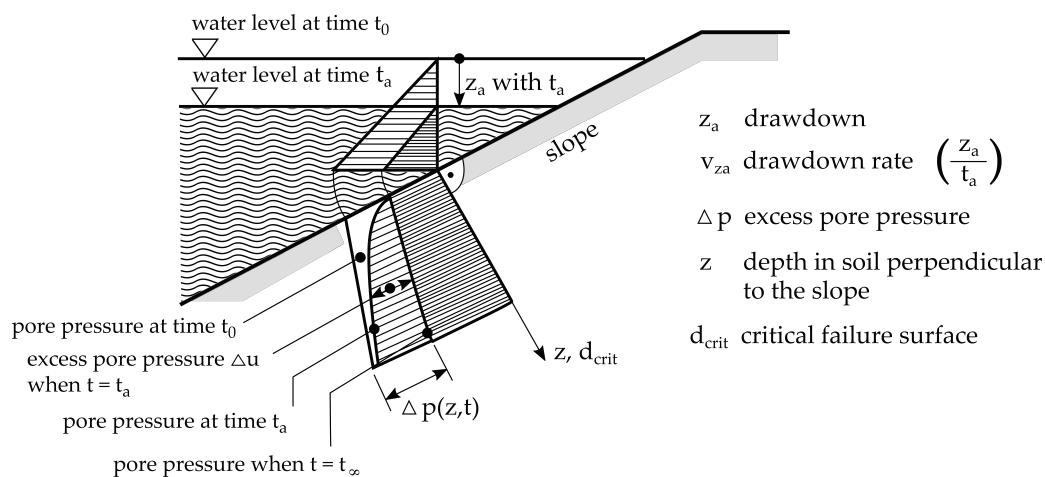


Figure 2.6: Hydrostatic pore water pressure and excess pore pressure during rapid drawdown; illustration based on GBB (2010, cf. p. 20).

Slope stability influenced by excess pore pressures has been investigated for many years in geotechnical engineering (Bishop, 1955; Terzaghi, 1943). The geotechnical design of revetments is distinguished in local and global stability analysis. The revetment design “must ensure local stability for the load case in which excess pore pressure occurs as a result of rapid drawdown

of the water level" (GBB, 2010, p. 109). It does not include global slope stability analysis, which has to be verified separately following the guidance of DIN 1054:2010-12 (2010). If the soil has a permanent effective cohesion under water which is greater than p , the local stability of permeable revetments can be assumed without further verification (GBB, 2010). Thus, subsequently presented investigation only considers non-cohesive materials.

Required armour stone layer thickness to impede slope sliding

The excess pore pressure Δp may cause driving forces to exceed resisting forces at the vertical slice of the infinite slope leading to local sliding. Current design standards (GBB, 2010; PIANC, 1987a; Rock Manual, 2007) refer to the investigations of Köhler (1985, 1989, 1993, 1997a,b) which provide the following equations to determine the required unit weight under buoyancy g' against slope sliding:

$$g' = \gamma'_D d_D = \frac{\Delta p \tan \phi' - c' - \tau_F - \tau_A}{\cos \beta \tan \phi' - \sin \beta} - (\gamma'_F d_F + \gamma'_B d_{crit}) \quad (2.4)$$

with the effective friction angle of soil ϕ' , the armour stone layer thickness d_D , the buoyant unit weight of the armour stones below the groundwater table γ'_D , the filter layer thickness d_F , the buoyant unit weight of the filter layer below the groundwater table γ'_F , the buoyant unit weight of the soil below the groundwater table γ'_B and the critical depth d_{crit} , which denotes the depth at which the difference of resisting and driving forces reaches a minimum. A schematic illustration of these quantities is provided in Figure 2.7.

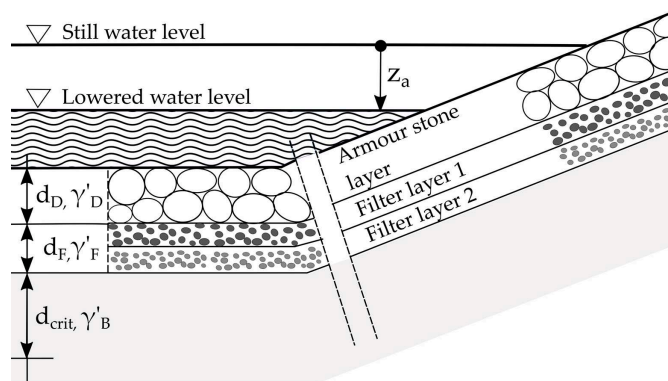


Figure 2.7: Constructional elements considered in a revetment design.

An effective cohesion c' reduces the required armour stone layer thickness. An additional toe support or a suspension of the armour stone layer can add a supporting additional stress from a revetment suspension τ_A or additional stress from a toe support τ_F , which leads to the reduction of the required armour stone layer thickness. However, for revetments with a toe blanket and/or a suspension, further failure mechanisms and thus, additional design equations are to be considered (GBB, 2010).

Required armour stone layer thickness to impede liquefaction

Excess pore pressures trigger a flow in the permeable river bed which may lead to considerable vertical hydraulic gradients at river bed and slope. This process is particularly promoted by a compressible pore fluid in soils of moderate to low hydraulic conductivity and moderate to large plasticity. The flow of pore water can lead to liquefaction of a near-surface layer of the river bed. In the case of a large toe support force, a revetment suspension or a very small slope inclination, the weight per unit area of the cover layer resulting from the design against slope sliding failure may not satisfy the equilibrium equations of liquefaction. Equation (2.5) allows to determine the required unit weight under buoyancy g' required to protect embankments against liquefaction caused by rapid drawdowns:

$$g' = \gamma'_D d_D \geq \frac{\Delta p}{\cos \beta} - (\gamma'_F d_F + \gamma'_B d_{\text{critB}}) \quad (2.5)$$

with the buoyant unit weight of soil below the groundwater table γ'_B and the critical depth of liquefaction d_{critB} , at which, again, the difference of resisting and driving forces reaches a minimum.

Besides the geotechnical requirements, the layer thickness is also defined on the basis of the various functions of the revetment as protective layer. Structure, anchor cast, vessel impacts, ice breakage and ultraviolet radiation must be considered (GBB, 2010; Rock Manual, 2007).

2.3.5 Summary and critical evaluation

As shown in the previous sections, a large number of equations exist in different deterministic design standards. The equations employed nowadays for revetment design against wave attack originate to a large extent from approaches developed for coastal engineering. Differences between ship-induced and coastal waves the design equations may not account for are, for example, load duration, load direction and shallow foreshore conditions. Moreover, the quality of the installation plays an important role regarding the stability of revetments. As found by Allsop and Jones (1993) and Bezuijen and Klein Breteler (1992), oblique wave attack, which is particularly a result of vessel-induced loads, is negligible.

Commonly, a similarity between breakwaters and armour stone layered revetments on the one hand and wind waves and ship-induced secondary waves on the other hand is assumed, which allows to transfer equations proposed for coastal structures to the design of revetment in inland areas (Boeters et al., 1993). Equations that specifically address revetments on inland waterways are found in GBB (2010), PIANC (1987a) and Rock Manual (2007). Still, the transformation process from coastal applications to inland waterways may lead to uncertainty.

Moreover, particularly in the case of inland waterways, additional parameter uncertainty is introduced by not using the measured loads, i. e. waves and currents, as input parameters for design, but calculating these values from preceding equations based on vessel passages. Especially concerning waterways, it is thus necessary to quantify the uncertainties arising from the calculation of characteristic values of actions.

At present, uncertainties in the design formulae are commonly accounted for by empirical factors which differ between the different design formulae. Depending on the design equations and the empirical factor, different damage or safety levels are targeted. Besides the use of different formulae, this complicates a comparison of different designs.

Several design codes (PIANC, 1987b; Rock Manual, 2007; US Army Corps of Engineers, 2002) recommend the application of probabilistic methods to consider the uncertainty and evaluate the conservativeness in particular inherent to hydraulic revetment design.

Conclusions: The literature review shows that a variety of design formulae are available to determine the armour stone diameter for revetments; commonly derived for coastal structures. Wave height, flow velocity or vessel passages as well as the geometrical boundary condition at the waterway serve as input parameters. Depending on the design equations and the empirical factor, different target damage or safety levels are targeted. Fewer equations are available for the geotechnical design; commonly, the equations of Köhler (1985) are used for local stability analyses.

2.4 Damage and failure

2.4.1 Damage and failure types

Failure is a 'state in which the performance requirements are not satisfied' (COST WG 1, 2019). It thus refers to specific performance goals, performance requirements and does not automatically refer to the collapse of a structure. Damage can contribute significantly to failure. It is defined as 'physical disruption or changes to the material and/or geometric properties of these a [sic!] systems, including changes to the boundary conditions and system connectivity, which adversely affect the system's performance' (COST WG 1, 2019). Failure modes are 'quasi-permanent or transient situations that violate code specifications or owner's/operator's provisions [...]' (COST WG 1, 2019). They occur when a limit state is exceeded.

Although Rock Manual (2007, p. 568) defines 'failure' as a state 'corresponding to reshaping of the armour layer such that the filter layer under the armourstone in a double layer is visible.', in design codes, there is often no clear distinction between damage and failure modes of revetments. In a fault tree analysis, Schiereck (1998) distinguishes between failure mechanisms causing overall instability and local instability. The overall instability is differentiated into micro and macro instability, which again is a result of toe erosion. The local instability may result from instability of the protective elements, wave overtopping and subsequent subsidence and vessel collision. Julien (2002) states four failure modes, being particle erosion, slide, riprap slump and sideslope failure. The Rock Manual (2007) lists a total of 14 predominately geotechnical failure mechanisms, which relate to global and local slope stability. Besides the already listed failures, they include wave overtopping, settlement, tilting, piping, liquefaction, ice drifting and ship collision. It should be noted that often failure modes are interrelated. As stated in GBB (2010), armour stone revetments are dimensioned against the following local "failure" mechanisms:

- erosion of the cover layer (Figure 2.8),
- sliding of the cover layer (revetments without toe support, Figure 2.11),
- liquefaction (Figure 2.12),
- slope failure at the base of the embankment or at the base of the toe support (Figure 2.13) and

- scour as a special form of erosion (Figure 2.9).

The main types of damage mentioned in literature (Blodgett and McConaughy, 1986; Julien, 2002; Kreyenschulte, 2020; Ouellet, 1972; Rock Manual, 2007) and in reports of the Federal Waterway Engineering and Research Institute (BAW) (Fleischer and Kayser, 2006; Kayser, 2003, 2006, 2007a,b, 2008; Stein, 2008) are

- single armour stone displacements (Figure 2.8)
- scouring in the bed area (Figure 2.10),
- deeper slope failure (Figure 2.15) and
- shallow slope failure (Figure 2.14).

Hydraulic damage and failure types; figures based on Julien (2002) and complemented.

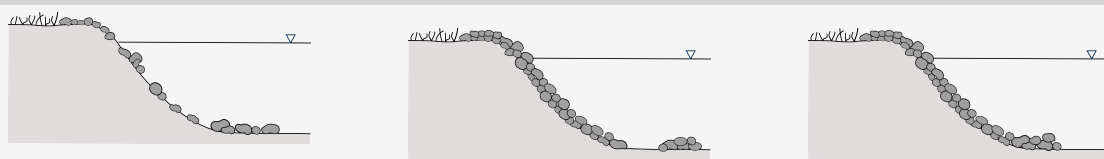


Figure 2.8: Erosion of the cover layer.

Figure 2.9: Scouring of the toe.

Figure 2.10: Scouring of the bed.

Geotechnical damage and failure types; figures based on Julien (2002) and complemented.

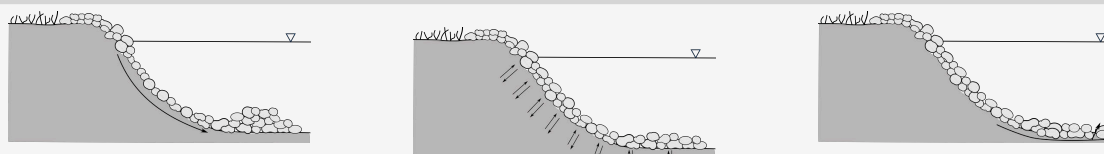


Figure 2.11: Sliding of the cover layer (local).

Figure 2.12: Liquefaction.

Figure 2.13: Failure of the toe support.

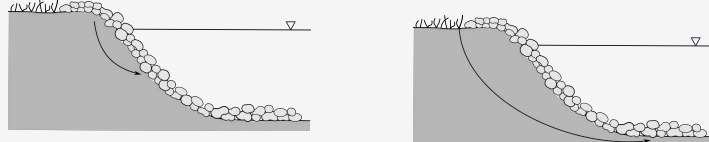


Figure 2.14: Shallow slope failure.

Figure 2.15: Deeper slope failure.

2.4.2 Causes of damage and failure

Damage is often a result of causes of damage listed below in combination with unfavourable circumstances, e. g. poor installation, passage of ships close to the bank or excessive speed. BAW reports (Fleischer and Kayser, 2006; Kayser, 2003, 2006, 2007a,b, 2008; Stein, 2008) mention hydraulic loads, pack ice, material ageing and vandalism as the most frequent causes of damage. A number of additional causes of damage are summarised by PIANC (1987a), Rock Manual (2007), Uliczka (2018) and USACE (1997). In summary, the following causes of damage and failure are identified:

- **Abrasion:** ice floes and debris, abrasive sediments and pack ice
- **Biological:** livestock, vermin, plant growth, seaweed and algae and microbes
- **Chemical:** oils and hydro-carbons, sulphates and other aggressive salts

- **Temperature:** frost heave, extremely low temperatures, high temperatures and freeze / thaw
- **Human action:** vandalism or theft, washing places and mooring of small crafts
- **Traffic:** ship / bank collision, dragging anchors and overdredging
- **Ultra-violet light** (sunlight)

Various guidelines such as PIANC (1987b, 2016) recommended fault tree analyses for a systematic review of failure mechanisms and reliability analyses of systems. Fault tree analyses illustrate the relationship between causes and events which may cause damage or failure of a structure. An example of such a fault tree, which is used as a basis for further investigations, is given in Figure 2.16. While macro stability mainly refers to global slope stability, micro stability encompasses various types of geotechnical failure. The displacement of armour stones, the hydraulic design, is of secondary importance and not considered in detail. Additionally, it is noted that not all of the above-mentioned causes of damage and failure as well as damage and failure mechanisms are included in the fault tree. The criticality of individual failure mechanisms is not evaluated. A connection between geotechnical and hydraulic failure mechanisms is established neither.

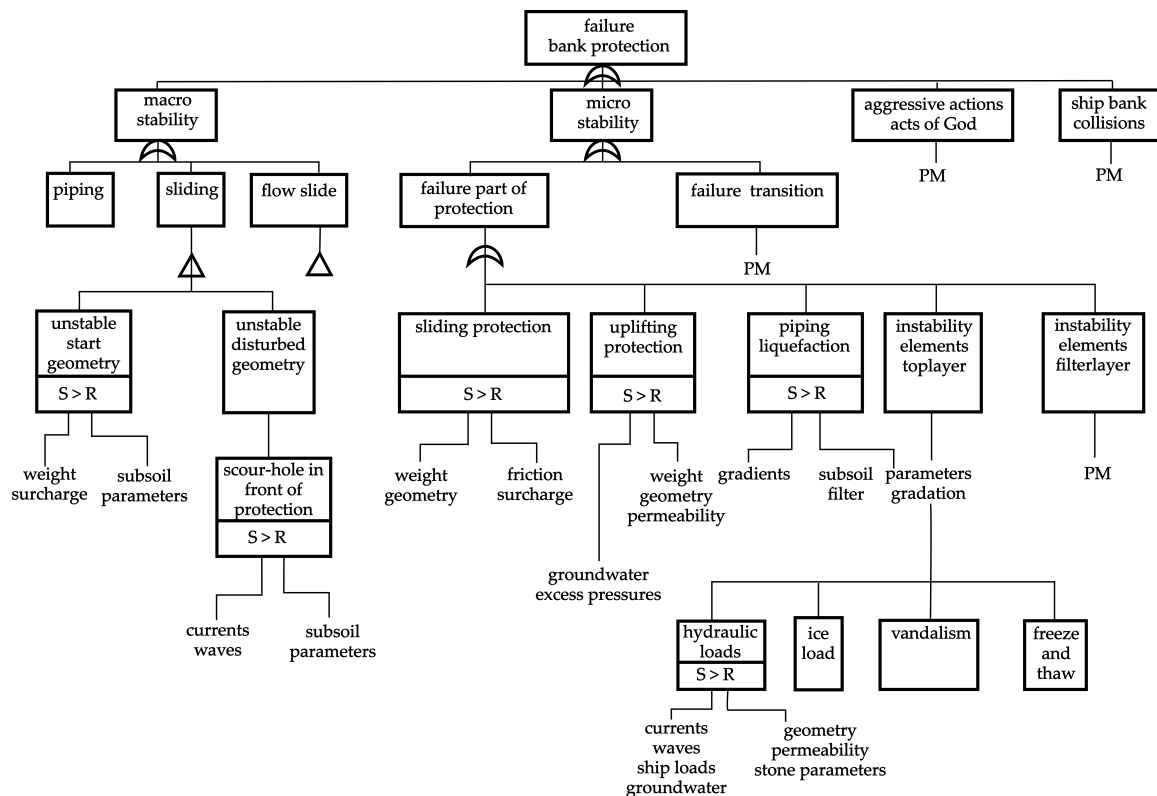


Figure 2.16: Fault tree for a bank protection; illustration based on PIANC (1987b, cf. p. 15).

2.4.3 Damage development

To allow for the definition of critical states of the revetment which may result in failure, a detailed observation of the course of damage and a damage classification is necessary. So far, there is no uniform definition of damage for armour stone revetments. Different classification approaches are followed in literature. A statement on the degree of damage can be

made on the basis of visual classification (Hedar, 1965; Kayser, 2015a; Ouellet, 1972), on the basis of the number of eroded stones (Font, 1970; Hudson, 1959; Thompson and Shuttler, 1975; van de Kreeke, 1969) or in relation to an eroded area (Broderick, 1983; Melby, 1999; van der Meer, 1988b). Often, these criteria are used as target values in a design, i. e. stability number N_S (Hudson, 1959) or dimensionless damage S_2 (Broderick, 1983; Pilarczyk and den Boer, K., 1983).

In the past, the development of damage was investigated by small-scale tests (Beyer, 2007; Daemrich et al., 1996; DST, 2006; Font, 1968; Hudson, 1959; Lee et al., 1987; Pilarczyk and den Boer, K., 1983; Pitt and Ackers, 1983; Thompson and Shuttler, 1975; Uliczka, 2018; van der Meer and Pilarczyk, 1984; Verheij and Bogaerts, 1989) and large-scale experiments (Ahrens, 1970; Bezuijen, Klein Breteler and Bakker, 1987; Gier, 2017; Köhler, 1985; Kreyenschulte, 2020; van der Meer, 1987; van der Meer and Pilarczyk, 1984; Westrich et al., 2003). These investigations mainly aimed at the development of design approaches for revetments, i. e. at the definition of a “failure point”, and less at the observation of the damage development. Minor to moderate armour stone displacements led to the termination of experiments. In addition, only few investigations (Uliczka, 2018; Verheij and Bogaerts, 1989) consider vessel-induced loads, which differ compared to coastal loads, e. g., by the angle of wave attack. A summary of relevant model tests and field investigations related to the design of revetments can also be found in Appendix A.2.

Figure 2.17 shows a model for the damage development of rock slopes and gravel beaches developed by van der Meer (1988b). Recent investigations confirm these findings (Sorgatz, 2019). The revetment stones move from the area exposed to waves towards the base of the slope. The upper edge of the slope rises slightly. An S-profile is formed. Additionally, an influence of storm duration, armour stone diameter and initial slope inclination is reported by van der Meer (1988b).

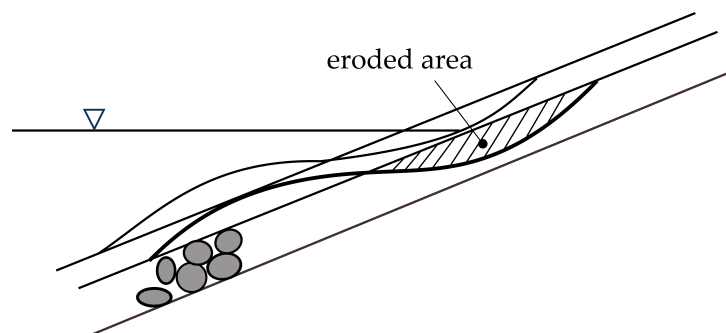


Figure 2.17: Damage development of rock slopes and gravel beaches; illustration based on van der Meer (1988b, cf. p. 21).

A mathematical description of damage development is introduced by Melby (2001), who outlines with eq. (2.6) a solution for cumulative damage S_d as a result of several storm events. Total damage is the sum of damages caused by n storms of different duration time t and mean wave period T_m for structures characterised by a stability number N_S ; b is a coefficient determined in experiments. Melby’s formula is only valid for a limited parameter range such as storm events of comparable strength, a slope inclination of 1:2 and structures with a rather impermeable core (Rock Manual, 2007). For the design equation of van der Meer (1988b), wave conditions, which cause equivalent damage, can be determined. Subsequently, the total number of waves is calculated and damage is computed for the total number of waves.

$$S_d(t_n) = S_{d0}(t_0) + 0.025 \frac{N_{s,n}^5}{T_{m,n}^b} (t_n^b - t_0^b) \quad (2.6)$$

2.4.4 Summary and critical evaluation

The literature review reveals that various types of damage and failure are observed for loose armour stone revetments. Besides hydraulic loads biological, chemical and other causes of damage are identified. However, often there is no clear distinction between damage and failure. Also, different terms are often used for the same type of damage. The course of damage is mainly described qualitatively. Studies describing damage development mathematically do not apply to revetment design.

With regard to Section 2.3, it must be noted that the current design equations only partially represent different failure mechanisms. For example, progressive failure due to the displacement of armour stones is neither from a hydraulic nor from a geotechnical point of view taken into account. This may lead to difficulties in describing and assessing appropriate limit states.

In general, few investigations consider vessel-induced loads which differ compared to coastal loads. Frequency and criticality of the individual damage patterns cannot be derived from previous investigations. This information, however, is required to draw conclusions about the nature of the limit state functions. So far, fault tree analyses only imply that hydraulic and geotechnical design may not describe equivalent limit state conditions.

Conclusions: Typical failure mechanisms, damage types and their causes are identified with the aid of literature. To specify the type of limit state associated with the design equations of revetment design, collected damages and failures must be evaluated with regard to their frequency and criticality at inland waterways. This may allow to specify limit states concerning revetments at inland waterways more precisely.

2.5 Methods of a probabilistic reliability assessment

The origins of a reliability-based design may be found in military-related aerospace engineering (AGREE, 1957; Lloyd and Lipow, 1962; US Department of Defense, 1987) promoted by high failure rates in military equipment during World War II. While at the beginning, reliability analysis mainly deals with systems featuring a large number of technical components, it is slowly adopted for the analysis of structures and structural components. As late as in the 1970s, reliability analysis starts to merge into structural engineering dealing with uncertainties that arise from limited information (Madsen and Egeland, 1989). Surely, pioneering in the field of reliability engineering is the work of Ang and Tang (1975, 1984) and Benjamin and Cornell (1976), who summarise methods of reliability analysis specifically for engineering applications.

It is beyond the scope of this thesis to provide a full background on mathematical definitions and methods applied in reliability-based engineering. This chapter aims to establish a common understanding of terminology and methods used in revetment design reliability-based engineering. Additional mathematical definitions are provided in Appendix B.

2.5.1 Conceptual definitions

Structural reliability

DIN EN 1990:2010-12 (2010) defines reliability as “ability of a structure or a structural member to fulfil the specified requirements, including the design working life, for which it has been designed. Reliability is usually expressed in probabilistic terms.” Thus, the reliability of a structure or component applies to the structural integrity, the serviceability and the durability in regard to the intended lifetime. Since failure refers to any situation where the structural performance during the service life is below the requirements, the corresponding definition of failure is broad. Failure can refer to a structural collapse in case of Ultimate Limit States (ULS) or an unsatisfactory behaviour in the case of Serviceability Limit States (SLS). In the context of ULS, reliability can therefore be interpreted as a measure of safety (Geißler, 2019).

Using the example of bank revetments, the structural reliability serves as a key figure to describe the probability of a revetment and its components meeting pre-defined specifications over the intended lifetime, even if deterioration or fatigue are encountered. A structural collapse may refer to the total failure of the slope, whereas an unsatisfactory behaviour may be reached when the functionalities of a revetment, i. e. protection of slope, ensure safety and ease of navigation on the waterway, are no longer met.

Reliability Index

Since structures are unique in nature and failure occurs due to the exceedance of a limit state function, the reliability of structures cannot be assessed through failure rates. Thus, models are established for resistances RE and actions LD , and the structural reliability is assessed through the probability of failure p_f , which is the complement of the reliability (Ditlevsen and Madsen, 2005). It describes the probability of the structure or system to perform unsatisfactory. Considering LD and RE as two independent stochastic variables with the density functions f_{LD} and f_{RE} and the distribution functions F_{LD} and F_{RE} , p_f is computed as follows:

$$p_f = P(RE \leq LD) = \int_{-\infty}^{\infty} P(RE \leq x)P(x \leq LD \leq x + dx)dx = \int_{-\infty}^{\infty} F_{RE}(x)f_{LD}(x)dx \quad (2.7)$$

A useful translation of the p_f into a more practical measure is the reliability index. The Cornell reliability index β_C , introduced by Cornell (1969), is given by mean μ_G and standard deviation σ_G of the joint probability density function (jpdf) of LD and RE . It is defined as

$$\beta_C = \frac{\mu_G}{\sigma_G} = \frac{\mu_{RE} - \mu_{LD}}{\sqrt{\sigma_{RE}^2 + \sigma_{LD}^2 - 2\rho_{RELD}\sigma_{RE}\sigma_{LD}}}. \quad (2.8)$$

As illustrated in Figure 2.18, eq. (2.8) describes the distance of the mean margin of the safety $G = RE - LD$ in terms of the standard deviation geometrically. The correlation coefficient ρ_{RELD} is zero for uncorrelated values. The definition of β_C depends on the distributions and the limit

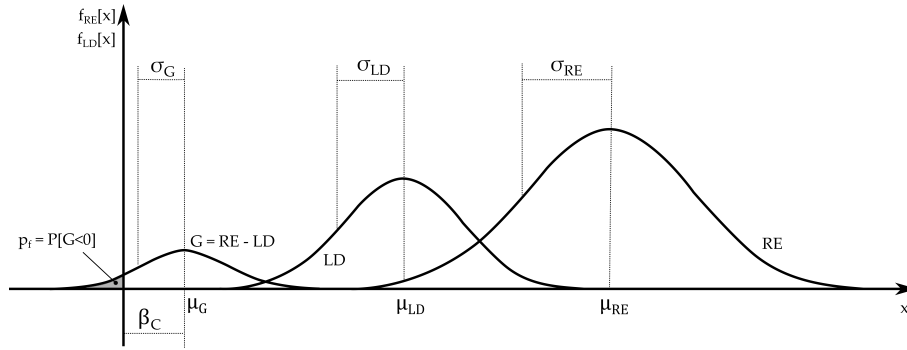


Figure 2.18: Probability of failure p_f and the Cornell reliability index β_C . Load and resistance are described by their mean, μ_{LD} and μ_{RE} , and standard deviation, σ_{LD} and σ_{RE} . Their difference yields the joint probability density function of the safety G , which is again characterised by its mean μ_G and standard deviations σ_G .

state function. Dependent variables increase the complexity of eq. (2.8) rapidly. Additionally, β_C varies for different representations of the limit state function.

To overcome the variability of β_C for different representations of the limit state function, Hasofer and Lind (1974) introduced a more comprehensive geometric definition of the reliability index by transforming independent Gaussian variables from physical space into a standard normal space U . As illustrated in Figure 2.19, the Hasofer-Lind reliability index β_{HL} is defined as minimum distance u^* between origin O and point P^* in U , see eq. (2.9). P^* corresponds to a point on the limit state function g where the probability density of the joint Gaussians is maximised. In physical space, P^* is also denoted as the design point. Assuming a Gaussian distribution, the p_f is obtained from β_{HL} by eq. (2.10) with Φ as the probability density function (pdf) of a Gaussian distribution in standard space.

$$\beta_{HL} = \|u^*\| \quad (2.9)$$

$$p_f \approx \Phi(-\beta_{HL}) \quad (2.10)$$

In the case of independent variables, the importance factors α_i , see eq. (2.11), are a measure for the relative contribution of the variance of each variable to the overall variance of the output. When considering dependent variables, the isoprobabilistic transformation, which is required to transfer the variables from physical to standard space, leads to importance factor which depend on the order of input (Lebrun, 2013). Thus, for correlated variables, importance factors only give an estimate of the contribution to failure, which should be reviewed cautiously.

$$\alpha_i^2 = \frac{(u_i^*)^2}{\sum_{i=1}^n (u_i^*)^2} = \frac{(u_i^*)^2}{\beta_{HL}^2} \quad (2.11)$$

2.5.2 Probabilistic methods

As discussed in JCSS (2001), methods of reliability assessment are sometimes resented arguing that data is scarce. Although this observation often holds true, when probabilities are under-

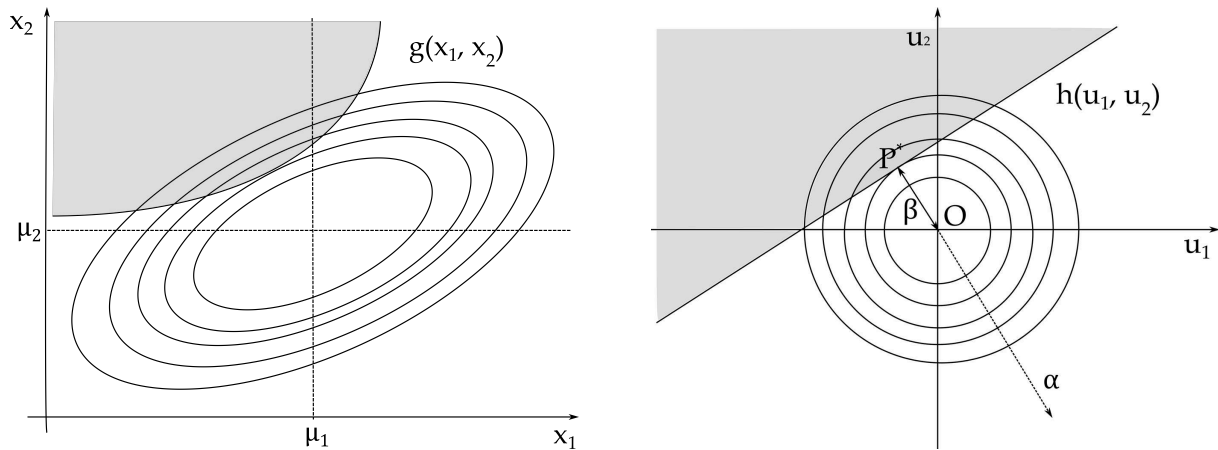


Figure 2.19: The physical space of the random variables x_1 and x_2 (left) and a representation of the Hasofer-Lind index in the standard space (right). The grey shaded area represents the ‘unsafe’ space; the white area the ‘safe’ space.

Table 2.3: Levels of reliability analysis (Teixeira, 2012).

Information	Reliability analysis level				
	0	I	II	III	IV
Hydraulic and/or geotechnical parameters	✓	✓	✓	✓	✓
Calculation method (deterministic)	✓	✓	✓	✓	✓
Design parameter (statistical basis)	x	✓	✓	✓	✓
Variability of parameters	x	x	✓	✓	✓
- mean and standard deviation	x	x	✓	✓	✓
- pdf	x	x	x	✓	✓
Costs	x	x	x	x	✓
Type of analysis	Global FoS ⁽¹⁾	Partial factors	FORM ⁽²⁾	MCS ⁽³⁾	Risk

⁽¹⁾ Factor of Safety

⁽²⁾ First Order Reliability Method

⁽³⁾ Monte-Carlo simulations

stood in the Bayesian way, they are suitable for decision making processes. The reliability assessments allow to generate comparable key figures which can assist in an effective and risk-informed assessment of the condition of existing structures, and, thus, the organisation of maintenance measures. The methods of a probabilistic reliability assessment are differentiated by their complexity and accuracy as shown in Table 2.3. Increasing accuracy requires an increasing computational effort. In the practical applications, thus, a trade-off between accuracy and computational efficiency is sought.

Deterministic approach (Level 0)

Level 0 analysis are fully deterministic solutions. The safety of the structure is investigated using single characteristic values of actions and material parameters. Characteristic values of these basic variables may be established by (statistical) data analysis. However, no information

regarding p_f are inferred. The targeted level of safety depends solely on the choice of characteristic values. Examples of deterministic approaches can be found in present design standards (GBB, 2010; Rock Manual, 2007; USACE, 1997).

Semi-probabilistic methods (Level I)

Semi-probabilistic methods do not calculate p_f , but account for uncertainty and variability of basic variables and design models by means of design values, partial factors and other additive quantities (ISO 2394:2015-03, 2015).

The partial factor approach is the current normative design approach (DIN EN 1997-1:2014-03, 2010) aiming to bridge the probabilistic and the deterministic design approach (Prästings et al., 2019; Schuppener and Heibaum, 2012). Partial factors are applied to characteristic values of actions and material parameters to account for the uncertainty of input values. At present, the partial factors are defined in the National Annexes and mainly calibrated to maintain the safety level of the previous global safety concept (Schuppener and Heibaum, 2012).

Characteristic values are “selected as a cautious estimate of the value affecting the occurrence of the limit state” (DIN EN 1997-1:2014-03, 2010). The selection of the characteristic values is either based on expert knowledge or statistical methods.

“If statistical methods are used, the characteristic value should be derived such that the calculated probability of a worse value governing the occurrence of the limit state under consideration is not greater than 5 %” and

“NOTE: In this respect, a cautious estimate of the mean value is a selection of the mean value of the limited set of geotechnical parameter values, with a confidence level of 95 %; where local failure is concerned, a cautious estimate of the low value is a 5 % fractile.” (DIN EN 1997-1:2014-03, 2010).

The first paragraph of the above definition implies that characteristic values are chosen in a way which leads to p_f of the structure smaller than 5 % (before application of partial factors). The second paragraph specifies the appropriate choice of the characteristic value with respect to the failure mode (Hicks, 2012). Prästings et al. (2019) observe that DIN EN 1997-1:2014-03 (2010) refers to two different characteristic values; one which addresses local failure and which shall be selected as the 5 % quantile of the probability function of the variable and another which addresses non-local failure, which shall be a selection of the mean value with 95 % confidence level. While the former represents a small volume of the soil, the latter accounts for a larger volume of soil allowing for averaging. In the case of slope stability, the failure which governs the design and, thus, the choice of characteristic values is strongly affected by the spatial correlation structure of the soil.

Approximate probabilistic methods (Level II)

Approximate probabilistic methods replace characteristic values and partial factors by probability functions. With these probability functions as input, the exceedance of g is evaluated resulting in an approximate p_f . Several methods are available to approximate p_f and β_C or β_{HL} . The most common are:

The First Order Second Moment (FOSM) uses the first terms of the Taylor series expansion of the limit state function g to determine β_C . Assuming uncorrelated variables X_1, X_2, \dots, X_n with values x and their correlation $\rho_{X_i X_j} = 0$, β_C is obtained as quotient of the expected value E given g and its standard deviation σ_g :

$$E[g] = \mu_g \approx g(X_1, X_2, \dots, X_n) \quad (2.12)$$

$$\sigma_g^2 \approx \sum_{i=1}^n \sum_{j=1}^n \frac{\partial g}{\partial x_i} \frac{\partial g}{\partial x_j} \rho_{X_i X_j} \sigma_{X_i X_j} \quad (2.13)$$

$$\beta_C = \frac{E(g) - 1}{\sigma_g} \quad (2.14)$$

FOSM assumes that the factor of safety is normally distributed. It inherits the same drawbacks as β_C (see Section 2.5.1), which depends on the distributions and the limit state function. Furthermore, it is not invariant to the definition of the limit state function (Baecher and Christian, 2003).

The Point Estimate Method (PEM) was proposed by Rosenblueth (1975). It approximates p_f by replacing continuous variables by discrete random variables whose probability mass function (pmf) has the same moments as the pdf of the continuous variables. A major drawback of the PEM is the rapidly increasing number of computations for the multivariate case. In the original formulation of Rosenblueth (1975), the number of simulations N is an exponential function of the number of variables \bar{n} with $N = 2^{\bar{n}}$. Additionally, as illustrated by Christian and Baecher (1999), the accuracy of the PEM decreases with increasing variance of the variables.

The First Order Reliability Method (FORM)

was introduced by Hasofer and Lind (1974). In standard space, β_{HL} is defined as minimum distance between the design point P^* and the origin O , where P^* is a point on the limit state surface characterised by the maximum probability density (see Section 2.5.1). FORM solves a constrained optimisation problem approximating the minimum distance through linearization in the design point. The approximation can be conducted with several methods such as Lagrangian Multiplier, Taylor Series or the Fiessler-Rackwitz approach (Abdo and Rackwitz, 1991; Rackwitz and Fiessler, 1978). For other than Gaussian distributions, the Rosenblatt transformation (Rosenblatt, 1952) or the Nataf transformation (Nataf, 1962) allow to transform the distributions into standard space. Correlated variables can be incorporated, e. g. by means of the Cholesky matrix or eigenvectors and eigenvalues (Baecher and Christian, 2003). Low and Tang (1997, 2004) proposed an interpretation of the reliability index in elliptical space, which thus does not require a transformation into normal space. FORM is based on the assumption that the design point is a unique point in standard space. This may lead to erroneous results, in particular for highly non-linear limit state functions.

The Second Order Reliability Method (SORM) is an extension of FORM which uses quadric or paraboloid approximation functions (Breitung, 1984; Der Kiureghian, Lin et al., 1987; Der Kiureghian and Thoft-Christensen, 1991; Fiessler et al., 1979). Although commonly more expansive in computational terms, SORM can give more accurate solutions in case of highly non-linear limit state functions.

Simulation-based probabilistic methods (Level III)

Level III methods compute p_f numerically Monte-Carlo simulations (MCS). They originate from the research on nuclear technology during the Second World War, where it was developed to describe neutron diffusion (Fermi and Richtmyer, 1948; Metropolis, Rosenbluth et al., 1953; Metropolis and Ulam, 1949). MCS are commonly applied to mathematical problems whose analytical solutions are tendentious or impossible.

By generating a set of discrete values from a jpdf of all random variables \mathbf{x} , the problem can be solved analytically. This procedure is repeated for N independent realisations. Several sampling algorithms such as the Wichmann-Hill algorithm (Wichmann and Hill, 1982) and the SIMD-Oriented Fast Mersenne Twister algorithm (Saito and Matsumoto, 2008) are used. Based on the simulation statistics, p_f is derived via the indicator function I which compares the simulation results to the failure domain defined with respect to g as follows:

$$I = \begin{cases} \text{stable (0),} & \text{if } g(\mathbf{x}) \geq 0. \\ \text{unstable (1),} & \text{if } g(\mathbf{x}) < 0. \end{cases} \quad (2.15)$$

As a result, p_f is calculated from the number of failures relative to the overall N :

$$p_f = p[I = 1] \approx \frac{1}{N} \sum_{i=1}^N I_i \quad (2.16)$$

Following the Central Limit Theory, the sample average approaches a true value as $N \rightarrow \infty$. Monte Carlo simulations thus rely heavily on the number of simulations performed. The accuracy of the method increases with the number of samples. Assuming a Gaussian distribution of the output, a maximum error $\epsilon = 0.0001$ and $p_f = 0.001$ the number of required MCS is calculated as follows:

$$N_r = p_f \cdot (1 - p_f) \left(\frac{u_{0.1/2}}{\epsilon} \right)^2 = 0.001 \cdot 0.999 \left(\frac{1.645}{0.0001} \right)^2 = 270332 \quad (2.17)$$

where $u_{0.1/2} = 1.645$ is the z-score of the standard Gaussian distribution at $P[U > u_{0.1/2}] = 0.1/2$ for a two-sided significance level of 10 % (Arnold, 2016; Fenton and Griffiths, 2008).

In particular for small probabilities of failure, the classical MCS is computationally expensive. Hence, a number of methods requiring less realisations while achieving the same accuracy such as directional simulation (Ditlevsen, Bjerager et al., 1988), importance sampling (Kahn and Marshall, 1953), adaptive sampling (Bucher, 1988), Latin Hypercube Sampling (LHS) (McKay et al., 1979) and subset simulation (Au and Beck, 2001, 2007) has been developed. These methods reduce the variance of the output by using information from previous realisations or approximate techniques (Baecher and Christian, 2003).

2.5.3 Limit states and target reliabilities

Limit states describe states “beyond which a structure no longer satisfies the design criteria” (ISO 2394:2015-03, 2015, p. 6). As commonly accepted in engineering, actions, environmental

influences, properties of material and geometrical properties of a system are assessed with “reference to a specified set of limit states which separate desired states of the structure from adverse states” (JCSS, 2001, p. 4).

According to Eurocode standards and Rock Manual (2007), the design of a structure should include the assessment of load bearing capacity (ULS) and serviceability (SLS) conditions. In contrast to that, GBB (2010) does not clearly differentiate between different limit states. Both design types, the hydraulic and the geotechnical design, are evaluated with respect to ULS; although, the empirical factors which are employed in the hydraulic design may be considered as relaxation of the ULS since they account for different damage and maintenance efforts. Rock Manual (2007) defines ULS and SLS conditions only for the geotechnical design.

A clear categorisation of limit states which applies to the geotechnical and hydraulic revetment design is proposed by Oumeraci et al. (1999) and PIANC (1987b), who propose an extension of the limit states specified in DIN EN 1990:2010-12 (2010) and DIN EN 1997-1:2014-03 (2010). The following four types of limit states are specified:

(1) Ultimate Limit State (ULS):

“corresponds to the ultimate load bearing capacity, collapse or instability of single elements, transformation into other failure mechanisms, etc.” (PIANC, 1987b, p. 10).

(2) Progressive collapse limit state (PCLS):

“corresponds to a state in which accidental loss or overloading of single elements may produce in the structure, or major parts of it, a condition in which progressive failure could take place. This state could occur when the stability of elements in a bank protection (riprap or concrete stones) is based on the supporting reactions of neighbouring elements and one of these elements fails” (PIANC, 1987b, p. 10).

(3) Serviceability Limit State (SLS):

“corresponds to, for example, excessive deformation or (cyclic) motion without loss of equilibrium, durability etc.” (PIANC, 1987b, p. 10).

(4) Fatigue criterion (FLS):

“corresponds to the occurrence of a large number of normal or accidental events which have cumulative damaging effects” (PIANC, 1987b, p. 10).

The reliability of the structure at ULS and/or SLS condition is compared to the target reliability. The target reliability is a “specified average acceptable probability of failure that is to be reached as close as possible” (ISO 2394:2015-03, 2015, p. 5). JCSS (2001) refers to target reliabilities as “appropriate levels of reliability” which suit the use of the structure, the type of structure and the design situation. Target reliabilities allow to relate the condition of a structure to the consequence associated with a failure in terms of damage, cost or loss of life. Consequences of failure, the effort required for risk reduction and the lifetime of the structure should be taken into account (JCSS, 2001).

According to PIANC (2003) and Vrijling (1999), target reliabilities over the entire lifetime of vertical breakwaters are categorised by their limit state and safety class and range between 0.05 and 0.40 (see Table 2.4). These target values for breakwaters are confirmed by the investigation of various failure mechanisms and additional parameter studies in the context of a life cycle analysis (PIANC, 2016).

Although Chowdhury and Flentje (2003) distinguish between five risk categories, the annual target reliabilities they propose for natural slopes roughly agree with the above outlined values of PIANC (2003, 2016) and Vrijling (1999). Since Chowdhury and Flentje (2003) refer to natural slopes, they solely provide ULS target reliabilities. Christian, Ladd et al. (1994) assume increasing consequences with the increasing height of dikes. They propose annual probabilities of failure from 0.01 ($\beta_{HL} = 1.63$) for dikes of 6 m height to 0.0001 ($\beta_{HL} = 1.43$) for dikes of 23 m height, always with respect to ULS conditions.

Table 2.4: Indicative values of acceptable (maximum) probabilities of failure within structure lifetime (PIANC, 2003).

Limit State	Safety class			
	Very low	Low	Normal	High
SLS	0.40	0.20	0.10	0.05
ULS	0.20	0.10	0.05	0.01

The Joint Committee on Structural Safety (JCSS, 2001) defines annual target reliabilities for ULS and SLS (see Table 2.5). The consequences are incorporated by dividing the classification into three consequence classes. USACE (1999) proposes target reliabilities for geotechnical structures with respect to the ultimate limit state (see Figure 2.20). The target reliabilities relate verbal condition descriptions to p_f and β_{HL} values. They mainly apply to major rehabilitation projects, flood damage reduction studies and levee planning studies.

Table 2.5: Target reliability indices β_{HL} (and associated probabilities of failure) related to one year reference period; ULS and SLS (JCSS, 2001).

Relative cost of safety measure	Ultimate Limit State (ULS)			Serviceability Limit State (SLS)	
	Minor consequences of failure	Moderate consequences of failure	Large consequences of failure	Relative cost of safety measure	Target index (irreversible SLS)
Large (A)	$\beta_{HL} = 3.1$ ($p_f \approx 10^{-3}$)	$\beta_{HL} = 3.3$ ($p_f \approx 5 \cdot 10^{-3}$)	$\beta_{HL} = 3.7$ ($p_f \approx 10^{-4}$)	High	$\beta_{HL} = 1.3$ ($p_f \approx 10^{-1}$)
Normal (B)	$\beta_{HL} = 3.7$ ($p_f \approx 10^{-4}$)	$\beta_{HL} = 4.2$ ($p_f \approx 10^{-5}$)	$\beta_{HL} = 4.4$ ($p_f \approx 5 \cdot 10^{-6}$)	Normal	$\beta_{HL} = 1.7$ ($p_f \approx 5 \cdot 10^{-2}$)
Small (C)	$\beta_{HL} = 4.2$ ($p_f \approx 10^{-5}$)	$\beta_{HL} = 4.4$ ($p_f \approx 5 \cdot 10^{-6}$)	$\beta_{HL} = 4.7$ ($p_f \approx 10^{-6}$)	Low	$\beta_{HL} = 2.3$ ($p_f \approx 10^{-2}$)

Conclusions: It was found that literature specifications regarding limit states and corresponding target reliabilities are transferable to geotechnical design of revetments which may refer to an ultimate limit state. The type of limit state assessed in the hydraulic design is not clearly specified. Since the criticality of damage is closely associated with its detectability and maintainability, it must be evaluated which types of damage are frequently observed and whether and when damage endangers stability. Based on this, corresponding target reliabilities can be selected.

2.5.4 Summary and critical evaluation

In literature, a number of probabilistic methods have been described and applied to the analysis of hydraulic structures. As almost for any other methods, increasing accuracy of the results requires an increasing computational effort and a broader data basis.

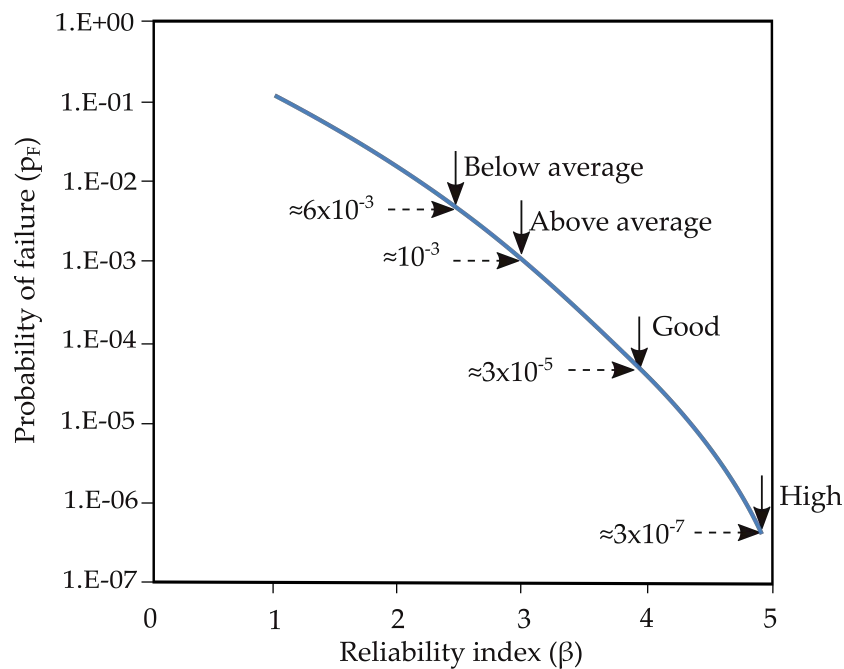


Figure 2.20: Target reliabilities for risk-based analysis in geotechnical engineering related to the condition of a construction; diagram based on USACE (1999, cf. p. B-138).

Although, the popularity of reliability-based methods seems to grow lately, it should be noted that the application of reliability-based methods in engineering has also been subject of fundamental criticism. As discussed in Schuppener and Heibaum (2012), a number of arguments have been forwarded against reliability-based methods such as the lack of data, ignoring human error and the limited ability to oversee to complete geotechnical design. On the other hand, advantages of probabilistic design methods include the consideration of the stochastic nature of input parameters such as material properties and hydraulic loads, the consideration of uncertainty in design models, the possibility to include different sources of information and update uncertainty estimates when introducing additional information. Moreover, probabilistic design methods allow to gain a better insight into the interaction of complex systems and the contribution of different sources of uncertainty to a final design, i. e. Baecher and Christian (2003), Kortenhaus (2003), Phoon (2004, July 9) and Phoon, Ching and Wang (2019).

Conclusions: The results of the literature analysis show that different methods to determine the probability of failure or reliability of a structure are available. They have already been successfully applied to various engineering problems. However, in the case of highly non-linear limit state functions, Level II procedures may cause difficulties. Within this thesis, Level III analyses are thus favoured. Additional investigations are conducted to evaluate the suitability of Level II analyses for probabilistic revetment design.

2.6 Revetment design under uncertainty

2.6.1 Reliability-based design of hydraulic structures

First recommendations regarding a probabilistic assessment concept of shore protection structures can be found in the Netherlands. Triggered by a severe storm event (31 January – 1 February 1953), van Dantzig (1956) presents a probabilistic approach for the geotechnical design of flood defence systems. In 1980, Bakker and Vrijling (1980) publish a first concept for the probabilistic design of sea defence structures (dikes and dunes). In 1984, Mol et al. (1984) first describe a probabilistic design concept for breakwaters which considers both the geotechnical and the hydraulic design. For the hydraulic design, Mol et al. (1984) investigate the probability of certain damage levels instead of a probability of failure of the structure. Barends and van Dijk (1985) provide a guideline for the probabilistic, computer-aided geotechnical design of breakwaters. The concept of van der Meer (1988a) employs a revised version of the Hudson (1959) equation with a probabilistic design approach to assess the probability of failure of rubble mound breakwaters over their lifetime. Again, different damage levels are assessed. In 1997, Vrijling and van Gelder (1997) extend the approach by van der Meer (1988a) towards maintenance. They present different methods to determine the probability of failure and subsequently, the evolution of damage by means of Monte-Carlo simulations (MCS). The evolution of damage itself is described by an empirical equation, which is derived from field tests.

Bruining (1994) and Christiani (1997) both propose probabilistic design concepts for vertical breakwaters. A detailed guideline for vertical breakwaters is provided by the project PRObabilistic design tools for VERTical BreakwaterS (PROVERBS), which ran from February 1996 to January 1999. Relevant failure modes and parameters for a reliability-based design of vertical breakwaters are assessed, acceptable probabilities of failure and a partial factor system are defined (Vrijling, 1999).

Upon the reliability concept of Vrijling (1993), which establishes new standards for the design of flood defences, Voortman (2003) proposes a general framework for a risk-based design applicable to large-scale flood defence systems. Classical reliability analysis is combined with optimisation algorithms in order to identify a cost-effective design under the constraint of required protection levels. At about the same time, Kortenhaus (2003) outlines a probabilistic design concept for German North Sea dikes. Similar to Vrijling (2001), he assesses the different failure mechanisms related to dike failure and merges them in a fault-tree-analysis to determine the joint probability of failure.

In 2007, the FLOODsite project is initiated. Within this framework, various investigations focusing on the reliability of coastal structures in case of flood events are conducted by a European consortium of different research institutions. Amongst others, the influence of uncertainties on the reliability of flood defence systems (Kanning, 2007), the reliability of flood and sea defence structures and systems (van Gelder, 2009) and the determination of hydraulic loads by means of the extreme value theory (Sánchez-Arcilla et al., 2010; van Gelder and Mai, 2008) are assessed. Also, in the late 2000s, the reliability analysis of coastal structures is extended to a time-dependent analysis taking into account a deterioration process of the structure (Buijs et al., 2009; van Noortwijk et al., 2007).

Starting approximately ten years ago, the hydraulic (Jafarnejad, Pfister, Brühwiler et al., 2017; Jafarnejad, Pfister and Schleiss, 2012) and geotechnical stability (Möllmann, 2009; Pham Quang

et al., 2010; Weißmann, 2014) of river and canal embankments has been investigated. The investigations focus on flood events and waterways subjected to natural flow. So far, ship-induced loads have not been considered.

Conclusions: The literature study reveals that on an international level, probabilistic methods have already been applied at the interface of hydraulic and geotechnical engineering. They are used in particular when actions are of predominately stochastic nature such as wave events and water levels during a storm surge. In contrast, there is hardly any experience in the probabilistic design of revetments at inland waterways. It should thus be examined to what extent probabilistic methods provide information for design and condition assessment of revetments. Therefore, input parameters, their distributions and correlations must be specified. Different types of uncertainty should be considered.

2.6.2 Definition and sources of uncertainty

The term *uncertainty* refers to any imprecision regarding a model parameter, but also regarding the model itself (COST WG 1, 2019). Although various classifications of uncertainties exist, i. e. (COST WG 1, 2019; ISO 2394:2015-03, 2015; JCSS, 2001), the most common is the differentiation into *aleatory* and *epistemic* uncertainty introduced by Hacking (1975). *Aleatory uncertainty* refers to an inherent uncertainty due to natural variability such as a variation of soil properties and load intensity, while the *epistemic uncertainty* describes a lack of knowledge caused by limited, insufficient or imprecise data or models. *Epistemic uncertainty* can be reduced by additional measurements or advanced models, e. g. Baecher and Christian (2003) and Phoon, Prakoso et al. (2016). A third category of uncertainties are the so-called “unknown unknowns” which refer to unidentified aleatory and epistemic uncertainties. It is stressed that a clear categorisation of uncertainties inherent to a design is impossible, as all types of uncertainty contribute to the total uncertainty and depend on the context of application (Der Kiureghian and Ditlevsen, 2009). For instance, human impact can be both aleatory and epistemic uncertainty - often as “unknown unknowns”.

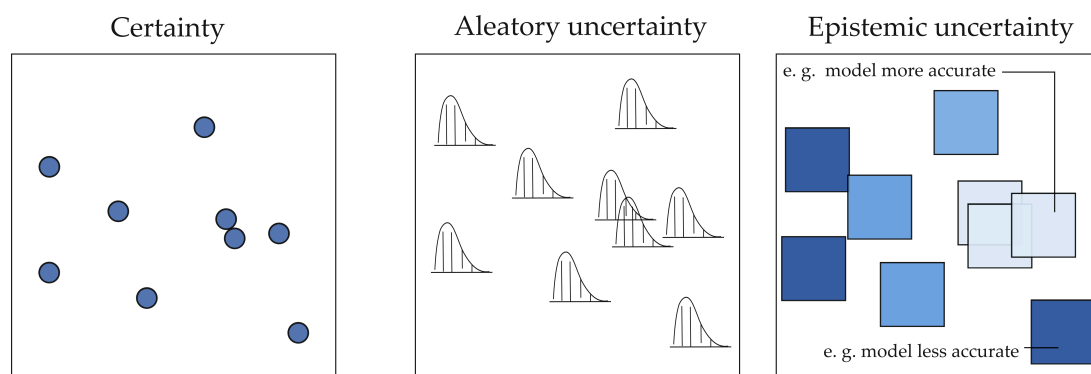


Figure 2.21: Visualisation of types of uncertainty. *Aleatory uncertainty* represents the intrinsic uncertainty of the material, whereas *epistemic uncertainty* describes the lack of knowledge. For instance, the different shaded rectangles indicate that models ‘generate’ less uncertainty in a specific range; illustration adapted from Hou et al. (2019) and complemented.

The difference between aleatory and epistemic uncertainty is often related to the different interpretation of the probability as frequency and subjective probability. While the former, the Frequentists’ approach, understands the probability as “frequency with which things occur in a long series of trials”, the latter, referred to as Bayesian probability, understands probability as

the “degree of belief” (Baecher and Christian, 2003, p. 65). In the Bayesian sense, “probability is our best estimate of what would occur in a certain number of imagined observations; it depends, therefore, on our knowledge and our ability to make estimates, and for this reason, it is always subjective and based on our common sense” (Marsili, 2018, p. 24).

The notion of probability substantially affects how data are analysed and what conclusions can be drawn from the analyses (Baecher and Christian, 2003). Although, in some cases, the distinction is vague; for instance, the epistemic uncertainty can also be assessed in a frequentist manner with methods such as bootstrapping, which is a common non-parametric method for the assessment of errors in a statistical estimation problem. For large data, the Bayesians’ interpretation of probability coincides with that of the Frequentists’ (ISO 2394:2015-03, 2015). The presented analyses address uncertainty predominantly from a Frequentist point of view, since it intends to assemble basics for a reliability-based revetment design. However, it is recommended to employ the findings of this thesis in Bayesian analyses in the future. Bayesian statistics allow to deal with the vagueness associated with the statistical model by engaging different sources of information. Initial estimates, e. g. based on expert knowledge or previous investigations, can be supplemented by additional data from new measurements through Bayesian inference, which may allow to reduce the number of required measurements or the uncertainty associated with basic variables.

The uncertainty inherent to the design of hydraulic structures is the result of the uncertainties of the parameters and the design model. If not considered in the design process, any of these uncertainties can bias the reliability of a structure. Figure 2.22 illustrates the sources of uncertainty schematically.

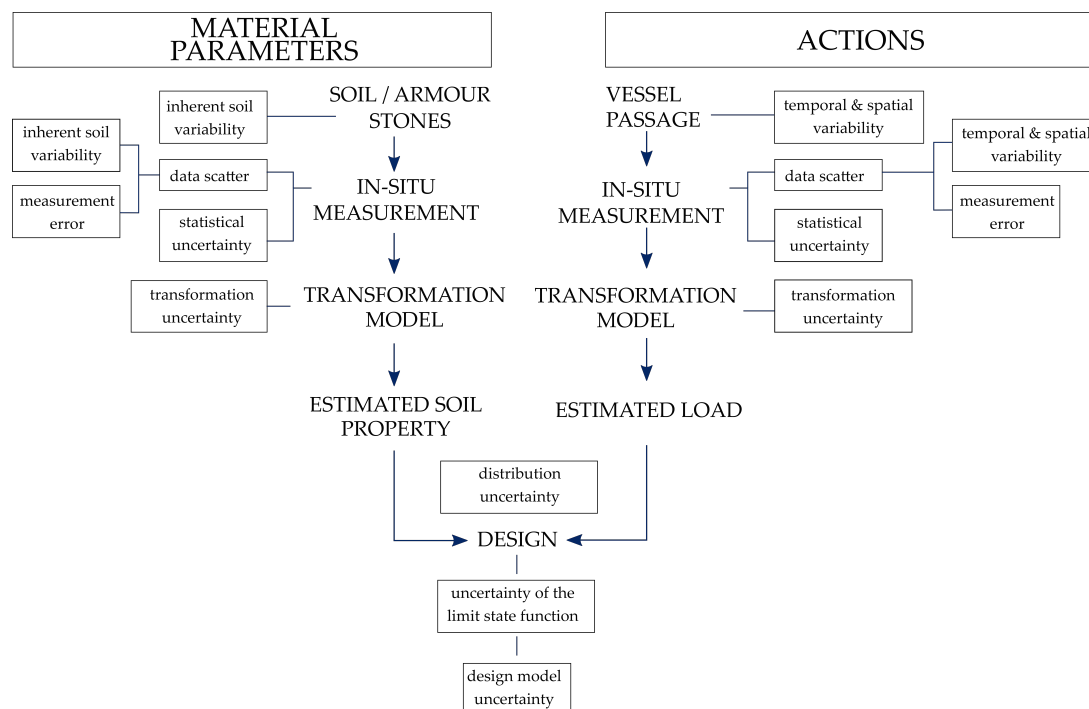


Figure 2.22: Sources of uncertainty contributing to the total uncertainty of revetment design; illustration adapted from ISO 2394:2015-03 (2015, cf. p. 72) and supplemented.

Uncertainty of hydraulic parameters comprises (1) the spatial variability, (2) variability over time, for example due to seasonal and usage-related changes in traffic, (3) measurement error,

(4) statistical uncertainty and (5) transformation error. Primary sources of uncertainty of material parameters are (1) natural (inherent) variability, (2) measurement error, (3) statistical uncertainty and (4) transformation error (Phoon and Retief, 2016). The natural (inherent) variability results mainly from the genesis of soil, which is not a standardised pre-fabricated material such as steel or concrete, but made of different materials by various physical, chemical and biological processes. The interaction of climate, relief, organisms and the initial rock material (magmatic, sedimentary or metamorphic) leads to inhomogeneity and anisotropy of soil. Statistical uncertainty is a result of limited information such as a limited number of field observations or soil strength values from laboratory tests (DNVGL-RP-C207:2017-05, 2017). Additionally, when fitting a parametric distribution to limited data, the parameters of the distribution are of random nature. This uncertainty is also referred to as statistical uncertainty; it decreases with the number of observations (Oumeraci et al., 1999). The transformation error arises when values measured through field or laboratory tests are transferred to material properties by means of expert knowledge, empirical or other correlation models.

In addition, it is stressed that the design models that allow to determine the required armour layer thickness and mean armour stone diameter inhibit model uncertainty, which is mainly a result of the underlying empirical equations and correlations.

The relative contribution of the sources of uncertainty to the total uncertainty of the design depends, amongst others, on site-conditions, available testing equipment and its accuracy (Phoon and Retief, 2016). However, as Christian, Ladd et al. (1994) point out, different sources of uncertainty have different implications on the stability of a structure. A 1 % probability of failure which results from spatial variability alone indicates that, on average, 1 % of the length of, e. g., a dike would fail. In contrast, a 1 % probability of failure resulting from model or statistical uncertainty - Christian, Ladd et al. (1994) refer to it as *systematic* error - implies that, on average, one out of 100 of similar structures would fail completely.

2.6.3 Parameter uncertainty

Uncertainty inherent to actions

Statistical uncertainty

Although PIANC (1987a) states that load-effects, which are the effects of ship or wind-induced water motion, have a random character, so far, little information is available on statistical uncertainty of characteristic ship-induced loads. Most experience and data for a probabilistic description of hydraulic loads is available from coastal engineering. Often, statistical and model uncertainty are considered as a single parameter and estimated subjectively (PIANC, 1989; Schüttrumpf et al., 2008).

Hussaarts et al. (1999), Kortenhaus (2003) and PIANC (1989, 1992a) suggest approximating the significant wave height by a Gaussian probability density function; van Gelder (2000), van Gelder and Mai (2008) and Vrijling (1993, 2001) propose the application of the extreme value theory and the corresponding distributions such as the Generalized Pareto function and the Generalized Extreme Value function. Moreover, van Gelder (2000) and Vrijling and van Gelder (1998) investigate the effects of distribution uncertainty on the reliability of flood protection. They conclude that with an increasing number of observations and assuming an undamaged structure, the uncertainty and, thus, the probability of structural failure decreases. PIANC (1992a) presents a detailed analysis of uncertainty related to environmental data required for

breakwater design such as wave heights. Expert surveys conducted by Schüttrumpf et al. (2008) supply standard deviations σ for the significant wave height, which range depending on observation method and observed structure between $2.2 \leq \sigma \leq 5.5$. Investigations of the significant wave height in shallow water indicate that nearshore wave heights are characterised by larger variability than wave heights of offshore sea waves (PIANC, 1992a). Rock Manual (2007) recommends Gaussian distributions with corresponding mean values and standard deviations for the constants in the equations of van der Meer (1988b).

Uncertainty of currents is commonly associated with the flow in rivers (Froehlich and Benson, 1996; Jafarnejad, Pfister, Brühwiler et al., 2017; Jafarnejad, Pfister and Schleiss, 2012). However, the transferability of these results to revetment design is even more debatable than for wave heights obtained from coastal engineering.

Spatial variability

While for the design of coastal protection structures, i. e. dikes, the consideration of spatial variability of extreme loads is of high importance (Fröhle, 2000), the spatial variability of extreme loads plays a minor role for revetment design at inland waterways. Hydraulic loads along inland waterways vary as a result of changes in geometry of the waterway and driving behaviour of the vessels. A precise statement on the spatial variability of hydraulic loads is impossible on the basis of available literature and data. The selection of representative observation locations can reduce spatial variability. For example, curves or areas in the vicinity of berths and ports are not suitable as observation locations, as the driving behaviour of ships deviates significantly from the behaviour on regular canal or river stretches.

Transformation uncertainty

Transformation uncertainty of hydraulic loads results from the transformation of observed vessel passages with parameters such as velocity, passing distance and vessel geometry to actual hydraulic loads, i. e. waves, currents and drawdown. Various standards such as GBB (2010) and Rock Manual (2007) provide a number of design equations to ascertain the actions on banks resulting from passages of typical inland navigation vessels (e. g. motorised freight vessels, pushed barge units, sport boats) in stationary movement parallel to the bank and for few simplified cross-section geometries. In order to solve these equations, a number of assumptions and simplifications are required, which are passed to the transformation uncertainty. To the knowledge of the author, transformation uncertainty inherent to these calculations has not been investigated yet.

Uncertainty inherent to material parameters

Statistical uncertainty

JCSS (2006, p. 4) distinguishes the statistical uncertainty of geotechnical parameters into “inaccurate statistics of soil property distributions (continuum parameters and continuous soil layer boundaries)” and “potential errors in soil stratigraphy (e. g. missing local phenomena, anomalies)”. While the latter is a purely site-specific issue, the point statistics (μ , σ & cov) of different soil types have, despite their local uniqueness (Phoon, Ching and Wang, 2019), been investigated on a more generalised basis. They have been gathered by various authors in conjunction with particular applications, e. g. Arnold (2016), JCSS (2006), Lacasse and Nadim (1996), Lumb (1966, 1974), Phoon and Kulhawy (1999a,b), Phoon, Prakoso et al. (2016), Rawls et al. (1982),

Schultze (1972) and Uzielli, Lacasse et al. (2006) and summarised in standards and reports, e. g. Arnold (2016) and JCSS (2006).

Armour stone characteristics are defined by present standards (DIN EN 13383-1:2015-07 - Entwurf, 2010; DIN EN 13383-2:2017-03-Entwurf, 2010; TLW, 2003). While for newly constructed revetments, statistical uncertainty of armour stone characteristics is limited (Sorgatz, Kayser and Schüttrumpf, 2018), for existing structures there is a purely site-specific issue which, amongst others, requires a thorough study of maintenance reports.

Spatial variability

Vertical and horizontal variability of soil properties is caused by a combination of geologic, environmental and physical-chemical processes (ISO 2394:2015-03, 2015). To date, information on the spatial correlation structure of soil properties is sparse. Few studies such as Fenton (1999a,b), ISO 2394:2015-03 (2015), Jaksa (1995) and Uzielli, Vannucchi et al. (2005) indicate a wide range of values depending on soil type and soil property.

Typically, random fields are employed to accomplish an appropriate representation of the spatial correlation structure defined by the scale of fluctuation, the correlation function and a trend function (see Figure 2.23). The scale of fluctuation describes the distance at which values are spatially correlated. Values within the scale of fluctuation are correlated, albeit decreasingly so with increasing distance, see also Vanmarcke (2010). The correlation function defines the decrease of correlation with increasing distance. The most common correlation function is a single exponential function introduced by Vanmarcke (1977), although in recent years, several other functions were published, e. g. Cao and Wang (2014) and Fenton and Griffiths (2008).

Random field analyses with a simple infinite slope approach have been applied by various authors to investigate the stability of slopes with spatially variable soils under rainfall infiltration (Cho, 2014; Santoso et al., 2011; Zhang et al., 2014). An extension towards the analysis of unsaturated slopes is presented by Zhou et al. (2016). Cai et al. (2017) propose an analytical solution for the reliability analysis of slope stability in the presence of spatially variable shear strength parameters.

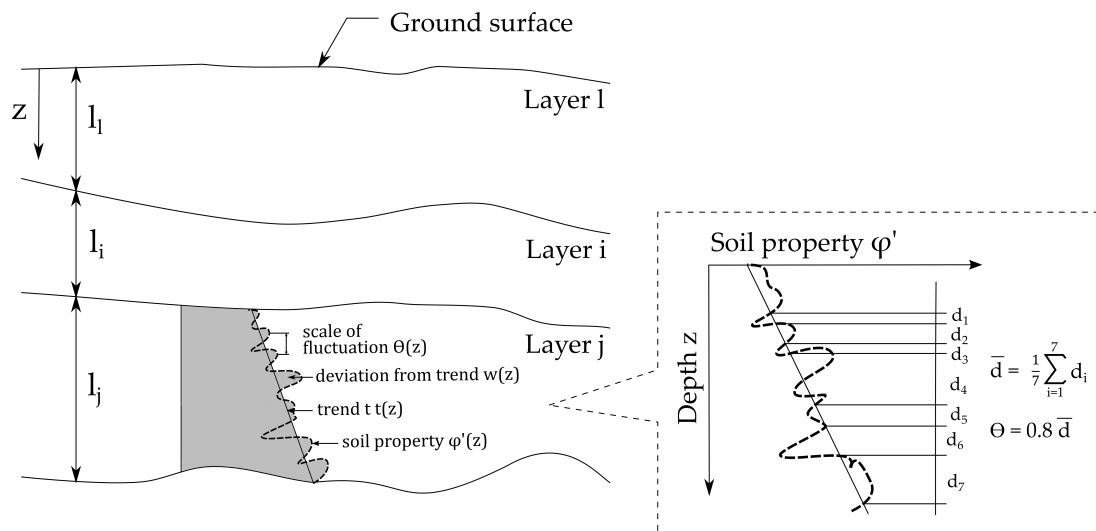


Figure 2.23: Random field model for natural soil variability; illustration based on ISO 2394:2015-03 (2015, cf. p. 74).

Transformation uncertainty

The transformation uncertainty of soil parameters is “related to the accuracy of physical or statistical models” (ISO 2394:2015-03, 2015). Often, transformation uncertainty of soil parameters is thus result of empirical or other correlation models.

For instance, the friction angle is commonly determined by means of direct shear tests, which allow determining the friction angle via the Mohr-Coulomb failure criterion based on the relationship between the measured shear stress failure and the normal stress applied in the test. Thus, model uncertainty arises. For slope stability analysis, McGuire and VandenBerge (2017) investigate the shear strength uncertainty resulting from the assumption of a constant variance applied to the Mohr-Coulomb failure criterion. As demonstrated by Ching, Phoon et al. (2016), the transformation uncertainty of CPT-based measurements can be decomposed into systematic bias for a local site and a component partly associated to measurement errors. A method to reduce the uncertainty of CPT-based site characterisation by a site-specific transformation model is proposed by van der Krogt et al. (2019). Phoon and Kulhawy (1999b) provide statistics for a number of tests and parameters commonly employed in geotechnical engineering. Ching, Li et al. (2016) compiles transformation models and their uncertainty for properties of clay and sand/gravel under the assumption of multivariate data. Multivariate data assessment couples the information of different soil tests and parameters to reduce the uncertainty, e. g. Ching, Li et al. (2016) and Phoon, Ching and Huang (2012).

Regarding the choice of statistical models, JCSS (2006), Lacasse and Nadim (1996) and Schultze (1972) assume that material weights are distributed normally. For the probability density function of the effective friction angle ϕ' , JCSS (2006), Lacasse and Nadim (1996), Lumb (1966) and Wolff et al. (1996) suggest a Gaussian distribution. Schultze (1972) recommends a Lognormal distribution for ϕ' . The hydraulic conductivity is commonly considered as lognormally distributed (Carsel and Parrish, 1988; de Rooij et al., 2004; Mallants et al., 1997). However, as pointed out by Phoon, Prakoso et al. (2016), the present summaries do not account for the range of different testing and evaluation methods available in geotechnical engineering.

2.6.4 Model uncertainty

Each mathematical formulation of a physical process, subsequently also referred to as model, may be subject to uncertainty. This applies, for example, to the calculation of excess pore pressures required for geotechnical revetment design and the determination of ship-induced loads for hydraulic revetment design. In this thesis, these uncertainties are mainly addressed as transformation uncertainties, whereas model uncertainty refers to the mathematical formulation of the limit state function. However, the difference between transformation and model uncertainty is not always obvious and may also depend on the research question.

Hydraulic design

Information on model uncertainty associated with the determination of the armour stone diameter is vague. One reason for this may be the large number of design equations available for dimensioning. The following explanations briefly outline existing findings on model uncertainty associated with common design equations, which are summarised in Section 2.3.3 and Appendix A.1. Within this thesis, model uncertainty is not considered in detail. As a matter of principle, however, especially in the case of the empirical design equations used for revetment design, model uncertainty should be taken into account in a fully probabilistic analysis.

Burcharth (1993) states “the uncertainty of a formula [such as Hudson (1959) and van der Meer (1988b)] can be considerable. [...] Coefficients of variation of 15 % - 20 % or even larger are quite normal.” The uncertainty of the equations arises from the random behaviour of the rock slopes, the accuracy of the damage measurement and the subsequent curve fitting (Pilarczyk, 2017). In addition, model uncertainty may also include uncertainty resulting from the assumption of deep water waves at shallow foreshores. By comparing the differences between measured and predicted damage values, van Gent (2005) investigates the performance of the design equations of Hudson (1959), van der Meer (1988b) and van Gent et al. (2003) for rubble mound breakwaters. Observed standard deviations range between 10 % to 50 % with the equations of Hudson (1959) being the least reliable. Pilarczyk (2017) suggests introducing two normally distributed model factors to account for the model uncertainty in the equations of van der Meer (1988b). For the Hudson equation, Pilarczyk (2017) mentions a variation coefficient of 18 %.

Geotechnical design

As argued by Dithinde et al. (2016), the complex soil-structure interactions encumber an exact prediction of the behaviour of a geostructure. To allow for an analytical solution of stability and serviceability calculations, empirical and semi-empirical methods have been proposed, which commonly lead to model uncertainty.

Although difficulties in the evaluation of model uncertainty of the geotechnical parameters arise from the natural variability of the soil, measurement errors of the initial parameter and the reaction of the structure which cannot be separated from the model uncertainty (Lesny et al., 2017, June 4–July 7), model factor statistics are available for a number of models such as footings, pile foundations and slopes (Phoon and Tang, 2019). Literature does not provide any model factors targeting specifically geotechnical revetment design. The model uncertainty for the global stability assessment of soil slopes varies between $0.95 \leq \mu \leq 1.07$ and $0.15 \leq \text{cov} \leq 0.21$ depending on the design method (Phoon and Tang, 2019; Travis et al., 2011). Site-specific model uncertainty for common geotechnical models is summarised in Dithinde et al. (2016).

For model factor analyses, special attention must be paid to soil characteristics at the test-site, interpretation of load test results and test scale (Lesny, 2017, June 4–July 7). Model factors available from literature which are determined for slope stability, thus, cannot be transferred to revetment design directly, since they were determined for different boundary conditions. For example, loading as a result of rapid drawdown is usually not considered in stability analyses of slopes.

Within this thesis, model uncertainty is not considered. Once more, however, it is stressed that model uncertainty should be considered in a fully probabilistic analysis.

2.6.5 Summary and critical evaluation

The literature review on the current state of knowledge has shown that statistical, spatial and transformation uncertainty constitute the parameter uncertainty inherent to actions and material parameters.

Investigations on hydraulic loads are mainly conducted for coastal structures. At present, neither statistical nor transformation uncertainty have been assessed for ship-induced loads. Moreover, there is no evidence on distributions and correlations of ship-induced waves and currents.

Distributions for the soil parameters can be derived from literature; friction angle and hydraulic conductivity are commonly approximated by Lognormal distributions. In contrast, there is little evidence on characteristic distributions for armour stones. Random field analyses have been applied by various authors to investigate slope stability with spatially variable soils. However, the effect of rapid drawdowns in a spatially variable soil has not been investigated. The quantification of the transformation error for soil properties is subject of ongoing research. However, since transformation uncertainty of material parameters is not strictly confined to revetment design, as it affects all forms of geotechnical constructions, it is not considered in this thesis.

Furthermore, literature (GBB, 2010; PIANC, 1987a; Rock Manual, 2007) gives little guidance on the selection of characteristic values for actions and material parameters. Maximum wave heights and current velocities are commonly considered as design loads. The characteristic hydraulic conductivity is commonly chosen as a value at the lower end of the possible range of values. For the choice of the characteristic friction angle, no specific recommendations are provided.

Following the definition of the characteristic values, characteristic values of hydraulic loads shall be selected as the 95 % quantile of the probability density function; characteristic soil parameters must either be defined as conservative mean with 95 % confidence or as 5 % quantile. Consequently, distributions of hydraulic loads and associated parameter uncertainties must be quantified in order to define characteristic values which are neither too much on the safe nor on the unsafe side.

In addition, the literature review shows that model uncertainty inherent to the geotechnical and hydraulic design equations contributes to the total design uncertainty. Despite its relevance for a quantification of the total uncertainty, however, this aspect cannot be considered in detail within this thesis. Model uncertainty in geotechnical and hydraulic design depends strongly on the set of design equations employed. In the case of geotechnical design, this concerns the equations for slope stability and the excess pore pressure model. In the hydraulic design, it concerns all equations for the purpose of determining the required armour stone size. An investigation would require numerous field and model tests as well as numerical analyses, which is beyond the scope of this thesis.

Conclusions: With the help of the literature review, it is shown that for some uncertainties to be considered in a design, some data is already available, i. e. statistics of soil parameters. A knowledge gap has been identified in the description of ship-induced uncertainties, which are primarily relevant for inland waterways. Descriptive statistics of the armour stone diameter must be assessed. Suitable distributions and correlations of ship-induced waves and currents must be evaluated. Since measurements on inland waterways are costly and thus limited, the parameter uncertainty is to be discussed as a function of the sample size. Moreover, the transformation of vessel passages to characteristic values of actions is object of uncertainty due to the use of empirical equations. Since the stability of a slope in rapid drawdown situations depends on the local excess pore pressure and shear strength, the effects of spatial variability of soil on the revetment dimensions must be assessed.

2.7 Specification of the research objective and methodology

2.7.1 Research objective

The present design approaches are mainly based on worst-case assumptions regarding actions and material parameters. In addition, at present, neither the type of limit state for geotechnical and hydraulic design nor respective target values are specified. The limit state functions yield the required mean armour stone diameter and armour layer thickness, which, however, do not serve as comparable key figures for site-specific safety levels. Neither the stochastic nature of basic variables nor uncertainties of the models are considered in present design approaches. Therefore, probabilistic design methods - despite the shortcomings discussed in Section 2.5.4 - offer a structured methodology to improve the design of bank revetments.

Within this thesis, the following topics and research questions summarised by bullet points are covered:

1) Specification of limit states

- *What are the most relevant damage mechanisms at inland waterways?*
- *Which criticality is associated with different damage types?*
- *Which limit states, thus, apply to the hydraulic and geotechnical design or assessment of bank revetments? What does this imply for possible target reliabilities?*

2) Evaluation of field observations

- *What demands should be made regarding field observations if employed to define parameter distributions in a design?*
- *How can data quality be assessed?*

3) Identification of input parameters

- *Which parameters should be included in a reliability-based revetment design?*
- *Which distributions and correlations suit the required parameters best?*

4) Addressing parameter uncertainties inherent to actions and material parameters

- How does parameter uncertainty affect the hydraulic and geotechnical revetment design?
- How can these uncertainties be taken into account?
- What recommendations can be provided regarding characteristic values of actions and material parameters?
- How can a reliability-based revetment design assist in accounting for local traffic and safety requirements?

2.7.2 Methodology

Subsequent investigations employ the design procedure outlined in GBB (2010). The choice of GBB (2010) offers the advantage that in the corresponding MAR (2008), standard revetment designs are summarised which can be used as benchmark for the presented probabilistic investigations. By comparing the revetment dimensions obtained by probabilistic analyses with the benchmark design, conclusions can be drawn regarding the degree of conservativeness.

In order to close the knowledge gaps identified above, the following approach is taken to investigate parameter uncertainties associated with the revetment design and supplement the current design approach for revetments at inland waterways (Figure 2.24):

- **Specification of the design model and limit states:** By means of a literature review, sources of uncertainty and common ways to deal with them are identified. As discussed by Panenka et al. (2020), the criticality of damage, and, thus, the specification of the limit state conditions is closely associated with detectability and maintainability. Expert interviews are employed to explore the most significant causes of damage and damage types as well as current maintenance procedures.
- **Identification of the most significant input variables:** In order to minimise the measurement effort and, thus, to ensure the applicability of the methodology, a sensitivity analysis is performed to identify relevant input parameters. Amongst others, the sensitivity analysis elaborates which parameters are not significant and can therefore be eliminated from the final model; which input parameters contribute most to the variance of the result; and which parameters interact with each other.
- **Assessment of current measurement procedures and available data:** While the in-situ measurement of soil parameters is part of the standard repertoire of revetment design, hydraulic loads have not been recorded on a standardised basis so far. Thus, current procedures of field measurements are summarised. Data quality measures are discussed. Recommendations regarding future measurements are provided.
- **Assessment of the statistical uncertainty inherent to actions:** As the measurement and subsequent analysis of hydraulic loads is cumbersome, the measurement period is often limited to a few days. With the help of probabilistic methods, uncertainty resulting from the measurement duration is quantified. Recommendations regarding the measurement duration are provided.
- **Assessment of the transformation uncertainty inherent to actions:** The measurement effort may be reduced by observing vessel passages (vessel dimensions, velocity, passing distance) instead of hydraulic loads (waves, currents, drawdown). As the observed vessel passages are transferred to actions by means of semi-empirical equations, additional

uncertainty is generated, which must be taken into account when defining characteristic values. By means of reliability-based methods, model factors are assessed. Recommendations regarding the use of field observations for a revetment design are outlined.

- **Evaluation of characteristic soil parameters considering spatial variability:** The stability of a slope in rapid drawdown situations depends on the local excess pore pressure and shear strength. Therefore, in the case of soil parameters, it is not sufficient to examine the statistical variability of soil parameters. With the help of random fields, the influence of spatially variable soil properties on the armour stone layer thickness is investigated aiming for recommendations regarding the choice of characteristic soil parameters.

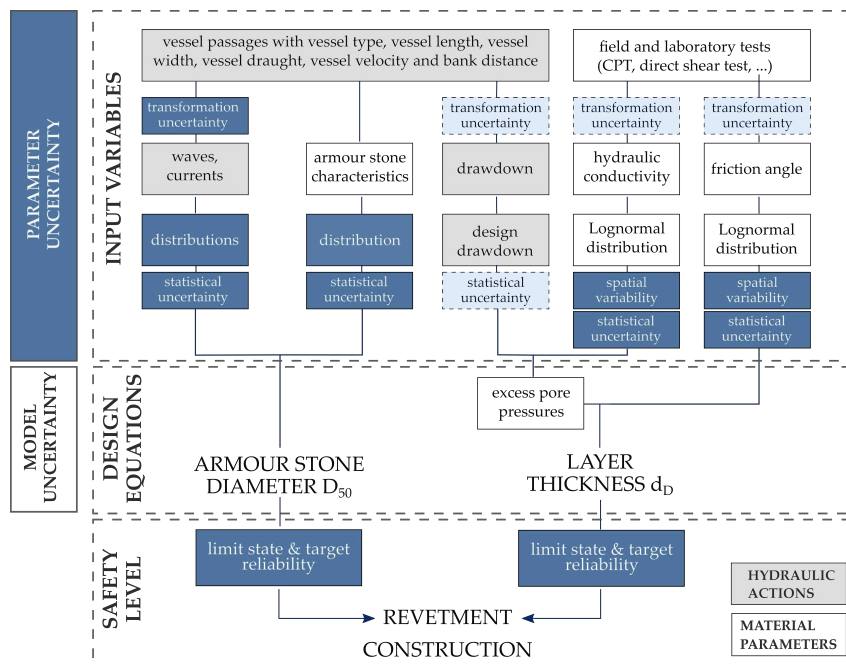


Figure 2.24: Methodology for the purpose of describing parameter uncertainties inherent to revetment design. Within this thesis, research aspects highlighted in the dark blue shaded boxes are investigated in detail.

3 | TRAFFIC AND TRAFFIC LOADS: FIELD DATA COLLECTION

‘Data is not information, information is not knowledge, knowledge is not understanding, understanding is not wisdom.’

–Clifford Stoll, American Astronomer

Contents

3.1	Introduction	48
3.2	Exemplary datasets	48
3.2.1	Waterway characteristics	48
3.2.2	Geometry and construction	49
3.3	Load parameters	50
3.3.1	Field measurements	50
3.3.2	Summary of data statistics	51
3.4	Material parameters	52
3.4.1	Soil characteristics	52
3.4.2	Armour stone characteristics	52
3.5	Quality assurance	55
3.5.1	Introduction of quality indicators for field observations	55
3.5.2	Discussion of quality indicators with respect to the data	57
3.6	Conclusions	60

3.1 Introduction

Hubbard (2010, p. 31) states a measurement is a “quantitatively expressed reduction of uncertainty based on one or more observations”. Field observations of vessel passages and measurements of resulting loads can assist in quantifying and eventually reducing uncertainties inherent to design procedures. In this thesis, they serve as basis for the investigation of statistical and transformation uncertainty of revetment design. By doing so, conservative assumptions regarding actions and material parameters are replaced by more precise, site-specific knowledge.

While few investigations of traffic flow exist, e. g. Biles et al. (2004), Fischer et al. (2014) and Xiao et al. (2015), the actual hydraulic loads caused by vessel passages, i. e. waves and currents, or parameters of a vessel passage, i. e. bank distance and vessel velocity, are rarely observed or published. Moreover, it must be differentiated between traffic observations, which record the “average” traffic, and driving tests, where selected vessels of different types are instructed to navigate at a defined bank distance and velocity. Commonly, load measurements are conducted during driving tests as they provide defined boundary conditions for the extension of existing design standards. Actual traffic observations are carried out for individual, site-specific studies commonly related to a revetment assessment or design. This thesis focuses on traffic observations.

This chapter introduces four exemplary datasets which are used throughout this thesis to evaluate the effects of parameter uncertainty on revetment design. First, in Section 3.2 site-specific characteristics of four datasets are highlighted. Secondly, the load measurement procedure is briefly presented and statistical parameters are determined (Section 3.3). Section 3.4 summarises measurements of material parameters. To conclude with, a procedure for the quality assessment of field observations is described and demonstrated.

3.2 Exemplary datasets

3.2.1 Waterway characteristics

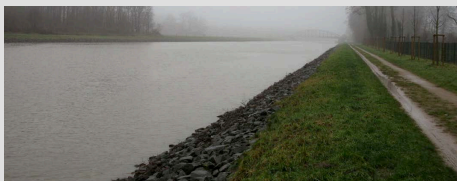

During the last twenty years, a number of measurements has been conducted on behalf of BAW. The measurements aimed at providing data for an extension of existing design standards or additional site-specific information for design purposes. Thus, traffic observations and driving tests have been conducted. At present, twenty of these measurement campaigns for a total of eleven canals and rivers have been processed and stored in a database owned by BAW. A campaign is commonly supplemented by a report which outlines location, cross-section profile(s), instrumentation and measurement processing.

Since canals are generally characterised by well-defined boundary conditions, e. g. an almost constant water level throughout the year, no or hardly any natural flow and a standardised cross-section geometry, this thesis focuses on canals. From a statistical point of view, the water level is not constant over time. Moreover, the local water level is an important input parameter for determining the hydraulic loads by means of calculations. However, the measurements of waves and currents are conducted at an approximately constant water level. This is beneficial as the measured values initially do not include any drift due to water level fluctuations, which would have to be deducted. For subsequent analyses, the four most recent campaigns that

were conducted at four different canals are chosen. They are the most reliable and comparable regarding employed measurement devices and data post-processing.

Basic information on the four waterways are compiled in a fact sheet (see Table 3.1). The four exemplary datasets comprise waterways of different waterway categories, traffic densities, and expansion and maintenance conditions. Traffic regulations regarding allowed vessel sizes and vessel velocities at the example canals are outlined in Appendix C, Table C.1.

Table 3.1: Fact sheets characterising four waterways whose measurements are employed throughout this thesis. The information is based on a short summary of expert interview and corresponding questionnaires (see Chapter 4), (Photos: Sorgatz).

<p>Dortmund-Ems Canal (DEK), north</p> <ul style="list-style-type: none"> • Category A • $A = 103 \text{ m}^2$ • $b_{ws} = 35.0 \text{ m}$ • $\approx 15\,000$ cargo vessels, $\approx 1\,500$ pleasure crafts per year • construction: 1921 - 1935 • enlargement: 1965 - 1975 	<p>The canal was partly enlarged. Damage occurs at regular intervals in not enlarged sections. Ship waves, propulsion and pack ice are the main damage causes. Steep embankments and no filter layer require a rigorous maintenance schedule.</p>	
<p>Küsten Canal (KuK)</p> <ul style="list-style-type: none"> • Category C • $A = 123 \text{ m}^2$ • $b_{ws} = 39.8 \text{ m}$ • $\approx 5\,000$ cargo ships, ≈ 500 pleasure crafts per year • construction: 1921 - 1935 • enlargement: 1965 - 1975 	<p>This canal shows considerable damage. In particular, stone displacements are frequently observed. It is not clear whether a lack of maintenance in the past or an insufficient design in regard to expected actions led to damage.</p>	
<p>Silo Canal (SiK), Untere-Havel-Wasserstraße</p> <ul style="list-style-type: none"> • Category C • $A = 186 \text{ m}^2$ • $b_{ws} = 55.0 \text{ m}$ • ≈ 900 cargo ships, $\approx 12\,000$ pleasure crafts per year • construction: 1910 • enlargement: 2002 - 2005 	<p>The canal was enlarged only recently and is well maintained. Damage refers to single armour stone displacement and is mainly caused by vandalism. Maintenance consists of rare, local measurements. It is aimed for a nature-oriented maintenance.</p>	
<p>Wesel-Datteln Canal (WDK)</p> <ul style="list-style-type: none"> • Category A • $A = 183 \text{ m}^2$ • $b_{ws} = 55.0 \text{ m}$ • $\approx 25\,000$ cargo ships, $\approx 1\,500$ pleasure crafts per year • construction: 1930 • enlargement: 1970 - 1989 	<p>Canal is well designed in relation to expected loads. Damage is rare. Ship waves, propulsion and vandalism are identified as main causes of damage. Revetment changes are regarded as a naturally occurring degradation process due to rare extreme events.</p>	

3.2.2 Geometry and construction

In the case of the four exemplary datasets, the information on geometry and construction originate from the measurement reports and from maintenance reports in the vicinity of the observation locations compiled by the BAW (IBS, 2006, 2007a,b, 2008a,b, 2015, 2016; Kayser, 2007a, 2008; Sorgatz and Soyeaux, 2019; Soyeaux, 2009). Figure 3.1 summarises cross-section profiles and revetment construction at the four example canals.

The investigations are based on the simplified assumption that there is no additional weight and, thus, stability support from a mineral filter layer, which corresponds to common conditions in the field. A geotextile is often found on extended waterways. At older, not extended

waterways it is unclear to what extent a filter layer is still present. The assumptions illustrate that if a revetment is assessed for maintenance purposes, a comprehensive investigation of the existing structure can assist in reducing uncertainty. In the future, geometrical uncertainty such as the existence of a filter layer or toe support may also be taken into account by means of random variables.

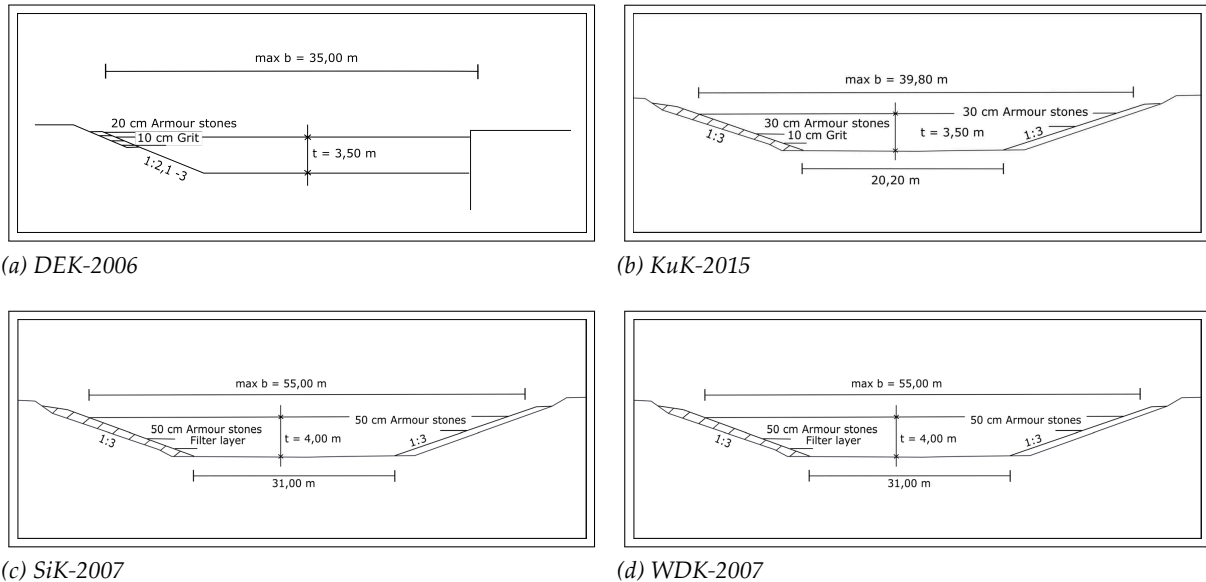


Figure 3.1: Cross-section geometries used for analyses throughout this thesis. The figures represent approximations of the actual in-situ conditions; illustrations based on field reports (IBS, 2006, 2007a,b, 2008a,b, 2015, 2016; Kayser, 2007a, 2008; Sorgatz and Soyeaux, 2019; Soyeaux, 2009).

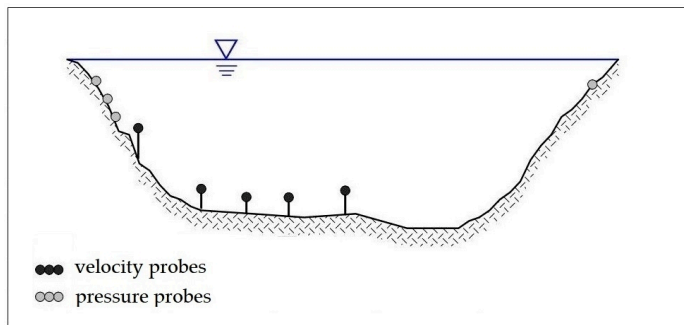
3.3 Load parameters

3.3.1 Field measurements

A measurement campaign commonly lasts between one to two weeks during which all vessels passing the observation location are registered. The measured values generally encompass dimensions and draught of the vessel, vessel velocity, passing distance as well as resulting water level fluctuations and flow velocities. Vessel velocity, vessel dimensions, vessel type and passing distance are determined by laser or radar, from image sequences or Automatic Identification System (AIS). Moreover, additional information on the vessels can be queried at the locks. Wave heights are recorded by pressure probes (absolute or relative) at a minimum of two different heights. Ship-induced flow velocities are measured in a minimum of two directions by acoustic doppler velocimeters (ADCP) or electro-mechanical current meters (inductive or electro-magnetic). Figure 3.2a shows a cross-section with the common instrumentation set-up, although, measurement devices and locations differ slightly between different campaigns as summarised in Appendix C, Table C.2.

From the measured water level fluctuations and flow velocities ship-induced loads, waves, currents and drawdown parameters, are determined for each vessel passage. This process is illustrated in Figure 3.2c for the example of the wave heights at bow and stern and in Figure 3.2d

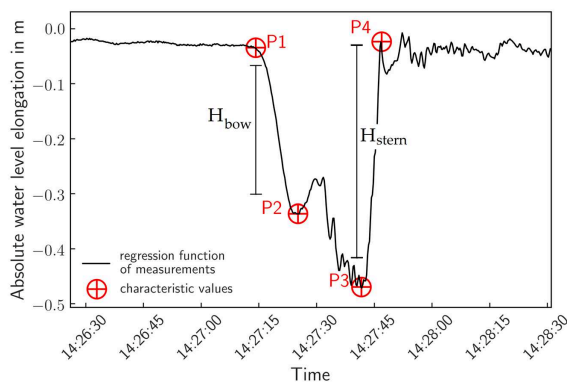
for the example of flow velocities. For each wave event the points marked in the graph are picked manually by the consultant in charge, which yields possible “characteristic” waves. For instance, the difference between P1 and P2 is defined as H_{bow} ; the difference between P4 and P3 yields H_{stern} . The manual procedure may lead to different results when changing the consultant. The uncertainties resulting from this procedure cannot be reconstructed with the existing data and are therefore not considered in this thesis. In the future, an automated evaluation of field measurements should be aimed at.



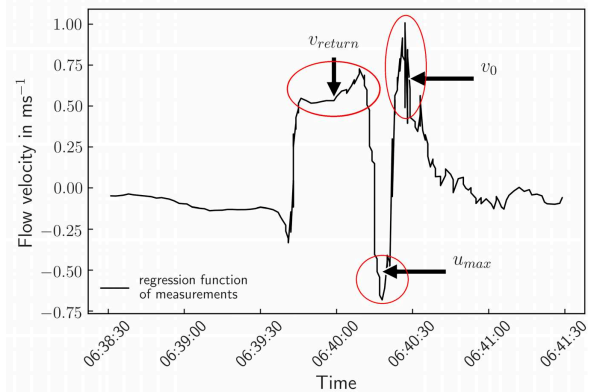
(a) Cross-section with common instrumentation set-up.



(b) Measurement set-up at the shore.



(c) Primary wave event with characteristic values; H_{stern} refers to the sternal wave height and H_{bow} to the bow height



(d) Flow velocities with characteristic values; v_{return} refers to the return current velocity, u_{max} to the slope supply flow and v_0 to the propeller jet velocity

Figure 3.2: Current measurement set-up and post-processing of field observations; illustrations based on (IBS, 2006, 2007b), (Photo: BAW).

3.3.2 Summary of data statistics

A summary of descriptive statistics of the four example datasets is given in Table 3.2. A comprehensive, but anonymised list of the measurements is provided digitally.

From the summary in Table 3.2 it is apparent that the supply flow velocity u_{max} is not included in any dataset. This may be reasoned by the difficulties arising when trying to quantify u_{max} in field observations. The drawdown parameters, z_a and t_a , are only available for KuK-2015. On the other hand, the return current velocity v_{return} is not available for KuK-2015. Furthermore, it is derived that the largest and fastest vessels are observed at SiK-2007 and WDK-2007.

The average vessel velocity ranges between 2.41 m s^{-1} and 3.16 m s^{-1} . The shore distance depends on the available cross-section area, the cov, however, varies moderately between 0.11 - 0.17. The mean values of H_{stern} range between 0.12 m and 0.27 m; the standard deviation (std) takes values from 0.08 m to 0.14 m resulting in a coefficient of variation (cov) between 0.37 and 0.75. The mean values of v_{return} range between 0.33 m s^{-1} and 0.88 m s^{-1} with std values of 0.15 m s^{-1} to 0.27 m s^{-1} . The corresponding cov values vary between 0.27 to 0.45. The mean values of t_a vary within 12.21 s to 28.14 s with cov values ranging between 0.31 and 0.47. Larger mean values are observed for $t_{a,\text{stern}}$, whereas larger cov values are observed for $t_{a,\text{bow}}$.

The histograms in Figure 3.3 disclose information on observed passing distances and vessel velocities. The data is normalised with respect to the water surface width b_{ws} and the permitted speed z_{perm} according to BinSchStrO (Bundesministerium der Justiz, 2011). The normalised passing distances are similar. On waterways of 'standard' cross-section (Figure 3.3b), the vessels navigate predominantly in the centre of the canal, as indicated by the peak of the histogram. The slight shift to the opposite side of the embankment observed for DEK-2006 (Figure 3.3b) is likely a result of the rectangular trapezoidal profile. The vessels navigate closer to the sheet pile wall.

The analyses of vessel velocities show that the majority of vessels passes the canals at velocities close to, but below the permitted velocities; however, speeding is also observed. This behaviour is particularly pronounced for SiK-2007, where many smaller vessels are sailing at increased speed. However, due to the large n-ratio (cross-section area / submerged part of the vessel, also known as blockage ratio), the speeding at SiK-2007 does not lead to extremely large waves and currents.

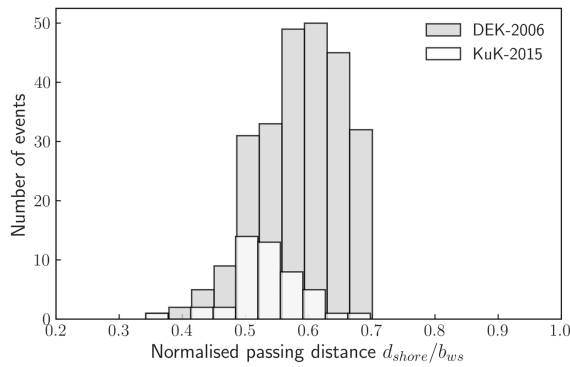
3.4 Material parameters

3.4.1 Soil characteristics

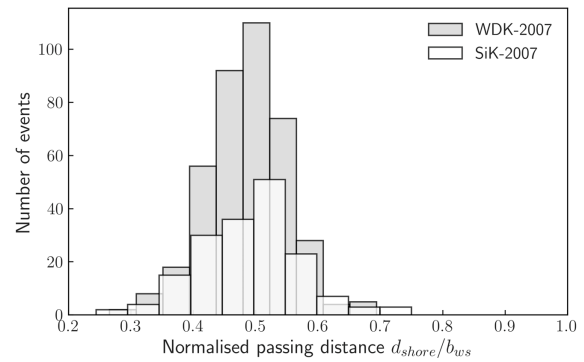
Commonly, information on the soil parameters such as friction angle and hydraulic conductivity are retrieved from field and laboratory tests. In the case of the four exemplary datasets, only the soil type originates from maintenance reports in the vicinity of the observation locations compiled by BAW (Kayser, 2007a, 2008; Sorgatz and Soyeaux, 2019; Soyeaux, 2009), whereas the soil parameters are based on recommendations for these soil types provided by current guidelines (EAU, 2012; MAR, 2008). At DEK-2006 and SiK-2007 a medium-wide graded sand is dominant, whereas at KuK-2015 and WDK-2007 a silty sand governs the design. This fact serves primarily to describe the measurement location. Throughout this thesis, parameter studies are conducted with both materials in order to assess parameter uncertainties. Detailed information on the investigated soil properties are therefore summarised in the chapters in which the geotechnical design is examined.

3.4.2 Armour stone characteristics

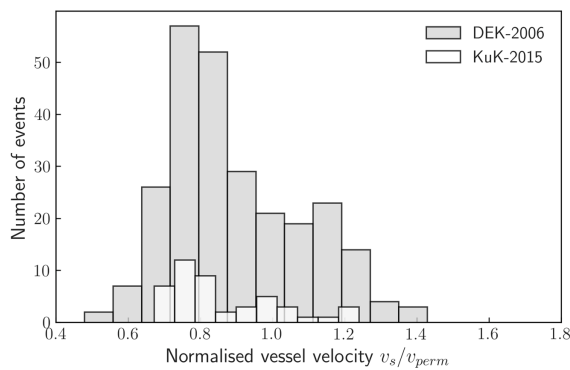
The armour stones are characterised by unit weight $\gamma_s = 26.5 \text{ kNm}^{-3}$, angle of repose $\phi'_{\text{D,hydr}} = 45.0^\circ$ and diameter. Armour stones are either classified by their length, CP classes, or weight, LMB classes, (TLW, 2003). Sampling a large number of armour stones in the field for distribution



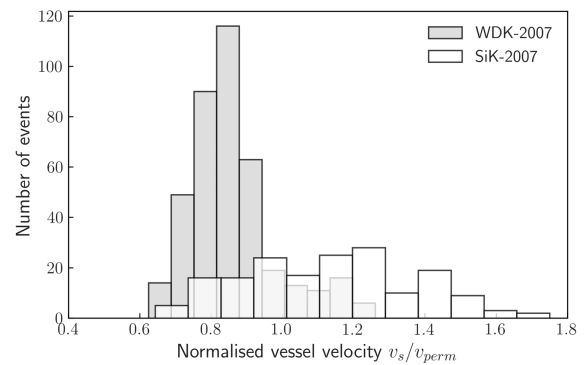
(a) Passing distances at canals of smaller cross-sections.



(b) Passing distances at canals of "standard" cross-sections.



(c) Vessel velocities at canals of smaller cross-sections.



(d) Vessel velocities at canals of "standard" cross-sections.

Figure 3.3: Statistics of passing distances and vessel velocities observed in the field.

fitting is very ineffective. Therefore, in order to obtain a data basis for subsequent analyses, a general statistical description valid for different armour stone classes is derived from a grain-size analysis in the laboratory. Thousand armour stones of two armour stone classes ($CP_{90/250}$ and $CP_{45/125}$) are weighted; their length, width, height and sieve diameter are recorded. The full set of measurements is provided digitally.

The measurement procedure yields a discrete quantity. Thus, the data is fitted with a Poisson distribution $\mathcal{P}(\nu_P)$ with ν_P as mean occurrence rate. As shown in Figure 3.4a the Poisson distribution represents regular distances between the classes. The spacing of the sieves, on the other hand, is irregular. At first glance, the fit of the Poisson distribution is therefore an imprecise approximation. However, the results must be considered with regard to the measurement procedure. Only selected sieve diameters are available for sieving. By nature, the mean armour stone diameter is a continuous variable and may be represented by a Gaussian distribution. For large ν_P , $\mathcal{P}(\nu_P)$ approaches a Gaussian distribution $\mathcal{N}(\nu_P, \sqrt{\nu_P})$ as shown in Figure 3.4.

The results of the sieving (Table 3.3) indicate that μ varies depending on the armour stone class and delivery batch, whereas σ is constant at ≈ 12 mm for $CP_{90/250}$ and ≈ 10 mm for $CP_{45/125}$.

Table 3.2: Summary of statistical measures describing the four example datasets. A complete data set should contain the following parameters: vessel length L , vessel width B , vessel draught T , vessel velocity v_s , shore distance d_{shore} , drawdown time at bow $t_{a, bow}$, drawdown time at stern $t_{a, stern}$, drawdown height at bow $z_{a, bow}$, drawdown height at stern $z_{a, stern}$, bow wave height H_{bow} , stern wave height H_{stern} , secondary wave height H_{sec} , return current velocity v_{return} and supply flow velocity u_{max} .

Measure	L	B	T	v_s	d_{shore}	$t_{a, bow}$	$t_{a, stern}$	$z_{a, bow}$	$z_{a, stern}$	H_{bow}	H_{stern}	H_{sec}	v_{return}	u_{max}
	m	m	m	ms^{-1}	m	s	s	m	m	m	m	m	ms^{-1}	ms^{-1}
DEK-2006 (km 111.100 - 111.300, 11 July 2006 - 25 July 2006)														
count	257	257	255	257	257	-	-	-	-	257	253	256	244	-
median	80.00	8.20	2.30	2.38	20.73	-	-	-	-	0.22	0.24	0.04	0.89	-
mean	75.92	8.38	1.86	2.51	20.53	-	-	-	-	0.22	0.25	0.05	0.88	-
std	12.24	0.95	0.76	0.52	2.34	-	-	-	-	0.09	0.10	0.04	0.27	-
cov	0.16	0.11	0.41	0.21	0.11	-	-	-	-	0.41	0.41	0.85	0.31	-
min	12.90	3.95	0.60	1.34	12.00	-	-	-	-	0.04	0.07	0.01	0.25	-
max	95.00	9.50	2.70	4.00	24.52	-	-	-	-	0.47	0.69	0.29	1.64	-
KuK-2015 (km 15.960, 09 June 2015 - 23 June 2015)														
count	47	47	46	46	47	47	47	47	47	47	47	47	-	-
median	80.00	8.20	2.15	2.25	21.10	12.25	27.25	0.16	0.22	0.17	9.23	0.03	-	-
mean	76.56	8.39	1.83	2.41	21.18	12.70	28.14	0.19	0.25	0.19	0.27	0.03	-	-
std	11.07	0.91	0.65	0.43	2.34	4.63	8.81	0.09	0.11	0.09	0.14	0.03	-	-
cov	0.14	0.11	0.36	0.18	0.11	0.36	0.31	0.48	0.46	0.47	0.54	0.78	-	-
min	31.50	6.02	0.75	1.88	13.60	5.75	6.00	0.06	0.09	0.07	0.09	0.01	-	-
max	100.00	9.50	2.50	3.47	27.75	25.25	56.00	0.44	0.58	0.47	0.72	0.16	-	-
SiK-2007 (km 58.200 - 58.400, 30 May 2007 - 05 June 2007)														
count	174	174	123	174	174	154	154	-	-	154	154	167	133	-
median	67.00	8.00	1.50	3.10	27.31	10.71	21.29	-	-	0.08	0.09	0.03	0.30	-
mean	63.26	7.38	1.43	3.16	26.97	12.21	21.74	-	-	0.10	0.12	0.04	0.33	-
std	24.33	1.74	0.52	0.67	4.55	5.58	10.22	-	-	0.07	0.09	0.03	0.15	-
cov	0.38	0.24	0.36	0.21	0.17	0.46	0.47	-	-	0.68	0.75	0.81	0.45	-
min	13.00	3.20	0.60	1.80	13.42	2.75	3.58	-	-	0.01	0.01	0.01	0.06	-
max	124.00	11.40	2.45	4.90	41.23	32.42	58.17	-	-	0.39	0.65	0.22	0.97	-
WDK-2007 (km 33.450 - 33.800, 08 August 2007 - 22 August 2007)														
count	397	397	397	397	397	397	397	-	-	397	397	397	397	-
median	80.00	9.00	2.48	2.77	27.00	15.75	26.75	-	-	0.23	0.21	0.05	0.70	-
mean	84.82	8.88	2.25	2.83	26.71	16.30	27.90	-	-	0.23	0.23	0.06	0.71	-
std	19.76	1.18	0.56	0.40	3.55	5.49	9.56	-	-	0.07	0.08	0.02	0.19	-
cov	0.23	0.13	0.25	0.14	0.13	0.34	0.34	-	-	0.31	0.37	0.38	0.27	-
min	39.00	5.05	0.55	2.06	14.60	3.50	8.75	-	-	0.06	0.07	0.02	0.14	-
max	181.00	11.48	2.83	4.16	38.15	45.25	77.00	-	-	0.49	0.65	0.21	1.38	-

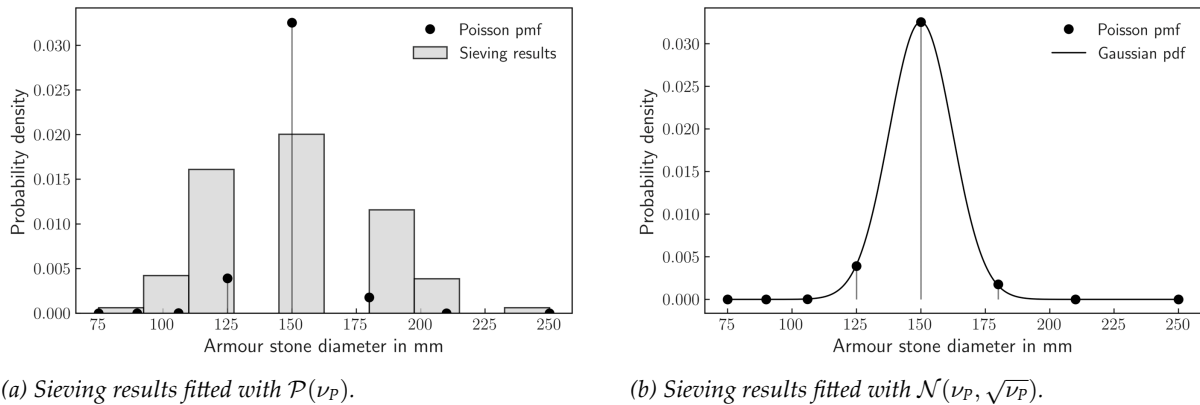


Figure 3.4: Relation between Poisson and Gaussian probability function.

Table 3.3: Test statistics of armour stone diameters. The table summarises parameters of a Poisson distribution $\mathcal{P}(\nu_P)$ and a Gaussian distribution $\mathcal{N}(\mu, \sigma)$ for different sample sizes and two armour stone classes.

		CP _{45/125}			CP _{90/250}			
		Poisson dist.	Gaussian dist.		Poisson dist.	Gaussian dist.		
No of samples		ν_P	μ	σ	No of samples	ν_P	μ	σ
1-199		97.91	97.91	9.89	1-199	152.241	152.241	12.339
200-399		94.35	94.35	9.71	200-399	161.312	161.312	12.701
400-599		94.83	94.83	9.74	400-599	152.568	152.568	12.352
600-799		90.71	90.71	9.52	600-799	143.377	143.377	11.974
800-999		96.16	96.16	9.81	800-999	142.276	142.276	11.928
1-1000		94.82	94.82	9.74	1-1000	150.259	150.259	12.258

3.5 Quality assurance

3.5.1 Introduction of quality indicators for field observations

Traffic observation must provide a representative impression of the site-specific traffic if used in a design or assessment of revetments. The total number of vessel passages along a waterway over a period of one year is defined as the reference value or total population, which the sample, the limited number of traffic observations, is compared to. The hereinafter presented quality assurance aims at a qualitative assessment of the data collection with respect to the specific target application. Comparable, albeit more sophisticated, approaches can be found in the field of economics and information technology (ISO/IEC 25012:2008-12, 2008; ISO/IEC 25024:2015-10, 2015; Sebastian-Coleman, 2012), ecological life cycle assessment (Veiga et al., 2017; Weidema, 1998; Weidema and Wesnæs, 1996) and recently in engineering (Klerk et al., 2018).

Sebastian-Coleman (2012, p. 40) defines data quality in relation to the consumers' expectations "based on their intended uses of the data" and thus, the "perceived or established purposes of the data." It is the "degree to which the characteristics of data satisfy stated and implied needs

when under specific conditions” (ISO/IEC 25012:2008-12, 2008, p. 4). Consequently, the following quality goals adopted from Weidema and Wesnæs (1996) and modified for an application to the above introduced field observations are proposed:

- (1) All variables required for a design (either vessel passages or hydraulic loads) are available in sufficient quantity (Completeness).
- (2) The data shows the design traffic (Temporal correlation).
- (3) The data is gathered for a specific waterway. The location of the observation is chosen in a way that it is representative for the respective waterway, for instance, not directly in a curve, near a lock or docking places (Geographical correlation).
- (4) The data is determined using state-of-the-art measurement methods. Documentation and raw data are available (Validity & Consistency).

(1) Completeness:

According to Sebastian-Coleman (2012, p. 62) “the dataset must be defined so that it includes all the attributes desired (width); the dataset must contain the desired amount of data (depth); and the attributes must be populated to the extend desired (density).” Figure 3.5 illustrates the different aspects of completeness schematically. The width refers to the number of variables (X_1 to X_n .) The number of available observations is described by the depth. The density deals with the number of single values measured visualised by the grey-shaded boxes.

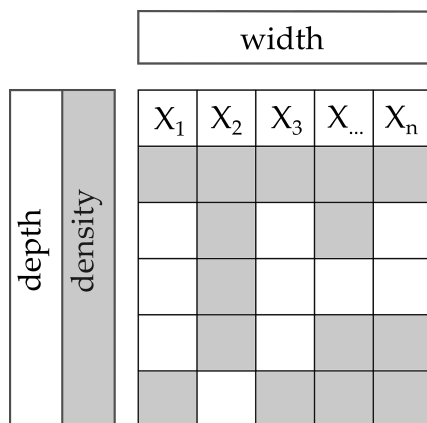


Figure 3.5: Dimensions of completeness as described by Sebastian-Coleman (2012).

(2) Temporal correlation:

The temporal correlation refers to the currentness of the data. It represents the time correlation between the year of the observation and the year of data applications (Weidema and Wesnæs, 1996). English (1999) denotes this indicator as timeliness, which is the degree to which data represents the real world from the required point of time. In the cases of a revetment design or assessment, it must be ensured that all vessel types relevant for dimensioning are included in the observations. The geometry of the observation cross section should not have changed between measurements and analyses.

(3) Geographical correlation:

The geographical correlation describes the spatial proximity of observation and design location. In the design or assessment case it is not only required to have information on the observation location, but also on construction details. For instance, if the cross-sectional areas or the cross-section profiles vary significantly between different areas at one waterway, measurements may not be applicable to the entire waterway.

(4) Validity & Consistency:

These two criteria deal less with the subject-specific suitability of a dataset than with its technical suitability. According to Sebastian-Coleman (2012, p. 62f) the term validity describes the “the degree to which data is conform to a set of business rules, sometimes expressed as a standard or represented within a defined data domain.” Consistency is “the degree to which data has attributes that are free from contradiction and are coherent with other data in a specific context of use” (ISO/IEC 25012:2008-12, 2008, p. 6). In the context of the presented application, these criteria relate in particular to the degree of standardisation realised in data collection, data evaluation and data storage. The data should be collected by state-of-the-art measuring devices, automatically evaluated and stored in a standardised format, which allows different consultants to access the same data at all times.

3.5.2 Discussion of quality indicators with respect to the data**(1) Completeness:**

A soft indicator of depth is the mix of vessel passages which should correspond to the average fleet observed at the particular waterway over the year. It is evaluated by comparing the observed vessel passages to lock statistics (see Figure 3.6). The lock statistics are queried at the lock closest to the observation location (WSA Brandenburg, 2018; WSA Duisburg-Meiderich, 2018; WSA Meppen, 2018; WSA Rheine, 2018). The different, partly area specific terminology of the vessel types proved difficult to compare observations with lock statistics without making assumptions, for instance, for a transformation of the vessel type using their width and length. If available, it is therefore recommended to rely on AIS data instead. The graphs shown in Figure 3.6 contrast observed vessel passages and lock statistics. From the similar bar heights, it can be deduced that the observed fleet approximately corresponds to the average fleet.

However, the evaluation of the datasets in Section 3.2 shows that the data is incomplete with respect to the dimensions ‘width’ and ‘density’. One parameter, u_{\max} , is missing (width) and there are few gaps within the parameter sets (density) indicated by the fluctuating number of counts in Table 3.2. Gaps in the data usually lead to a reduction in the number of samples. In few cases, such as when determining model factors, the single measurement can no longer be used. The extent to which the number of samples has significance for the uncertainties in the design is investigated within this thesis. Missing parameters are required for further analyses and, therefore, have to be determined by approximate calculations increasing inaccuracies in the design. Furthermore, the significance of the mathematically determined parameters for the overall result may be over- or underestimated. In the presented analyses only u_{\max} is calculated.

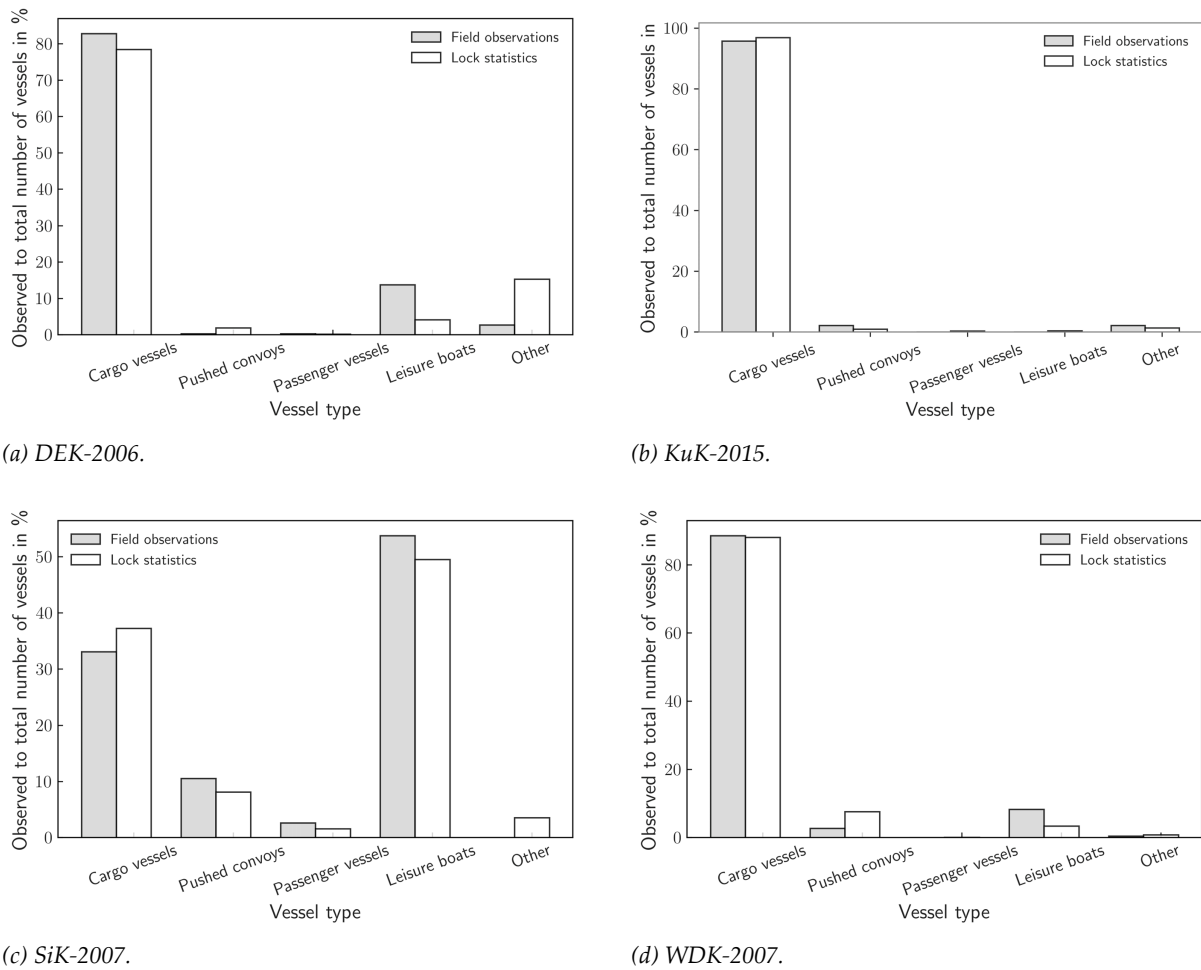


Figure 3.6: Vessel types derived from field measurements (left) and lock statistics (right).

An investigation of the uncertainties resulting from this procedure is beyond the scope of this thesis due to the existing database.

(2) Temporal correlation:

The investigations presented within this thesis do not require the latest data. To ensure the comparability between the analyses at different canals, the four most recent campaigns are chosen. They are the most reliable in regard to employed measurement devices and data assessment. In fact, for the reliabilities evaluated throughout this thesis this implies that they may not represent the current situation at the canals. They describe the condition at the time of the measurements. Any comparisons of damage, damage development and maintenance costs which may serve for validation of the analyses must therefore refer to the time of the measurement campaigns.

(3) Geographical correlation:

As a matter of fact, a measurement location should be representative for the waterway under consideration, e. g. not in curvy areas, near berths or in the vicinity of structures. These boundary conditions are met for all of the four example campaigns. In the course of this thesis, the data are gathered as accurately as possible for the measurement locations. The evaluation of the reliability is therefore primarily a measure for this location, but can also be regarded as an approximation for other sections due to the representatively selected observation location. Model factors are less confined to the observation location. Despite these facts, for the interpretation of the results of this thesis it is stressed that the results do not allow drawing conclusions about the condition of the entire waterway based on the presented results.

(4) Validity & Consistency:

At present, the available field campaigns are characterised by a lack of standardisation, since there is neither a standardised measurement set-up nor are there standardised specifications for the evaluation and storage of measurements (see also Table C.2). The employed measurement devices and their accuracy vary between the different campaigns. Quality and content of the reports differ between the individual campaigns. Raw data are not available for consultants.

Within the scope of this thesis, the lack of standardisation can be partially compensated for by extensive research and processing of data. Additionally, the subsequent analyses focus on the development of a probabilistic design approach for revetments rather than a design of revetments. For this purpose, minor concessions may be tolerable regarding validity and consistency of the data. However, it is strongly recommended to work towards a standardisation of field observations.

Summary

The inspection of data quality reveals that the four example campaigns are carried out, processed and documented differently. Even if they are comparable with regard to the employed measurement devices and data processing, the data itself is partly heterogeneous and/or incomplete. On the one hand, this is due to the varying questions investigated in the field campaigns. On the other hand, this is caused by a lack of measurement standardisation. Despite this fact, the evaluation of the quality indicators with respect to the proposed investigations indicates that the available data can be used for generic investigations of uncertainty inherent to the revetment design. The quality indicators the data does not fully comply to are mainly relevant for a site-specific revetment design. The aspect of data completeness is examined in this thesis. In short, the data and subsequent analyses results do not allow drawing conclusions about the condition of the entire waterway, but are suitable for generic uncertainty analyses.

3.6 Conclusions

Identification of input parameters

- ☑ *What demands should be made regarding field observations if employed to define parameter distributions in a design?*
- ☑ *How can data quality be assessed?*

In this chapter field measurements and supplementary material describing the data are presented. Armour stone characteristics are identified based on laboratory tests with two armour stone classes and 1000 armour stones each. The inspection of four example measurement campaigns reveals that at present available campaigns differ in their quality. On the one hand side, this is due to the varying questions investigated in the field campaigns. On the other hand, side, this is caused by a lack of measurement standardisation. Currently, there is neither a completely standardised measurement set-up nor are there standardised guidelines for the evaluation of the measurements. Despite this fact, the quality indicators discussed in this chapter are mostly met. Some criteria are of minor relevance in the context of the investigations of this thesis. Although, the data and subsequent analyses do not allow drawing conclusions about the condition of the entire waterway and describe the condition of a waterway only at the time of measurement, they are thus suitable for generic uncertainty analyses.

The presented concept for the quality assurance of field observations proposes quality indicators (completeness, temporal correlation, geographical correlation, validity and consistency) and procedures for their assessment. To improve its applicability in practice, it may be conceivable to introduce a scoring system. However, it is important to remember that the relative importance of the quality indicators may depend on the task at hand.

The investigations highlight the importance to store measurements and boundary condition, raw data and interpreted data together in one database or alternate data storage system. It must be ensured that different consultants access the same data at all times. Future work should focus on the automation and standardisation of measurements to increase usability and comparability of measurement campaigns.

4 | DEFINITION OF LIMIT STATES: EXPERT INTERVIEWS

‘We can start measuring only when we know what to measure: qualitative observation has to precede quantitative measurement, and by making experimental arrangements for quantitative measurements we may even eliminate the possibility of new phenomena appearing.’

–Heinrich Casimir, Dutch Physicist

Contents

4.1	Introduction	62
4.2	Elicitation of expert knowledge	62
4.2.1	Definitions	62
4.2.2	Experimental set-up	63
4.3	Interview results	66
4.3.1	Questionnaires	66
4.3.2	On-site inspections	67
4.3.3	Interviews	70
4.4	Discussion	71
4.5	Summary	73
4.6	Conclusions	74

4.1 Introduction

In contrast to Eurocode standards, e. g. DIN EN 1997-1:2014-03 (2010), current design standards applicable to revetment design do not differentiate between different limit states. Damage that endangers slope stability is not distinguished from damage that affects the serviceability of a structure. A resource-efficient and economic design, however, accounts for risk as the product of failure probability and extent of damage, which differs significantly between Limit States of Serviceability and Ultimate Limit States. In addition, the formulation of the design equations only allows to determine minimum design specifications as categorical information. Empirical factors shall account for different levels of damage. Conclusively, the design does not yield a comparable measure for system performance.

Furthermore, as discussed by Panenka et al. (2020), the criticality of damage is closely associated with its detectability and maintainability. If maintenance can be conducted easily, i. e. placing armour stones, damage may be less severe. In contrast, the reconstruction of a slope after slope sliding demands more effort and funding. It is therefore required to assess current procedures of maintenance and documentation of damage and maintenance in order to establish standardised, risk-based limit state functions, which are in line with feasible maintenance options.

Expert judgements provide a systematic way of eliciting information about events that elude a stochastic description due to a lack of representative data. As a scientific method originating from human sciences, expert interviews are used to collect qualitative data. In the following, expert interviews are employed to systematically assess the most significant failure mechanisms and failures as a result of damage. Following a brief introduction that summarises terminology and theory of expert interviews, this chapter presents results of expert interviews conducted at different German inland waterways.

4.2 Elicitation of expert knowledge

4.2.1 Definitions

Expert interviews are a scientific method aiming for the understanding of so far unknown context and hidden processes. In human sciences, expert interviews are a widely accepted method to analyse knowledge about the social context of actions and social structures (Bogner et al., 2009; Gläser and Laudel, 2010; Meuser and Nagel, 1991). In natural sciences and engineering, eliciting expert knowledge becomes attractive when quantitative data is not available in sufficient quality, e. g. Kuhnert et al. (2010), McBride and Burgman (2012) and Schüttrumpf et al. (2008).

The term

“‘Expert’ describes the specific position of the interview partner as source of specialist knowledge about [human] facts to be researched. Expert interviews pose a method that allows assessing that knowledge.’ (Gläser and Laudel, 2010, p. 12, own translation).

Criteria that allow to choose experts are discussed extensively in literature (Bogner et al., 2009; Gläser and Laudel, 2010). The interviewer him-/herself awards the expert status to the interviewees (Meuser and Nagel, 1991). Therefore, the choice of an interview partner depends strongly on the subjective selection criteria. Despite this fact, the selected experts, also referred to as sample, should meet criteria such as statistical representativeness and the typical nature of the interviewee regarding the research topic reasoned by competence criteria like education, position or function (Honer, 1994; Mieg and Näf, 2005).

Interview types can be formally classified according to their degree of standardisation. According to Gläser and Laudel (2010), one can distinguish between:

- **(Fully)Standardised interviews** where interviewees answer questions with pre-defined options to answer.
- In **semi-standardised interviews**, the interviewee receives a pre-defined catalogue of questions, but can formulate his/her own answers.
- **Non-standardised interviews** without pre-defined questionnaire and answers are classified as following:
 - In **(structured) guided interviews**, the interviewer uses a catalogue of subjects and questions summarised in a guideline. Formulation and order of questions can be customised by the interviewer depending on the course of conversation. The guideline ensures that all topics are covered and thus, the comparability of different interviews.
 - For **open interviews**, no guideline is required. Thus, several interviews on the same topic may explore different angles. The interviewer asks questions to interesting aspects developing within the conversation.
 - In **narrative interviews**, the interviewee answers in a monologue a complex question given at the beginning of the interview. Subsequently, the interviewer can ask additional questions to clarify information or to investigate specific aspects in more detail.

4.2.2 Experimental set-up

Sampling scheme

A sample is defined as a reduced group of people or institutions out of the overall population relevant to the research question. Schreier (2011) describes a categorisation scheme of sampling methods, which is illustrated in Figure 4.1. On the one hand, the sample can be chosen randomly. On the other hand, non-probabilistic sampling methods can be differentiated in incurring and purposive sampling. Incurring samples comprise a group of people or institutions being present at a certain time and place, e. g. resulting from a newspaper advertisement. Prior to the sampling, purposively chosen samples require knowledge of the underlying theory, theory-driven sampling, or of the object of investigation, data-driven sampling (Corbin and Strauss, 2015). This work applies a theory-driven sampling approach with a sampling scheme which assists in structuring the samples by characteristic features (Kelle and Kluge, 2010).

The sampling scheme results from the structure of the Federal German Waterways and Shipping Administration (WSV) and the categorisation of German waterways. In Germany, the WSV is responsible for the inspection of river beds including shore areas and revetments as well as

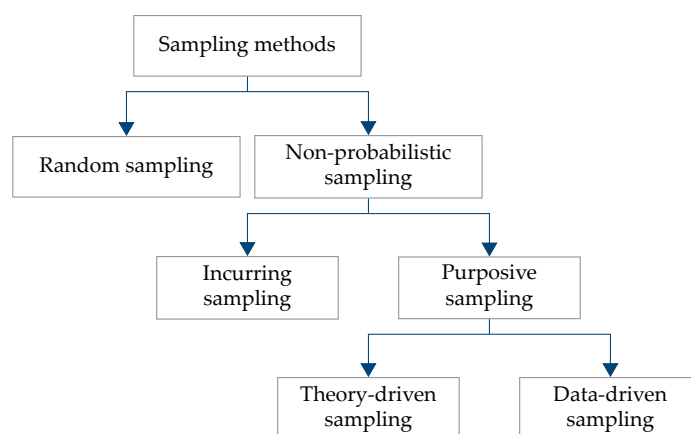


Figure 4.1: Sampling methods employed in qualitative research as categorised by Schreier (2011).

their maintenance. The Local Offices for Waterways and Shipping (WSA) operate regional field departments (Abz), which, amongst others, maintain revetments. The categorisation is based on current and projected transport demands at the waterways. The main inland waterways are subdivided in category A, category B, category C and other. Larger investments for extension measures are budgeted in category A. In category B, optimisation measures (excavation, embankment extension) may be scheduled, whereas for waterways in category C and other, only already existing assets will be maintained. As no category B waterway satisfies the criteria (canal, loose armour stone revetment), the study does not contain any waterway of that category. However, this is of marginal importance for the presented study, since categories A and C cover worst and best case situations.

Overall, 17 experts from nine field departments, primarily engineers and technicians, have been chosen by their function as field engineer. It is assumed that due to their daily work on site, they can describe damage and corresponding measures taken in most detail. The number of possible interviewees was limited by the number of field departments that regularly maintain loose armour stone revetments at canals. Thus, to avoid further reducing the number of interviewees, the professional experience of the interviewees is noted, but not taken into account when selecting the interviewees. In the interviews it was found that all interviewees have at least 10 years of experience maintaining revetments. Thus, it can be assumed that the selected sample is representative. Waterways of different traffic volumes, categories and maintenance standards located in different parts of Germany are included (Table 4.1).

Table 4.1: Qualitative sampling scheme for the compilation of expert interviews.

Maintenance standard	Non-standard design	Standard design
Waterway category		
A	Dortmund-Ems Canal, north Wesel-Datteln Canal	Dortmund-Ems Canal, south Kiel Canal
C	Küsten Canal Silo Canal Sacrow-Paretz Canal	Oder-Havel Canal Junction Canal Hildesheim

Interview process

The following work makes use of guided interviews. In contrast to fully standardised interviews, this method allows to explore research questions comprehensively without sanctioning expectations by the interviewer (Honer, 1994). Guided interviews require the interviewer to compile a catalogue of subjects and questions summarised in a guideline. Formulation and order of questions can be customised by the interviewer depending on the course of conversation. The guideline features main research aspects and corresponding research questions, ensures that all topics are covered, and thus, different interviews are comparable.

Prior to the interview, a semi-quantitative questionnaire is sent to the experts with questions that require preparation by the experts, e.g. number of vessel passages per year and current revetment constructions along the waterway. In addition, the questionnaire asks for causes of damage and typical types of damage. A semi-quantitative rating system with four categories ranging from 'occurs very often/main cause' (++) to 'does not occur/no influence' (-) is applied. Possible ambiguities in answering the questionnaire are clarified during the expert interviews by discussing selected aspects of the questionnaire in detail.

Figure 4.2 illustrates a workflow for the expert interviews. In theory and as indicated in Figure 4.2, the first phase of interviews could be followed by a second interview phase, e.g. in the form of group discussions, in order to verify the results once again. In the context of this thesis, this second iteration stage will be omitted, since the main goal of this study is to gain insights on main causes of damage and failure and on their development. However, if the interviews are used as basis for planning actual measures in the field departments, it is strongly recommended to conduct the second interview phase. Interview guideline and questionnaire used for the presented interviews are supplied in Appendix D.1 and Appendix D.2.

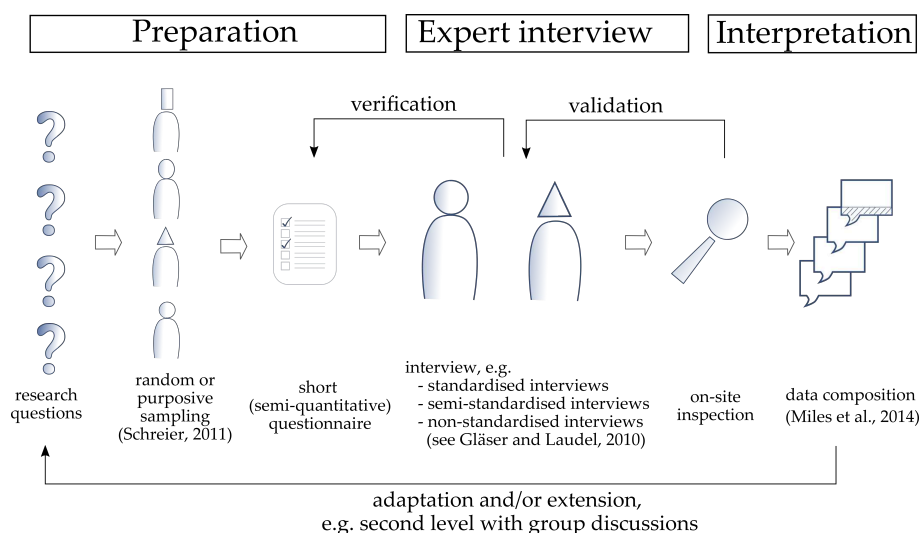


Figure 4.2: Essential elements of expert interviews from interview preparation to data evaluation.

Damage development is discussed utilising the classification proposed by Kayser (2015a) and MSV (2018). The experts are asked to assess the technical accuracy and practical relevance of the classification system, which graphically distinguishes the following five damage classes:

- S0 – No change or max. armour layer thickness of $\frac{1}{2}$ of armour stone diameter is eroded.
- S1 – Armour layer thickness of one armour stone diameter is eroded.
- S2 – Filter / geotextile layer is exposed.

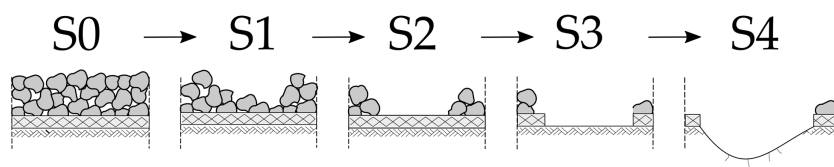


Figure 4.3: Damage classification for maintenance purposes; illustration based on Kayser (2015b, cf. p. 17).

S3 – Filter / geotextile layer is destroyed.

S4 – Subsoil or seal eroded in decimetre range or more.

Following the interview, joint on-site inspection where the interviewees are given the opportunity to show critical or damaged areas discussed in the interview is asked for. The inspection allows to compare the observations described by the interview partner to observations at other waterways.

Analysis method

Each interview is recorded and transcribed. The analysis consists of an à priori determination of relevant categories of information and a corresponding classification of the data content. Key subjects are subdivided into sub-categories to provide an overview of the data content (Miles et al., 2014). If a key subject is, for example, “documentation”, possible sub-categories may be “documentation of damage”, “documentation of maintenance measures”, “widely accepted damage classes” and “data management”. Sub-categories can also be compiled over several key subjects. After analysing about half of the interviews, the sub-categories are revised; if necessary, sub-categories are merged or new categories created. The final sub-category matrix is given in Appendix D.3.

The interviews were conducted and evaluated in German. Statements, which are crucial for understanding the conclusions drawn in this thesis, have been translated as accurately as possible (see Appendix D.3). For presentation, the data is anonymised referencing each interview by a single letter and a number indicating the waterway category (1 - category A, 2 - category C).

4.3 Interview results

4.3.1 Questionnaires

Table 4.2 displays the questionnaire answers on damage patterns. Obviously, the displacement of armour stones is the most frequently observed damage pattern, followed by scouring and erosion. This applies to all waterways independently of their category or maintenance condition. Slope sliding can be observed occasionally, but on a limited scale and more likely at waterways of category A. The same applies to cliff development, which mainly occurs at waterway of category A. An exception is B2, where both types of damage are observed. However, at B2 hardly any of the revetment structure has been retained (see Section 4.3.2). Moreover,

scouring contributes strongly to damage at waterways of category A, which may be a result of larger vessels passing the shore as at waterways of category C.

Table 4.2: Answers to semi-quantitative questionnaire regarding damage patterns and failures at German inland waterways. The following indicators are used: ++ occurs very often, + occurs, - occurs rarely, - - does not occur, NA - no answer. Answers which were altered as a result of the expert interviews are written in parentheses.

Observed damage	Armour stone displacement	Cliff development	Scouring	Slope sliding	Sagging
Abz					
A1	+	--	+	NA	NA
B2	++	+	+	+	++
C1	+	+	+	++	+
D2	+	-	++	--	NA
E2	+	-	-	--	NA
F2	+	(-)	--	--	NA
G1	+	+	++	NA	++
H1	(+)	NA	++	+	NA
I2	+	NA	+	NA	-

Table 4.3 shows that mainly ship-induced loads lead to damage. Critical sections close to constructions such as bridges and locks as well as areas, where navigation is required, are particularly endangered. Yet, vandalism, pack ice and material, even when complying to standards, equally contribute to damage, although they are beyond the scope of design standards. Local boundary conditions seem to affect the causes of damage the most. Canals in the north of Germany seem to be more strongly affected by pack ice. Vandalism seems to be slightly more prevalent at smaller waterways than on waterways with heavy traffic and at waterways that are less affected by vessel-induced loads.

Table 4.3: Answers to semi-quantitative questionnaire regarding causes of damage at German inland waterways. The following indicators are used: ++ main cause of damage, + causes damage, - may cause damage, - - has no influence on damage, NA - no answer. Answers that were altered as a result of the expert interviews are written in brackets.

Causes of failure/damage	Construction	Shipping	Wave surge	Currents	Draw-down	Collision	Vandalism	Pack ice	Installation	Material	Animals
Abz											
A1	++	+	NA	+	+	NA	+	-	--	+	--
B2	NA	+	+	+	+	--	--	-	++	+	NA
C1	NA	+	+	+	+	-	+	-	+	+	NA
D2	++	++	++	NA	NA	--	-	+	-	+	NA
E2	NA	+	NA	NA	NA	--	(+)	+	-	-	NA
F2	NA	(+)	NA	NA	NA	NA	++	NA	NA	NA	NA
G1	++	++	+	NA	NA	NA	-	+	-	NA	+
H1	NA	++	NA	NA	NA	--	--	-	--	+	NA
I2	NA	++	NA	NA	(++)	--	--(+)	--	NA	--	NA

4.3.2 On-site inspections

Table 4.4 summarises the site-inspections which were conducted following the interviews. In addition, photos illustrating the situation at the canal are provided. The descriptions indicate that the revetment conditions differ strongly between the interview locations. Initial conditions such as traffic and available maintenance options differ significantly between different waterway categories, types of damage, location of damage and time of damage detection. While local displacements of armour stones by swimmers and anglers represents the largest damage observed at some waterways like A1, F2 and H1, other waterways such as B2, D2 and I2 are characterised by vast areas of strongly displaced armour stones, cliff development and soil erosion. It may be noteworthy that this applies in particular to waterways of category C whose design does not fulfil present standards.

Table 4.4: Summary of waterway conditions at interview locations (Photos: Sorgatz).










<p>A1</p>	<p>Well-dimensioned canal cross section where hardly any damage is observed. Minor damage is fixed by the field department. Larger damages are put out to public tender once a year. Vandalism and material defects are identified as the main causes of damage. Major damage types are scour and landslides.</p>	
<p>B2</p>	<p>Canal is not constructed according to current standards. The revetment is only partly retained. A number of landslides result from unfavourable soil conditions. Maintenance measures are almost completely restricted in anticipation of new construction. Damage is repaired by the field department pulling armour stones from the bottom to the slope. Ship waves, propulsion and the current revetment construction are identified as main causes of damage.</p>	
<p>C1</p>	<p>Canal is constructed according to current standards. Revetment damage occurs rarely. Ship waves, propulsion and vandalism are identified as the main causes of damage. Damage is predominantly caused by the quality of armour stones and vandalism and is usually repaired by the field department before damage class S2 occurs.</p>	
<p>D2</p>	<p>Canal is not constructed according to current standards. Damage occurs frequently. The canal is in moderate condition, large sections range between S2 to S3. Ship waves and pack ice have been identified as the main causes of damage. Smaller maintenance measures are carried out by the field department. Annually, larger sections are put out to tender for maintenance. For this purpose, the field department uses its own damage classification.</p>	

Table 4.4: Summary of waterway conditions at interview locations (Photos: Sorgatz), continued.

E2	Canal is well maintained. Locally, there is little damage, i. e. caused by anglers. Due to the condition of the revetment in combination with low traffic, little maintenance is required.	
F2	Canal is well maintained. Locally, there is little damage, i. e. caused by vandalism. Due to the condition of the revetment, little maintenance is required.	
G1	Canal is not constructed according to current standards. Damage occurs at regular intervals. Ship waves, propulsion and pack ice are identified as the main causes of damage. The field department ensures a regular and regulated tendering of maintenance measures. In general, very 'small-scale' maintenance is conducted, as without filter layer, damage would develop quickly from S2 to S3.	
H1	Canal is in good condition. Maintenance measures are hardly necessary (on average one location per year). Larger measures are put out by public tender. Ship-induced loads and subsoil are considered as main causes of damage.	
I2	Canal is not constructed according to current standards. The revetment is only partly retained. Damage in terms of cliff development and erosion is correlated with the soil type. Ship waves, sinking and a missing filter are identified as the main causes of damage. Maintenance mostly comprises pulling armour stones from the bottom to the slope.	

4.3.3 Interviews

Table 4.5 summarises main results of the expert interviews for each waterway individually.

Table 4.5: Evaluation of expert interviews: Compilation of categorical data for each waterway.

Waterway	Interviewees	Experience	Damage classification	Damage documentation	Maintenance documentation	Point of intervention	Monitoring	Time to maintenance
A1	3	high	own	x	x	S1/S2	weekly	4-5 years
B2	2	high	unknown	(✓) ¹⁾	x	S2	fortnight	regularly
C1	1	moderate	unknown	✓	x	S2	fortnight	> 2 years
D2	1	moderate	own	✓	✓	S2	< monthly	> 5 years
E2	3	high	known	✓	x	S1/S2	< weekly	3 - 5 years
F2	1	high	known	✓	✓	S2/S3	< monthly	< 5 years
G1	2	high	unknown	x	✓ / x	S1/S2	fortnight	8 years
H1	2	high	unknown	✓	x	S1	< 6 months	5 - 10 years
I2	2	unknown	moderate	x	x	S2	irregular	10 years

⁽¹⁾ temporarily

The results show that the presented damage classification is barely known. Two field departments use their own classification system, i. e. D2 uses a risk-based classification. Regarding the proposed damage classification, A1 recommends introducing an intermediate damage class between S1 and S2 as a result of the point of intervention ('Maybe you have to insert an intermediate stage. With S1, I assume that [...] we will not yet take action as a rule. S2 already shows too much damage.'). Commonly, a damage classification is, if employed at all, used for guidance to determine the degree of urgency for maintenance (E2, D2).

Damage documentation is more popular than maintenance documentation. Often, Excel lists or photo documentations are compiled for internal use to keep track of damages and required measures in the field departments (G1, B2, H1, E2, F2). For instance, H1 states, 'Whenever we pass the track and find damaged areas, they are documented. But we only indicate the damaged area and estimate the amount of material needed to repair the damage. Then, the damage is fixed with the material we already have on site.' Only B2, D2 and F2 keep a damage and installation register. F2 outlines, for example, 'I record damage, also in terms of maps and locations, and where we have made the last repairs. [...] We have an Excel chart with waterway, kilometre range and what we have done there [...]. We document everything in tables, but also in maps.' D2 additionally updates a shore monitoring for the zone of water level fluctuation once or twice a year. Field department A2 and I2 argue against a standardised building inspection of bank revetment as '[...] the effort is extraordinary. [...]. In the field departments, there is basic knowledge available to say, this area is already damaged, I'll have a look at it. I know there is damage, I am keeping an eye on it, I haven't seen anything at this location, yet, and something has to be done in this area. That's the area that's going to be next.'

All field departments except for H1, define the point of intervention - when maintenance should be scheduled - as the point when the filter layer is exposed (damage class S2) or some time before or after. A1 indicates that action should be taken when approximately two layers of armour stones have been eroded. H1 'would leave S1 as an observation ...', but continues that at '[S2] it would be urgent to do something. It depends on the area affected by damage. If there was damage at 50 m, maybe we'd do something there [S1], too.' In short, maintenance is conducted when a revetment no longer fulfils its functions. 'When we see that there are no more armour stones on the slope. We need them against wave impact, because otherwise the ground is eroded directly. At this point, we would already try to do something. Or at least observe and plan for it.' (I2) The interviewees cannot provide a clear relation between loading and damage. However, all field departments confirm that at locations, where flow conditions

change, for example, at the beginning or end of structures like sheet pile walls, damage occurs more frequently.

A standardised monitoring is not conducted, but the track is inspected at regular intervals. In seven out of nine field departments, the track is checked at least once a month. Besides regular scheduled inspections, it is common that ‘colleagues pass the waterway every day or at least three times a week and then, of course, see where such damage develops.’ (E2) ‘Whenever the colleagues are outside and there are changes, then they react.’ (D2) Depth soundings at least once a year complement the monitoring strategy.

The maintenance efforts depend strongly on the conditions at the waterways. For instance, G1 states that ‘if we have normal winters, mild winters, they [the armour stones] can be left five to six years [...]’ [before intervention is required]. Some field departments state that scoured areas are more likely to require maintenance. ‘Once the revetment is damaged, the damage progresses faster. The area to attack has increased.’ (B2, C1, D2, H1) Whereas, I2 notes that ‘Approximately, I would say we have 40 km, and we do an area of 7 km to 10 km each year where we go and repair damage. But sometimes, there are 20 damages in almost 10 km, and sometimes there are 80, but it is also possible that they are on 2 m.’ In particular at waterways of category C such as D2, damage development is a creeping process. ‘That doesn’t happen overnight. It is a long process. It’s getting worse and worse here. [...] The revetment is not changing that fast. It’s not like everything changes from one day to the next. You have enough time.’

When it comes to maintenance intervals, there is no significant difference between waterways of different categories. According to the interviewees, at waterways of category A like A1, ‘It doesn’t have to be done annually, maybe every four or five years, and that is always in different areas, not always at the same place.’ Instead of the waterway categories, it is more likely that installation, material and current condition of the revetment defines the maintenance intervals (B2, D2, H1).

Since the required armour stone quantity is commonly determined by experience, armour stones are often stored for years and maintenance is conducted as a combination of public tender and self-directed, it is difficult to draw conclusions on revetment conditions based on statistics of armour stone orders. In some field departments, long preparation times for maintenance work must be expected due to shortages of staff (G1, H1). For smaller waterways of category C in particular, maintenance must be pictured as described by B2 ‘[...] there’s a shovel here, a shovel there. And it’s not every meter, but 200 m, 500 m, there are places like that. But you have to stay on the ball, otherwise it won’t work.’

4.4 Discussion

As for any scientific method relying on the knowledge of individuals, the “establishment of the truth” by means of expert interviews can be troublesome. The analysis of data from multiple experts may be difficult due to the ambiguity inherent to language or semi-qualitative grading formats. Using expert knowledge introduces uncertainty which derives from the vagueness in the description of the semantic meaning of a statement or judgment (Zimmermann, 2012). To overcome these drawbacks, Meuser and Nagel (1991) recommend a method called

‘cross checking’, a comparison of statements given by different interviewees, during data evaluation. Besides that, expert interviews encompass the same difficulties as any other qualitative data collection: qualification and skills of the interviewer. Interview technique, relation interviewee-interviewer and spontaneity regarding the guideline alter the quality of the results greatly (Hopf, 1978; Pfadenhauer, 2009). In summary, a number of factors may affect the interviews, whose influence cannot be reconstructed from the results.

In the case of the presented interviews, it is assumed that the quality of the interviews improves with an increasing number of interviews conducted. On the other side, it must be noted that the first interviews were conducted in a tandem of an experienced and a less experienced interviewer. In addition, as shown in Section 4.3.2, the conditions at the interview locations differ. While at category C waterways, the available maintenance measures are commonly limited to dumping armour stones by the field department, at category A waterways, public tenders for more extensive maintenance measures are standard procedure. In conjunction with different traffic (moderate or high), this may lead to the following issues which the interpretation of interviews and questionnaires may not fully account for:

- Due to different revetment constructions and revetment conditions, the interviewees assess the criticality of a particular damage differently.
- Different geotechnical boundary conditions such as local silty layers or very sandy soils increase the probability of certain failure mechanisms. For example, in areas of predominantly sandy soil, the absence of a filter layer may promote soil erosion. Silty layers are more prone to slope sliding.
- The different approach to maintenance combined with different staffing levels also lead to differences in the planning of maintenance measures

Despite these limitations, some general conclusions regarding the limit state functions can be derived from the expert interviews. The interviews show that no measures are taken in the case of single armour stone displacements at the slope. Only when the filter layer is exposed, a condition is reached which no longer meets the performance requirements of a revetment, also defined as failure. With reference to current design equations outlined in Section 2.3.3, it can therefore be concluded that the equations do not describe an Ultimate Limit State (ULS), but rather a Limit State of Fatigue (FLS). The occurrence of a large number of normal or accidental events has a cumulative damaging effect on the revetment. This results in less stringent requirements in terms of reliability or degree of utilisation.

With regard to the fault tree presented in Section 2.4.2, the interviews disclose further information. Armour stone instability can also lead to failure of the sliding protection as damage progresses. So far, this connection is not clearly accounted for in the fault tree; presumably because there are no equations yet which adequately describe this condition. The current design equations for the geotechnical design summarised in Section 2.3.4 assume undamaged conditions with an even distribution of the armour stone layer along the slope. Here, further investigations are required for the specification of a limit state function which considers damaged revetments. Moreover, further investigations of damage progression are required.

4.5 Summary

Failure and damage patterns, causes of damage and failure: The semi-quantitative questionnaires and the interviews indicate that ship-induced loads are of utmost importance regarding the occurrence of damage and its progression. Some damage patterns suggested in the questionnaire are rarely observed in nature. Armour stone displacements are the most common damage pattern. Geotechnical failure is more likely to occur at waterways of category A. If maintenance is conducted at an early stage, armour stone displacements do not interfere with slope stability and do not pose a risk to the waterways' reliability. Single armour stone displacements are thus classified as damage which contributes to failure mechanisms, e. g. slope sliding or soil erosion.

Deterioration: Damage of loose armour stone embankments progresses slowly. Often, it can be observed for years before an intervention will become urgent. For waterways of lower traffic density, category C, deterioration may take more than 15 years, until a critical deterioration state is reached. Due to the current maintenance strategy, however, these waterways now require regular maintenance by the field departments. For waterways of category A, deterioration takes place within five to six years. Subsequently, maintenance should be scheduled. Especially the transition from the exposure of the filter layer (S2) to the destruction of the filter layer (S3) and/or subsequent soil erosion (S4) takes place within a few days to weeks. A good quality installation of the armour stone layer increases its long-term stability. Furthermore, the damage development depends on traffic in relation to revetment design. The degree of utilisation of the revetment determines the pace of damage progression. Therefore, in the case of a comparable degree of utilisation, the existing categorisation of waterways may be one element to schedule maintenance measures.

Monitoring, maintenance and documentation: Maintenance works well in the field departments using location-specific experience. Measures up to approximately 50 t are conducted by the field departments. Larger measures require public tenders. The periods in which maintenance measures can be carried out are often limited to four to six weeks during the year for reasons of nature conservation and work schedules. A systematic and objective monitoring of canal embankments does only exist on a very basic level in form of regular field trips. Annual depth soundings supplement the present monitoring strategy. Often, maintenance is carried out over larger waterway sections, which does not allow to conclude on the severity of damage based on installed material. Observed damages and/or maintenance measures are documented (temporarily) for internal use. Conclusions regarding the revetment condition can only be drawn to a limited extent from current documentations, since data of varying quality has to be queried at different instances.

Classification: Despite being published for three years (MSV, 2015, 2018), the classification system is not familiar to most interviewed field department representatives. Some field departments have their own classification systems, for example, based on installation tonnage or photos. In principle, the experts agree with the classification suggested by Kayser (2015a). However, since the point of intervention aimed for is localised just before S2, it is suggested to introduce an intermediate damage class between S1 and S2.

Limit states: From the description of damage and failure it is deduced that the current design against armour stone displacement, the hydraulic design, refers to the FLS. The ULS condition is reached when the filter layer or soil is exposed locally, because, at that point, a major function of the armour stone layer - the protection against erosion - is no longer fulfilled. This condition corresponds roughly to the preferred moment of intervention, which should be scheduled prior to

the exposure of filter layer or soil. Areas once affected by damage are more likely to be object of deterioration. However, in order to describe this process by means of a model, further investigations of damage progression are required. The equations valid for a local slope sliding describe an ULS. If the design load is exceeded, the structure will fail locally.

Based on the results of the expert interviews the following limit state functions are defined. The limit state function g_{hydr} compares the armour stone diameter in-situ $D_{50,\text{pres}}$ to the required mean armour stone diameter $D_{50,\text{req}}$. It represents a FLS and is defined as follows:

$$g_{\text{hydr}} = D_{50,\text{pres}} - D_{50,\text{req}}(\text{hydraulic loads, armour stone characteristics and canal geometry}) \quad (4.1)$$

where failure is defined as $g_{\text{hydr}} \leq 0$.

The geotechnical design computes the required armour layer thickness required to ensure slope stability under rapid drawdown conditions. It refers to an ULS and the limit state function g_{geo} is defined as follows:

$$g_{\text{geo}} = d_{\text{D,pres}} - d_{\text{D,req}}(\text{hydraulic loads, soil characteristics and canal geometry}) \quad (4.2)$$

where failure is described by $g_{\text{geo}} \leq 0$.

4.6 Conclusions

Specification of limit states

- What are the most relevant damage mechanisms at inland waterways?*
- Which criticality is associated with different damage types?*
- Which limit states, thus, apply to the hydraulic and geotechnical design or assessment of bank revetments? What does this imply for possible target reliabilities?*

The presented expert interviews provide a better understanding of current maintenance procedures in the field departments. It was found that at present, existing damage and/or maintenance documentation cannot be used for comparative long-term analyses of revetment conditions, as, if documentations exist at all, they differ in detail and objective. If, in future, a prediction of damage and its development is required, long-time observations of damage progression are vital. New methods of data collection for a comparable damage and maintenance documentation should be established. However, this can only be achieved by increased automation of the documentation process taking into account economic efficiency. For instance, a simple database system could assist in reporting damage. It allows to record essential information about damage and associated repair measures, including a photo documentation, directly on site. A summary of annual maintenance costs may supplement regular condition assessments and, thereby, assist in identifying critical infrastructure.

Vessel-induced loads, and, depending on the waterway location and condition, also vandalism and pack ice are identified as main causes of damage. The most significant damage pattern is the displacement of armour stones. Generally speaking, damage of loose armour stone embankments progresses slowly. Often, damage can be observed for years before an intervention will become urgent. When filter layer or soil is exposed, the damage rate increases rapidly. Major and more extensive maintenance measures are required in a short time. The conclusion

can therefore be drawn that design equations which encompass the hydraulic design refer to a fatigue criterion. ULS conditions are reached the functionalities of the armour stone layer, the protection against soil erosion and local slope failure, are no longer fulfilled. There are currently no limit state functions that describe this condition. Further investigations are required for the specification of a limit state function considering of damage progression and damaged revetments. The assessment of slope stability at different levels of armour stone displacement requires further investigation. However, it can be assumed that an additional armour stones at the toe of the slope will increase slope stability. The limit states considered in the geotechnical design represent ULS conditions.

For demonstration purposes, subsequent investigations use target reliabilities for ULS and SLS provided in literature. Since at present there are no target reliabilities available for the FLS, the target values of the SLS are employed. The design equations of the geotechnical design describe an ULS. Target reliabilities are selected on basis of the safety class (JCSS, 2001).

5 | IDENTIFICATION OF INPUT PARAMETERS: SENSITIVITY ANALYSIS

'Cynics say that models can be made to conclude anything provided that suitable assumptions are fed into them.'

—The Economist

Contents

5.1	Introduction	78
5.2	Basic formulation and methods	78
5.2.1	Problem definition and objectives	78
5.2.2	Model definition	79
5.2.3	Assessment procedure	80
5.3	Results of the sensitivity analyses	84
5.3.1	Hydraulic design	84
5.3.2	Geotechnical design	86
5.4	Discussion	90
5.5	Conclusions	91

5.1 Introduction

A reliability-based design and assessment of structures involves an elaborate understanding of the actual system behaviour, limit states, input variables and the necessary resolution level of the analysis. The first two and the fourth aspect have already been covered in the previous chapters. The principles of revetment design are outlined in Chapter 2 and specify the relation between actions, material and geometrical parameters and, in the case of the presented investigations, the resolution of the analysis. Based on the expert interviews (see Chapter 4), the limit state conditions are assigned.

Amongst others, the demands concerning input parameters depend on the model itself, the desired accuracy of the analysis and the available data. In case of a probabilistic design, a more detailed analysis of the uncertainty inherent to the design can be conducted when using an increased number of random input parameters. At the same time, the effort required for the analysis increases with an increasing number of parameters. Thus, for reasons of computational efficiency, the most significant parameters should be identified prior to the probabilistic analysis.

In this chapter, sensitivity analyses are used to investigate which input parameters are required. Sensitivity analyses allow to elaborate the variability of the model output with respect to the input parameters. Thereby, the methodology assists in gaining insight into the relative importance of the various input parameters of a design model and into identifying the limitations of the employed models. To be more precise, in the context of revetment design this means that (a) for the hydraulic design and (b) for the geotechnical design, it is investigated which hydraulic loads, geometric and geotechnical boundary conditions have the greatest influence on (a) the required armour stone size and (b) the required armour stone layer thickness.

The first part of this chapter briefly summarises the state of knowledge regarding sensitivity analyses and methods applied in this thesis. Moreover, the design model is briefly outlined. Subsequently, sensitivity analyses are conducted for the hydraulic and geotechnical design. Based on the results of the analyses, the random input variables required for a probabilistic revetment design and model limitations are discussed.

5.2 Basic formulation and methods

5.2.1 Problem definition and objectives

As opposed to uncertainty analyses, sensitivity analyses do not attempt to determine the maximum variance of the model output. Sensitivity analysis seek to assign the uncertainty of input factors to the uncertainty of the model output (Saltelli, Aleksankinac et al., 2019). It can answer various questions, including (1) which variables require additional investigations to enhance the reliability of the model; (2) which variables are not significant and can therefore be eliminated from the final model; (3) which input variables contribute most to the variance of the result; (4) which variables interact with each other; (5) is there a physical explanation for each output or is the model erroneous; and (6) when using the model for calculation, what consequences result from the change of an input variable (Chan et al., 1997; Hamby, 1994). Figure 5.1 illustrates

an ideal scheme of a (sampling-based) sensitivity analysis introduced by Saltelli, Aleksankinac et al. (2019).

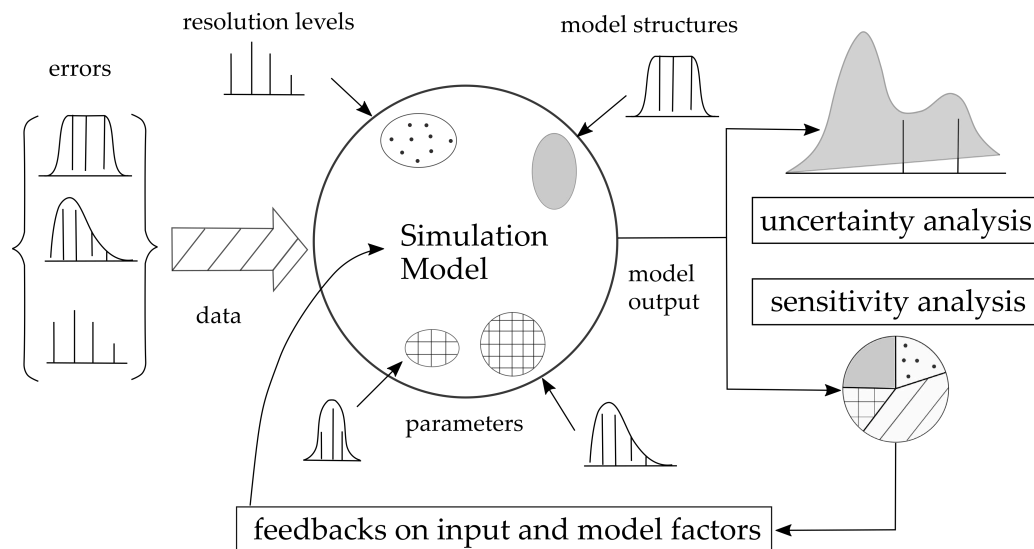


Figure 5.1: (Sampling-based) sensitivity analysis scheme; illustration based on Saltelli, Aleksankinac et al. (2019, cf. p. 30).

The presented sensitivity analyses address the following issues:

- (1) evaluation of the correctness of the implemented model,
- (2) evaluation of the sensitivity of model output with regard to the input parameters and
- (3) evaluation of interactions between input parameters with regard to the model output.

5.2.2 Model definition

The term ‘model’ refers to the mathematical formulation of the limit state function g , which requires a number of yet to be determined input parameters. Design equations and limit state conditions constitute the model. As specified by common design approaches (see Chapter 2), one model is used for hydraulic design and one for geotechnical design. The models presented below are used for sensitivity analyses, subsequently for uncertainty and reliability analyses. The sensitivity analyses also serve to verify the calculation model. In this thesis, the design equations are transferred to a Python-based implementation. A documentation of the code outlining the simulation models is provided in Appendix E.1

In the case of the hydraulic design, the limit state function g_{hydr} compares the armour stone diameter in-situ $D_{50,\text{pres}}$ to the required mean armour stone diameter $D_{50,\text{req}}$. Load and material parameters are treated as random variables. As outlined in Chapter 4, eq. (5.1) refers to FLS conditions. Failure is defined as $g_{\text{hydr}} \leq 0$.

$$g_{\text{hydr}} = D_{50,\text{pres}} - D_{50,\text{req}}(\text{hydraulic loads, armour stone characteristics and canal geometry}) \quad (5.1)$$

The equations applied in subsequent analyses originate from GBB (2010). Since different equations can be used to determine the armour stone diameter required to resist waves and currents, a weighting concept from GBB (2010) is adopted. GBB (2010) employs a weighting concept

which incorporates physical relations of different load types. While different load types are treated as equally important, the competing design equations for the same load type are weighted. A graphical illustration of the weighing system is depicted in Figure A.1. The full set of equations is presented in Appendix A.3.

The geotechnical design computes the required armour layer thickness required to ensure slope stability under rapid drawdown conditions. The limit state function g_{geo} is defined as follows:

$$g_{\text{geo}} = d_{\text{D,pres}} - d_{\text{D,req}}(\text{hydraulic loads, soil characteristics and canal geometry}) \quad (5.2)$$

where failure is described by $g_{\text{geo}} \leq 0$. As stated in literature and verified by the expert interviews in Chapter 4, g_{geo} describes ULS conditions. The equations from Section 2.3.4 are used. The required armour layer thickness is determined as the maximum of armour layer thicknesses required against slope sliding, eq. (2.4), and liquefaction, eq. (2.5). Minimum layer thicknesses resulting from other requirements regarding the revetment (interlocking of the armour stones, UV protection of the geotextile) are not considered in this model.

5.2.3 Assessment procedure

The methods available for sensitivity analyses are manifold (see Table 5.1). In general, a distinction is made between local sensitivity analyses and global sensitivity analyses as well as gradient-based and variance-based methods.

Table 5.1: Common methods of sensitivity analyses.

Local methods	Global methods
<i>Uncorrelated variables</i>	
<ul style="list-style-type: none"> • One-at-a-Time (OAT), • Adjoint modelling (Cacuci, Ionescu-Bujor et al., 2005; Cacuci, Navon et al., 2005) 	<ul style="list-style-type: none"> • Morris method (Campolongo et al., 2007; Morris, 1991) → screening method, • Sobol indices (Saltelli, 2002; Sobol, 1993, 2001), • Fourier amplitude sensitivity analysis (FAST) (Cukier et al., 1973; Saltelli, Tarantola et al., 1999; Schaibly and Shuler, 1973), • Derivative-based Global Sensitivity Measure (DGSM) (Sobol and Kucherenko, 2009)
<i>Correlated variables</i>	
	<ul style="list-style-type: none"> • Regression-based variance measure (Xu and Gertner, 2008), • ANCOVA, (Caniou, 2012; Mara and Tarantola, 2012)

In local sensitivity analyses, change in the model output is examined in relation to a single input parameter using either the derivative or linear regression to monitor changes in the output values. For this purpose, the parameters are varied one at a time within specified physic-

ally relevant limits. The interaction of different input parameters with each other is not considered. Local sensitivity analyses are commonly employed to investigate the effect of minor to moderate changes in the model output when changing input parameters within a limit range, i. e., to assess the stability (robustness) of pre-selected parameter combinations (Siebertz et al., 2017).

In global sensitivity analyses, input variables are modified to explore the entire variable space. Global sensitivity analyses evaluate the dispersion of the model output by attributing it to input parameters and input parameter combinations. Input and output are described by probability distributions. Global methods are employed to achieve a better understanding of the significance of individual parameters in a model and to compare the influence of different parameters (Siebertz et al., 2017). They are less susceptible to so-called type II errors, which means an important input parameter is thought to be noninfluential (Saltelli, 2008). Sobol indices analysis is one of the most popular methods of variance-based sensitivity analyses. Fourier amplitude sensitivity analysis is characterised by lower computation costs, but less popular due to its complexity (Saltelli, 2008). The Derivative-based Global Sensitivity Measure is, as the name implies, a gradient-based method, which may be less applicable to highly non-linear models.

Local methods mainly evaluate the model based on the gradient of the output (gradient-based), global methods can either be gradient-based approaches, e. g. Derivative-based Global Sensitivity Measure, or variance-based approaches, e. g. Sobol indices and Fourier amplitude sensitivity analysis. In contrast to gradient-based methods, variance-based methods allow to account for parameter interactions, and non-linear responses of the model. The Morris method is also referred to as screening method characterised by low computational costs and commonly used in preliminary analyses to reduce the number of input parameters prior to a detailed sensitivity analysis (Saltelli, 2008). The above-mentioned methods do not allow for the inclusion of correlated input variables. Only in recent years, a number of variance-based methods have emerged that account for correlated parameters (Caniou, 2012; Mara and Tarantola, 2012; Xu and Gertner, 2008), which, on the other hand, require knowledge on distributions and correlation structure. Finally, it is stressed that different methods do not necessarily provide identical results (Hamby, 1994).

Morris method

The Morris method emerged from OAT (One-factor-At-a-Time) screening methods, which are searching for a set of important input factors among a large number of input parameters. It offers a simple sampling algorithm that reduces the number of samples and, thereby, the calculation effort, while ‘sharing positive qualities of the variance-based techniques’ (Campolongo et al., 2007, p. 1). It examines which input parameters may be considered to have effects, which are (a) negligible, (b) linear and additive, or (c) non-linear with regard to the model output (Campolongo et al., 2007).

Mathematically, the Morris method is based on Elementary Effects EE_i . In a model with n independent input parameters X_i , $i = 1, \dots, n$ that vary in an n -dimensional unit cube across q selected levels, the elementary effect of the i th input parameter of the parameter combination $(X_1, X_2, \dots, X_{i-1}, X_i, \Delta, \dots, X_n)$ is defined as

$$EE_i = \frac{Y(X_1, X_2, \dots, X_{i-1}, X_i, \Delta, \dots, X_n) - Y(X_1, X_2, \dots, X_n)}{\Delta} \quad (5.3)$$

with the model output Y and the increment Δ in $0, 1/(q-1), 2/(q-1), \dots, 1$ in which the i th input parameter varies.

The Morris method as proposed by Morris (1991) yields two sensitivity measures, μ , the mean value of all elementary effects of an input parameter, represents the total effect of the input parameter on the model result, and σ , the standard deviation of the elementary effects an input parameter, describes second order and higher order effects, for instance, resulting from non-linear contribution to the model variability and/or interactions with other parameters (Saltelli, 2008). Based on the work of Campolongo et al. (2007), μ can be replaced by μ^* , which uses the mean of the absolute values of all elementary effects. With this procedure, eliminating significant input parameters cancelled out by positive and negative elementary effects or interaction with other parameters can be avoided. With regard to the evaluation, in simple terms, the larger the Morris parameters, the stronger the contribution of the input parameter to the model's variability.

Sobol Indices

Sobol indices are obtained by random sampling with the Sobol sequence (Saltelli, 2002; Saltelli, Annoni et al., 2010; Sobol, 2001), which is a quasi-random sampling method designed to facilitate the assessment of Sobol indices. Sobol indices allow to decompose the overall variance of the model output in the variance of the inputs. As introduced by (Saltelli, Annoni et al., 2010), the following three Sobol indices are evaluated:

The first order (FO) indices characterise the importance of one random variable X_i to the unconditional output variance $V(Y)$ as a function of the model output Y while averaging the other variables. For mutually independent variables, $V(Y)$ can be decomposed into the contributions associated with each X_i . The FO index is then defined as quotient of the conditional variance of the average output $E(Y|X_i)$ given all possible values of X_i and $V(Y)$:

$$FO = S_i = \frac{V_i}{V(Y)} = \frac{V(E(Y|X_i))}{V(Y)} \quad (5.4)$$

The second order (SO) indices evaluate the variance V_{ij} of every pair of variables X_i and X_j with regard to the total variance $V(Y)$. It is defined as follows:

$$SO = S_{ij} = \frac{V_{ij}}{V(Y)} \quad (5.5)$$

The total order (ST) indices are a measure of the output variance caused by a single variable X_i including all variance caused by its interactions with other variables. It therefore indicates the effect of all groups of variables that contain X_i . In one-dimensional variable space $\mathbf{X}_{\sim i}$ it is defined as follows:

$$ST = ST_i = \frac{E_{\mathbf{X}_{\sim i}} V_{X_i}(Y|\mathbf{X}_{\sim i})}{V(Y)} \quad (5.6)$$

Analysis workflow

To accomplish the objectives listed in Section 5.2.1, two methods of global sensitivity - the Morris method and Sobol indices - are employed subsequently. Both methods are widely accepted for model assessment and classified robust against non-linear models (Saltelli, 2008). First, the Morris method is used to search for the most significant variables that contribute the most to the variability of the model output. Secondly, Sobol indices are computed with a reduced parameter set to investigate the interactions of the input variables in more detail. Figure 5.2 illustrates the outlined workflow of the sensitivity analysis.

The investigations employ the Python package “SALib” (Herman and Usher, 2017), which provides an implementation of the Morris method and Sobol indices. The package performs the sampling of the input parameters according to the selected method of sensitivity analysis and based on the parameter ranges provided by the user. A uniform distribution of the input parameters is assumed. The sampling results are then transferred to the calculation model, in the presented case, the geotechnical and hydraulic revetment design, and the model output is calculated for all input parameter combinations provided. The model output is then further examined with the help of the SaLib package. Based on the model output, the SALib package calculates the Morris parameters or Sobol indices. Figure 5.3 illustrates the process.

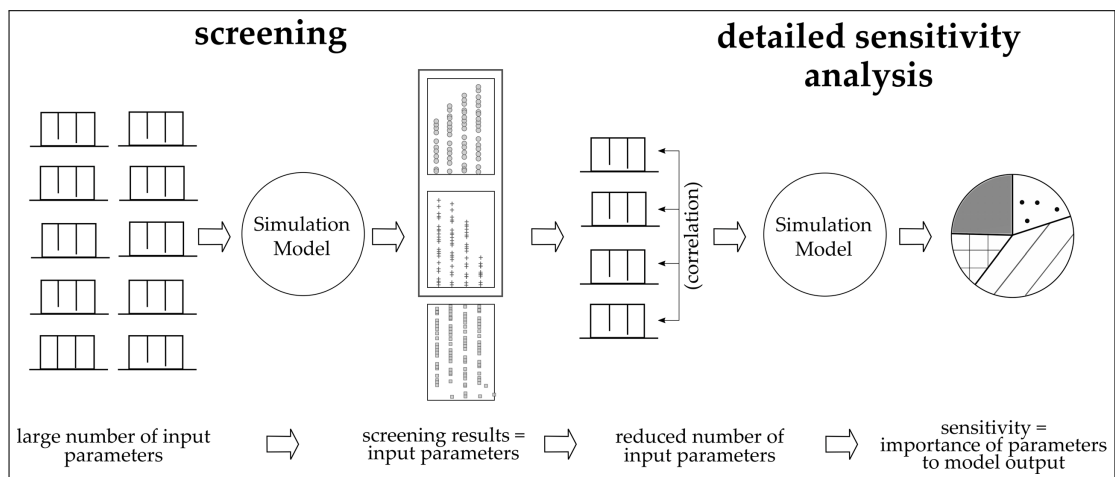


Figure 5.2: Workflow of a sensitivity analysis combining screening and sensitivity measures.

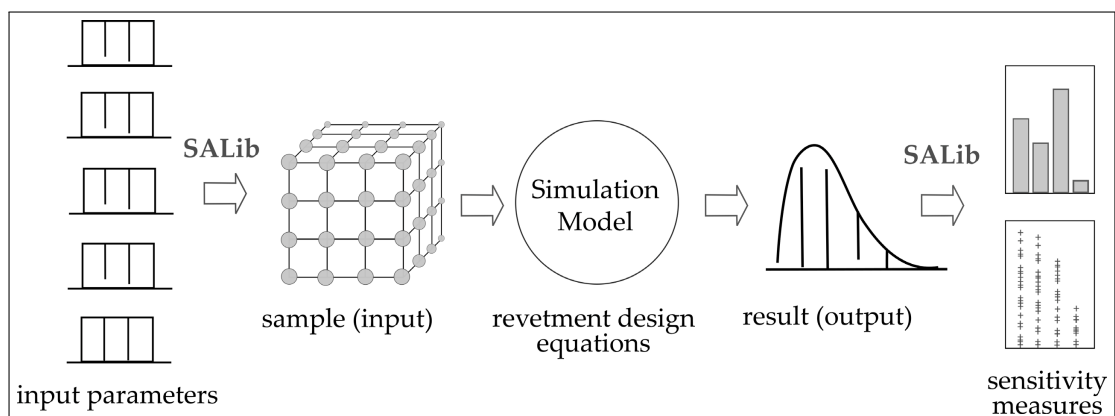


Figure 5.3: Workflow of a sensitivity analysis using the SALib package in Python.

5.3 Results of the sensitivity analyses

5.3.1 Hydraulic design

Variability of the input variables

The hydraulic design requires the following input variables, the *transversal stern wave height* H_{stern} , the *secondary wave height* H_{sec} , the *return current velocity* v_{return} and the *maximum slope supply flow* u_{max} . Furthermore, characteristics of the armour stones are required: the *armour stone density* ρ_s , the *angle of repose of the armour stones* $\phi'_{\text{D,hydr}}$ and the *in-situ mean armour stone diameter* $D_{50,\text{pres}}$. The *slope angle* m and the *waterway cross-section area* A complete the parameters measurable in nature required for a revetment design. The measurable parameters are supplemented by empirically determined stability factors B'_B and B^*_B , which shall account for the desired occurrence of the design case or maintenance efforts. B'_B and B^*_B were derived from field and laboratory tests and used in a rather simplified manner as deterministic description to describe risk associated with the final revetment dimensions in a deterministic way.

The parameter range for the hydraulic revetment design is summarised in Table 5.2. It is based on standard design values (MAR, 2008) and field observations (see Chapter 3). The armour stone characteristics range in the order of twice the standard deviation as determined by laboratory investigations (see Chapter 3). Under the assumption of a Gaussian, distribution this approach includes approximately 95.0 % of possible values.

The sensitivity analysis does not cover different cross-sections, e. g. due to different waterway categories. The standard cross-section geometry of an inland canal featuring a T-profile has a cross-section area of 182 m^2 (BMVBS, 2011). For sensitivity analysis a deviation of 10.0 % is assumed. This simplification is reasonable, as it can be assumed that for any design or assessment, approximate information on the cross-section geometry are available. A similar procedure is used to specify the range of density and friction angle of the armour stones. Here, too, it is assumed that approximate information on these parameters are available for design or assessment. Thus, a large variability, which essentially means different armour stone types, does not have to be considered.

Table 5.2: Ranges of variables employed in the sensitivity analysis of the hydraulic design.

H_{stern}	H_{sec}	v_{return}	u_{max}	$D_{50,\text{pres}}$	A	m	ρ_s	$\phi'_{\text{D,hydr}}$	B'_B	B^*_B
m	m	m s^{-1}	m s^{-1}	mm	m^2	–	kg m^{-3}	°	–	–
MIN 0.25	0.05	1.00	1.00	155.00	164	2.70	2300.00	35.00	1.50	2.00
MAX 1.10	0.25	1.75	2.80	205.00	200	3.30	3000.00	45.00	2.60	3.00

Results of the sensitivity analysis

The results of the Morris analysis are displayed in Table 5.3 and Figure 5.4. The investigations are conducted with regard to the limit state function g_{hydr} . A negative difference $D_{50,\text{pres}} - D_{50,\text{req}}$ characterises failure, while a positive value indicates a sufficient armour stone size in-situ.

From the small μ^* and σ values in Table 5.3 it is concluded that A , h_w and H_{sec} do not affect the variability of the model output. The input parameter v_{return} , B'_B , B_B^* , m and $\phi'_{D,\text{hydr}}$ are of moderate importance; the moderate σ of v_{return} indicate that v_{return} may interact with other parameters or contribute non-linearly to the model output. The remaining input parameters, H_{stern} , u_{max} , ρ_s and $D_{50,\text{pres}}$ affect the model output significantly. It is noteworthy that $\sigma(D_{50,\text{pres}}) = 0.000$ suggests that the effect of $D_{50,\text{pres}}$ does not result from parameter interactions or higher order effects. This observation corresponds to the provided calculation model, which assumes $D_{50,\text{pres}}$ to be an independent input parameter characterising resistance.

Table 5.3: Morris test statistics of hydraulic design with μ and μ^* as mean of the elementary effects, μ^*_{conv} as confidence interval of μ^* and σ as standard deviation of the elementary effects.

Parameter	μ^*	μ	μ^*_{conv}	σ
Stern wave height H_{stern}	66.928	-66.812	1.878	32.134
Secondary wave height H_{sec}	0.015	-0.015	0.025	0.421
Return current velocity v_{return}	19.717	-19.717	2.137	35.559
Supply flow velocity u_{max}	116.406	-116.406	3.319	54.157
Stability parameter B'_B	17.126	17.126	0.704	11.432
Stability parameter B_B^*	17.082	17.082	0.718	10.825
Cross-section area A	0.000	0.000	0.000	0.000
Water depth h_w	0.000	0.000	0.000	0.000
Slope inclination m	8.980	8.980	0.252	4.247
Armour stone density ρ_s	71.646	71.646	1.576	27.350
Armour stone friction angle $\phi'_{D,\text{hydr}}$	13.268	13.268	0.420	7.314
In-situ armour stones $D_{50,\text{pres}}$	50.000	50.000	0.000	0.000

The scatter plots (Figure 5.4) provide more insights regarding the effects of the input variables on the limit state. The graphs display the model output as a function of different input parameter combinations. A linear relation between H_{stern} and $D_{50,\text{pres}} - D_{50,\text{req}}$ as well as between $D_{50,\text{pres}}$ and $D_{50,\text{pres}} - D_{50,\text{req}}$ is observed; v_{return} , u_{max} and ρ_s are characterised by a quadratic relation to $D_{50,\text{pres}} - D_{50,\text{req}}$. This observation corresponds to the underlying design equations, where plain wave heights and squared flow velocities are included to determine the required armour stone diameter (see Appendix A.3). In summary, the screening indicates that A , h_w and H_{sec} do not affect the model output strongly. Thus, these values are considered to be deterministic values in subsequent analyses using the mean values of the ranges presented in Table 5.2.

The results of the Sobol analysis are presented in Figure 5.5. First order (FO) and total order (ST) indices are presented using a barplot in Figure 5.5a, where a larger Sobol index indicates a higher importance of an input parameter for the output variance. From the graph, a strong contribution of H_{stern} , u_{max} , ρ_s and $D_{50,\text{pres}}$ to the output variance is inferred. A minor importance of v_{return} , B'_B and B_B^* is observed. In general, ST and FO indices do not differ significantly. The importance of H_{stern} , u_{max} , ρ_s and v_{return} increases slightly when additionally accounting for the interactions with other parameters. Second order (SO) indices are displayed in the colourmap in Figure 5.5b. This simplified chart only represents the upper part of a symmetrical matrix. The shading illustrates the interaction of the parameters; the brighter a square, the greater the SO index and, thus, the parameter interaction. The colourmap confirms the minor importance of variable interactions. Interactions should be highlighted by a lighter or darker shaded square, which is only the case for v_{return} and u_{max} and u_{max} and ρ_s .

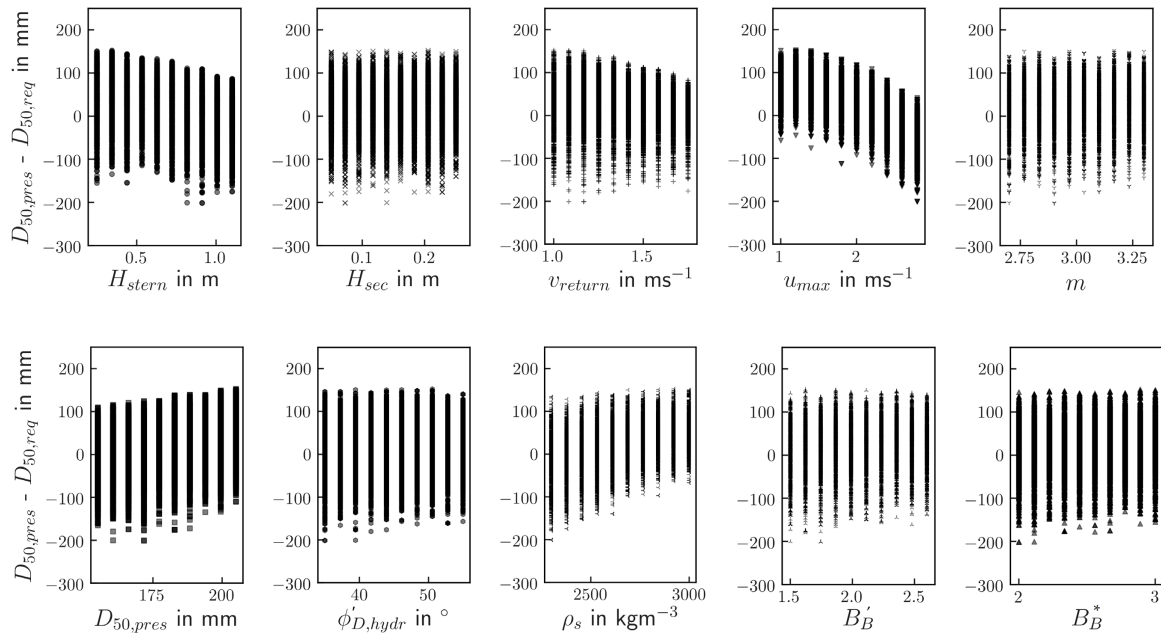


Figure 5.4: Results of sensitivity analysis of the hydraulic design using the Morris method. A negative difference $D_{50,pres} - D_{50,req}$ characterises failure, whereas a positive value indicates a sufficient armour stone diameter in-situ. A significant change in the scatter caused by a moderate change of the input parameter points to a larger importance of that parameter for the model output.

To evaluate the model implementation, (a) semi-probabilistic calculations with selected parameter sets from Table 5.2 are performed and compared with results of MAR (2008); (b) the probability of failure is derived from the model output statistics of the Morris analysis.

(a) For the semi-probabilistic calculations, a maximum required armour stone diameter of 220 mm is obtained. (b) The number of failures denoted by $g_{hydr} \leq 0$ is compared to the total number of failures. The Morris sample is used because, compared to Sobol indices, the sampling strategy is computationally more efficient, which allows to generate more values. For the analysis of the hydraulic model, the population, all samples of the Morris analysis, consists of 100 000 values. The analysis results in $p_f = 27.9\%$ for the probability of armour stone displacements. Considering the large variability of the input data and the small armour stone size in-situ ($CP_{90/250}$), the result is reasonable and an indication for the veracity of the model implementation. A fully probabilistic assessment should yield significantly smaller p_f values due to the uncertainty reduction, amongst others, resulting from the adequate choice of input parameters and their distributions.

5.3.2 Geotechnical design

Variability of the input variables

To determine the required armour layer thickness, the following input parameters are required: The range of the drawdown parameters, *drawdown height* z_a and *drawdown time* t_a are defined on basis of field observations (see Chapter 3) and design vessel passages summarised in MAR (2008). The *effective friction angle* ϕ' , the *unit weight of the soil* γ_B and the *hydraulic conductivity* k

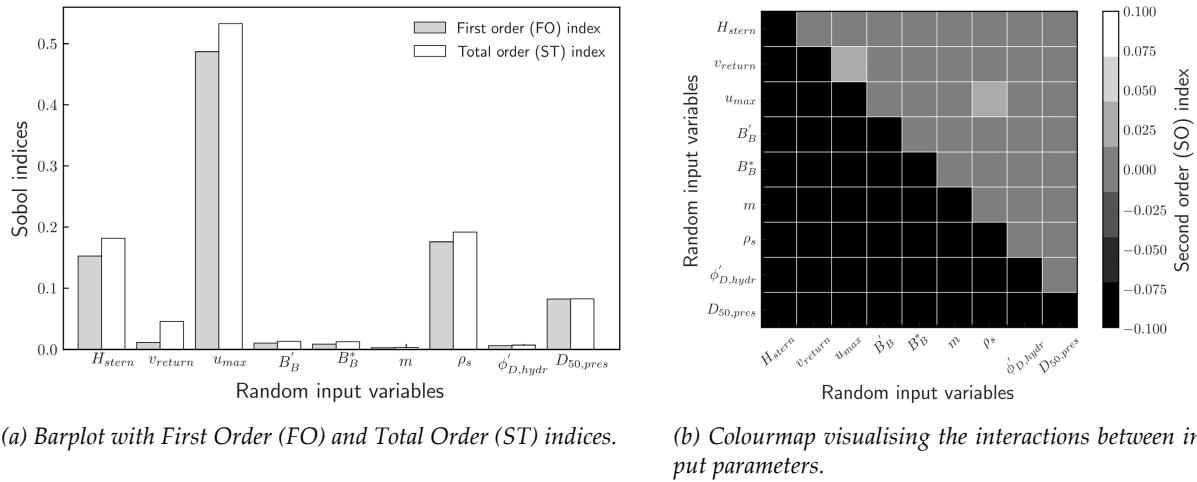


Figure 5.5: Results of sensitivity analysis of the hydraulic design using Sobol indices and $D_{50, pres} - D_{50, req}$ as model output. White squares indicate a strong variable interaction, black squares indicate minor to no variable interaction.

are generally obtained from cone penetration tests, drilling and subsequent laboratory investigations. For the presented sensitivity analyses their parameter range is defined on basis of EAU (2012) for a silty sand, which is a common material type along waterways. The definition, thus, assumes that at least the soil type is known during design or assessment.

The armour layer thickness is a function of the *slope inclination* m , the *density of armour stones* ρ_s and the *porosity of the armour layer* n_r , which depends on the type of revetment construction. For instance, when armour stones are dumped under water, the porosity ranges between 50.0 % and 55.0 %, whereas for material packed by hand, a low porosity ranging between 30.0 % to 40.0 % is observed (GBB, 2010). For all of the above mentioned variables, the minimum and maximum as outlined in GBB (2010) are assumed for sensitivity analyses. If there is only one value provided, the minimum and maximum is estimated based on expert knowledge.

The range of the *in-situ armour layer thickness* $d_{D, pres}$ is based on MAR (2008) recommendations which demand 0.60 m of armour layer thickness for silty sand without additional weight of a geotextile. Experience in construction shows that an installation accuracy of about 5 cm can be achieved. Consequently, the variability of $d_{D, pres}$ represents the installation accuracy. Table 5.4 summarises the investigated parameter ranges.

Table 5.4: Ranges of variables employed in the sensitivity analysis of the geotechnical design.

	t_a	z_a	ϕ'	γ'_B	k	ρ_s	n_r	m	$d_{D, pres}$
	s	m	°	kN m^{-3}	m s^{-1}	kg m^{-3}	–	–	m
MIN	2.00	0.05	30.00	9.00	5×10^{-6}	2300.00	0.30	2.50	0.55
MAX	80.00	0.80	35.00	12.00	5×10^{-5}	3000.00	0.55	3.50	0.65

Results of the sensitivity analysis

The results of the Morris analysis for the geotechnical design are displayed in Table 5.5 and Figure 5.6. Likewise to the hydraulic design, the analyses are conducted with regard to the limit state function g_{geo} . A negative difference $d_{\text{D,pres}} - d_{\text{D,req}}$ characterises failure, whereas a positive value indicates a sufficient armour layer thickness.

Contrary to the hydraulic design, the Morris parameters calculated for the geotechnical design (see Table 5.5) are less informative. Besides for z_a , μ^* ranges for all parameters below 1.0. Moderate σ values do not indicate significant second or higher order effects. Negligible to none interactions of $d_{\text{D,pres}}$ with other parameters are indicated by $\sigma(d_{\text{D,pres}}) = 0.000$. This corresponds to the design model which assumes $d_{\text{D,pres}}$ as independent resistance parameter. Ranked by their μ^* values, the load parameters z_a and t_a are the most significant parameters; the soil characteristics k , m , γ_B , ρ_s and ϕ' contribute moderately to the variability of the model output and the effect of the variability caused by $d_{\text{D,pres}}$ is low.

Table 5.5: Morris test statistics of geotechnical design with μ and μ^* as mean of the elementary effects, μ^*_{conv} as confidence interval of μ^* and σ as standard deviation of the elementary effects.

Parameter	μ^*	μ	μ^*_{conv}	σ
Drawdown time t_a	0.576	0.139	0.027	0.689
Drawdown height z_a	1.050	-0.223	0.041	1.267
Effective friction angle ϕ'	0.140	0.140	0.009	0.163
Unit weight of soil γ_B	0.116	0.006	0.005	0.143
Hydraulic conductivity k	0.356	0.039	0.017	0.452
Armour stone density ρ_s	0.168	0.168	0.009	0.160
Porosity n_r	0.180	-0.180	0.010	0.172
Slope inclination m	0.255	0.244	0.019	0.286
Armour layer thickness $d_{\text{D,pres}}$	0.100	0.100	0.000	0.000

Figure 5.6 shows the model output of the geotechnical design as a function of the input parameters obtained from the Morris analysis. The drawdown parameters z_a and t_a seem to affect g_{geo} the most; with larger z_a , the scatter seems to rise linearly indicating a ‘safer’ design. Interestingly, at the lower end of the inspected parameter range $0.05 \text{ m} \leq z_a \leq 0.25 \text{ m}$, the graph shows that the difference of $d_{\text{D,pres}} - d_{\text{D,req}}$ increases towards failure. With increasing z_a , $d_{\text{D,pres}} - d_{\text{D,req}}$ decreases until it reaches a minimum at which failure is the least likely at approximately 0.25 m from where it rises again. A similar, albeit not as pronounced behaviour, can be observed for t_a . This behaviour may be explained by the combination of t_a and z_a required to reach a quasi-stationary state. It may also depend on the soil permeability. Subsequent chapters pursue this observation in more detail. Meanwhile, the results highlight the necessity to explore the full variable space to detect relevant drawdown combinations. For the remaining parameters, the output variability cannot clearly be attributed. From the results of the Morris analysis it is inferred that the variability of the geotechnical design depends on a variety of input parameters. On the basis of Morris analysis, thus, none of the parameters considered can be excluded from the subsequent sensitivity analysis with Sobol indices.

Figure 5.7 visualises the results of the Sobol sensitivity analysis, which confirm the results of the Morris method. The Sobol first order (FO) and total order (ST) indices shown as barplot in Figure 5.7a emphasise that t_a and z_a contribute the most to the variability of the model output. In addition, the ST indices attribute a strong influence of the interaction of these two variables on the model output. As shown by the white square in the simplified colourmap

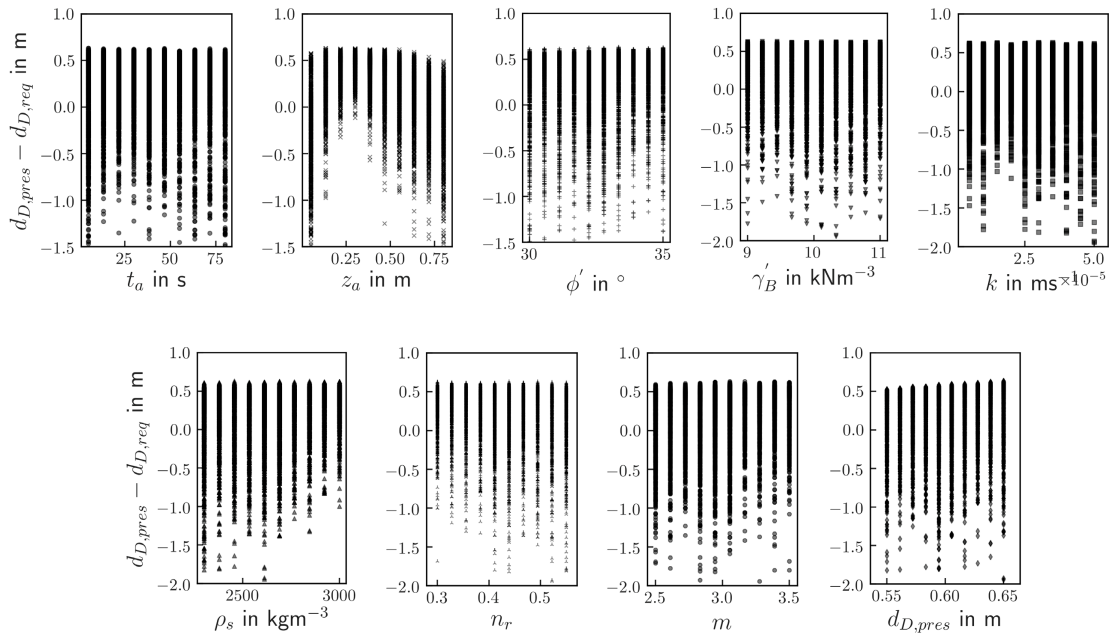


Figure 5.6: Results of the sensitivity analysis of the geotechnical design using the Morris method. The difference between in-situ and required armour layer thickness $d_{D,pres} - d_{D,req}$ serves as reference value with negative values indicating failure. A significant change in the scatter caused by a moderate change of the input parameter points to a larger importance of that parameter for the model. The current investigations do not take a toe support into account, which can reduce the required armour layer thickness by 0.60 m to 0.90 m.

(Figure 5.7b), this is mainly caused by the interaction between t_a and z_a . The remaining random input variables of the geotechnical design show a minor contribution to the variance of the model output. The combination of z_a and k affects the model moderately. For now, it is concluded that z_a , t_a and their combination have the greatest influence on the required armour layer thickness. Moreover, due to parameter interactions, which concerns k in particular, soil characteristics may have to be considered as random variables in design. For a fully probabilistic revetment design, the slope inclination m may have to be added to the set of random variables.

Again, to evaluate the correct implementation of the design equations, (a) semi-probabilistic calculations with selected parameter sets from Table 5.4 are performed and compared with results of MAR (2008); (b) the probabilities of failure are investigated using the model output of the Morris analysis.

(a) For the semi-probabilistic calculations, a maximum required armour layer thickness of 1.5 m is obtained. (b) Based on 100 000 Morris samples, the probability of failure is investigated separately for liquefaction and slope sliding. The analysis indicates that in approximately 72.0 % of the investigated variable combinations, failure is caused by slope sliding. For the remaining combinations liquefaction causes failure. Assuming an armour layer thickness ranging between $d_{D,pres} = 0.55 \text{ m} - 0.65 \text{ m}$, the total probability of failure amounts to $p_f = 84.5\%$. However, it must be considered that the presented analyses do not include a toe support. Based on exemplary calculations with a toe support, it can be assumed that a toe support reduces the required armour layer thickness by 0.60 m to 0.90 m resulting in a significantly lower p_f . Furthermore, as already outlined for the hydraulic design, p_f values obtained for a fully probabilistic assessment should be smaller due to the uncertainty reduction resulting from the choice of suitable,

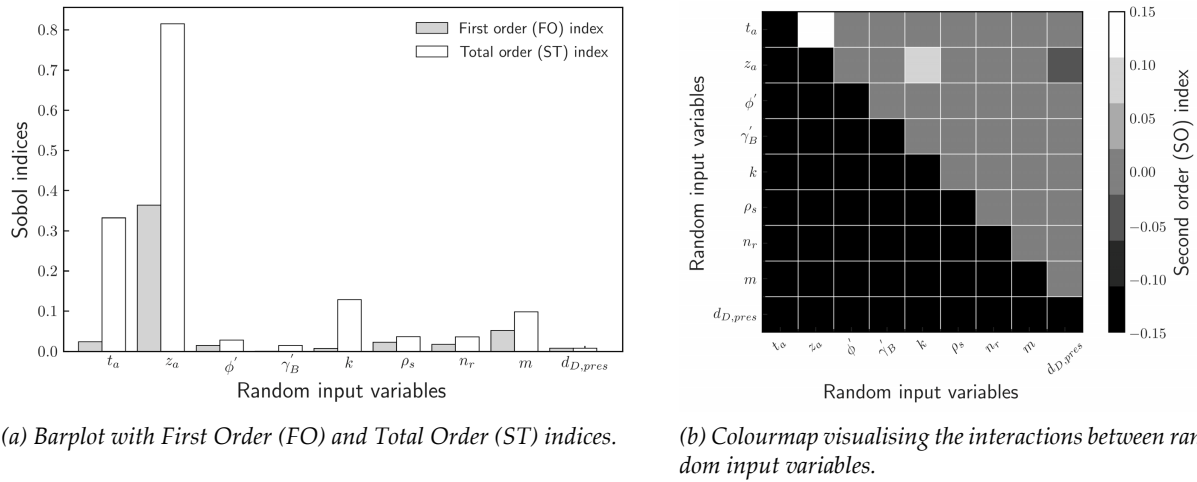


Figure 5.7: Results of sensitivity analysis of the geotechnical design using Sobol indices and d_D as model output. White squares indicate a strong variable interaction, black squares indicate minor to no variable interaction.

location-specific distributions and correlations for the input parameters. The model implementation is therefore considered valid.

5.4 Discussion

Since this thesis focuses on the description of uncertainties inherent to actions and material parameters required for a revetment design, the presented sensitivity analyses solely consider hydraulic loads, material parameters and geometrical data as model input. Parameters describing vessel passage, i. e. vessel velocity and dimensions, from which in turn hydraulic loads are determined, are not considered. Such an approach would lead to an extension of the current simulation model, which would introduce additional uncertainty resulting from different assumptions inherent to the extended calculation framework, e. g. simplified cross-section geometry, empirical parameter describing the vessel shape. Accordingly, further investigations are required for a model extension.

In the case of the hydraulic design, the employed model includes different assumptions such as a weighting system of hydraulic loads and the damage factors B'_B and B_B^* . These procedures reduce the transparency of the model output with regard to the model input. For example, the weighting system may prevent actual damaging actions from being identified. The empirical factors already include a certain amount of maintenance in the final design. For the sensitivity analysis, the information may not be of direct relevance since the empirical factors are of minor importance for the design result. However, if used in a probabilistic assessment, attention should be paid to the choice of target reliabilities.

The analyses assume a slope, alternative cross-section types such as a trapezoidal profile are not considered. With this simplification, common constructions of bank revetments are covered. For constructions with sheet piling and other cross-sectional areas, additional considerations may be required. Additionally, the standard design of newly built revetments as specified by MAR (2008) comprises a toe support, which significantly reduces the required armour layer

thickness due to the activation of additional supporting shear stresses. The current investigations do not take a toe support into account. Such a simplification is reasonable, as the sensitivity analysis conducted in this thesis aims at identifying input parameters which are valid for a large number of revetment constructions. Older revetment constructions, which maintenance focuses on, either rarely have a toe support or it is unclear what condition the toe support is in. If a toe support exists, additional failure mechanisms must be considered. In this case, the importance of specific soil characteristics such as γ_B and ϕ' may have to be re-evaluated for revetments with toe support.

From the sensitivity analyses it is concluded that the hydraulic loads and their combination have the strongest influence on the required armour layer thickness. Moreover, the analyses point to a strong interdependency of t_a and z_a regarding the model output. The significance of the soil mechanical properties can be regarded as almost negligible compared to the draw-down parameters. On a physical level, this observation is consistent, however, places increased demands on the description of the input parameters.

Soil parameters are not only characterised by their point statistics but also vary spatially. The employed methods of sensitivity analysis do not account for the spatial variability of soil properties. Further investigations are necessary to investigate this aspect in detail.

In addition, the applied methods of sensitivity analysis do not account for parameter correlation. Thus, the choice of input parameters should not solely depend on the sensitivity analyses. Parameters that are related to significant input parameters should also be included as random parameters, since a correlation may affect the variability of the model output.

The sensitivity measures, the semi-probabilistic calculations and the determined p_f values allow to evaluate whether the selected design models are implemented correctly. The core of the model, i. e. the underlying equations, is not reviewed, as this process is part of the development of design equations which is beyond the scope of this thesis. Since a similar contribution of failure mechanisms to the exceedance of the limit state functions as found in the expert interviews (see Chapter 4) is observed, and the sensitivity measures and semi-probabilistic calculations meet the expected values, the models are assumed to be correctly implemented. They can therefore be used for subsequent uncertainty and reliability analyses. It is stressed that the determined p_f values do not provide information about the actual p_f of a revetment, which must be calculated individually for each structure considering local boundary conditions.

5.5 Conclusions

Identification of input parameters

- Which parameters should be included in a reliability-based revetment design?*

The presented sensitivity analyses examine the variability of the model output with regard to a number of input parameters. Geotechnical and hydraulic design are considered as two independent models.

The output variance of the hydraulic design is strongly affected by H_{stern} , u_{max} , ρ_s and moderately by $D_{50, \text{pres}}$ and v_{return} . It is, thus, required to find and describe distributions and correlations of these variables. Furthermore, uncertainties, i. e. transformation uncertainty and statistical uncertainty, inherent to these parameters must be investigated. For reliability-based

assessments or designs in particular, it is recommended to reduce the number of empirical factors such as B'_B and B_B^* to a minimum. The internal weighing system should be omitted to examine the significance of individual input parameters.

The sensitivity analyses of the geotechnical model show that the hydraulic loads affect the required armour layer thickness the most. Moreover, the analyses point to a strong interaction of t_a and z_a and a moderate interaction of z_a and k . Due to their interaction, drawdown parameters must be considered as a set of parameters which cannot be varied one at a time without significant effects on the model output. For probabilistic considerations, this observation indicates that if the drawdown parameters are uncorrelated, which physical considerations and a recent study (Sorgatz and Kayser, 2020) imply, deterministic input parameters based on worst-case vessel passages should be used for design purposes. A best practice approach would investigate different drawdown combinations, i. e. based on field observations or MAR (2008), to identify worst-case combinations for local soil conditions. Furthermore, since the employed methods of sensitivity analysis do not allow to account for the spatial variability of soil properties and correlated parameters, it is recommended to consider at least ϕ' , γ_B and k as random variables in a probabilistic design approach.

6 | ADDRESSING STATISTICAL UNCERTAINTY: DISTRIBUTION PARAMETERS

'Anything you need to quantify can be measured in some way that is superior to not measuring it at all.'

–Gilb' Law

Contents

6.1	Introduction	94
6.2	Exploratory data analysis	94
6.2.1	Outliers	94
6.2.2	Distribution analysis	97
6.2.3	Correlation analysis	98
6.2.4	Summary of exploratory data analysis	100
6.3	Random sampling for sample size analysis	100
6.4	Uncertainty of load variables	103
6.4.1	Distribution type and parameters	103
6.4.2	Results of sample size analysis	103
6.5	Uncertainty of material parameters	107
6.5.1	Variation of distribution parameters for uncertainty analysis	107
6.5.2	Distribution type and parameters	107
6.5.3	Results of sample size analysis	108
6.6	Discussion	110
6.7	Conclusions	112

6.1 Introduction

Since field observations and subsequent data analyses required to determine hydraulic loads are neither standardised nor automated, they are time-consuming and expensive. Often, they are conducted for a very limited measurement period. On the resistance side, characteristic soil parameters are defined on the basis of standardised field and laboratory tests, which are limited in number for reasons of cost-effectiveness. Thus, uncertainties arise regarding the distributions and distribution parameters of loads and soil properties, which, in turn, affects the choice of characteristic values.

The following investigations aim at quantifying the statistical uncertainty and its effect on the armour stone diameter and the armour layer thickness. For this purpose, the available data introduced in Chapter 3 are first examined with respect to applicable distributions and correlations (Section 6.2). Subsequently, the statistical uncertainty of load variables and soil properties is investigated as a function of the sample size (Section 6.4 and 6.5). For this purpose, a procedure based on bootstrapping is developed, which is outlined in Section 6.3. Ensuring reliability analyses illustrate the effects of statistical uncertainty on the revetment design. Based on the results, recommendations regarding the least required measurement duration are provided. In addition, the integration of statistical uncertainty in current design procedures is discussed.

6.2 Exploratory data analysis

6.2.1 Outliers

Extreme values (low and high) that deviate significantly from the main data body are referred to as outliers (Dithinde et al., 2016). They may result from human error, measurement error and/or large natural deviations. If outliers are included in the final data evaluation, they may bias the calculated statistics. On the other hand, it is stressed that data points classified as outliers by standard methods of outlier detection may represent valid observations. Thus, it is strongly advised not to eliminate data without strong evidence of errors. Although a number of novel methods (Aggarwal and Yu, 2008; Yuen and Mu, 2012) are available, this thesis applies boxplots as a simple yet common method of outlier assessment.

The line in the box of the boxplot shows the median. The edges of the box describe the upper and lower quartiles. The position of the median within the box describes the skewness of the dataset. The length of the box corresponds to the interquartile range (IQR). The IQR indicates the interval width in which 50 % of the sample sorted by size are encompassed. The whiskers are a measure for 1.5 · IQR. Values that are mapped as points above and below the whiskers are defined as outliers.

Figure 6.1 provides an overview of the available data from which a similar range of H_{stern} and v_{return} for DEK-2006, KuK-2015 and WDK-2007 is observed. H_{stern} and v_{return} at SiK-2007 are significantly smaller. The measured t_a values of KuK-2015, SiK-2007 and WDK-2007 vary within a comparable range. For KuK-2015 in particular it is noted that H_{stern} is right skewed. In addition, from the larger size of box and whisker it is apparent that H_{stern} of KuK-2015 is characterised by a larger variability compared to the other campaigns. This may result from the smaller number of available measurements at KuK-2015. Additionally, the boxplots of H_{stern} and t_a show a

number of outliers indicated by the scatter points above the whiskers. However, when the data are skewed, points may be erroneously classified as outliers, since the outlier classification in boxplots is solely based on measures of location and scale and assumes a Gaussian distribution. As discussed later, this may not suit the data. For example, values at the tail of a Lognormal distribution are considered as outliers.

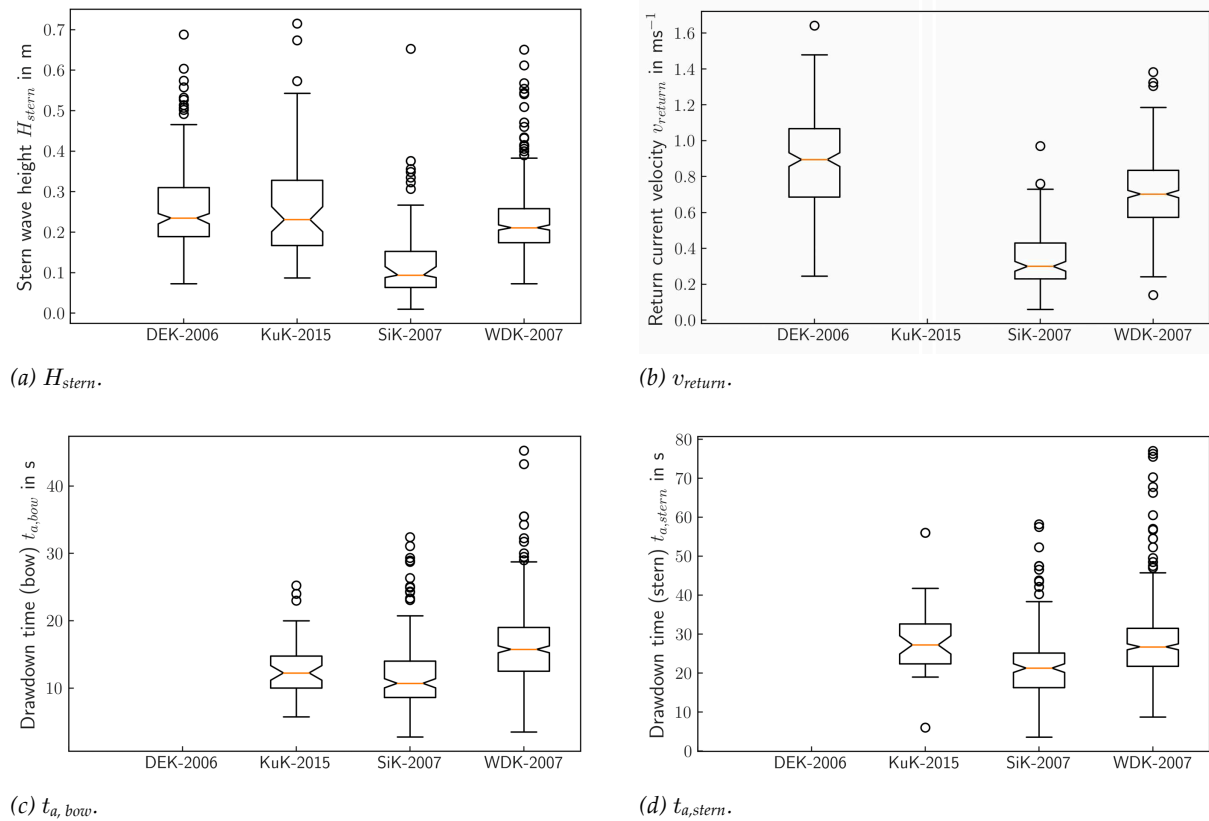


Figure 6.1: Boxplots of basic variables H_{stern} , v_{return} and t_a extracted from the field measurements. The line in the box of the boxplot shows the median. The edges of the box describe the upper and lower quartiles. The position of the median within the box describes the skewness of the dataset. The whiskers are a measure for $1.5 \cdot IQR$. Values that are mapped as points above and below the whiskers are defined as outliers.

The mean values of H_{stern} range between 0.09 m and 0.23 m; the standard deviation (std) takes values from 0.33 m to 0.74 m, resulting in a coefficient of variation (cov) between 1.60 and 2.00 for DEK-2007, KuK-2015 and SiK-2007. Only for SiK-2007 a larger cov = 8.0 is observed. The mean values of v_{return} range between 0.33 m s^{-1} and 0.88 m s^{-1} with std values of 0.15 m s^{-1} to 0.27 m s^{-1} . The corresponding cov values vary between 0.30 to 0.50. The mean values of t_a vary between 12.00 s to 28.00 s with cov values ranging between 0.30 and 0.47. Larger mean values are observed for $t_{a,stern}$, whereas larger cov values are observed for $t_{a,bow}$. It is stressed that in the case of t_a , a moderate or small t_a may cause larger excess pore pressures as larger t_a . Moreover, as discussed in Chapter 4, there is a strong interdependency between t_a and z_a . Since the criticality of drawdown is a function of drawdown velocity, drawdown height and hydraulic conductivity of the soil, contrary to wave height or flow velocity, the statistical description of the drawdown loads eschews information on the criticality of the observed drawdowns.

In detail, the detected outliers are displayed in Figure 6.2 as a function of vessel velocity v_s and

shore distance d_{shore} . Data is filtered for outliers using the approximate definition of outliers $\mu \pm 3\sigma$. Size and colour of the scatter correspond to outlier values (H_{stern} , v_{return} , $t_{a, \text{bow}}$ and $t_{a, \text{stern}}$). The observed outliers are characterised by high vessel velocity and/or moderate to high shore distance. In contrast to the boxplots, in Figure 6.2 a Lognormal distribution is assumed for H_{stern} and t_a , which reduces the number of observed outliers substantially. For v_{return} , on the other hand, the outlier analysis presented in Figure 6.2 is based on a Gaussian distribution as indicated by the boxplots.

Yet, based on these investigations, individual values still cannot be categorised as outliers. The observed outlier values, which are shown in each scatter point, are in similar and physically reasonable range. Compared to ‘standard’ design values provided by MAR (2008), the observed ‘outliers’ are in a reasonable range. MAR (2008) even recommends larger design values than the observed values for H_{stern} and v_{return} . Therefore, due to the limited number of observations, values that range within the MAR (2008) definitions and the lack of evidence regarding measurement errors, the outliers are not removed from the data.

The assessment highlights the importance of making both processed and raw data available to the consultant. Moreover, it is recommended to ensure data quality according to the framework discussed in Chapter 3 before storing it in a central database. Even if the evaluation of data validity only begins with the analysis, serious measuring errors or data that do not comply with pre-defined standards must be filtered in order to provide a consistent data basis which does not solely depend on the judgement of the individual engineer.

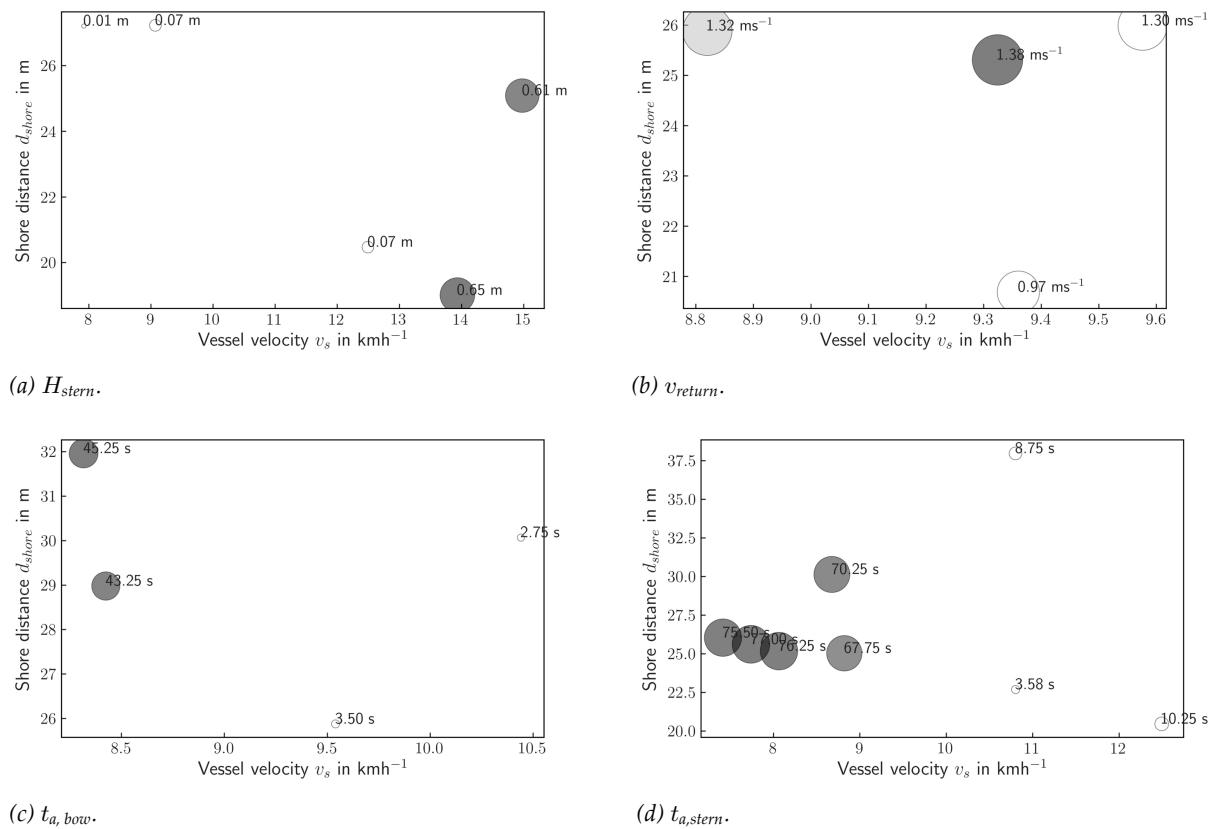


Figure 6.2: Outliers of basic variables H_{stern} , v_{return} and t_a ; H_{stern} and t_a are considered as lognormally distributed. Data is filtered for outliers defined as $\mu \pm 3\sigma$. Size and colour of the scatter correspond to outlier value, whereby the different waterways are considered separately. Numbers in each scatter point represent the outlier values.

6.2.2 Distribution analysis

The realisation of a variable derived from measurements happens within a range of possible yet random values. Probability functions transfer these random values into a mathematical model. A discrete random variable is described by its probability mass function (pmf); a continuous random variable by its probability density function (pdf) (Ang and Tang, 2007). Mathematical definitions of frequently used probability functions and the corresponding terminology are provided in Appendix B.

To identify the most suitable distribution for a given finite sample, methods such as the Method of Moments Estimate (MME) or the Maximum Likelihood Estimate (MLE) are applicable. MME is based on the relation between the moments of the random variables, see Appendix B.1, and the parameters of a distribution. These relations allow determining the distribution parameters directly. MLE, in contrast, searches for the most likely value of a parameter. It is assumed that the likelihood of obtaining a value of a random sample corresponds directly to its probability function. A likelihood function defines the likelihood of obtaining a sample of a number of independent observations by random sampling. The maximum of this likelihood function is evaluated by partial differentiation with respect to the unknown distribution parameter. When there is more than one parameter to estimate, a set of likelihood functions, one for each parameter, is maximised (Ang and Tang, 2007).

The determined distribution with its parameters approximates the data best; although, it is still to be considered as a “best guess” and, therefore, referred to as point estimate. Depending on the distribution type and the available data it may under- or overestimate potential characteristic values at the lower or upper end of a distribution (van Gelder and Vrijling, 1997).

In order to validate the distribution choice, Goodness-of-Fit (GoF) tests are conducted, e. g. by means of visual tests such as comparative plots of theoretical and empirical probability functions, Q-Q and P-P plots, or by means of hypothesis tests. Hypothesis tests are methods of statistical interference, where, in the context of GoF tests, a sample is compared to a theoretical distribution. Common hypothesis tests are the Anderson-Darling (AD) test (Anderson and Darling, 1952; Stephens, 1974) and the Kolmogorov-Smirnov (KS) test (Kolmogorov, 1933; Smirnov, 1948) for continuous data and the χ^2 -test for discrete or categorical data. Additionally, the GoF can be assessed by the *Akaike-Information-Criterion* (AIC, Akaike (1998)) and *Bayesian-Information-Criterion* (BIC, Schwarz (1978)), which evaluate the GoF by comparing different distributions fitted into the same data. An overview of distribution fitting methods together with quality assurance methods is provided by Figure 6.3. Appendix F.1 explains the hypothesis tests in more detail.

Figure 6.4 shows the results of the distribution analysis for the investigated example campaigns. Besides the visual apparent distribution type, it summarises mean, std, number of available samples (N) and GoF, which is assessed by means of the AD test for a significance level of 5%. For lognormally distributed data, the log(variable) is assessed. If the first value, the test statistics, is smaller than the second value, the critical test value, the data follows the applied distribution type. Based on a number of hypothesis tests (see also Appendix F.1), the analysis of distribution types suggests that H_{stern} is lognormally distributed, whereas v_{return} is best approximated by a Gaussian distribution.

A comprehensive summary of all test statistics is provided in Appendix F.1. Therefore, below, only selected, particularly noteworthy test statistics are discussed in detail.

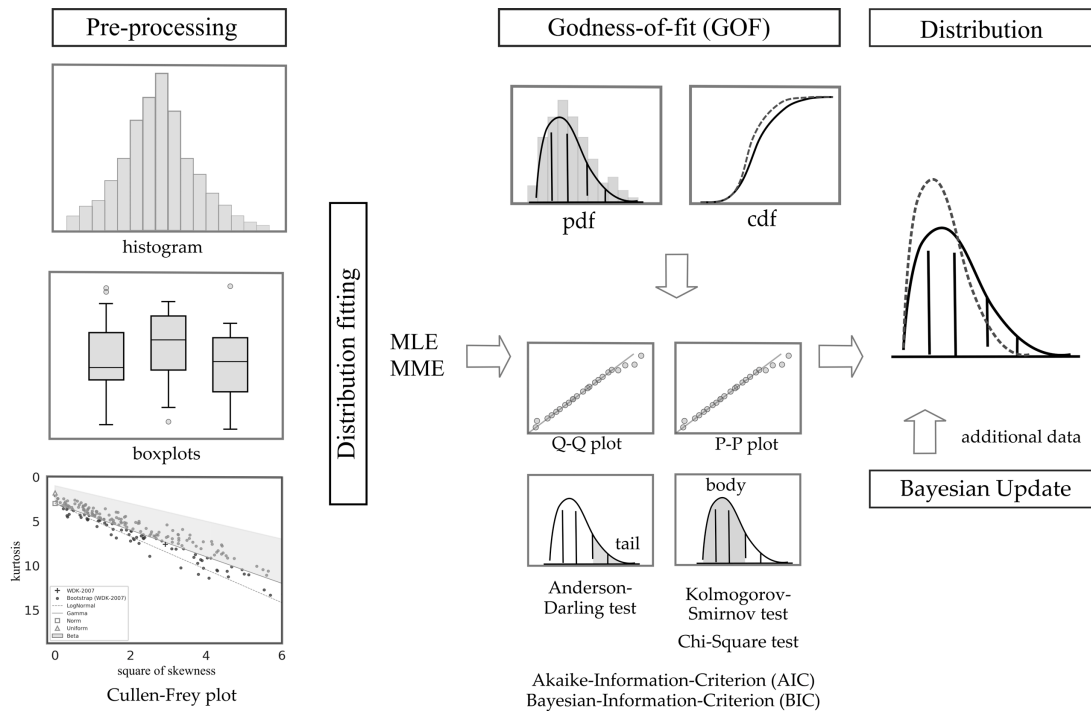


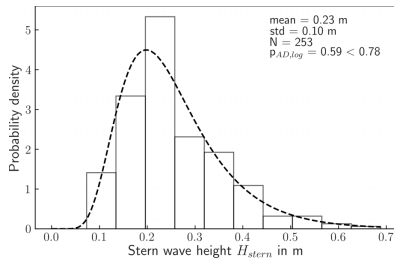
Figure 6.3: Common methods of distribution fitting presented in a potential workflow which may standardise the fitting process.

In the case of H_{stern} of WDK-2007, the test against a Lognormal distribution with the AD test fails, while the KS test indicates that the Lognormal distribution is the most suitable choice as shown by the test results summarised in Table F.21. The test result of 0.054 is slightly higher than the required test statistics of 0.045 for a significance level of 5%. BIC and p-value of the χ^2 -test confirm the choice of the Lognormal distribution. It can therefore be concluded that a Lognormal distribution approximates the body of H_{stern} of WDK-2007 well, while a heavier skewed distribution like a Gamma distribution may be more suitable for the tail. For v_{return} of SiK-2007, the AD test of normality fails, whereas the KS test is successful with a test result of $0.062 < 0.077$. Again, a heavier skewed distribution may approximate the tail slightly better than the Gaussian distribution, whereas the Gaussian distribution suits the distribution's body best.

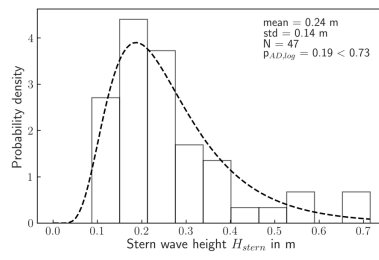
The currently available drawdown parameters do not allow for conclusions regarding suitable distributions; z_a could possibly be approximated by a Johnson or Lognormal distribution, t_a can, at present, only be reasonably represented by a uniform distribution. Further investigations are required in order to characterise the statistics of these parameters.

6.2.3 Correlation analysis

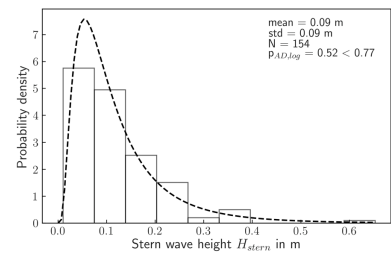
If a model requires more than one input variable, the dependence between variables must be described mathematically. An unconditional dependence of several variables can be described by multivariate probability functions. However, since these are difficult to construct and data on multivariate correlation are rare, the dependence is often reduced to bivariate observations. The linear relationship of two variables is evaluated by the Pearson correlation coefficient ρ_P , which varies within the limits of $[-1.00, 1.00]$. (Ang and Tang, 2007; Baecher and Christian,



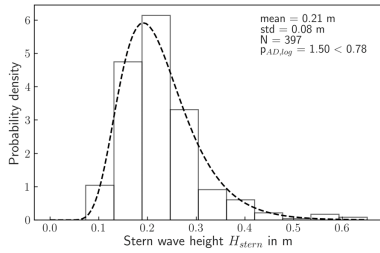
(a) DEK-2006, H_{stern} , Lognormal dist.



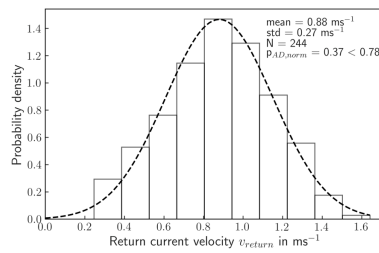
(b) KuK-2015, H_{stern} , Lognormal dist.



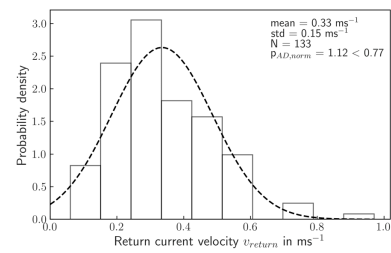
(c) SiK-2007, H_{stern} , Lognormal dist.



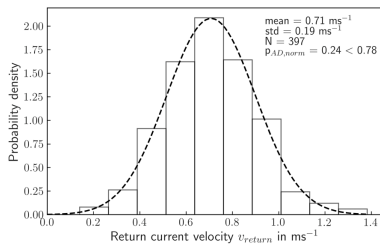
(d) WDK-2007, H_{stern} , Lognormal dist.



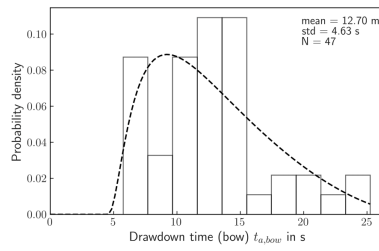
(e) DEK-2006, v_{return} , Gaussian dist.



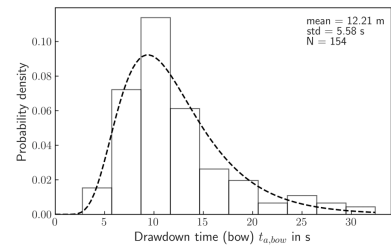
(f) SiK-2007, v_{return} , Gaussian dist.



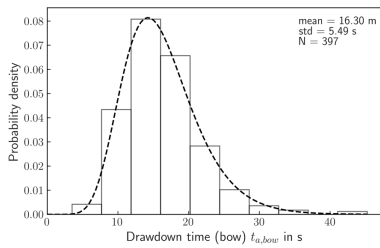
(g) WDK-2007, v_{return} , Gaussian dist.



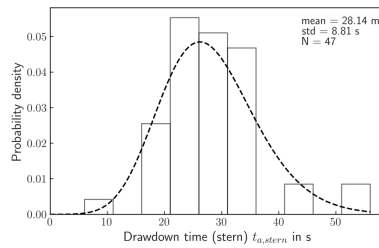
(h) KuK-2015, $t_{a,bow}$, Johnson dist.



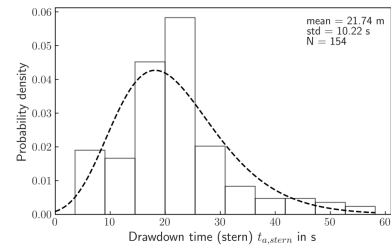
(i) SiK-2007, $t_{a,bow}$, Johnson dist.



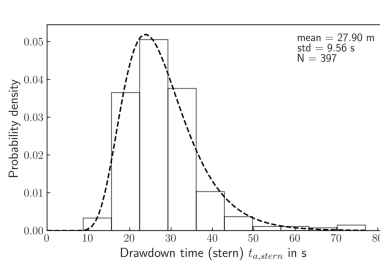
(j) WDK-2007, $t_{a,bow}$, Johnson dist.



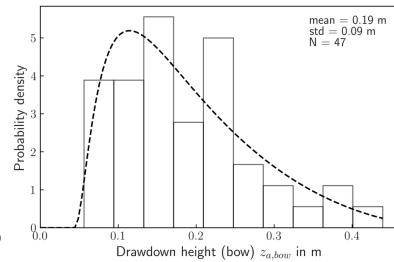
(k) KuK-2015, $t_{a,stern}$, Johnson dist.



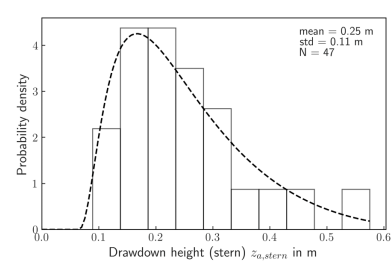
(l) SiK-2007, $t_{a,stern}$, Johnson dist.



(m) WDK-2007, $t_{a,stern}$, Johnson dist.



(n) KuK-2015, $z_{a,bow}$, Johnson dist.



(o) KuK-2015, $z_{a,stern}$, Johnson dist.

Figure 6.4: Probability functions fitted to the basic variables H_{stern} , v_{return} , t_a and z_a available from field measurements.

2003). A correlation is to be considered as moderate for $\rho_P > 0.4$, and as strong for $\rho_P > 0.6$ (Phoon and Ching, 2015). The same applies to negative correlation.

As an example, the correlation of H_{stern} and v_{return} is displayed in Figure 6.5, where $\rho_P = 0.69$ indicates a moderate linear relation. From the analysis it is deduced that the correlation coefficient may depend on the investigated data, e. g. for WDK-2007 $\rho_P = 0.58$ was identified, while for SiK-2009 $\rho_P = 0.71$ is observed. Information on the drawdown parameters is scarce. The analysis of the KuK-2015 measurements does not show a significant correlation of t_a and z_a . However, due to the limited number of samples, no definitive statement can be inferred. A summary of all determined correlation coefficients is provided in Appendix F.2. In short, the parameter set at different waterways is characterised by different correlation coefficients. Especially for the correlation of measured flow velocities it is difficult to establish a general trend. More research is required in this area.

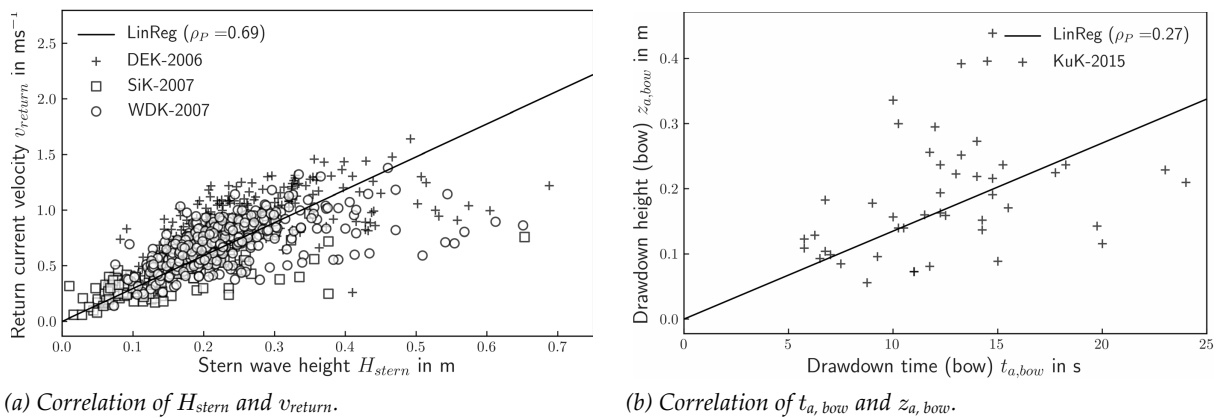


Figure 6.5: Correlation of basic variables available from field measurements.

6.2.4 Summary of exploratory data analysis

The results highlight that the choice of suitable distribution types, distribution parameters and correlations is - even after a thorough exploratory data analysis - ambiguous. For subsequent analysis, it is assumed that H_{stern} is lognormally and v_{return} normally distributed. Additionally, a positive correlation of H_{stern} and v_{return} is assumed.

The four example campaigns do not provide sufficient information on the drawdown parameters t_a and z_a as well as the slope supply flow u_{max} . Thus, in subsequent investigations, these parameters are either modelled as deterministic worst case estimates or based on calculations using observed vessel passages.

6.3 Random sampling for sample size analysis

To allow for a systematic investigation of uncertainty of distribution parameters, a methodology to compute the required sample size presented by Newman et al. (2000) is modified. The uncertainty of the sample size is passed through the model using a bootstrapping approach. Bootstrapping is a common non-parametric method for the assessment of errors in a statistical

estimation problem. In simple terms, bootstrapping assigns measures of accuracy (bias, variance, confidence intervals, prediction error, etc.) to sample estimates in order to obtain a sample that complies with predefined statistics (Efron, 1982; Efron and Tibshirani, 1993). Comparable investigations exist, amongst others, for the analysis of extreme events, the fields of climatology and hydraulic engineering, e. g. Ebtehaj and Moradkhani (2009), Katz et al. (2002), Pandey et al. (2003) and van Gelder (2000).

Bootstrapping is distinguished into a *non-parametric* and *parametric* approach. The former randomly samples from a given sample with replacement, while the latter generates random samples for an underlying parametric distribution. Investigations by Kysely (2008) suggest that non-parametric bootstrapping underestimates the samples' variance for heavy tailed samples. Therefore, the presented investigations employ a parametric bootstrapping approach.

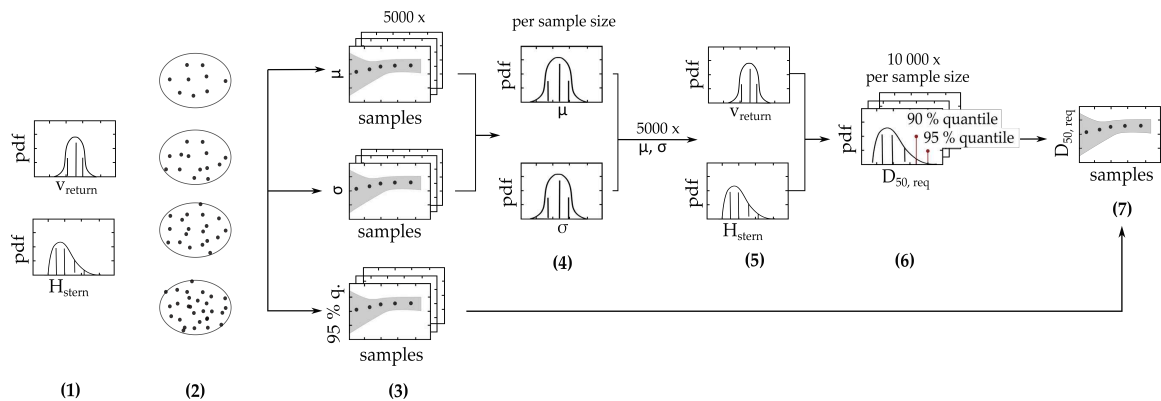


Figure 6.6: Proposed bootstrapping approach to assess distribution uncertainty.

Figure 6.6 displays the proposed workflow schematically. The underlying code is graphically illustrated in Figure 6.7. A full code documentation is available in Appendix E.1. The following steps are implemented in a Python-based simulation:

- (1) Firstly, a large number of samples is drawn from a given pdf, which is assumed to represent a "perfect" observation.
- (2) Secondly, the random sampling procedure is started. A limited number of samples is drawn randomly from the "perfect" observation. The term "random" refers to a pseudo-random number generation, which is based on the Mersenne-Twister algorithm (Saito and Matsumoto, 2008). The samples are drawn without replacement in order to approximate the field observations as a random series of measurements.
- (3) Subsequently, the first moments of the subset sample are calculated. The workflow is repeated 5000 times to obtain the variability of the underlying distribution parameters at different sample sizes.

The technical procedure is illustrated in Figure 6.7a with `sample_load` referring to the "perfect" observation and `no_samples` to the number of samples drawn from the "perfect" observation. The command `random.choice` provides a random sample of defined size from the previously specified pdf, while `random.normal` or `random.lognormal` generates a pdf with the specified distribution parameters. In the inner loop the moments of the `sample` and, subsequently, the underlying `dist_params` are determined. The outer iteration yields the pdf of the underlying distribution parameters `dist_params_no` and moments `moments_no` for each `no_samples`.

The propagation of the statistical uncertainty through the design model for revetments is, amongst others, affected by the importance of the input parameters (see Chapter 5). In order to quantify the effects of distribution uncertainty on the actual revetment design, the random sampling approach is extended as follows:

- (4) For each sample size, a Gaussian probability density function(pdf) is fitted to the distribution parameters μ and σ obtained from (3) by MLE.
- (5) The Gaussian pdf are used to draw 5000 samples of $\mu_\mu, \mu_\sigma, \sigma_\mu$ and σ_σ . Each parameter set, (μ_μ, σ_μ) and $(\mu_\sigma, \sigma_\sigma)$, characterises the underlying pdf of μ and σ , which, in turn, provide the basis for the pdf of the random input variables.
- (6) Finally, 10 000 MCS are run to determine the variability of the required armour stone diameter or armour layer thickness with the uncertain probability density functions as input. The choice of 1000 distribution parameters and 10 000 MCS was considered as a reasonable compromise between model performance and model accuracy.
- (7) This procedure is repeated for each sample size in order to determine the effect of the sample size on the armour stone diameter or armour layer thickness.

The technical procedure of the second part of the analysis is shown in Figure 6.7b. The distribution parameters of the underlying pdf are denoted by μ_{1_dist} , μ_{2_dist} , σ_{1_dist} and σ_{2_dist} . They define the distribution parameters, $dist_mu$ and $dist_sigma$, which, in turn, build the distribution of a basic variable $dist_load$. In the case of the hydraulic design, the variables H_{stern} and v_{return} are considered as random in the analyses. D_{50} is a function that encompasses the stability analysis against armour stone displacements. The sample size analysis of the geotechnical design is evaluated in the same way as described for the D_{50} ; k and ϕ' are considered as random variables.

```

sample_load = random.lognormal(size=2000)
no_samples = ([10, 20, 50, 75, 100, 250, 500, 750, 1000, 1500, 2000])
For no in no_samples:
  For i = 1:5000:
    sample = random.choice(replacement=False)
    moments (sample)
    dist_param (sample)
  End
  dist_param_no, moments_no
End

```

(a) Random sampling scheme (part I)

```

no_samples = ([10, 20, 50, 75, 100, 250, 500, 750, 1000, 1500, 2000])
For no in no_samples:
  mu1_dist = random.choice (dist_param_no[no], size=5000)
  sigma1_dist = random.choice (dist_param_no[no], size=5000)
  mu2_dist = random.choice (dist_param_no[no], size=5000)
  sigma2_dist = random.choice (dist_param_no[no], size=5000)
  For i = 1:5000:
    dist_mu = random.normal(mu1_dist[i], sigma1_dist[i])
    dist_sigma = random.normal(mu2_dist[i], sigma2_dist[i])
    dist_load = random.lognormal(dist_mu[i], dist_sigma[i])
    For i = 1:10000:
      D50 = StabilityAnalysis(dist_load)
    End
  End
End

```

(b) Random sampling scheme (part II)

Figure 6.7: Calculation procedure to investigate the effects of statistical uncertainty using the example of hydraulic revetment design.

6.4 Uncertainty of load variables

6.4.1 Distribution type and parameters

Although the proposed methodology is applicable to all kinds of parameters observed in the field, u_{\max} , z_a and t_a are not included in current analyses, as the available field observations do not provide sufficient information regarding parameter statistics and applicable distributions. This once more emphasises the importance of sufficient data for uncertainty or reliability analyses. If the weighing system described in GBB (2010) is applied, $u_{\max} = 1.25 \text{ m s}^{-1}$ and $H_{\text{sec}} = 0.08 \text{ m}$. This order of magnitude corresponds approximately to the mean values of these quantities, which is supposed to neither over- nor underestimate the contribution of u_{\max} and H_{sec} to the final result.

In the context of this thesis, only the uncertainties resulting from H_{stem} and v_{return} are investigated using the existing data. Following the results of the exploratory data analysis, H_{stem} is approximated by a Lognormal and v_{return} by a Gaussian pdf. For demonstration purposes, the mean values correspond to the WDK-2007 data, while the cov values vary within the ranges assessed in the exploratory data analysis. A summary of the investigated parameter combinations is given in Table 6.1.

Table 6.1: Distribution and their parameters employed in the analysis of statistical uncertainty inherent to hydraulic revetment design.

Parameter	Probability function	μ	$\sigma_1, \sigma_2, \sigma_3$	COV ₁ , COV ₂ , COV ₃
H_{stem}	Lognormal	0.2 m	0.1, 0.3, 0.6	0.5, 2.5, 3.0
v_{return}	Gaussian	0.7 m s^{-1}	0.14, 0.21, 0.28	0.2, 0.3, 0.4

6.4.2 Results of sample size analysis

Effects of sample size on distribution uncertainty

The uncertainty of the underlying distribution parameters μ and σ as a function of the sample size can be observed in Figure 6.8. The grey shaded areas refer to the 5 % and 95 % quantiles of the determined samples of μ and σ . An increasing number of samples leads to an exponentially decreasing statistical uncertainty, albeit a larger cov always results in larger uncertainty. Figure 6.8 also points to a deficiency as a result of the choice of a Gaussian distribution for the underlying distribution parameters: $\mu_{H_{\text{stem}}}$ includes negative values, which are not considered in further stability calculations, though. The results suggest that approximately 250 observations may be required to find a Lognormal or Gaussian pdf that characterises the given data well, although the uncertainty related to the underlying distribution parameters is also a function of the cov. For larger cov, more measurements may be necessary.

Effects of distribution uncertainty on the armour stone diameter

In addition, the minimum required number of observations depends on the sensitivity of the input model regarding the input variables. H_{stem} and v_{return} may contribute differently to the

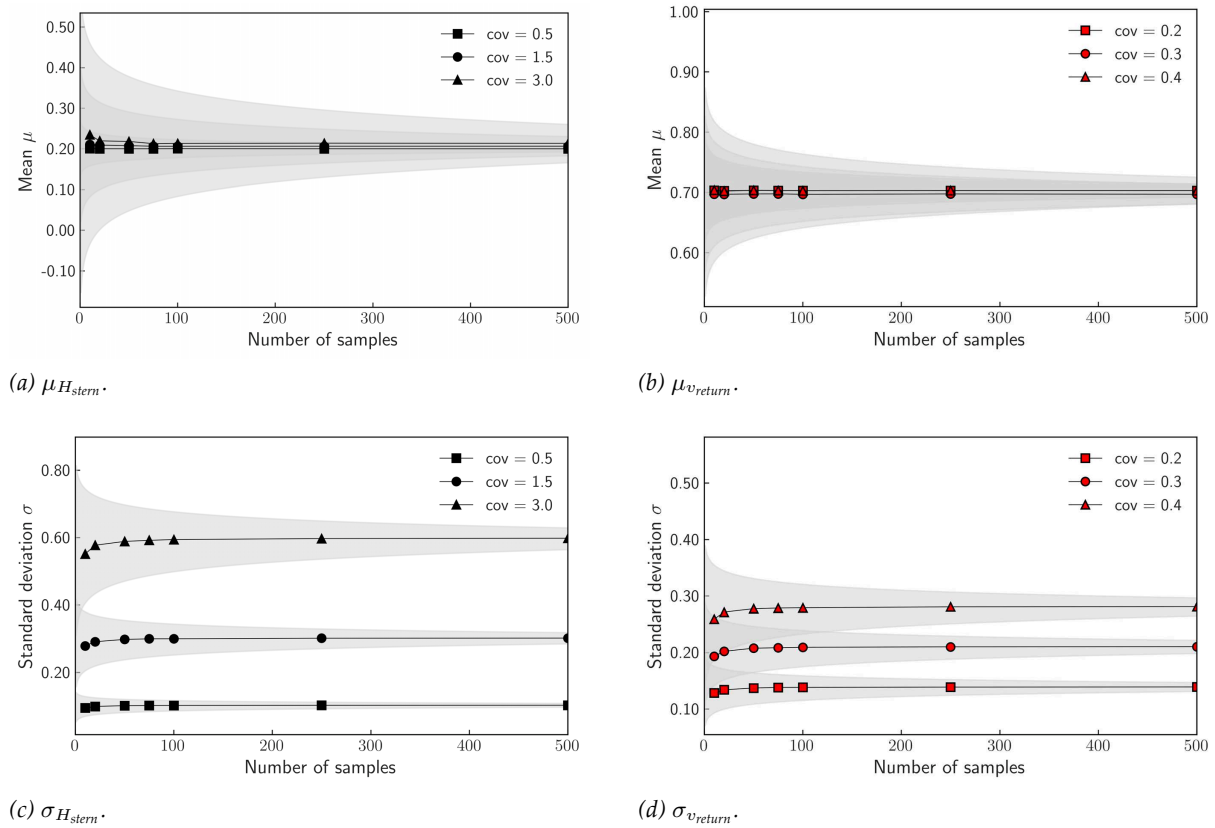


Figure 6.8: Uncertainty of distribution parameters of selected hydraulic loads as a function of the sample size. Each line represents a mean value. Corresponding 5% and 95% quantiles are shown as grey shaded areas.

total uncertainty of the revetment design. Figure 6.9 visualises the uncertainty of the required armour stone diameter as a function of the required sample size. Since the required armour stone diameter defines the design, the analysis focuses on the 95% quantile of the determined diameter and its 5% and 95% quantiles. To investigate the effects of each variable independently, the concept of weighing specified in GBB (2010) is omitted.

The results show that H_{stern} defines the required armour stone diameter under the assumptions of the presented investigations, e. g. Lognormal pdf and deterministic u_{max} . Again, an increasing number of samples reduces the uncertainty associated with the required armour stone diameter. For cov= 3.0 and 250 field observations, the determined armour stone diameter varies by approximately 40 mm for the lognormally distributed H_{stern} , whereas a moderate cov= 1.5 yields approximately 10 mm difference. Similar figures apply to v_{return} .

The graphs illustrate that despite statistical uncertainty, the required armour stone diameter approaches a constant uncertainty, which is a function of cov. The current analyses do not account for correlation between different hydraulic loads. In the case of the investigated parameters, the correlation is predominately positive. Moreover, it is stressed that the current analysis does not consider measurement uncertainty, which, however, should be negligible in comparison to the investigated statistical uncertainty.

If deterministic design methods are used in conjunction with field observations, the uncertainty resulting from small sample sizes would have to be compensated by means of partial factors. Table 6.2 shows the effect of the sample size a partial factor would have to account for in a

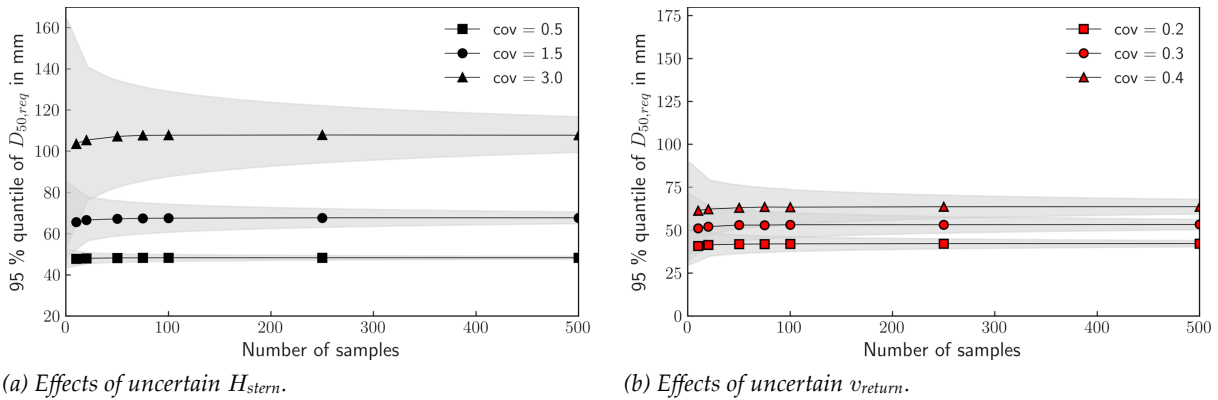


Figure 6.9: Effects of statistical uncertainty on the required armour stone diameter.

very simplified way using an additive factor. The additive factor is calculated as the difference between lower (5 %) and upper (95 %) confidence interval of the estimated 95 % quantile of $D_{50, req}$. The determined values are added to the initially calculated, deterministic armour stone diameter to ensure that the occurrence of extreme events is not underestimated. Naturally, especially for small cov, the additive factor is negligible. It is, however, of interest at the boundary between two armour stone classes, where the additive factor as a result of a small sample size would result in a larger armour stone class. Since revetments are line structures that cover larger areas, this may lead to significantly increased maintenance or construction costs. In addition, it must be noted that neither the addition of a factor nor the multiplication by a partial factor may supply a comparable safety level at different waterways.

Table 6.2: Additive factor relating statistical uncertainty to sample size derived from bootstrapping for different cov and sample sizes in mm. The results are based on $cov_{H_{stern}}$, since the current investigations indicate that it defines the required armour stone diameter. The factor may have to be adjusted after examining the effects of u_{max} .

Samples	10	20	50	75	100	250	500	750	1000	1500	2000
$cov_{H_{stern}} = 0.5$	5	3	2	2	2	1	1	1	1	1	0
$cov_{H_{stern}} = 1.5$	17	13	8	7	6	4	3	3	3	2	2
$cov_{H_{stern}} = 3.0$	52	37	26	22	19	13	10	9	8	7	6

Effects of distribution uncertainty on the probability of failure

To assess the effects of the statistical uncertainty on the probability of failure, the above presented case studies are evaluated with respect to the limit state functions as a function of the armour stone diameter. The following parameter combinations are investigated:

- H_{stern} : cov = 0.5, 1.5, 3.0; sample size=50, 250
- v_{return} : cov = 0.3, 0.4, 0.5; sample size=50, 250

For the armour stone diameter in-situ $D_{50, req}$ a Gaussian distribution $\mathcal{N}(\mu, 12)$ is assumed. The reliability assessment is then conducted for different mean armour stone diameters ranging from 30 mm to 180 mm, while the standard deviation is kept at a constant value. Following the guidelines outlined in Chapter 2, an annual $p_f = 0.05$ ($\beta_{HL} = 1.7$) is targeted for irreversible SLS

conditions and normal investment costs (JCSS, 2001). The probability of failure results from the number of failures over the total number of MC simulations.

Figure 6.10 shows the mean p_f as a function of the armour stone diameter. As expected from the results of the sensitivity analysis, H_{stern} governs the design. A larger variability of actions requires larger armour stones to achieve the same reliability level. Neither for H_{stern} nor for v_{return} the mean p_f is affected by the sample size indicated by the superimposed lines.

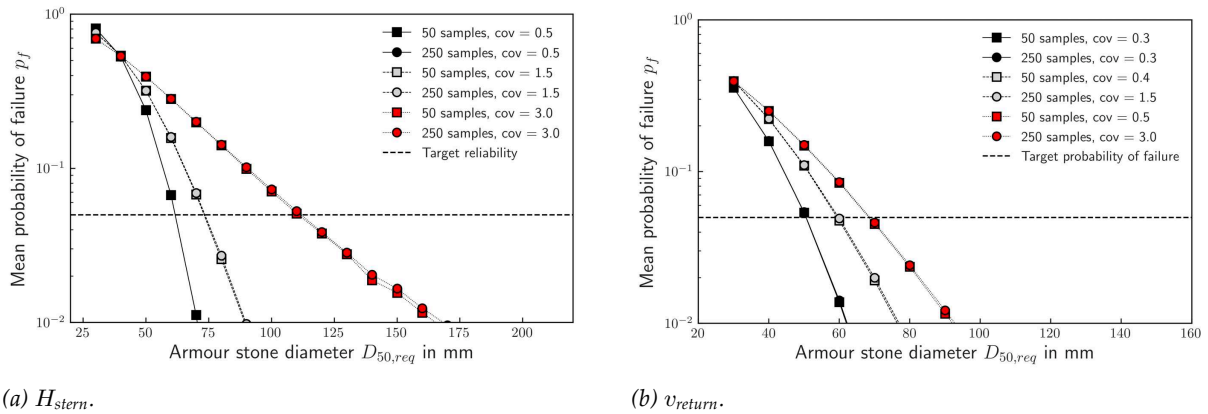


Figure 6.10: Mean probability of failure as function of the required armour stone diameter.

A different situation arises when the 95 % quantile of p_f is examined. Figure 6.11 shows the 95 % quantile of p_f as a function of the sample size. Considering $cov = 0.3$, p_f differs by a maximum of 5 % between a sample of 50 values and a sample of 250 values of H_{stern} . Similar observations are made for v_{return} .

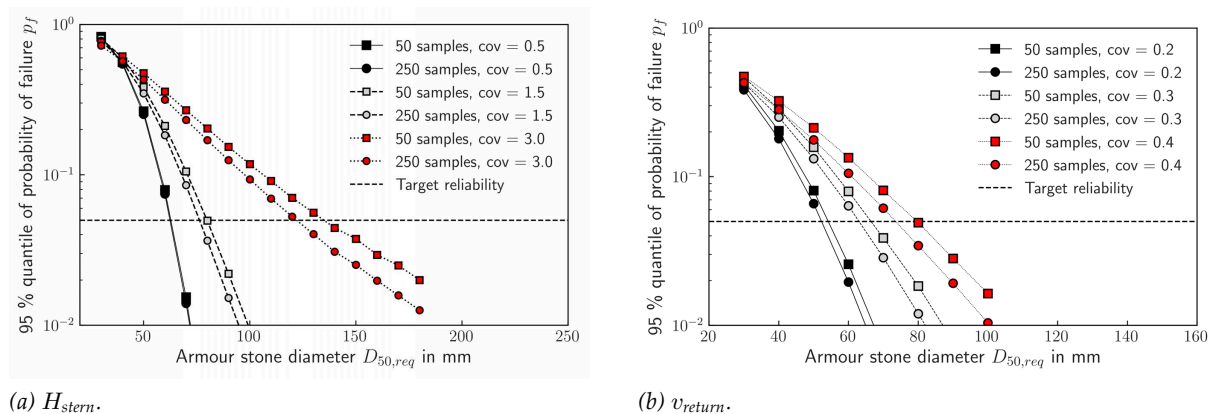


Figure 6.11: 95 % quantile of the probability of failure as function of the required armour stone diameter.

Comparing the results to the design specifications of MAR (2008), it is noticed that smaller armour stone diameters are required. The graphs illustrate that depending on the expected cov $D_{50, req} = 90 \text{ mm} - 150 \text{ mm}$ fulfils the target reliability, while MAR (2008) requires $D_{50, req} = 150 \text{ mm}$ to 180 mm . The results highlight the importance of evaluating the degree of conservativeness site-specifically and adapt revetment dimensions accordingly.

6.5 Uncertainty of material parameters

6.5.1 Variation of distribution parameters for uncertainty analysis

In the following section, the effect of statistical uncertainty of the material parameters on the geotechnical design is examined analogous to the investigations of the hydraulic loads. With respect to current test procedures of subsoil, a maximum sample size of 50 samples is defined, which exceeds the size of samples per soil type commonly available for revetment design approximately by a factor of 3. The main reason for the reduced sample size is the effort required for subsequent laboratory tests; each test result requires a laboratory test in addition to the efforts required for field testing. More advanced considerations may thus consider a combination of test methods, i. e. CPT, shear and triaxial test, by means of Bayesian methods.

6.5.2 Distribution type and parameters

Investigated soil types and drawdown combinations are selected based on the existing German design standards EAU (2012) and MAR (2008). Serving as an example, permeable sand (SW) and silty sand (SU) are investigated. The variability of the soil is expressed via the mean and the cov of each variable. The cov values are defined on the basis of the ranges provided by EAU (2012) for specific soil types. It is assumed that the upper and lower boundary represent approximately $\pm 2\sigma$ of a Lognormal distribution. Literature offers different potential distribution types for soil parameters, but as discussed in Sorgatz and Kayser (2020), the results of the most common distribution types, Gaussian and Lognormal distribution, do not yield a notable difference in the case of revetment design.

The analysis does not consider the spatial variability of soil parameters. Furthermore, due to the lack of representative drawdown measurements, the selected drawdown combinations are based on worst case assumptions of a vessel passage in a standardised rectangular trapezoidal profile of a waterway cross-section (MAR, 2008). From the load combinations available in MAR (2008), the most unfavourable are chosen. Merging load combinations and soil types, the four case studies summarised in Table 6.3 are investigated. In order to obtain realistic revetment dimensions, a toe support ($\tau_F = 1.5 \text{ kN}$) is taken into account. This results in armour layer thicknesses that are comparable to the standard revetment dimensions summarised in MAR (2008).

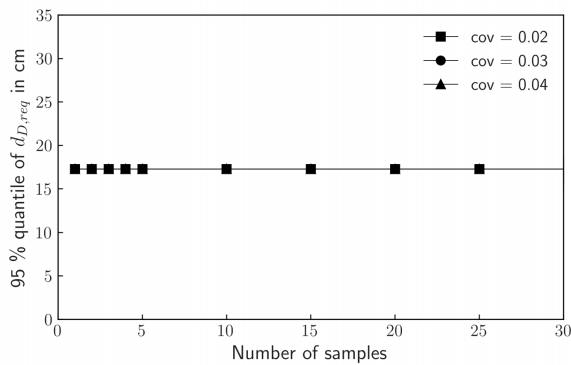
Table 6.3: Combinations of actions and soil parameters employed in the analysis of statistical uncertainty inherent to geotechnical design.

Soil type	ϕ'	cov	k	cov	γ'_B	t_a	z_a
–	°	–	m s^{-1}	–	kN m^{-3}	s	m
SW1 Sand, widely graded	32.5 - 37.5	0.01 - 0.04	$1 \times 10^{-4} - 1 \times 10^{-5}$	0.05 - 0.50	11.5	4.5	0.63
SW2 Sand, widely graded	32.5 - 37.5	0.01 - 0.04	$1 \times 10^{-4} - 1 \times 10^{-5}$	0.05 - 0.50	11.5	27.6	0.83
SU1 Silty sand	32.5 - 37.5	0.01 - 0.04	$1 \times 10^{-5} - 1 \times 10^{-6}$	0.05 - 0.50	9.5	4.5	0.63
SU2 Silty sand	32.5 - 37.5	0.01 - 0.04	$1 \times 10^{-5} - 1 \times 10^{-6}$	0.05 - 0.50	9.5	27.6	0.83

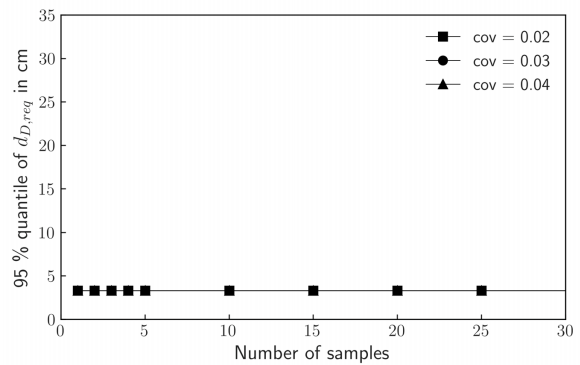
6.5.3 Results of sample size analysis

Effects of distribution uncertainty on the armour layer thickness

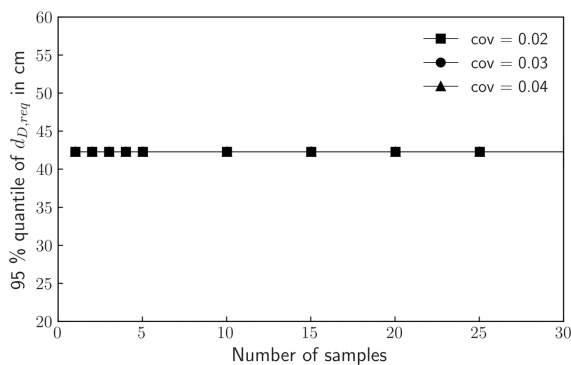
Solving the design equations with characteristic values at lower end of the selected parameter range reveals that the limit state of slope sliding, see eq. (2.4) in Chapter 2, governs the revetment dimensions. Figure 6.12 shows that the statistical uncertainty of the examined range of ϕ' does not affect the required armour layer thickness considerably. Additionally, for different $\text{cov}_{\phi'}$ the same armour layer thickness is obtained. In contrast to ϕ' , the uncertainty of k results in a maximum difference of 5 cm of armour layer thickness depending on soil type, drawdown combination, cov_k and the number of available samples (see Figure 6.13). With an increasing number of samples, the uncertainty decreases.



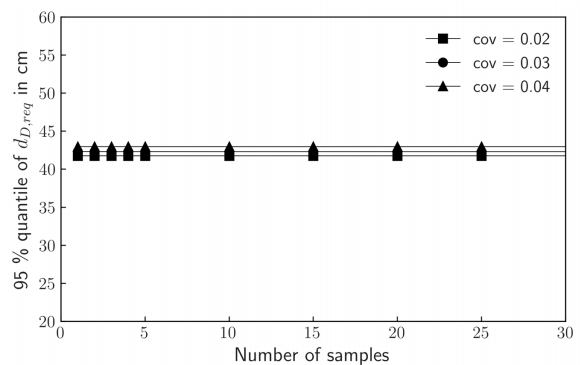
(a) B3 soil, Lognormal ϕ' , $t_a = 4.5$ s, $z_a = 0.63$ m.



(b) B3 soil, Lognormal ϕ' , $t_a = 27.6$ s, $z_a = 0.83$ m.



(c) B4 soil, Lognormal ϕ' , $t_a = 4.5$ s, $z_a = 0.63$ m.

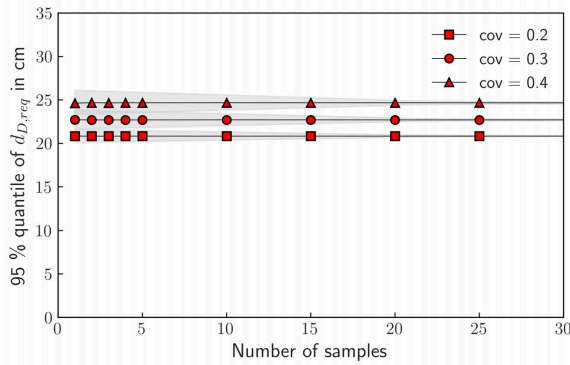


(d) B4 soil, Lognormal ϕ' , $t_a = 27.6$ s, $z_a = 0.83$ m.

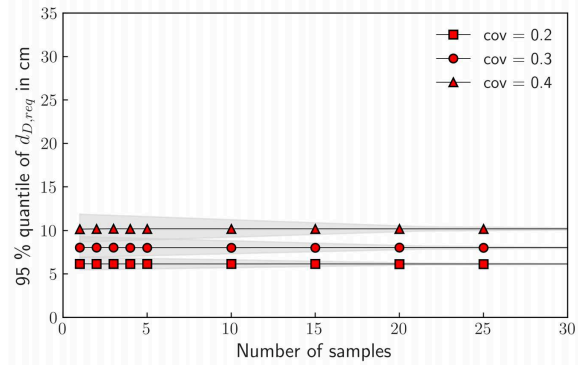
Figure 6.12: Effects of statistical uncertainty of the friction angle ϕ' on the required armour layer thickness $d_{D, req}$.

In addition, it is observed that the armour layer thickness required in the SW cases is governed by small t_a at moderate z_a (SW2), whereas the armour layer thickness of the SU cases is governed by large t_a in combination with large z_a (SU1). This behaviour may be explained by the time to reach quasi-stationary state and, thus, the maximum excess pore pressure. In soils of smaller hydraulic conductivity, it takes longer to reach a quasi-stationary state, while in permeable soils, the quasi-stationary state is reached faster. In less permeable soils the maximum excess pore pressure is thus reached with large t_a , whereas at small t_a the excess pore pressure does not fully build up. Consequently, the SU cases require larger armour layer thicknesses with

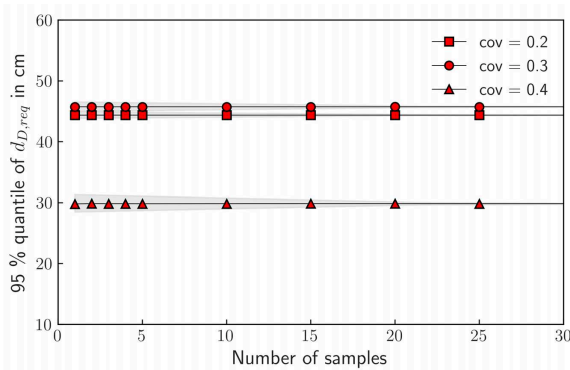
larger, but slower drawdowns, whereas the SW cases require larger armour layer thicknesses with smaller, but faster drawdowns.



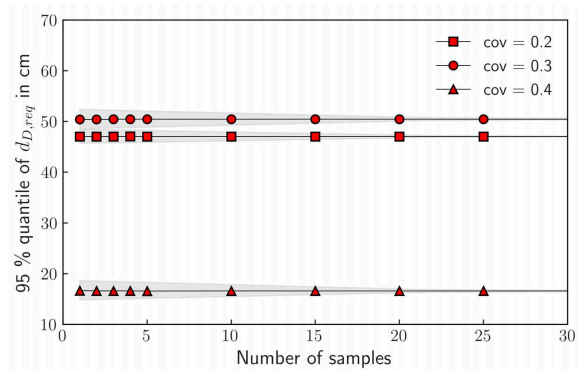
(a) B3 soil, Lognormal k , $t_a = 4.5$ s, $z_a = 0.63$ m.



(b) B3 soil, Lognormal k , $t_a = 27.6$ s, $z_a = 0.83$ m.



(c) B4 soil, Lognormal k , $t_a = 4.5$ s, $z_a = 0.63$ m.



(d) B4 soil, Lognormal k , $t_a = 27.6$ s, $z_a = 0.83$ m.

Figure 6.13: Effects of statistical uncertainty of the hydraulic conductivity k on the required armour layer thickness $d_{D, req}$.

For the investigated parameter range it is observed that statistical uncertainty of ϕ' and k has a negligible effect on the required armour layer thickness. Only the variance or, in the case of a deterministic design, the choice of characteristic values affect the required layer thickness. These conclusions apply to a homogeneous soil neglecting the spatial variability of soil parameters.

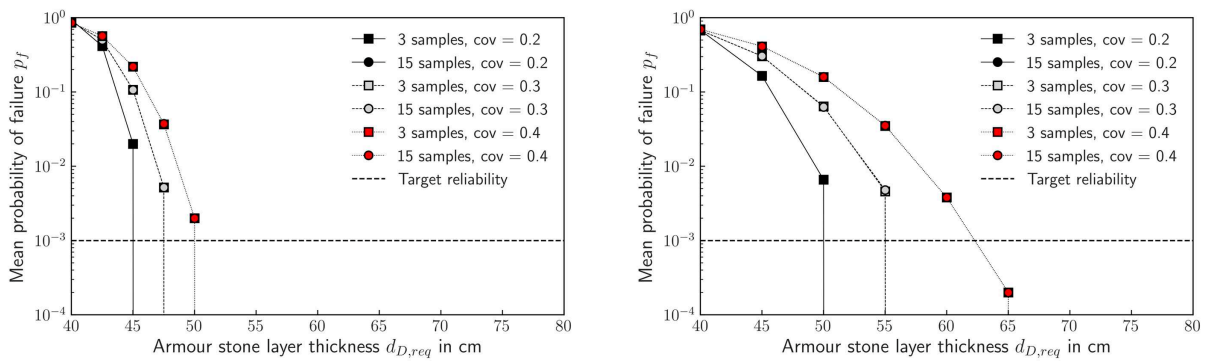
Effects of distribution uncertainty on the probability of failure

Based on the findings outlined in Section 6.5.3, it is decided to examine only the effect of a statistically uncertain k on the probability of failure in detail. Following the specifications of JCSS (2001), a target reliability of $\beta_{HL} = 3.1$ ($p_f = 1 \times 10^{-3}$) may be acceptable for ULS conditions leading to minor consequences while being characterised by high costs for safety measures.

Figure 6.14 and Figure 6.15 show the mean p_f and the 95 % quantile of p_f as a function of the armour layer thickness. It is observed that there are moderate differences between different sample sizes in the range of $p_f > 1 \times 10^{-2}$. In the range of the target reliability, a minor influence of the sample size is observed. Depending on the coefficient of variation, however, differences

of several centimetres in the required armour layer thickness are determined. The analyses therefore confirm, as already described in GBB (2010), a permeability at the lower end of the applicable range of values determines the design.

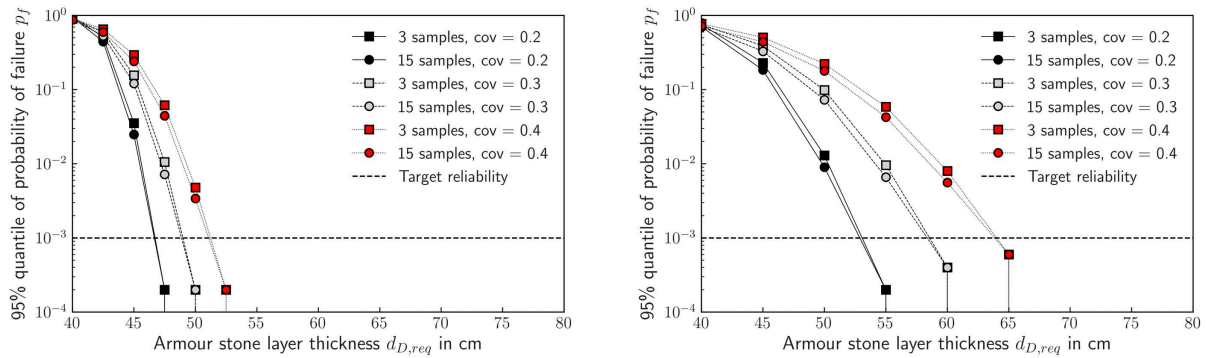
The reliability analysis yields armour layer thicknesses that are close to MAR (2008) standards. Following the guideline, a minimal armour layer thickness ranging between 0.70 m to 0.80 m is required for revetments without the additional weight of a filter layer. The four investigated case studies result in layer thicknesses ranging between 0.05 m and 0.55 m. Thus, assuming an equivalent toe support, the probabilistic design approach results in slightly smaller armour layer thicknesses than the deterministic approach.



(a) B4 soil, Lognormal k , $t_a = 4.5$ s, $z_a = 0.63$ m.

(b) B4 soil, Lognormal k , $t_a = 27.6$ s, $z_a = 0.83$ m.

Figure 6.14: Mean probability of failure as function of the required armour layer thickness. The statistical uncertainty of two different sample sizes is examined.



(a) B4 soil, Lognormal k , $t_a = 4.5$ s, $z_a = 0.63$ m.

(b) B4 soil, Lognormal k , $t_a = 27.6$ s, $z_a = 0.83$ m.

Figure 6.15: 95 % quantile of the probability of failure as function of the required armour layer thickness.

6.6 Discussion

As described in Chapter 2, the number of required MCS is a function of the required accuracy. For target reliabilities ranging between 0.05 and 0.001, 7500 to 300 000 simulations are required. In order to shorten the calculation time, a value at the lower end of the scale is chosen with 10 000 MCS. This simplification is reasonable, as the presented investigations serve as qualitative description of the effect of statistical uncertainty on the revetment design. However,

particularly when interpreting the results of the geotechnical design, it must be considered that the determined probabilities of failure represent approximate values.

The calculations are based on a simplified approach that approximates the effects of statistical uncertainty of the basic variables on the revetment design using a bootstrapping approach. This methodology relies on a realistic description of the initial parameter variance. The performed calculations use field observations and literature values. However, it must be considered that the true natural variance could be larger.

Besides this fact, a Gaussian distribution is assumed for the underlying distribution parameters. This assumption may not be the most suitable choice, as some analyses include negative values for μ and σ , which are, however, not considered in further stability calculations. For first investigations of statistical uncertainty, however, it is a valid assumption, which may need to be examined in depth by further investigations.

In the case of the hydraulic design, the current evaluations are based on field observations lasting a maximum of 14 days. This may lead to an underestimation of the variability of actions. The probability of extreme events may be underestimated or the shape of the distributions may differ compared to the presented fits. Long-term observations or a more substantiated data basis that encompasses more than four canals could assist in validating the results.

From the results of the bootstrapping procedure it is derived that the statistical uncertainty decreases with the number of available samples. A minimum sample size of 250 measurements should be available to determine a probability function of the hydraulic loads. Depending on the traffic at the waterway, this translates into a measurement period of one week to approximately one month. The present measurements at DEK-2006 just meet these requirements and the measurements at WDK-2007 comprehensively, whereas the measurements at KuK-2015 and SiK-2007 contain less observations.

The hydraulic design currently employs empirical stability parameters, which cannot be set to 1 due to their scaling. Therefore, the armour stone sizes and reliabilities determined within this chapter must be considered with respect to the semantic meaning of the empirical factors. For the herein outlined analyses, the most common stability parameter combination is used. It allows for moderate damage and maintenance. Future investigations should examine whether design or assessment may be carried out without stability parameters. In the future, maintenance efforts could be targeted via the target reliability.

Although from sensitivity analyses it is derived that the variability of u_{\max} may have considerable influence on the required armour stone size, present measurements do not encompass u_{\max} . Thus, the presented investigations cannot consider the effects of u_{\max} . Moreover, the design loads reported in MAR (2008) are rarely observed. If necessary, the additive factors may have to be adjusted to account for u_{\max} . In addition, it must be noted that neither the additive factor nor the multiplication by a partial factor may supply a comparable safety level at different waterways. These measures are only supposed to limit the probability of underestimating the required revetment dimensions.

In the case of the geotechnical design, it should be noted that the stability of a slope in rapid drawdown situations depends on the local excess pore pressure and shear strength. From the investigations, the conclusion can be drawn that statistical uncertainty in the considered range has a minor effect on the required armour stone layer thickness. However, as outlined in Chapter 2, further investigations regarding spatial variability are required. Moreover, as a result of the findings presented in Chapter 5 and previous studies (Sorgatz and Kayser, 2020),

load parameters are considered as deterministic input, which may underestimate the statistical uncertainty inherent to the geotechnical design.

Within this thesis, only a limited parameter range is studied assuming homogeneous soil, which is a common assumption for revetment design. From preliminary investigations (Sorgatz and Kayser, 2020), it is apparent that the minimum of ϕ' and k determines the soil mechanical parameters. This observation also applies to the presented investigations, which, thus, allows to use a moderate parameter range for the uncertainty analysis. However, a large factor of uncertainty, the geological model with the stratification of individual soil layers, is not covered within this thesis, since existing design models do not account for stratigraphic layers. Future investigations should aim at quantifying the uncertainty of the geological model and its effect on the required armour stone layer thickness.

Compared to MAR (2008), standards that apply partial factors $\gamma_{G,d} = \gamma_Q = 1.0$ to actions and material parameters in slope stability analysis, the selected target reliability at ULS conditions is strict. ULS conditions commonly require partial factors greater 1.0 in a deterministic design (DIN EN 1997-1:2014-03, 2010). JCSS (2001) achieves a differentiation by taking consequences and costs into account. In the case of the revetment design, traffic may serve as an additional criterion for a differentiation of risk at waterways. This criterion is directly related to damage development. More traffic volume may advance damage more quickly. Thus, further research is required to mathematically describe the process of damage development.

Neither the investigations of the hydraulic design nor the investigations of the geotechnical design account for a correlation of input parameters. Further investigations should consider a correlation for parameters, where based on the sensitivity analyses, a strong effect of parameter interaction on the model output is found, i. e. z_a and t_a .

To conclude, the presented analyses address uncertainty from a Frequentist point of view. In the future, it is recommended to employ the findings of this chapter in Bayesian analyses. Variance of mean and standard deviation determined in the course of this thesis can be employed as initial values in Bayesian inference.

6.7 Conclusions

Identification of input parameters

- Which distributions and correlations suit the required parameters best?
- What demands should be made regarding field observations?

Addressing parameter uncertainties inherent to actions and material parameters

- How does parameter uncertainty affect the hydraulic and geotechnical revetment design?
- How can these uncertainties be taken into account?
- What recommendations can be provided regarding characteristic values of actions and material parameters?

The results of the distribution and correlation analysis emphasise that the choice of a suitable distribution types, distribution parameters and correlations is ambiguous even after thorough exploratory data analyses. Based on the analyses, it is concluded that H_{stern} follows a Lognormal and v_{return} a Gaussian distribution. A positive correlation of H_{stern} and v_{return} is found. The four example campaigns do not provide sufficient information on the drawdown parameters t_a and

z_a as well as the slope supply flow u_{\max} . Thus, in subsequent investigations, these parameters are either deterministic worst case estimates or based on calculations using observed vessel passages.

From the results of the bootstrapping procedure it is derived that the statistical uncertainty decreases with the number of available samples. When conducting a hydraulic revetment design with field observations, a minimum sample size of 250 measurements should be available. The measurements at DEK-2006 considered within this thesis just meet these requirements and the measurements at WDK-2007 comprehensively, whereas the measurements at KuK-2015 and SiK-2007 contain less observations.

The reliability analyses show that the required armour stone diameter in the range of the target reliability only slightly differs between the two investigated sample sizes. From the results, a robustness of the presented methodology with regard to potential outliers is derived. Opposed to the definition of characteristic values on basis of field observations, the probability functions allow to account values that exceed the observed load maxima.

The geotechnical design is marginally affected by statistical uncertainty provided that only the uncertainty of the material parameters is considered. The investigated parameter range yields minor differences of the required armour layer thickness as a result of different sample sizes. Only the variance or the choice of characteristic values of effective friction angle and in particular hydraulic conductivity affects the required armour layer thickness.

In comparison to MAR (2008) standards, armour stone sizes and layer thicknesses derived by probabilistic analyses result in similar or smaller revetment dimensions. In particular for the hydraulic design, it can be concluded that probabilistic calculations offer saving potentials, because (i) based on the new definition of the limit state different less strict target values apply; and (ii) the addition of approaches on the safe side is avoided, instead, uncertainties of input parameters are explicitly considered.

7 | ADDRESSING TRANSFORMATION UNCERTAINTY: MODEL FACTORS FOR LOAD PARAMETERS

‘The use of reliability methods is the next logical step toward greater rationality in design, and their potential benefits should not be discarded heedlessly because of the reluctance to advance beyond the current level of complexity in design.’

–Kok-Kwang Phoon, Professor at National University of Singapore

Contents

7.1	Introduction	116
7.2	Basic formulation and methods	116
7.2.1	Load calculation from vessel passages	116
7.2.2	Determination of probabilistic model factors	117
7.2.3	Application of model factor calculations to ship-induced loads	118
7.2.4	Reliability assessment with model factors	118
7.3	Results of model factors for vessel-induced loads	120
7.3.1	Verification of randomness of model factors	120
7.3.2	Statistics of generalised model factors for vessel-induced loads	120
7.4	Probability of failure	122
7.5	Discussion	124
7.6	Conclusions	126

7.1 Introduction

For a design of revetments that is more oriented towards actual traffic, either information on ship-induced loads or information on the driving behaviour of the vessels must be available. As indicated in previous chapters, measurements of vessel-induced loads are resource-intensive. However, if only the vessel passages are measured and subsequently transferred to hydraulic loads, transformation uncertainty arises. It is expected that a design based on observed vessel passages will require larger armour stone diameters and armour layer thicknesses than a design based on measured hydraulic loads; a design based on the design vessel passages will require the largest armour stone diameters and armour layer thicknesses.

This chapter examines the uncertainties resulting from the transformation of the vessel passages into ship-induced hydraulic loads. First, model factors for each available load parameter are determined. Subsequently, the model factors are applied in exemplary reliability analyses to evaluate comparability, advantages and disadvantages regarding the two design approaches, load measurements versus observation of vessel passages.

Drawdown parameters are not included in this study. As shown by Sorgatz and Kayser (2020), a simple combination of the drawdown parameters without information on the correlation and realistic drawdown distributions leads to unrealistically large armour layer thicknesses. Therefore, before describing the model factors, further investigations are necessary to describe the drawdown parameters statically.

7.2 Basic formulation and methods

7.2.1 Load calculation from vessel passages

If data on individual vessel passages is available, the prescribed design vessel passages (97 % v_{crit} , passing 1 m above the toe of the bank) can be substituted by load calculations using individual vessel passages. Ship-induced loads are then calculated on the basis of the equations outlined in GBB (2010). In the course of the presented investigations, the calculated loads serve as input for the calculation of model factors. The following vessel-related parameters are required to determine the hydraulic loads by means of *GBBSoft+*, a software for designing bank and bed protection for inland waterways based on GBB (2010):

- passing distance d_{shore} ,
- vessel length L ,
- vessel width B ,
- vessel draught T (full / empty / partially loaded),
- vessel velocity v_s and
- vessel type.

In addition to the observed vessel passages, the calculations require a cross-section geometry, which should be collected in conjunction with field observations. Currently, *GBBSoft+* replaces the cross-section geometry observed in nature with a simplified trapezoidal profile, which must be adapted by the consultant in charge.

As for almost any design method, the calculation requires a number of simplifications. The cross-section of the canal can only be approximated by a substitute trapezoidal profile of the

canal. The vessel shape and other parameters describing the vessel are specified by predefined parameter sets depending on the type of ship. For the draught of the vessel, it can only be distinguished between full, empty and partially loaded (as the mean of full and empty). Furthermore, the calculations are based on the 1D-channel theory, which provides an approximation of the actual loads especially for waterways with larger cross-sections.

7.2.2 Determination of probabilistic model factors

The translation of real-world problems into mathematical models commonly entails making conservative assumptions and introducing simplifications to create models that gain acceptance in the daily design practice due to their practical applicability. As a consequence, predicted values deviate from calculated values. The introduction of model factors allows to account for '(1) a bias if the model leads to overprediction or underprediction of a quantity in question and (2) a randomness associated with the variability in the predictions from one prediction of the quantity to another' (DNVGL-RP-C207:2017-05, 2017, p. 7).

The simplest representation of the model uncertainty is the model factor M , which is defined as the ratio of the measured response X_m over the calculated response X_c (ISO 2394:2015-03, 2015).

$$M = \frac{X_m}{X_c} \quad (7.1)$$

M takes a range of values, which allows estimating the hidden conservativeness or non-conservativeness of the model. In terms of revetment design, the model is considered conservative if the mean < 1 , whereas a mean > 1 implies a non-conservative model. M can be introduced in design calculations as a random factor. It is usually considered to be lognormally distributed (Dithinde et al., 2016).

If M varies systematically depending on the input variables, reliability calculations have to account for a correlation of the input variables including M . Since the inclusion of a correlation complicates the reliability analysis significantly, it is often preferred to remove the correlation of M and the input variables in order to apply M as independent variable (Dithinde, 2007).

Under the assumption of a Lognormal distribution, the generalised model factor M is determined from the regression of the logarithms of the measured loads Q_m and calculated loads Q_c with the following regression model:

$$\ln Q_m = \beta_0 + \beta_1 \ln Q_c + \epsilon \quad (7.2)$$

where β_0 and β_1 represent two regression constants and ϵ accounts for the error as a Gaussian random variable with zero mean and non-zero variance.

Eq. (7.2) can be rewritten as

$$Q_m = M Q_c^{\beta_1} \quad (7.3)$$

with

$$M = \exp(\beta_0 + \epsilon) \quad (7.4)$$

The distribution parameters of M are then calculated as follows:

$$\mu_M = \exp(\beta_0 + 0.5\xi^2) \quad (7.5)$$

$$\sigma_M^2 = \mu_M^2 [\exp(\xi^2) - 1] \quad (7.6)$$

with ξ as the standard deviation of ϵ (Dithinde, 2007). Eq. (7.3) is not dimensionless. Normalisation is required to obtain dimensionless model factors. However, since the revetment design as outlined by current design standards follows a standardised, unit-dependent scheme, normalisation is omitted. The determined model factors are valid when using the parameter-specific SI units, i. e. wave height in m and flow velocities in m s^{-1} .

Due to the random nature of M , the calculation method can be unconservative when applied to a specified case, despite being conservative on average. This formulation of the model factor is thus consistent with the concept of empirical approaches, which are commonly determined by means of a regression which yields a conservative estimate for the majority of the investigated cases. For the practitioner, M is a measure of the conservatism inherent to the model, which either reduces or increases the global factor of safety (Phoon and Tang, 2019).

7.2.3 Application of model factor calculations to ship-induced loads

Within the scope of these investigations, the calculated loads are derived from calculations with *GBBSofit+* as described in Section 7.2.1, whereas measured loads are the waves and currents observed at the waterways. The calculated loads are determined for each vessel passage individually using the parameters listed in Section 7.2.1. Subsequently, the model factors for $M_{H_{\text{stern}}}$ and $M_{v_{\text{return}}}$ are evaluated using the equations outlined in Section 7.2.2.

This procedure does not allow to evaluate model factors separately, e. g. according to passing distance or vessel velocity. Such an analysis would require systematic driving tests at defined velocities and passing distances. However, the presented investigations use observations of regular traffic. At the same time, available data confirm a low to moderate correlation of passing distance and vessel velocity as indicated by $\rho_P = 0.38$ (see Figure 7.1). Thus, if a correlation between a model factor and v_s is found, a correlation between the model factor with d_{shore} is likely to be observed, too. This may require additional efforts regarding the consideration or removal of correlations for the model factor analyses.

7.2.4 Reliability assessment with model factors

The performance of the model factors is examined by means of reliability analyses. Using the four example datasets, the reliability of the hydraulic design is determined with measured hydraulic loads, observed vessel passages and observed vessel passages multiplied by the determined model factors. Eq. (7.3) delivers the mathematical expression of the generalised model factor, which allows to derive the hydraulic loads on the waterway on basis of observed vessel passages while accounting for transformation uncertainty. The introduction

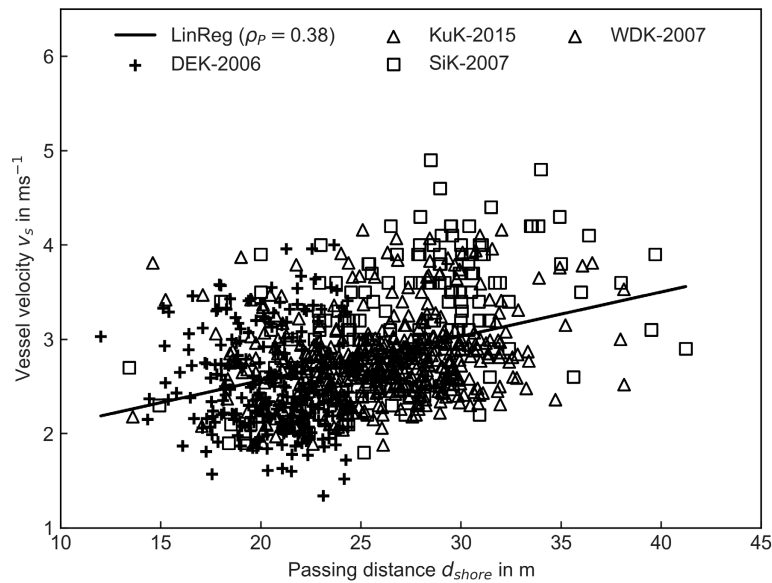


Figure 7.1: Correlation of passing distance and vessel velocity.

of model factors aims at obtaining the same reliabilities as obtained with measured hydraulic loads. The presented analysis accounts neither for statistical uncertainty nor for measurement uncertainties. For investigation purposes, it is assumed that the available measurements represent a statistically representative and accurate description of hydraulic loads at the four example waterways. The fact that this only applies to a limited extent has already been discussed in Chapter 6.

As outlined in Chapter 3, the currently available data lacks measurements of u_{\max} , which is thus evaluated by solving the equations of GBB (2010) for each observed vessel passage individually. Subsequently, the determined u_{\max} are employed as random variable. This procedure is necessary to allow for the comparison of the results obtained with measured and calculated loads. The weighing procedure, which has been discussed several times, averages H_{stern} and u_{\max} . If a deterministic value for u_{\max} is specified, the importance of H_{stern} and u_{\max} for the design would be misleading. Therefore, realistic values, which depend on the respective vessel passages, must be entered for u_{\max} . As already discussed in previous chapters, the choice of distribution is not always obvious. In the following reliability analyses, a Lognormal distribution is used for H_{stern} and u_{\max} ; v_{return} and $D_{50, \text{pres}}$ follow Gaussian distributions. It is assumed that the calculated hydraulic loads can be approximated by the same type of probability function as the respective measured loads. Independently of the waterway, the calculations assume an armour stone diameter of 150 mm, which equals the armour stone class CP_{90/250}.

For the present investigations, a moderate positive correlation of v_{return} and H_{stern} of 0.7 is assumed. In view of the existing data (see Chapter 6, Section 6.2), this assumption is justified, but certainly requires a more profound database in future.

The reliability analysis is performed with FORM and MCS using the OpenTURNS package in Python (Baudin et al., 2015). The optimisation of FORM is based on the Abdo-Rackwitz algorithm. A convergence of the MCS is reached at a maximum variance of 5 % of the calculated probability estimates.

7.3 Results of model factors for vessel-induced loads

7.3.1 Verification of randomness of model factors

Figure 7.2 shows two examples of the correlation between model factors and selected input parameters. The model factors result from the simplified representation of M as the ratio of measured and calculated values, see eq. (7.1). The correlation is described by the Pearson correlation coefficient ρ_P . A correlation is to be considered as moderate for $\rho_P > 0.4$ and as strong for $\rho_P > 0.6$ (Phoon and Ching, 2015). The results indicate a moderate negative correlation between v_s and $M_{v_{\text{return}}}$, which means the larger v_s the smaller $M_{v_{\text{return}}}$. The conservativeness of the design equations decreases with increasing v_s . A similar behaviour is observed for d_{shore} and $M_{H_{\text{stern}}}$ and d_{shore} and $M_{v_{\text{return}}}$; an increasing passing distance leads to a reduction of M . As explained in Section 7.2.3, existing data does not allow to conclude on the variable that causes the correlation of the model factors.

From the results of the correlation analyses it is apparent that the model factors scatter; model factors above and below 1 are observed. In addition, assuming the driving behaviour of the studied vessels reflects their actual driving behaviour, correlations imply that the closer the vessel to the shore the less ‘safe’ becomes the design. Conversely, the faster the ship the ‘safer’ the design. This observation applies to H_{stern} and v_{return} . From this observation, it may be derived that considerable safety reserves are inherent to a design which is based on $0.97 \cdot v_{\text{crit}}$ and a shore distance of 1 m above the toe of the embankment.

Overall, the number and strength of correlations is moderate; although, there may be additional parameters such as a correlation between draught of the vessels and vessel type or waterway geometry and vessel dimensions (n-ratio), which are not considered in this assessment and which may also affect M .

7.3.2 Statistics of generalised model factors for vessel-induced loads

Table 7.1: Generalised model factor statistics for H_{stern} in m using the example waterways.

Data	Regression parameters				Generalised M statistics		
	R^2	β_0	β_1	ξ	μ_M	σ_M	cov
DEK-2006	0.37	-1.03	0.52	0.33	0.38	0.13	0.34
KuK-2015	0.48	-0.47	0.85	0.35	0.66	0.24	0.36
SiK-2007	0.11	-1.96	0.34	0.70	0.18	0.14	0.79
WDK-2007	0.13	-1.15	0.35	0.31	0.33	0.11	0.32

Table 7.2: Generalised model factor statistics for v_{return} in m s^{-1} using the example waterways.

Data	Regression parameters				Generalised M statistics		
	R^2	β_0	β_1	ξ	μ_M	σ_M	cov
DEK-2006	0.43	-0.27	0.57	0.27	0.79	0.22	0.27
KuK-2015	NaN	NaN	NaN	NaN	NaN	NaN	NaN
SiK-2007	0.05	-1.12	0.20	0.48	0.36	0.19	0.51
WDK-2007	0.30	-0.22	0.70	0.25	0.83	0.21	0.25

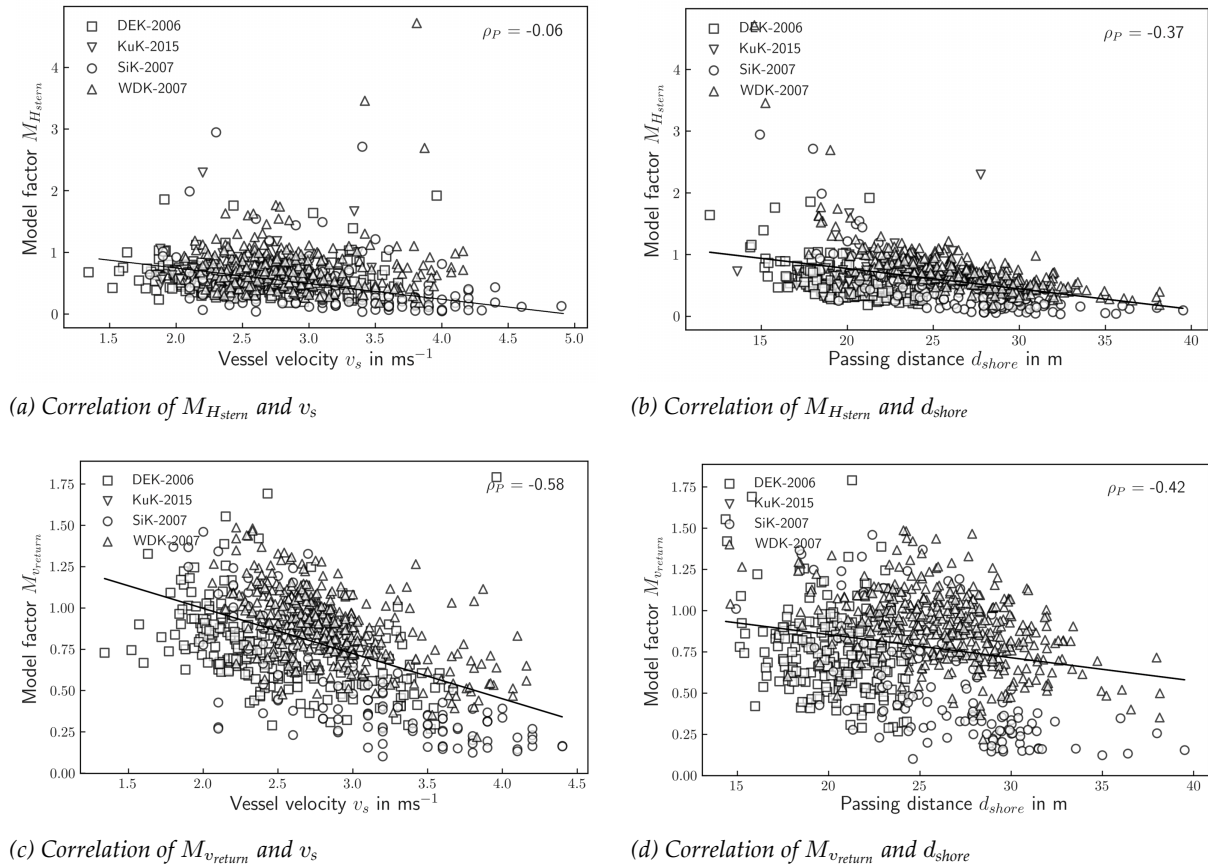


Figure 7.2: Correlation between model factors M of different vessel-induced loads and selected input parameters (vessel velocity v_s and passing distance d_{shore}).

As a result of the discussed correlations, M is determined by the generalised model factor approach. The regression parameters and the ensuing generalised model factor statistics for H_{stern} and v_{return} are summarised in Table 7.1 - Table 7.2. The following observations result from the determined generalised model factor statistics:

- The goodness of fit (R^2) of the linear regression functions is comparatively low for some of the results presented. The quality of the fit does not correspond to the sample size. The smallest sample KuK-2015 shows the highest R^2 values.
- It can be noticed that all obtained mean values of M are smaller than 1. The loads determined by GBB (2010) equations can therefore be regarded as conservative. When the regression constant β_0 is negative, the mean of M tends to be smaller than 1. With decreasing β_0 mean and standard deviation of M decrease. The standard deviation of M increases with increasing regressor β_1 .
- The reduction as well as the increase of hydraulic loads when applying the model factors is a function of μ , σ and β_1 . Small σ and β_1 values tend to increase the reliability index. Higher μ_M are compensated for by smaller σ_M and β_1 values. On the other hand, larger σ and β_1 are counterbalanced by low μ_M .
- Comparable model factors are identified for DEK-2006 and WDK-2007. These two waterways are characterised by a similar n-ratio (see Chapter 3). The values determined for

KuK-2015 and SiK-2007 differ significantly from the above-mentioned waterways. Considerably more passenger vessels and leisure boats pass at SiK-2007, which may show a difference in driving behaviour compared to commercial shipping. Moreover, a large portion of vessels are characterised by smaller dimensions and lower engine power.

- The importance factors indicate that, similarly to the results of the sensitivity analysis, the variability of the armour stone diameter affects the probability of armour stone displacement less than hydraulic loads. This allows to draw the conclusion that, in the event of damage, measures that lead to a reduction of loads such as prescribed passing distances and speed limits may be more effective to slow down the process of damage development.

7.4 Probability of failure

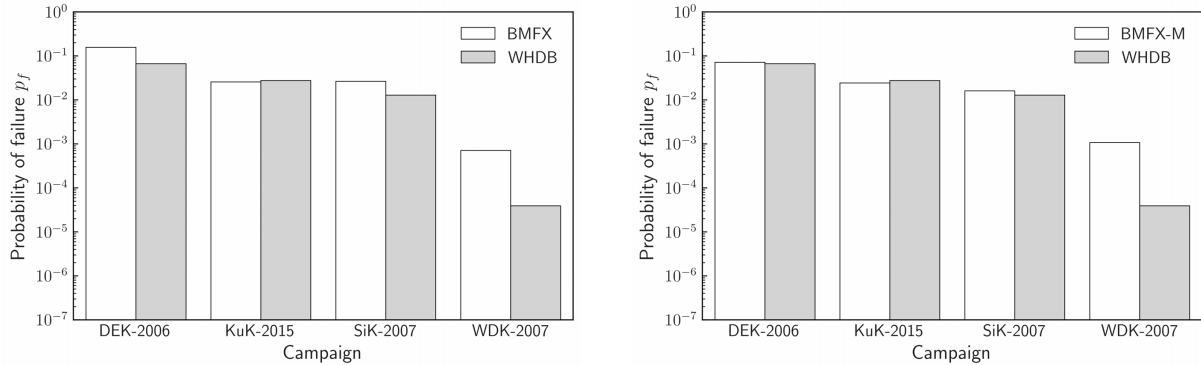
Table 7.3 summarises the results of the reliability assessment using FORM and MCS. Besides the probability of failure, Table 7.3 provides information on the FORM design point, which refers to the most probable point of failure. The abbreviation ‘BMFX’ refers to the reliability assessment with vessel passages, but without model factor; ‘BMFX-M’ refers to the reliability assessment with vessel passages and model factor; ‘WHDB’ indicates reliabilities obtained with measured hydraulic loads.

The p_f values vary strongly between the waterways and, in the case of the grey highlighted row also between the different methods. FORM is based on the assumption that the design point is a unique point in standard space. This may lead to erroneous results, in particular for highly non-linear limit state functions as most likely observed in the case of WDK-2007 (BMFX-M). An indicator for an erroneous design point is the physically implausible combination of input parameters. For example, as a result of $\rho_P = 0.7$, large u_{\max} are expected to occur in the presence of large H_{stern} . In the case of WDK-2007, it can be observed that the FORM design points differ significantly from the values determined for WHDB and BMFX.

Table 7.3: Probability of failure and design points using MCS and FORM (Abdo-Rackwitz algorithm). FORM / MCS deviations are highlighted in grey. The abbreviation ‘BMFX’ refers to the reliability assessment with vessel passages, but without model factor; ‘BMFX-M’ refers to the reliability assessment with vessel passages and model factor; ‘WHDB’ indicates reliabilities obtained with measured hydraulic loads.

Design case	Method	MCS		FORM	FORM design point			
		number	p_f	p_f	H_{stern}	v_{return}	u_{\max}	$D_{50,\text{pres}}$
					m	m s^{-1}	m s^{-1}	mm
DEK-2006	BMFX	3000	1.58×10^{-1}	1.28×10^{-1}	0.61	1.74	1.66	148.26
DEK-2006	BMFX-M	6000	7.23×10^{-2}	6.30×10^{-2}	0.70	1.72	2.38	148.50
DEK-2006	WHDB	6000	6.68×10^{-2}	6.51×10^{-2}	0.37	1.18	2.37	147.94
KuK-2015	BMFX	16000	2.57×10^{-2}	1.73×10^{-2}	0.60	1.73	1.57	144.86
KuK-2015	BMFX-M	17000	2.44×10^{-2}	1.74×10^{-2}	0.60	1.73	1.57	144.88
KuK-2015	WHDB	15000	2.76×10^{-2}	1.74×10^{-2}	0.50	1.73	1.58	144.89
SiK-2007	BMFX	15000	2.67×10^{-2}	1.66×10^{-2}	0.85	1.26	2.04	148.35
SiK-2007	BMFX-M	25000	1.62×10^{-2}	4.09×10^{-29}	0.17	0.58	0.32	16.34
SiK-2007	WHDB	31000	1.29×10^{-2}	1.23×10^{-2}	0.28	0.58	2.39	148.26
WDK-2007	BMFX	567000	7.09×10^{-4}	5.16×10^{-4}	0.84	1.43	1.97	142.34
WDK-2007	BMFX-M	371000	1.08×10^{-3}	9.81×10^{-5}	0.79	1.48	2.35	143.99
WDK-2007	WHDB	1000000	3.97×10^{-5}	3.07×10^{-5}	0.70	1.28	2.11	140.56

A graphical illustration of MCS results with and without mode factors is presented in Figure 7.3. Figure 7.4 shows the importance factors derived from MCS.



(a) Probability of failure without application of model factors. (b) Probability of failure with application of model factors.

Figure 7.3: Reliability assessment without (left) and with (right) application of model factors using MCS.

The following conclusions can be drawn based on the illustrations:

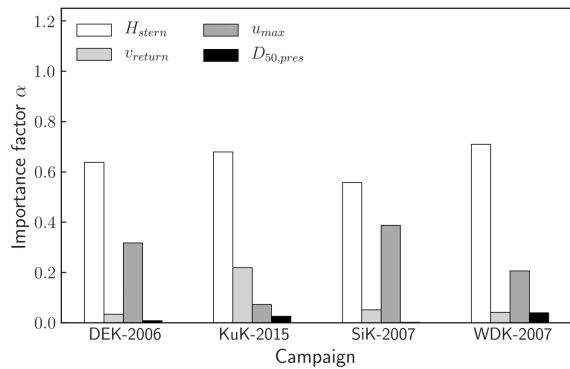
The introduction of M reduces difference between WHDB and BMFX calculations in all except for the WDK-2007 case. Compared to WHDB calculations, the BMFX calculations are on the safe side and, thus, more conservative. Through the application of model factors WHDB and BMFX-M, calculations approach similar results.

The importance factors derived from MCS indicate that H_{stern} is the most relevant parameter for design. This observation is in line with the sensitivity analysis (Chapter 5). However, in contrast to the sensitivity analysis, the contribution of u_{max} to failure is only moderate. This may be due to the use of specified probability functions in the reliability analysis, whereas the sensitivity assumes a uniform distribution. Moreover, the sensitivity analyses investigate a broad parameter range, which does not apply to a specific waterway, whereas the reliability analyses consider the location-specific loads derived from measurements.

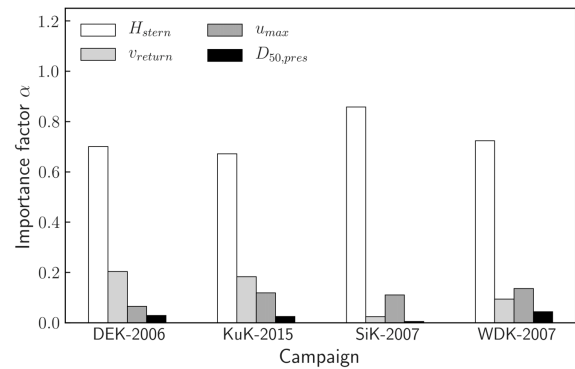
WHDB and BMFX importance factors differ; i. e., DEK-2006 (WHDB) shows a moderate importance of u_{max} , which DEK-2006 (BMFX) does not account for. The introduction of model factors harmonises the importance factors derived from WHDB and BMFX calculations in all but the WDK-2007 campaign. In the case of WDK-2007, the importance of v_{return} increases with the application of M . This behaviour may also provide an explanation for the lacking adjustment of p_f after the introduction of M_{return} in the case of WDK-2007. In some cases, the determined M_{return} lead to the augmentation of v_{return} . A particular reason for this may be that the determination of flow velocities on the waterway is associated with considerable inaccuracies.

The results of the reliability analyses suggest that in the case studies SiK-2007 and WDK-2007, smaller armour stone diameters may be more stable under the expected loads than prescribed in the design standards (MAR, 2008). The results correspond to the results of the expert interviews (see Chapter 4) that attribute SiK-2007 and WDK-2007 a good structural condition, whereas the studies DEK-2006 and KuK-2015 are waterways, which are attributed a lower stability.

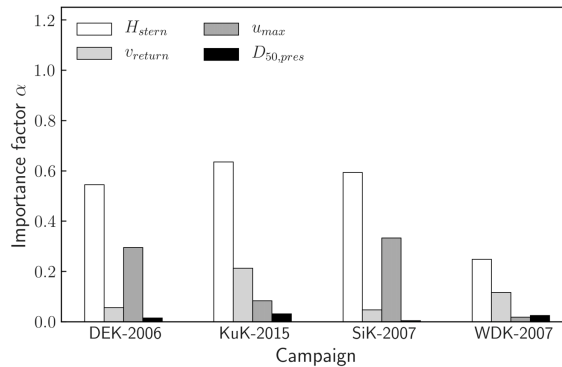
From the FORM design points, it is deduced that in narrower cross-sections, i. e. DEK-2006 and SiK-2007, the flow velocities seem to determine the design. The calculated $D_{50, \text{pres}}$, which



(a) Importance factors resulting from reliability assessment with measured loads (WHDB).



(b) Importance factors resulting from reliability assessment with calculated loads without model factors (BMFX).



(c) Importance factors resulting from reliability assessment with calculated loads with model factors (BMFX-M).

Figure 7.4: Importance factors resulting from reliability assessment using hydraulic loads and vessel passages as input variables. The abbreviation ‘BMFX’ refers to reliabilities obtained with vessel passages, but without model factor; ‘BMFX-M’ refers reliabilities obtained with vessel passages and model factor; ‘WHDB’ indicates reliabilities obtained with measured hydraulic loads.

indicate at which armour stone diameter most likely failure occurs corresponds approximately to the mean armour stone diameter. This is consistent with current design approaches. However, given a target reliability $p_f = 0.01$, only SiK-2007 and WDK-2007 would meet the safety requirements with armour stones of size $CP_{90/250}$.

7.5 Discussion

For further validation the results of the analyses are compared to previous investigations on revetment conditions and maintenance costs (Fleischer and Kayser, 2009; WgV, 2018). Fleischer and Kayser (2009) list annual maintenance costs of 0,00 Euro/m² for WDK, 0,16 Euro/m² for DEK north and 0,01 Euro/m² to 0,15 Euro/m² for DEK south. In an unpublished guideline for waterways of moderate traffic (WgV, 2018), annual maintenance costs of 0,24 Euro/m² are presented for KuK.

The maintenance costs summarised above correspond well with the predicted probabilities of failure; low maintenance costs coincide with $p_f < 1 \times 10^{-3}$ at SiK-2007 and WDK-2007, whereas

large maintenance costs occur at DEK-2006 and KuK-2015 with $p_f > 1 \times 10^{-2}$. This observation may not allow to define universally accepted target reliabilities, but it can be noted that target reliabilities above the design value selected within these investigations ($p_f < 1 \times 10^{-2}$) may result in increased maintenance efforts. In addition, it is stressed that the presented analyses still use stability factors that describe acceptable maintenance efforts. Without these factors, the determined probabilities of failure would increase.

Theoretically, model factors should be of random nature, because the represented differences between measured and calculated loads are the result of numerous minor facts not considered in the model. In practice, model factors are obtained from the comparison of measured and calculated loads. They may entail measurement errors, human errors or site-specific deviations causing extraneous uncertainties. In any case, the loads derived from the calculations are an approximation of the local boundary conditions at the waterway. Moreover, even though the data are screened in the course of this thesis with regard to outliers and measurement errors, for more than ten years old measurements it is no longer possible to clearly determine whether errors exist on the basis of the existing documentation. The results therefore emphasise the importance of modern data management and storage systems as well as corresponding data quality frameworks.

Furthermore, it is assumed that the calculated hydraulic loads can be approximated by the same type of probability density function as the respective measured loads. However, an analysis of the calculated loads shows that an assignment of probability density functions to calculated loads is less clear than an assignment to measured hydraulic loads. This behaviour may be caused by the use of various empirical factors, for example, to describe the vessel shape, which causes in real-life continuous quantities to tend towards categorical quantities. Deviations between calculated and measured hydraulic loads thus may also result from a less accurate distribution fitting. The probability of larger wave heights and flow velocities may be over- or underestimated. Further investigations of the distributions of the input parameters obtained from calculations are required. The assumed correlation of the input parameters must be validated.

Since u_{\max} was not measured in any campaign, the current calculations do not account for transformation uncertainty of u_{\max} . Nor is it possible to quantify the effect of the simplifications such as the calculation of u_{\max} made for the presented investigations. The total effect of transformation uncertainty on $D_{50, \text{req}}$ is thus most likely underestimated. The analyses emphasise the requirement of completeness of the data for probabilistic assessment approaches.

The current model factor approach employs model factors determined for each waterway. In the future, it may be of use to find general model factors from generic databases, for example depending on the waterway category. Based on a generic database, local model factors may then be determined efficiently using supplementary measurements and Bayesian statistics. So far, information calibrated on site-specific data can only be applied to specific sites of similar conditions. In the future, deep learning techniques may assist in identifying ‘similar’ site-conditions.

In addition, further investigations regarding the transformation of a random model factor towards an application in deterministic calculations, i. e. such as partial factors, may be required. The presented model factors are an estimate of the calculation model bias ($1/\mu$). However, particularly when performing level I analyses with partial factors (γ_{mod}), it may be required that the introduced model factors establish a certain reliability of the design model, ensuring that only

certain percentage of calculated values fails to match the ‘real’ values (see Figure 7.5). Thus, further research is needed in this area.

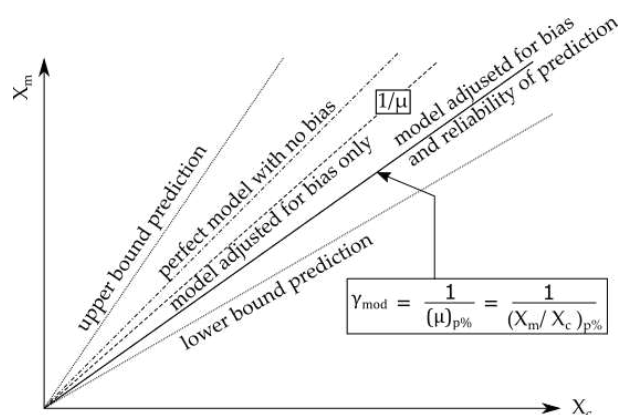


Figure 7.5: Illustration of model bias and reliability prediction as components of model factors; illustration based on Lesny et al. (2017, June 4–July 7, cf. p. 2).

The calculations only represent damage induced by overloading. Vandalism, collisions or material degradation may also cause damage. The expert interviews, though, have shown that these are less frequently observed (see Chapter 4). The presented model factor approach cannot be considered independently of this human component. In addition, once more it is stressed that the load distributions are established from measurements lasting one to two weeks. The determined p_f primarily assist in validating the presented methodology by comparing the results obtained for BMFX, BMFX-M and WHDB. Similarly to the previous chapters, long-term measurements are recommended to verify the estimates made in the course of these investigations.

Finally, it is emphasised that model uncertainty considered in the context of this thesis only applies to the uncertainties resulting from the parameters. Uncertainty inherent to the design model such as the equations describing the armour stone stability are not investigated. As discussed in Chapter 2, however, these model uncertainties may also have a considerable effect on the revetment design. Further investigations are thus required.

7.6 Conclusions

Addressing parameter uncertainties inherent to actions and material parameters

- How does parameter uncertainty affect the hydraulic and geotechnical revetment design?
- How can these uncertainties be taken into account?
- How can a reliability-based revetment design assist in accounting for local traffic and safety requirements?

As a result of the herein outlines investigations, it is shown that model factors can assist in account for transformation uncertainty inherent to calculations of hydraulic loads required for revetment design. Without model factors, transformation uncertainty leads to a conservative design; design loads are overestimated. Within this thesis, model factors for H_{stern} and v_{return} are determined.

Consequently, a probabilistic revetment design does not necessarily require measurements of waves and currents to substitute conservative design vessel passages by site-specific information. Time-consuming and expensive measurements of ship-induced loads may be replaced by observations of vessel passages or AIS data.

The current data basis does not allow to draw conclusions regarding transformation uncertainty inherent to load variables required for the geotechnical design. However, at the same time, reference is made to the study of Sorgatz and Kayser (2020), in which the use of drawdown parameters as random variables is not recommended, since a simple combination of the drawdown parameters without information on the correlation and realistic drawdown distributions leads to unrealistically large armour layer thicknesses.

The probability of failure p_f or the reliability index β_{HL} support the decision-making process in design and maintenance management as meaningful key figures. The comparison of maintenance costs and predicted probabilities of failure shows that the chosen target reliabilities for SLS conditions suit the observations in the field.

Compared to a deterministic approach, the proposed reliability-based methodologies provide additional information concerning the importance of the input parameters. This allows essential design parameters to be identified and, if necessary, account for their significance by ensuing measurements or more conservative characteristic values. FORM analyses additionally provide the design point which is a measure for the required revetment dimensions. Care must be taken as FORM may detect a local instead of a global maximum.

8 | ADDRESSING SPATIAL VARIABILITY: GEOTECHNICAL DESIGN

‘The premise here is that probabilistic and stochastic methods lead to more realistic definitions of response, reflecting the variable nature of the materials being analysed. They also lead to an improved understanding of how soils behave and, ultimately, to economy of design. However, they also involve the use of new technologies and ideas that are unfamiliar to many geotechnical engineers.’

–Michael Hicks, Professor of Soil Mechanics at Delft University of Technology

Contents

8.1	Introduction	130
8.2	Basic formulation and methods	130
8.2.1	Design equations of the infinite slope model	130
8.2.2	Determination of excess pore pressure profiles in response to drawdown	132
8.2.3	Generation of the random fields	133
8.2.4	Revetment design in presence of random fields	134
8.2.5	Parameter combinations	135
8.3	Results of the random field analysis	136
8.3.1	Influence of random fields on the embankment stability	136
8.3.2	Influence of a non-homogeneous friction angle	137
8.3.3	Influence of a non-homogeneous hydraulic conductivity	138
8.3.4	Influence of a non-homogeneous friction angle and hydraulic conductivity	139
8.4	Probability of slope failure	140
8.5	Discussion	141
8.6	Conclusions	142

8.1 Introduction

The stability of an embankment in rapid drawdown situations depends on the profile of the limit state function, which is a function of the local excess pore pressure and shear strength. This chapter investigates the effects of vertically non-homogeneous soil parameters on the design of revetments. A stability analysis of an infinite slope subjected to a rapid drawdown in the presence of a spatially variable friction angle and a spatially variable hydraulic conductivity is conducted. It is assumed that the location of permeable and less permeable areas in combination with the location of a spatially variable shear strength may strongly affect the embankment stability. The introduction of spatially variable soil parameters may therefore allow identification of the safety margins inherent to the revetment design. A more sophisticated understanding of the uncertainties resulting from spatial variability may also support the selection of characteristic values for soil parameters.

Following the introduction of the infinite slope model in Section 8.2, briefly touching on aspects such as the pore pressure determination, the random field generation and the parameter combinations used for the analysis, the results of the random field analyses are presented with regard to the required thickness of the armour stone layer (Section 8.3). Subsequently, in Section 8.4 the probability of a slope failure when considering non-homogeneous soil parameters is investigated.

8.2 Basic formulation and methods

8.2.1 Design equations of the infinite slope model

An infinite slope assumes a constant slope of infinite extent. The herein outlined equations follow the formulation of Zhou et al. (2016), which has been modified to account for the drawdown induced excess pore pressure Δp . A schematic representation of the quantities described in this section can be found in Figure 8.1. In short, the figure visualises that the stability of a slope with an inclination of β is a function of the excess pore pressure Δp , a response to the drawdown (z_a , t_a), and the load of soil and revetment $\gamma' + [(\gamma_s - \gamma_w) \cdot (1 - n_r)]$.

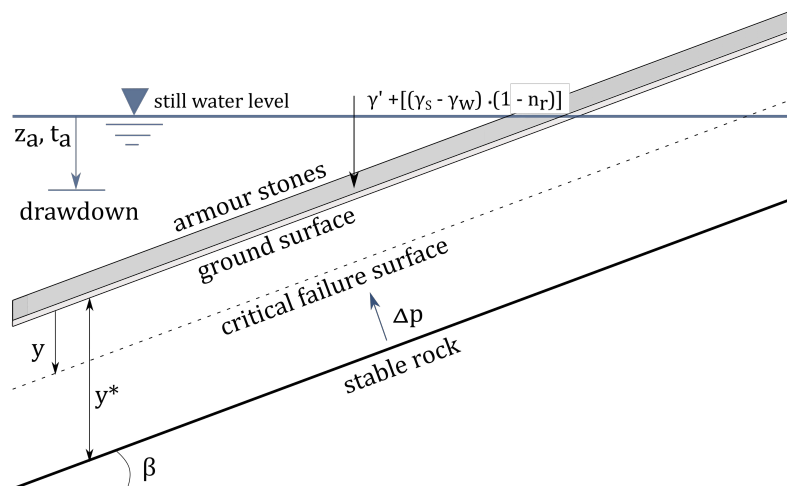


Figure 8.1: Infinite slope subjected to rapid drawdown.

For an infinite slope, the failure criterion for an arbitrary plane is that the shear stress $\tau(\mathbf{x}, y)$ on the plane exceeds the shear strength $\bar{\tau}(\mathbf{x}, y)$ on the plane. Following the notation commonly used in reliability engineering, the failure criterion is expressed as the limit state function g as follows:

$$g(\mathbf{x}, y) = \bar{\tau}(\mathbf{x}, y) - \tau(\mathbf{x}, y) \quad (y \in [0, y^*]) \quad (8.1)$$

where y is the depth of the plane below the ground surface and y^* is the thickness of the layer under consideration. \mathbf{x} represents stochastic variables that are included in the calculation.

The shear stress τ is caused by the effective vertical overburden stress σ'_v which results from the self-weight of the soil mass and the pore water. For a given depth y it can be written as

$$\tau(y) = \sigma'_v(y) \sin \beta \cos \beta \quad (8.2)$$

where the effective vertical overburden stress σ'_v without a revetment is determined by eq. (8.3) as a function of slope inclination β and unit weight of soil under buoyancy γ'_B and with a revetment by eq. (8.4):

$$\sigma'_v(y) = \gamma'_B y \quad (8.3)$$

$$\sigma'_v(y) = \gamma'_B y + [(\gamma_S - \gamma_W) \cdot (1 - n_r)] \cdot \left(\frac{d_D}{\cos \beta} \right) \quad (8.4)$$

The equations include the unit weight of soil under buoyancy γ'_B , the unit weight of water γ_W , the saturated unit weight of the armour stones γ_S , the porosity of the armour stone layer n_r and the thickness of the armour stone layer d_D .

The shear strength $\bar{\tau}(\mathbf{x}, y)$ is described by the Mohr-Coulomb criterion, which features the effective friction angle ϕ' and the effective cohesion c' and reads as follows:

$$\bar{\tau}(y) = \sigma'_n(y) \tan \phi'(y) + c' \quad (8.5)$$

$$\sigma'_n(y) = \sigma'_v(y) \cos^2 \beta - \Delta p(y). \quad (8.6)$$

where σ'_n is the effective normal stress acting on the soil skeleton. In the case of a vessel passage, σ'_n is reduced by Δp , see eq. (8.6). If the soil has a permanent effective cohesion under water, the local stability of permeable revetments can be assumed without further verification (GBB, 2010). Thus, the subsequently presented investigation only considers non-cohesive materials.

8.2.2 Determination of excess pore pressure profiles in response to drawdown

The response of excess pore pressure in the embankment to the drawdown is a time-dependent process. Based on the investigations of Köhler (1985), vessel wave induced drawdowns can be simplified as a decreasing water level of constant drawdown rate. The excess pore pressure attains a maximum at the end of the drawdown, which allows the assessment of equilibrium at just this moment.

The presence of even small volumes of entrapped gas in the voids, for example as a result of natural water level fluctuations and/or biogenic gas generation, in combination with ‘rapid’ external hydraulic or static load changes can lead to the build-up of excess pore pressure. The reason for such a response is primarily a consequence of the compressibility of the gaseous phase in the pore fluid. The expression ‘rapid loading’ must be considered with respect to the soil’s hydraulic conductivity and therefore involves a wide range of time scales.

To evaluate the vertical distribution of drawdown-induced excess pore pressure, a 1D coupled flow-deformation finite element (FE) model is employed. It is a simple, Python-based implementation based on the work of Montenegro (2016). A full code documentation can be found in Appendix E.4. The FE model, which is based on Biot’s theory of poroelasticity (Biot, 1956), was validated against analytical solutions of time dependent hydraulic and mechanical loading. Comparisons of 1D and 2D slope models resulted in comparable excess pore pressure distributions indicating an acceptable approximation of the 2D slope problem by the 1D computations (Ewers et al., 2017).

Within a continuum approach the (immobile) gas phase is accounted for by the partial saturation S (Fredlund et al., 2012; Montenegro, 1995). Considering mass and momentum balance principles under the assumption of uniaxial strain, the coupled flow-deformation problem reduces to a Boussinesq-type equation (Wang, 2000):

$$\frac{\partial \Delta p(t, y)}{\partial t} - c \frac{\partial^2 \Delta p(t, y)}{\partial y^2} = (1 - B^*) \frac{z_a}{t_a} \gamma_w \quad (8.7)$$

with the excess pore pressure Δp as a function of time t and depth y , the consolidation coefficient c , the hydraulic loading due to drawdown expressed via the drawdown rate z_a/t_a , the unit weight of water γ_w and the load efficiency parameter B^* as introduced by Wang (2000). The hydraulic and elastic properties of the soil-fluid system are accounted for by the consolidation coefficient c . The uniaxial loading efficiency parameter B^* defined in eq. (8.8) considers the ratio of the elastic properties of the soil matrix and the gas-water-mixture (Montenegro, 2016; Skempton, 1954; Wang, 2000).

$$B^* = \frac{1}{1 + \frac{nE_{\text{oed}}}{K_{\text{wg}}}} \quad (8.8)$$

Due to the assumed uniaxial loading condition the matrix elastic properties are considered by the oedometric modulus of the soil E_{oed} . The porosity n reflects the matrix-fluid volume ratio. The fluid compressibility of the pore fluid (water-gas-mixture) K_{wg} is given in eq. (8.9).

$$\frac{1}{K_{\text{wg}}} = \frac{S}{K_w} + \frac{(1 - S)}{K_g} \quad (8.9)$$

The elastic properties of the fluid depend on the amount of entrapped gas expressed by the saturation S and the respective bulk moduli of water K_w and gas K_g (Montenegro, 2016; Wang, 2000). K_g - exceeding K_w by orders of magnitude - is calculated based on Boyle's law and with respect to mean fluid pressure (Montenegro, 2016). The above presented equation applies to conditions below the water level where the gas phase is assumed to be discontinuous as small gas bubbles at the respective fluid pressure.

Field observations and laboratory experiments suggest a saturation between 85 % and 100 % in natural soils even under submerged conditions (Montenegro, Köhler et al., 2005; Montenegro, Stelzer et al., 2014). In this study the spatial variability of hydraulic conductivity and friction angle were considered, while the elastic properties were assumed to be constant and, thus, independent of these spatially varying parameters. Thus, conservative estimates of $S = 85\%$ and $B^* = 0.01$ are specified in the FE model.

Depending on the ratio of the drawdown velocity and the hydraulic conductivity, the excess pore pressure profile is characterised by a steep gradient close to the surface which requires a high model resolution. At present, the choice of 1000 equally spaced elements over a depth of 5 m was considered as a reasonable compromise between model performance and accuracy.

8.2.3 Generation of the random fields

The spatial variability of the soil parameters is approximated by random fields. From a parametric study it was deduced that a column with 500 slices that depict a discretisation of the random soil properties over a depth of 5 m is sufficient to observe a failure caused by the ship-induced excess pore pressure profile.

Numerous methods have been proposed for the generation of random fields, such as the covariance matrix decomposition (CMD) method (Clifton and Neuman, 1982; Davis, 1987), the moving average (MA) method (Gersch and Yonemoto, 1977), the turning bands method (TBM) (Matheron, 1973), the fast Fourier transform (FFT) method (Cooley and Tukey, 1965) and the local average subdivision (LAS) method (Fenton and Vanmarcke, 1990).

This work is restricted to stationary random fields where the covariance between two points depends solely on their distance. The random fields are generated by the covariance matrix decomposition method with a Cholesky decomposition. Firstly, a standard normal distribution is generated, in which the spatial variation of the standard values is incorporated by means of a correlation function with a scale of fluctuation $\theta_{k,\phi'}$. The following correlation function, adopted from Griffiths, Huang et al. (2011), is applied:

$$\rho_{ij} = \exp\left(-2\frac{|y_i - y_j|}{\theta_{k,\phi'}}\right) \quad (8.10)$$

The standard normal field is next transformed to the appropriate distribution based on mean and cov of the variable being modelled. A lognormal distribution of the random variables will ensure the variables are bounded by $\phi' > 0^\circ$ and $k > 0 \text{ m s}^{-1}$. The lognormal distribution is a common choice in geotechnical engineering as it offers the advantage of simplicity. The parameters are derived by a simple nonlinear transformation of the Gaussian distribution, e. g. Griffiths and Fenton (2007). Figure 8.2 illustrates the random field parameters schematically with regard to the infinite slope.

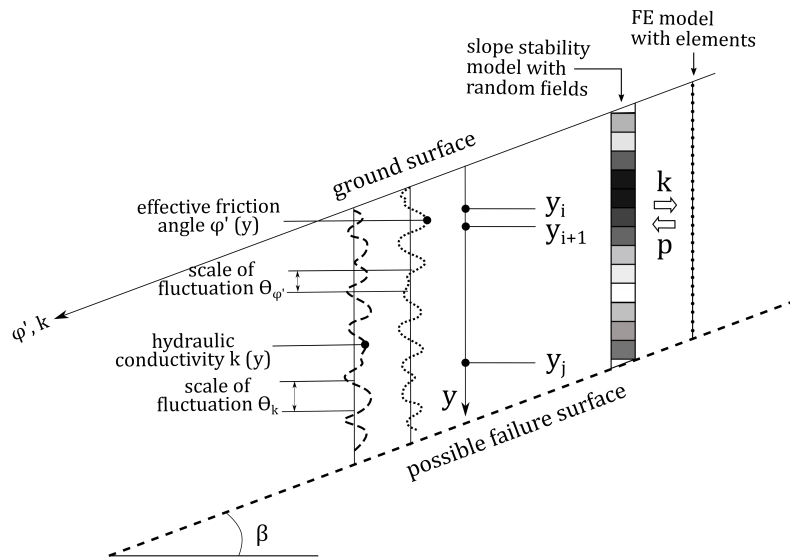


Figure 8.2: Schematic diagram of the random field method applied to an infinite slope. The random field of 500 slices is generated and k is mapped to the finite element model of finer resolution to determine the excess pore pressures p , which are subsequently re-assigned to the slope stability model by linear interpolation. Based on the material strength and excess pore pressures the required armour layer thickness is determined in the slope stability model.

8.2.4 Revetment design in presence of random fields

As a result of a fast drawdown, the limit state function g reaches a minimum g_{\min} at a certain depth, which is also referred to as the critical depth. If $g_{\min} < 0$, it may result in a local slope sliding failure. The armour layer thickness $d_{D, \text{req}}$ required to avoid slope sliding is derived from the infinite slope equations at g_{\min} :

$$d_{D, \text{req}} \geq \frac{g_{\min}}{(\sin \beta - \tan \phi \cos \beta) \cdot \gamma'_S} \quad (8.11)$$

Figure 8.3 clearly demonstrates the function of the armour stone layer. The limit state function and the shear strength are shifted from the negative, unsafe region to the positive, safe region while the excess pore pressure does not change. The formulation of the model, a theoretical construct, allows for negative values of the shear strength, which primarily occur in the theoretical set-ups without the armour stone layer. These set-ups are necessary to determine the required thickness of the armour stone layer, but lead to an initial factor of safety of the slope smaller than 1. It is therefore emphasized that a slope without any armour stone layer subjected to the design drawdowns will certainly fail.

For the stability analysis using the random field approach, a minimum of 1000 MCS are run to obtain a range of possible outcomes. With each simulation, a random field with the same mean and standard deviation, but with a different spatial distribution of soil properties within the 1D column is generated. Under the assumption that failure of any plane in the slope causes a local failure, g_{\min} is recorded after each simulation and compared to the following scheme:

$$I = \begin{cases} \text{stable (0),} & \text{if } g_{\min}(\mathbf{x}) \geq 0. \\ \text{unstable (1),} & \text{if } g_{\min}(\mathbf{x}) < 0. \end{cases} \quad (8.12)$$

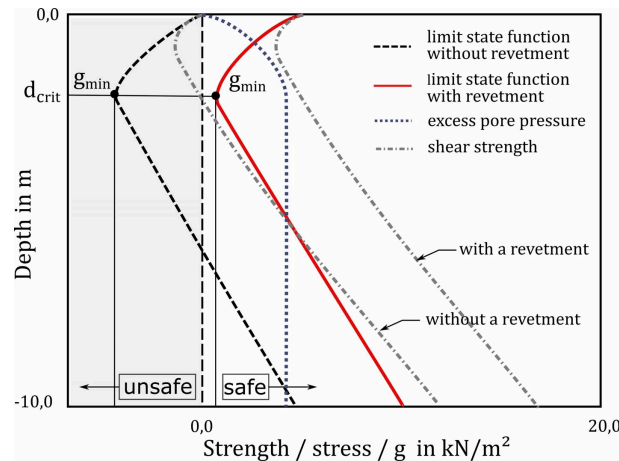


Figure 8.3: Limit state function as well as stress and strength profiles with and without revetment.

The probability of a slope failure p_f then results from the number of failures relative to the overall number of simulations N :

$$p_f = P [I = 1] \approx \frac{1}{N} \sum_{i=1}^N I_i \quad (8.13)$$

Reviewing eq. (8.2) and eq. (8.5), it becomes clear that the application of the armour stones will increase the vertical overburden load and, thereby, stress and strength. However, whereas the shear stress τ rises proportionally with increasing overburden load, the shear strength $\bar{\tau}$ rises non-proportionally due to the multiplication of σ'_n by $\tan \phi'$, see eq. (8.5). The resulting difference between stress and strength requires an additional safety margin, or, to be more precise, more armour stones.

Considering an example design case, where the initial calculation is conducted without a revetment, a first guess of the required armour layer thickness can be obtained by a first evaluation of eq. (8.11). However, as outlined above, the application of the additional weight of the armour stones alters the limit state function, and thereby, p_f . Eq. (8.11) only accounts for the load situation included in g_{\min} at the time of calculation, which includes not only the excess pore pressure and the weight of the soil, but also an initially assumed armour layer thickness. By means of the equilibrium calculations it can be determined, whether this initially assumed armour layer thickness is sufficient to ensure the local slope stability. If not, a second, third, and so on, evaluation of eq. (8.11) with the armour layer thickness determined in each step is required to verify that $g_{\min} \geq 0$ for the target value of p_f .

8.2.5 Parameter combinations

This chapter uses the same parameter combinations as Chapter 6, Table 6.3. The soil types and drawdown combinations investigated are selected based on the existing German design standards EAU (2012) and MAR (2008). The spatial variability is described by the scale of fluctuation θ . For the presented parameter study, it ranges from 0.00 m to 2.00 m.

For simplicity, the model variables k and ϕ' are defined as follows: The mean value for the random field is constant, while the variation of the properties relative to the mean is governed by

the cov. Since GBB (2010) does not state a particular bound to select the characteristic values, a range of ϕ' and k are considered for the deterministic benchmark solution. The lower bound is taken as the 5 % quantile of the distribution in accordance with DIN EN 1997-1:2014-03 (2010). The upper bound of the deterministic benchmark solution is the mean. Figure 8.4 illustrates the approach for two distributions of the same parameter, but with different standard deviations. Henceforth, results that consider the spatial variability are denoted by 'rf', whereas the corresponding benchmark results are indicated by the abbreviation 'bm'.

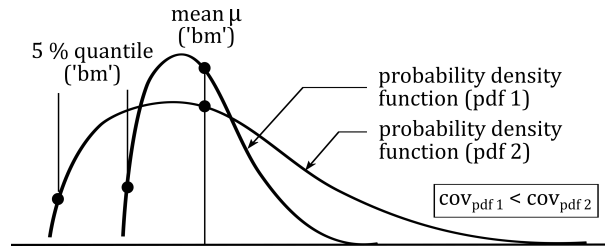


Figure 8.4: Parameter definition to compare the random field analyses to the benchmark solution.

8.3 Results of the random field analysis

8.3.1 Influence of random fields on the embankment stability

The inclusion of random fields leads to two competing mechanisms. While areas of larger ϕ' increase the stability of the embankment and thus require less armour stones, the presence of smaller k leads to larger excess pore pressures and thereby a thicker armour stone layer.

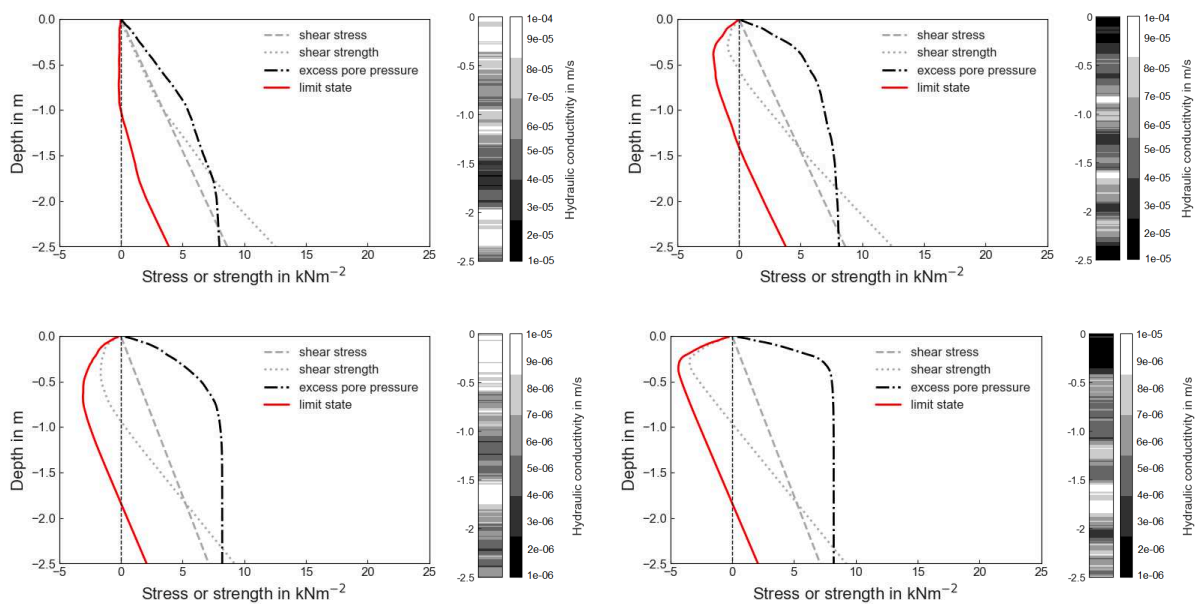
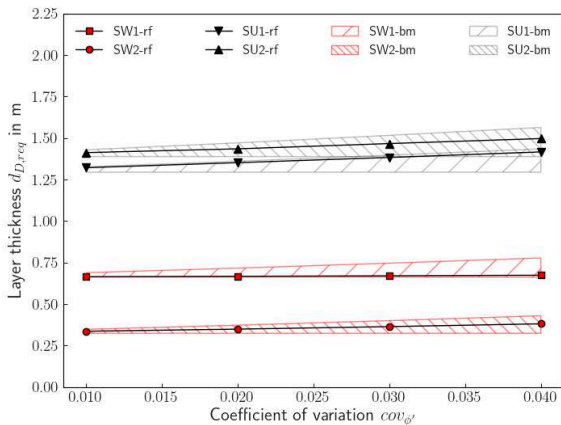


Figure 8.5: Stress, strength, excess pore pressure and limit state profiles with the corresponding random fields for maximum (left) and minimum (right) limit state out of a 100 MCS for SW2 (top) and SU2 (bottom).

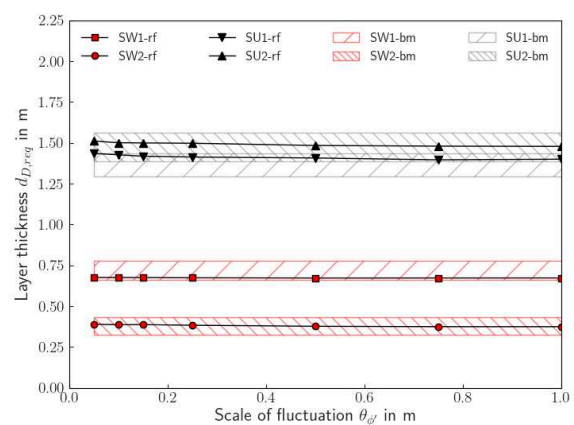
These observations can be best explained by Figure 8.3 and Figure 8.5. For illustrative purposes, the explanations focus on a random k . Figure 8.5 displays the stress, strength, excess pore pressure and limit state profiles over depth with the corresponding random fields for a best case and a worst case simulation of the sand and the silty sand. Naturally, large excess pore pressures occur in the presence of low values of k . A worst case scenario is characterised by a low k close to the surface; conversely, a higher k close to the surface leads to smaller excess pore pressures in the area of interest. Considering once more Figure 8.3, the required armour layer thickness is determined by g_{\min} . In particular, when areas of low k are located close to the surface, large excess pore pressures may occur in combination with a low overburden weight of the soil. As a result of the excess pore pressure the effective shear strength decreases which can be compensated by larger ϕ' . In areas of larger ϕ' , it is thus more likely that the maximum excess pore pressure can be compensated by the material strength.

Figure 8.5 also illustrates that with increasing v_a/k ratio ($v_a = z_a/t_a$), as inferred in the figure by a reduction in k , the excess pore pressure profile is less affected by the spatial variability of k . The shape of the excess pore pressure profiles and thus the limit state functions from the best and worst case scenarios of the SU case display less variation than the profiles of the SW case. It may therefore be concluded that soils of lower permeability display a smaller sensitivity to fluctuating k values than more permeable soils.

8.3.2 Influence of a non-homogeneous friction angle



(a) Required layer thickness as a function of $cov_{\phi'}$ with $\theta_{\phi'} = 0.25$ m.



(b) Required layer thickness as a function of $\theta_{\phi'}$ with $cov_{\phi'} = 0.04$.

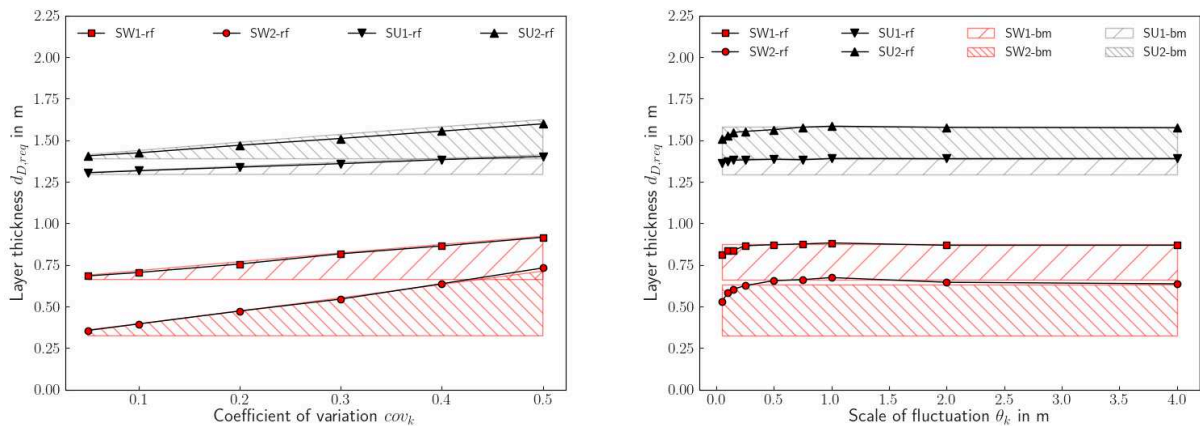
Figure 8.6: Influence of a non-homogeneous effective friction angle ϕ' on armour layer thickness (first iteration). The hatched areas indicate the deterministic benchmark solutions obtained with the 5% and 50% quantiles. The lines with markers depict the 95% quantiles obtained from the uncertainty analysis with random ϕ' .

Figure 8.6 shows that for the deterministic 'bm' and probabilistic 'rf' solutions, the layer thickness is a function of ϕ' . The results indicate that with an increasing $cov_{\phi'}$ the deterministic 5% 'bm' results require more armour stones than the 'rf' results, whereas deterministic mean 'bm' calculations require less armour stones. In contrast to this, increasing $\theta_{\phi'}$ values do not affect the required armour layer thickness. With regard to the revetment design, the results indicate that the choice of the 5% quantile of ϕ' as the characteristic value may overestimate the required armour layer thickness. Instead, a conservative mean may be a more suitable as characteristic

value of ϕ' . Depending on the load case and soil type, the thereby implied consideration of spatial variability can reduce the required armour layer thickness by 10 cm to 20 cm compared to the 5% 'bm' solution.

As described in Chapter 6, Section 6.5.3 a different reaction of the two soil types to the two draw-down combinations can be observed. The layer thickness required for the SW cases is governed by the small drawdown time at moderate drawdown height, whereas the layer thickness of the SU cases is governed by the large drawdown time at a large drawdown height.

8.3.3 Influence of a non-homogeneous hydraulic conductivity



(a) Required layer thickness as a function of cov_k with $\theta_k = 0.25$ m.

(b) Required layer thickness as a function of θ_k with $cov_k = 0.4$.

Figure 8.7: Influence of a non-homogeneous hydraulic conductivity k on armour layer thickness (first iteration). The hatched areas indicate the deterministic benchmark solutions obtained with the 5% and 50% quantiles. The lines with markers depict the 95% quantiles obtained from the uncertainty analysis with random k .

Figure 8.7a shows that an increasing variance of k does not affect the armour layer thickness notably. The increasing cov_k in the 'rf' cases demands a similar layer thickness as the 5% 'bm' results. Contrary to this, Figure 8.7b shows that small θ_k values yield slightly smaller layer thicknesses than the 5% 'bm' solutions. A thin 'layering' reduces the maximum excess pore pressure and thus the required armour layer thickness. For $\theta_k \rightarrow 0$, k reaches a harmonic mean, which is slightly smaller than the arithmetic mean of the probability density function, but larger than the 5% 'bm'. The harmonic mean of the hydraulic conductivity k_{eff} is determined from the sum of \bar{n} individual layer thicknesses $T_{L,i}$ over their hydraulic conductivities k_{s_i} compared to the total layer thickness, see eq. (8.14). For $\theta_k \rightarrow \infty$ the 'rf' results approach the 5% 'bm' results.

$$k_{\text{eff}} = \frac{\sum_{i=1}^{\bar{n}} T_{L,i}}{\sum_{i=1}^{\bar{n}} \frac{T_{L,i}}{k_{s_i}}} \quad (8.14)$$

Figure 8.7b indicates that in some cases the 5% quantile of k may not be as conservative as assumed. For moderate θ_k , the 'rf' armour layer thicknesses for the SW are larger than the layer thicknesses determined in the 5% 'bm' case. Comparing the two drawdowns considered, these observations are more prominent for the larger drawdown height at low(er) velocity (SW2) than

for a small(er) drawdown height at great(er) velocity (SW1). The results imply that, especially in those cases of a large cov_k and a moderate θ_k , the least permeable areas govern the design. If these areas are greater than 25 cm, they will act as a seal and the excess pore pressure will increase; hence, more armour stones will be required.

In the context of a revetment design, the results indicate a significant influence of the spatial variability of k on the required armour layer thickness. Especially soils of higher permeability exhibit a noteworthy sensitivity to fluctuating k values at moderate θ_k . In a few cases involving a large drawdown, the 5 % quantile of k may not yield a conservative design.

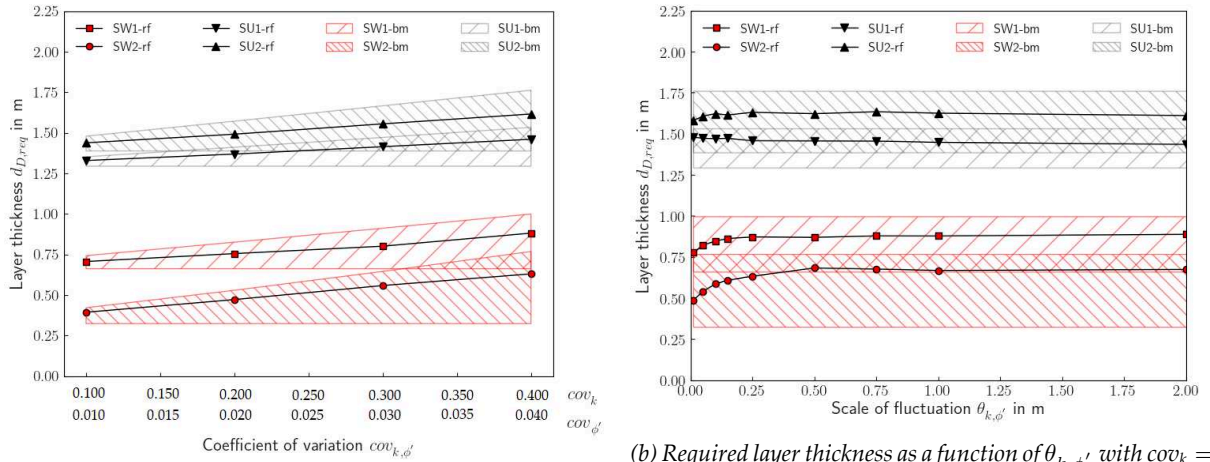
8.3.4 Influence of a non-homogeneous friction angle and hydraulic conductivity

Finally, the combination of a non-homogeneous friction angle and hydraulic conductivity is investigated, assuming no correlation between ϕ' and k . Figure 8.8a and Figure 8.8b illustrate that the mean 'bm' calculations greatly underestimate the required armour layer thickness. In contrast, the 5 % 'bm' cases overestimate the required armour layer thickness compared to the 'rf' analyses with different $\theta_{k,\phi'}$ and $\text{cov}_{k,\phi'}$ values. With increasing $\text{cov}_{k,\phi'}$, the difference between the 'rf' and 'bm' cases heightens due to the diverging rises of the 'bm' and 'rf' results. Consequently, the 'ideal' characteristic values of ϕ' and k are a function of $\text{cov}_{k,\phi'}$. Depending on the $\text{cov}_{k,\phi'}$ and $\theta_{k,\phi'}$, the 'rf' analyses require between 10 cm to 30 cm less armour stones than the 5 % 'bm' solutions.

Noteworthy is the different behaviour of the SW and SU cases with regard to an increasing $\theta_{k,\phi'}$ (see Figure 8.8b). In both SW cases, the required armour layer thickness initially rises until a maximum is reached and then it abates very slightly. The SU cases do not show a pronounced effect on the armour layer thickness with increasing $\theta_{k,\phi'}$. This behaviour may be explained by the larger variability of the excess pore pressure profiles in permeable soils (see Section 8.3.1). For values of $\theta_{k,\phi'}$ that are larger than the possible range of the critical depth, this effect becomes less defining.

Based on the four case studies, a worst case correlation length which is the correlation length that requires the most armour stones can be established. The examples indicate that a correlation length that ranges in the area of the critical depth affects the required armour layer thickness most. For the SU cases the critical depth ranges between 0.20 m and 0.50 m, whereas the SW cases are characterised by a greater critical depth of 0.40 m to 0.60 m. The 'worst case' scenario is most pronounced for sandy material subjected to a large drawdown of moderate velocity (SW2). For this particular case, a 'worst case' correlation length of 0.50 m is identified.

In summary, the results show that the few cases where the neglect of a spatially variable k leads to a non-conservative revetment design are compensated by larger ϕ' . Compared to the 5 % 'bm' solutions, the consideration of the spatial variability of ϕ' and k may allow for less armour stones. The spatial variability can account for uncertainties regarding the 'layering' of the soil and the complex interplay of ϕ' and k with regard to the local embankment stability. Especially for soils of higher hydraulic conductivity, the 'worst case' correlation length should be kept in mind. Moreover, correlation of the variables may serve to amplify the best and worst case scenarios.



(a) Required layer thickness as a function of $cov_{k,\phi'}$ with $\theta_{k,\phi'} = 0.25$ m.

(b) Required layer thickness as a function of $\theta_{k,\phi'}$ with $cov_k = 0.40$ and $cov_{\phi'} = 0.04$.

Figure 8.8: Influence of a non-homogeneous hydraulic conductivity k and friction angle ϕ' on armour layer thickness (first iteration). The hatched areas indicate the deterministic benchmark solutions obtained with the 5% and 50% quantiles. The lines with markers depict the 95% quantiles obtained from the uncertainty analysis with random k and ϕ' .

8.4 Probability of slope failure

The geotechnical design or assessment of a revetment may target a specific reliability. The reliability of the revetment is a function of the drawdown, the slope inclination, the soil parameters and the armour layer thickness. Since drawdown, geometry and soil parameters are commonly defined on the basis of available field information, the representative parameter sets of case studies SW2 and SU2 are selected to investigate the reliability as a function of the armour layer thickness. Each case study is investigated for all combinations of:

- $\theta_{k,\phi'} = 0.5$ m, $\theta_{k,\phi'} = 1.0$ m,
- $cov_{k,\phi'} = 0.20/0.02$ and $cov_{k,\phi'} = 0.40/0.04$.

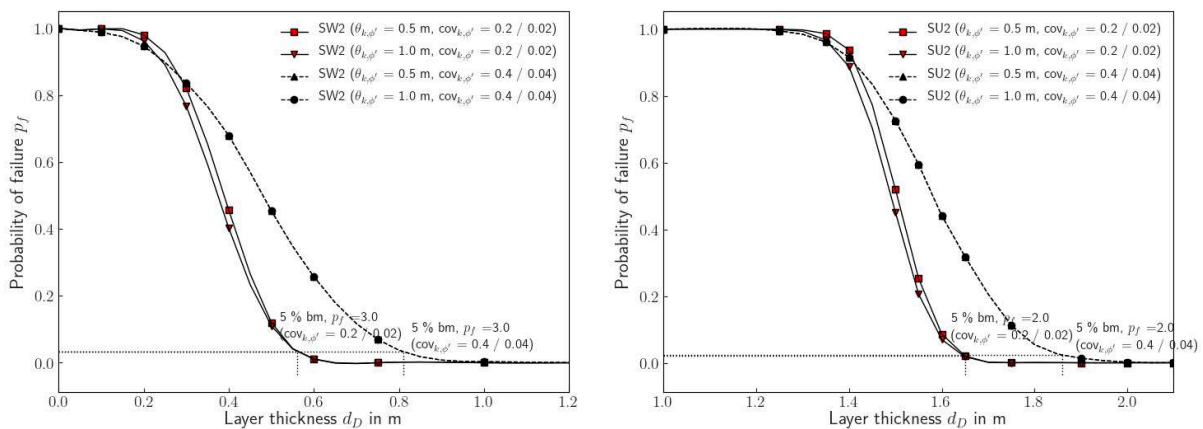
As shown in Figure 8.9, the probability of failure p_f decreases with increasing layer thickness rather rapidly after a certain threshold value has been reached. The larger the $cov_{k,\phi'}$, the larger the p_f , whereas $\theta_{k,\phi'}$ does not significantly influence p_f . For larger $cov_{k,\phi'}$ the p_f of the two investigated $\theta_{k,\phi'}$ are concordant.

Moreover, the obtained probabilities of failure highlight the importance of an iterative analysis or the use of probability charts when using the infinite slope model for a revetment design. Since the probability graphs of $cov_{k,\phi'} = 0.2/0.02$ are characterised by a steeper gradient in the area of interest, smaller iteration steps and, thereby, likely more iterations than for larger $cov_{k,\phi'}$ are required. The layer thickness obtained after one iteration yields approximately $p_f = 40\%$ for $cov_{k,\phi'} = 0.2/0.02$ and $p_f = 20\%$ for $cov_{k,\phi'} = 0.4/0.04$.

According to JCSS (2001), a target reliability of $\beta = 3.1$ ($p_f = 1 \times 10^{-3}$) may be acceptable for ultimate limit states leading to minor consequences in the case of a failure while characterised by high costs for safety measures. The armour layer thicknesses, which are determined with

the 5% 'bm' values, reach $p_f = 2\% - 3\%$ and, thus, do not meet the target reliability. However, since GBB (2010), for instance, defines partial factors for actions and material parameters as $\gamma_{G,d} = \gamma_Q = 1$, these larger probabilities of failure may be acceptable. If the current level of safety is satisfactory, the choice of limit state condition and target reliability should be discussed.

Independently of $\text{cov}_{k,\phi'}$, the deterministic 'bm' SW cases yield a larger p_f than the deterministic 'bm' SU cases. It is therefore concluded that sandy material is more strongly affected by the spatial variability than the silty material.



(a) Sand (SW2).

(b) Silty sand (SU2).

Figure 8.9: Probability of failure for different materials and variability parameters.

8.5 Discussion

The presented investigations illustrate the effects of a spatially variable friction angle and hydraulic conductivity on the revetment design. The applied methodology is not suitable for direct comparison with the existing German standard, since the excess pore pressures determined by an FE model based on Biot's approach are different to the excess pore pressures calculated using the analytical approximation defined in the GBB (2010). However, the parameter study indicates a strong model sensitivity to the excess pore pressure profiles, which once more emphasizes the significance of an accurate method to determine the excess pore pressure. Moreover, as a result of the chosen infinite slope approach the spatial variability is reduced to the variability in vertical direction. Yet, the spatial variability in longitudinal direction of an embankment is certainly of interest for the consideration of local damages. Further investigations are required.

The standard design of revetments comprises a toe support which significantly reduces the required armour layer thickness due to the activation of additional supporting shear stresses. The current investigations do not take a toe support into account. Such a simplification is justifiable as a toe support should not alter the observed mechanisms. This, however, results in rather large armour layer thicknesses for the current investigations. In general, it can be assumed that the construction of a toe support reduces the required armour layer thickness by 0.60 m to 0.90 m.

In summary, the results demonstrate that the level of safety obtained with the semi-probabilistic design approach depends strongly on the choice of the characteristic values. In the case of ϕ' , the 5 % quantile may overestimate the required armour layer thickness, while a conservative mean value may be a suitable choice. In the case of k , the 5 % quantiles may lead to slightly unconservative designs. For a combination of ϕ' and k the 5 % quantile may overestimate, and the mean value may underestimate, the required armour layer thickness.

For permeable soils, which are generally considered as non-critical from the point of view of a revetment design, special attention should be paid to θ_k . The results suggest that less permeable zones greater than 25 cm thickness located close to the surface, govern the excess pore pressure and the required armour layer thickness. A 'worst case' correlation length of 0.50 m is identified for sandy material subjected to a large drawdown at moderate velocity. This observation is especially interesting with regard to the GBB (2010) design standard which only accounts for layers thicker than 1 m.

The current analyses do not account for correlation between different soil parameters. In the case of the investigated parameters the correlation is slightly negative (Arnold and Hicks, 2011; Vardon et al., 2016). A zone that is characterised by small ϕ' is more likely to be associated with high k and vice versa. In this case, a negative correlation would tend to reduce best and worst case scenarios. However, if considering a correlation of the matrix stiffness K_s as well, competing mechanisms affecting the required armour layer thickness may be observable. While a correlation of ϕ' and k mainly governs the resistance, a correlation of K_s , k and the material porosity n influences the excess pore pressure development. Hence, more research is required.

To conclude with, it is stressed that, in contrast to the stratigraphic layer structure commonly used for slope stability analysis, the equations of the geotechnical revetment design are based on the assumption of homogeneous soil. In addition and as already discussed in Chapter 6, the variability of the soil properties is studied in a limited range. This assumption is justified by the dimensions of a revetment. In practice, it is not feasible to explore the soil stratification for large embankment structures exactly. For a design thus the most critical soil type is selected from all investigated stratification layers. Random fields offer the possibility to consider spatial variability within this framework. Uncertainties resulting from the assumption of homogeneity should be investigated separately within the framework of model uncertainty.

8.6 Conclusions

Addressing parameter uncertainties inherent to actions and material parameters

- ☑ How does parameter uncertainty affect the geotechnical revetment design?
- ☑ How can these uncertainties be taken into account?
- ☑ What recommendations can be provided regarding characteristic values of resistance parameters?

In summary, the investigations show that the level of safety obtained with the semi-probabilistic design approach depends strongly on the choice of the characteristic values. The best estimate of the characteristic value which accounts for the spatial variability of the soil parameters is a function of the soil type, $\text{cov}_{\phi'}$ and $\theta_{k,\phi'}$. For sandy material, a 'worst case' correlation length is identified.

The obtained probabilities of failure highlight the importance of an iterative analysis or the use of probability charts when using the infinite slope model for a revetment design. Since the proposed methodology allows targeting a specific reliability level under consideration of spatially variable soil parameters, it may be economically feasible, even if a larger number of field tests is required.

As a consequence for revetment design, during subsoil investigations and the choice of characteristic values for subsequent stability analyses special attention should be paid to the variability of k and ϕ' , in particular for soils close to the surface. To obtain a reliable design k should be selected as value at the lower end of the explored parameter range, whereas the characteristic value of ϕ' should be selected as conservative mean. For permeable soils, which are generally considered as non-critical from the point of view of a revetment design, special attention should be paid to θ_k . As the worst-case correlation length is closely associated with the critical depth, it is recommended that the selection of characteristic values should be based on the least permeable zone located between zero depth and the critical depth.

Further investigations regarding the comparability of the target reliabilities available in current probabilistic design codes and the level of safety of the current design are required. Moreover, the investigations should consider the correlation between the soil parameters and the spatial variability of the elastic soil properties. Finally, it is emphasized that further investigations of the probabilistic distribution of the loads are necessary in order to conduct a fully probabilistic revetment design.

9 | SUMMARY AND CONCLUSIONS

'Reliability analysis is not a panacea for all uncertainties affecting design calculations based on the factor of safety or the geotechnical practice in general. Reliability analysis is merely one of the many mathematical methods routinely applied to model the complex real-world for engineering applications. It is susceptible to abuse in the absence of sound judgement in the same manner as a finite element analysis. The importance of engineering judgement clearly has not diminished with the growth of theory and computational tools. However, its role has become more focused on those design aspects that remain outside of the scope of theoretical analyses.'

–Phoon, Ching and Wang (2019)

Contents

9.1	Introduction	146
9.2	Main findings	146
9.3	Usability of methods and results	148
9.4	Outlook and concluding remarks	150

9.1 Introduction

Uncertainties are inherent to design and construction in engineering. Deterministic design procedures, however, lack a systematic evaluation of uncertainty. This thesis aimed at complementing the revetment design process by introducing reliability-based methods.

For a first step towards a reliability-based design approach, the most significant uncertainties inherent to actions and material parameters are investigated. For this purpose, methods of data analysis were presented, the concept of a reliability-based design was adapted for revetments and compared to deterministically obtained standard designs. By doing so, the suitability of probabilistic design methods for revetments was demonstrated.

In order to allow for an application to real-life problems, a number of knowledge gaps regarding the description of damage, limit states, required input parameters and corresponding parameter uncertainties were investigated. While all findings were discussed in detail throughout this thesis and summarised in the conclusions of each chapter, the subsequent Section 9.2 recaps the main findings. Section 9.3 puts them in an overall context by outlining the applicability of the main findings and probabilistic methods to revetment design. Section 9.4 provides concluding remarks and an outlook regarding future research.

9.2 Main findings

Definition of limit states

Expert interviews were conducted at nine field departments at different German canals. Expert knowledge and field observations regarding damage, damage development and maintenance procedures were systematically gathered. It was found that damage of loose armour stone embankments progresses slowly. Often, damage can be observed for years before an intervention is urgently required. Only when the filter layer or soil is exposed, the damage rate increases rapidly. However, **initial displacement of armour stones does not pose a risk** to the reliability of the structure.

Based on these findings, it can be concluded that the current design against **armour stone displacements** refers to a **fatigue criterion**. Only when the functions of the armour stone layer, the protection against soil erosion and local slope failure, are no longer met, failure occurs. The equations of the **geotechnical** design describe an **Ultimate Limit State (ULS)**.

A comparison between determined failure probabilities and maintenance costs indicates that **target reliabilities** based on safety classes, i. e. JCSS (2001), may be suitable for a risk-based revetment design. Since literature does not provide target reliabilities for the Limit State of Fatigue, it is recommended to employ target values of the Serviceability Limit State (SLS).

Evaluation of field observations

A concept for **quality assurance** of field observations is proposed which assesses the following quality indicators: **completeness, temporal correlation, geographical correlation, validity** and **consistency**. The quality assessment of four field observation campaigns showed that available measurements of vessel passages and resulting hydraulic loads differ in validity, consistency

and completeness. The investigations highlight the importance of storing measurements and boundary conditions, raw data and interpreted data together in one database or alternative data storage system.

On the basis of the presented data review, generic requirements regarding data collection for a more site-specific, risk-orientated revetment design can be formulated. Put simply, the defined quality indicators should be met. Data should be as recent and site-specific as possible. Data evaluation and data storage should be as automated, structured and standardised as possible. With regard to completeness, it is recommended to record at least the parameters listed below. The measurement duration has to be adapted to the selected calculation approach (deterministic, semi-probabilistic, fully probabilistic).

- **Hydraulic loads:** wave heights at bow and stern, return current velocity and slope supply flow velocity or maximum ship-induced flow velocity, drawdown parameters
- **Geotechnical conditions:** soil and armour stone characteristics, i. e. friction angle, hydraulic conductivity
- **Geometrical conditions:** revetment construction, i. e. slope inclination, armour layer thickness, filter layer thickness, toe support
- **Meta data (useful, i. e. for model factor analyses, but optional):** vessel velocity, vessel type, vessel dimensions, shore distance

Identification of input parameters

By means of **sensitivity analyses**, it was shown that the hydraulic design is strongly affected by $H_{\text{stern}}, u_{\text{max}}, \rho_s$. It may be sufficient to observe these quantities in field measurements. Since canals are characterised by low to no natural flow, v_{return} is of secondary importance for the revetment design at canals. The geotechnical design is strongly affected by the hydraulic loads, t_a and z_a . Moreover, the analyses point to a strong interaction of t_a and z_a and a moderate interaction of z_a and k . Based on the findings of the sensitivity analyses, it is recommended to reduce the number of empirical factors such as B'_B and B_B^* in the hydraulic design to a minimum. B'_B and B_B^* have a minor effect on the variability of the hydraulic design but alter the design specifications, and thus, considering different revetments, lead to revetment dimensions which are not comparable.

The results of the **distribution and correlation analysis** highlight that the choice of a suitable distribution type, distribution parameters and correlation is ambiguous. Based on the analyses, it is concluded that H_{stern} follows a Lognormal distribution and v_{return} a Gaussian distribution. A positive correlation of H_{stern} and v_{return} was found.

Armour stone characteristics are identified based on laboratory tests with two armour stone classes and 1000 armour stones each. The results show that the mean value varies depending on the armour stone class and delivery batch, whereas the standard deviation is constant at $\sigma \approx 12$ mm for CP_{90/250} and $\sigma \approx 10$ mm for CP_{45/125}.

Accounting for uncertainty

A bootstrapping approach by Newman et al. (2000) was extended to investigate the effects of **statistical uncertainty** on hydraulic and geotechnical revetment design. From the results of the bootstrapping procedure, it is derived that the geotechnical design is marginally affected by statistical uncertainty if only the uncertainty of the material parameters is considered. Only the variance or the choice of characteristic values of effective friction angle and hydraulic conductivity affects the required armour layer thickness. In the case of the hydraulic design, it was shown that the statistical uncertainty decreases with the number of samples. The required armour stone size depends strongly on the variability of the hydraulic loads.

When conducting a **deterministic hydraulic revetment design** with field observations, a minimum sample size of 250 measurements should be available. For a smaller number of available measurements, statistical uncertainty increases significantly, which may be compensated by partial factors. Yet, it must be noted that such a semi-probabilistic approach may not result in a comparable safety level at different waterways.

As shown by the reliability-analysis combined with bootstrapping, the investigated **probabilistic methodologies** are characterised by a **robustness** regarding the underestimation of actions, since the probability functions account for the possibility that values occur, which exceed in nature observed load maxima.

The presented comparison of reliability analyses with measured and calculated hydraulic loads has shown that the revetment design becomes more conservative when using calculated loads. Subsequently, it was shown that the **generalised model factor approach** (Dithinde et al., 2016) can assist in accounting for this **transformation uncertainty**. Within this thesis, generalised model factors for H_{stern} and v_{return} are determined for four canals as summarised in Chapter 7.

The effects of **spatial variable soil properties** on slope stability was investigated by means of **random fields**. It was found that less permeable zones greater than 25 cm thickness close to the surface govern the required armour layer thickness. The best estimates of characteristic values of the soil properties are a function of the soil type, the coefficient of variation and the scale of fluctuation. As a consequence for revetment design, during subsoil investigations and for the choice of characteristic values for subsequent stability analyses, special attention should be paid to the variability of k and ϕ' , in particular for soils close to the surface.

To obtain a reliable design, k should be selected as value at the lower end of the explored parameter range, whereas the **characteristic value** of ϕ' should be selected as conservative mean. Moreover, as the worst-case correlation length seems to be closely associated with the critical depth, it is recommended to select the characteristic hydraulic conductivity based on the least permeable zone located perpendicular to the slope and up to a depth of the critical depth.

9.3 Usability of methods and results

Within the scope of this thesis, essential aspects of the **parameter uncertainty** were examined, and it was aimed for an **adaptation of a reliability-based design** for revetments. The **applicability** of a reliability-based concept should be evaluated. From the investigations, the following conclusions are drawn:

Statistical and transformation uncertainty have a significant effect on hydraulic revetment design. Model factors and reliability-based methods provide a robust framework to account for these uncertainties in hydraulic design. The results of probabilistic hydraulic design show that reliability-based methods offer saving potentials, because (i) based on the new definition of the limit state different, less strict target values apply and (ii) the addition of approaches on the safe side is avoided, instead, uncertainties of input parameters are explicitly considered.

Statistical uncertainty of hydraulic loads and spatial variability of soil properties have a strong influence on geotechnical revetment design. However, drawdown height and time must be considered as parameter set in combination with hydraulic conductivity. Moreover, a number of simplifications required for the presented analyses such as the 1D random field approach and the use of semi-empirical equations for the purpose of determining the excess pore pressure and slope stability only allow to account for some uncertainties inherent to geotechnical revetment design. At present and with regard to the presented investigations, a semi-probabilistic approach is thus recommended. As for the practitioner, the random field approach can be replaced by the choice of characteristic soil properties assuming homogeneous soil conditions.

In short, while in hydraulic design parameter uncertainty may be accounted for by a probabilistic design approach, in geotechnical design the presented investigations suggest to account for parameter uncertainty by the choice of characteristic values in a semi-probabilistic design approach. However, for both the hydraulic and the geotechnical design, further investigations are required to consider the model uncertainty in design.

With the above summarised findings, a first probabilistic design concept for bank revetments can be drafted. Recapping the proposed design model from Chapter 2, a holistic design concept must address parameter and model uncertainty inherent to geotechnical and hydraulic design. Both, geotechnical and hydraulic assessments must be considered together, as they are interdependent in terms of the final revetment dimensions. Resulting modifications in revetment design are indicated by the light blue coloured boxes in Figure 9.1 and briefly described hereinafter. A design example is provided in Appendix G.

The hydraulic design may use field observations to characterise location-specific distributions of vessel-induced loads; either (a) hydraulic loads or (b) vessel passages can be measured. If only vessel passages are observed, model factors may be introduced to account for transformation uncertainty. Actions and the in-situ armour stone diameter are considered as random variables. The required armour stone diameter is then obtained by means of FORM or Monte-Carlo simulations. FORM analyses offer the advantage of providing a design point, however, regarding the results care must be taken due to the non-linearity of design equations. The probability of failure p_f or the reliability index β_{HL} serve as key figures supporting the decision-making process in design and maintenance management.

In geotechnical design, the representation of drawdown time and drawdown height as random variables is not recommended since the random combination of these parameters results in unrealistic drawdown combinations. Instead, to account for local traffic and safety requirements in particular, it is recommended to explore a number of drawdown combinations. A best practice approach would investigate different drawdown combinations based on field observations to identify worst-case combinations for local soil conditions. Material parameters, e. g. friction angle and hydraulic conductivity, are represented as characteristic values. To achieve comparable revetment designs, the degree of utilisation of a design should be provided together with final revetment dimensions.

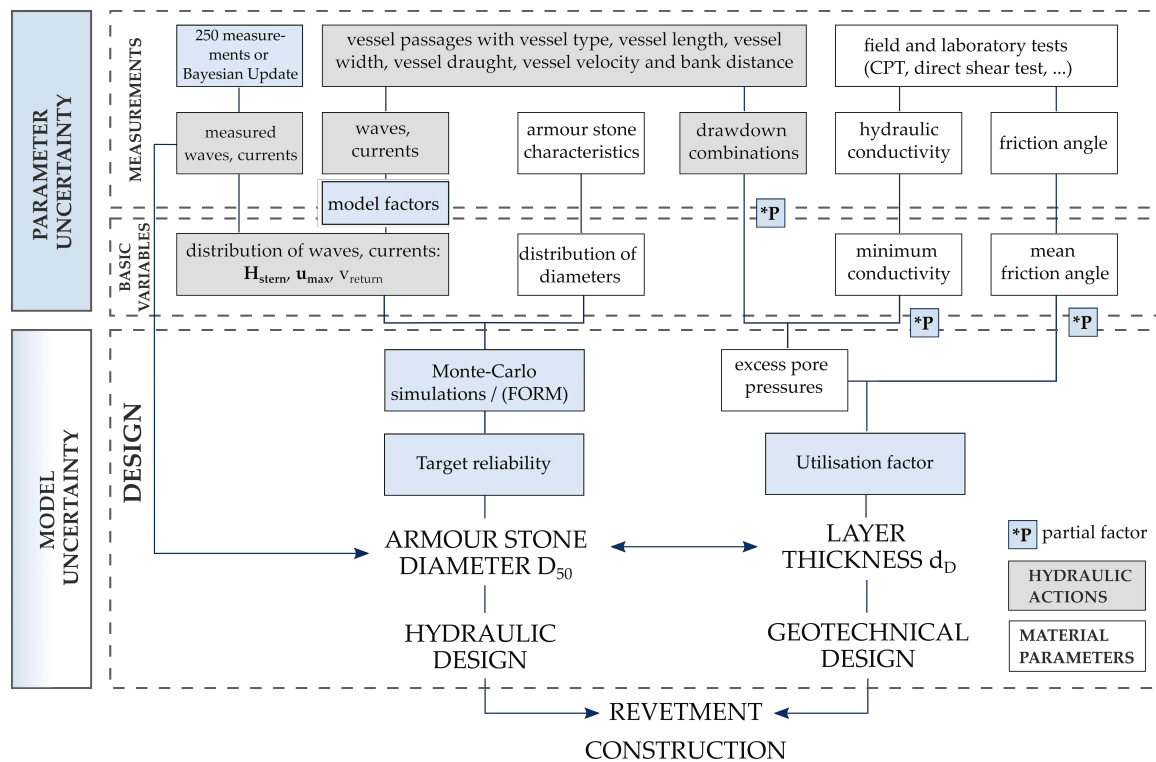


Figure 9.1: Probabilistic design model draft with input variables and uncertainties. Grey highlighted boxes indicate hydraulic actions; white boxes indicate material parameters. Blue boxes point to modifications in the revetment design as a result of the findings presented within this thesis.

9.4 Outlook and concluding remarks

Further investigations are necessary to validate and complement the proposed model approaches, to deepen the understanding of the damage development and to determine suitable target reliabilities. A detailed outlook on future research needs is provided at the end of each chapter. In the following, the need for research is thus only briefly described and recommendations for further investigations are given:

Research needs in the field of basic research

- Within the scope of this thesis, only a number of parameter uncertainties were investigated. **Uncertainty of design models** such as the equations describing armour stone stability or slope stability are not investigated. As discussed earlier, however, these model uncertainties may also have a considerable effect on the revetment design. Uncertainties regarding the revetment construction (geometry, filter layer) are considered neither. Nonetheless, these factors are of particular interest for the evaluation of existing structures and the planning of maintenance measures.
- A consequence of incomplete datasets is that only selected parameters could be examined within this thesis. Further investigations are required to determine the missing model factors, distributions and correlations. It is highly recommended to conduct **long-term observations** to validate the presented distributions and correlations.

- The presented analyses address uncertainty from a Frequentist point of view assembling basics for a reliability-based revetment design. It is recommended to investigate the application of **Bayesian methods** to the finding of this thesis. This may allow for smaller samples without increasing the uncertainty. Moreover, different sources of data such as measurements and expert knowledge can be included.
- For an integrated revetment design which combines hydraulic and geotechnical design, further research on damage progression and critical revetment conditions is required. **Damage development** must be described by a mathematical model. Moreover, damage progression must be linked to traffic. The herein presented condition assessment of revetments using probabilistic methods may serve as a starting point for the development of such a model.
- Reliability-based methods rely as much on the **underlying design equations** as analytical methods. Therefore, a continuous development of the design equations is a vital component towards a future-orientated and reliable revetment design. For instance, the presented studies on the geotechnical design indicate a strong model sensitivity to the excess pore pressure profiles, which emphasises the significance of an accurate method to determine excess pore pressure.

Research needs in the field of applied research

- This thesis primarily considers the revetment design approach outlined in GBB (2010). Since **other design approaches** are based on similar or identical design equations, it can be assumed that the results are applicable to other standards. Still, further investigations regarding the transferability of the results to other design approaches, i. e. PIANC (1987a) and Rock Manual (2007) should be conducted.
- **Target reliabilities** may be defined as a function of annual vessel passages and inspection intervals. If it is assumed that the probability of failure describes the probability of armour stone displacement per vessel passage, it must be specified in a way that allows for moderate, manageable damage propagation. Traffic density or waterway categorisation are potential criteria for a differentiation of target reliabilities. Further investigations are required to verify appropriate levels of safety.
- The assessment of the **cost-effectiveness** of investments over the **design-lifetime** of structures is crucial to provide a reliable infrastructure. In the future, it will be necessary to balance costs and benefits to cope with increasingly rapid changes with regard to economic, ecological and safety requirements. Thus, research is required to link maintenance costs, reliability and traffic.
- In order to use measurement data for design or assessment in the future, **automation and standardisation of field observations** and their evaluation should be pursued. Moreover, the proposed framework for **quality assurance of data** must be enhanced. To improve its applicability in practice, the introduction of a scoring system may be helpful.
- In addition, towards data-driven decision making of design and maintenance of revetments, engineers must begin to systematically collect and store data. Therefore, engineers must start to think about long-lasting **data storage concepts, data quality frameworks and data anonymisation**.

BOOKS, ARTICLES AND THESES

- Abdo, T. & Rackwitz, R. (1991). A New Beta-Point Algorithm for Large Time-Invariant and Time-Variant Reliability Problems. In A. Der Kiureghian & P. Thoft-Christensen (Eds.), *Reliability and Optimization of Structural Systems '90: Lecture Notes in Engineering*. Springer Berlin Heidelberg.
- Abt, S. R. & Johnson, C. J. (1991). Riprap Design for Overtopping Flow. *Journal of Hydraulic Engineering*, 17, 959–972.
- Abt, S. R., Wittler, R. J., Ruff, J. F., La Grone, D. L., Khattak, M. S., Nelson, J. D., Hinkle, J. D. & Lee, D. W. (1988). Development of Riprap-Design Criteria by Riprap Testing in Flumes: Phase II [Followup investigations].
- Aggarwal, C. C. & Yu, P. S. (2008). Outlier Detection with Uncertain Data. In M. J. Zaki, K. Wang, C. Apte & H. Park (Eds.), *Proceedings of the Eighth SIAM International Conference on Data Mining* (pp. 483–493). Cambridge University Press.
- AGREE. (1957). Reliability of Military Electronic Equipment: Report (US Department of Defense, Ed.).
- Ahrens, J. P. (1970). The influence of breaker type on riprap stability. In American Society of Civil Engineers (Ed.), *Proceedings of 12th Conference on Coastal Engineering, Washington D.C.* (pp. 1557–1566).
- Akaike, H. (1998). Information Theory and an Extension of the Maximum Likelihood Principle. In E. Parzen, K. Tanabe & G. Kitagawa (Eds.), *Selected Papers of Hirotugu Akaike* (pp. 199–213). Springer New York.
- Allsop, N. & Jones, R. J. (1993). Stability of rock armour and riprap on coastal structures. In K. W. Pilarczyk (Ed.), *Preprints International Riprap Workshop 1993* (pp. 99–119).
- Anderson, T. W. & Darling, D. A. (1952). Asymptotic Theory of Certain 'Goodness of Fit' Criteria Based on Stochastic Processes. *The Annals of Mathematical Statistics*, 23, 193–212.
- Ang, A. H. & Tang, W. H. (1975). *Probability concepts in engineering planning and design*. Wiley.
- Ang, A. H. & Tang, W. H. (1984). *Probability concepts in engineering planning and design*. Wiley.
- Ang, A. H. & Tang, W. H. (2007). *Probability concepts in engineering: Emphasis on applications in civil & environmental engineering*. Wiley.
- Arnold, P. (2016). *Probabilistic Modelling of unsaturated slope stability accounting for heterogeneity* (PhD thesis). University of Manchester, Faculty of Engineering and Physical Sciences. Manchester.
- Arnold, P. & Hicks, M. A. (2011). A stochastic approach to rainfall-induced slope failure. In N. Vogt, B. Schuppener, D. Straub & G. Brau (Eds.), *Proceedings of the 3rd International Symposium on Geotechnical Safety and Risk, ISGR 2011: Munich, Germany, June 2-3, 2011* (pp. 107–115).
- Au, S.-K. & Beck, J. L. (2001). Estimation of small failure probabilities in high dimensions by subset simulation. *Probabilistic Engineering Mechanics*, 16, 263–277.
- Au, S.-K. & Beck, J. L. (2007). Application of subset simulation methods to reliability benchmark problems. *Structural Safety*, 29, 183–193.
- Baecher, G. B. & Christian, J. T. (2003). *Reliability and statistics in geotechnical engineering*. Wiley.
- Bakker, K. J. & Vrijling, J. K. (1980). Probabilistic design of sea defences (TU Delft, Section Hydraulic Engineering, Ed.).
- Barends, F. B. J. & van Dijk, J. J. (1985). *Computer aided evaluation of the reliability of a breakwater design: Final report*. CIAD.

- Baudin, M., Dutfoy, A., Iooss, B. & Popelin, A.-L. (2015). OpenTURNS: An industrial software for uncertainty quantification in simulation [arXiv:1501.05242].
- BAW. (2009). Fahrversuche am Wesel-Datteln-Kanal und Modellversuche bei der DST zur Frage der Sohlen- und Deckwerksstabilität bei Schifffahrt [unpublished].
- Bayes, T. (1763). LII. An essay towards solving a problem in the doctrine of chances. By the late Rev. Mr. Bayes, F. R. S. communicated by Mr. Price, in a letter to John Canton, A. M. F. R. S. *Philosophical Transactions of the Royal Society of London*, 53, 370–418.
- Benjamin, J. R. & Cornell, C. A. (1976). *Probability, statistics, and decision for civil engineers*. McGraw-Hill Book Co.
- Beyer, T. (2007). *Vergleich von Modellversuchen zur Fahrt eines Grossmotorschiffes in zwei verschiedenen Kanalprofilen mit Berechnungen nach GBB* (Diplomarbeit). Universität der Bundeswehr München, Fakultät für Bauingenieur- und Vermessungswesen, Institut für Wasserwesen. München.
- Bezuijen, A. & Klein Breteler, M. (1992). Oblique wave attack on block revetments: Proceedings of 23rd Conference on Coastal Engineering.
- Bezuijen, A., Klein Breteler, M. & Bakker, K. J. (1987). Design criteria for placed block revetments and granular filters: 2nd Copedec, Beijing, China.
- Bezuijen, A., Wouters, J. & Laustrup, C. (1988). Block revetment design with physical and numerical models. *Coastal Engineering Proceedings*, 1, 2159–2173.
- Biles, W. E., Sasso, D. & Bilbrey, J. K. (2004). Integration of Simulation and Geographic Information Systems: Modeling Traffic Flow on Inland Waterways. In R. G. Ingalls (Ed.), *Proceedings of the 2004 Winter Simulation Conference: Washington Hilton and Towers, Washington, D.C., U.S.A., December 5-8, 2004* (pp. 331–337). Association for Computing Machinery.
- Biot, M. A. (1941). General Theory of Three-Dimensional Consolidation. *Journal of Applied Physics*, 12, 155–164.
- Biot, M. A. (1956). General solutions of the equations of elasticity and consolidation for a porous material. *Journal of Applied Mechanics*, 91–96.
- Bishop, A. W. (1955). The use of the Slip Circle in the Stability Analysis of Slopes. *Géotechnique*, 5, 7–17.
- Blaauw, H. G., van der Knaap, F. C. M., de Groot, M. T. & v, K. W. (1984). Design of bank protection of inland navigation fairways (Delft Hydraulics Laboratory, Ed.).
- Blodgett, J. C. & McConaughy, C. E. (1986). Rock Riprap for Protection of Stream Channels Near Highway Structures. Volume 2 - Evaluation of Riprap Design Procedures: U.S. Geological Survey. Water Resources Investigations Report 86-4128 [Prepared in cooperation with federal highway administration].
- Boeters, R. E. A. M., van der Knaap, F. M. & Verheij, H. J. (1993). Behaviour of armour layers of riprap bank protections along navigation channels. In K. W. Pilarczyk (Ed.), *Preprints International Riprap Workshop 1993* (pp. 193–206).
- Bogner, A., Littig, B. & Menz, W. (Eds.). (2009). *Experteninterviews: Theorien, Methoden, Anwendungsfelder*. VS Verlag für Sozialwissenschaften.
- Bouwmeester, J., van de Kaa, E. J., Nuhoff, H. A. & van Orden, R. G. J. (1977). Recent studies on push-towing as a base for dimensioning waterways: Paper presented at PIANC's XXIVth International Navigation Congress (Delft Hydraulics Laboratory, Ed.).
- Breitung, K. (1984). Asymptotic Approximations for Multinormal Integrals. *Journal of Engineering Mechanics (ASCE)*, 110, 357–366.
- Broderick, L. (1983). Riprap stability, a progress report. In J. R. Weggel (Ed.), *Proceedings of Coastal Structures '83, Arlington, Virginia* (pp. 320–330).
- Bruining, J. W. (1994). *Wave forces on vertical breakwaters* (Master thesis). Delft University of Technology. Delft.

- Bucher, C. G. (1988). Adaptive sampling — an iterative fast Monte Carlo procedure. *Structural Safety*, 5, 119–126.
- Buijs, F. A., Hall, J. W., Sayers, P. B. & van Gelder, P. H. A. J. M. (2009). Time-dependent reliability analysis of flood defences. *Reliability Engineering & System Safety*, 94, 1942–1953.
- Burcharth, H. F. (1993). Reliability Evaluation and Probabilistic Design of Coastal Structures. In Unyusho Kowan Gijutsu Kenkyujo (Ed.), *International Seminar on Hydro-Technical Engineering for Future Development of Ports and Harbours*.
- Cacuci, D. G., Ionescu-Bujor, M. & Navon, I. M. (2005). *Sensitivity and Uncertainty Analysis, Vol. II: Applications to large-scale systems*. Chapman & Hall/CRC.
- Cacuci, D. G., Navon, I. M. & Ionescu-Bujor, M. (2005). *Sensitivity and uncertainty analysis, Vol. I: Theory: Volume II: Applications to large-scale systems*. Chapman & Hall/CRC Press.
- Cai, J.-S., Yan, E.-C., Yeh, T.-C. J., Zha, Y.-Y., Liang, Y., Huang, S.-Y., Wang, W.-K. & Wen, J.-C. (2017). Effect of spatial variability of shear strength on reliability of infinite slopes using analytical approach. *Computers and Geotechnics*, 81, 77–86.
- Campolongo, F., Cariboni, J. & Saltelli, A. (2007). An effective screening design for sensitivity analysis of large models. *Environmental Modelling & Software*, 22, 1509–1518.
- Caniou, Y. (2012). *Analyse de sensibilité globale pour les modèles de simulation imbriqués et multi-échelles* (PhD thesis). Université Blaise Pascal - Clermont II. Clermont-Ferrand.
- Cao, Z. & Wang, Y. (2014). Bayesian model comparison and selection of spatial correlation functions for soil parameters. *Structural Safety*, 49, 10–17.
- Carsel, R. F. & Parrish, R. S. (1988). Developing joint probability distributions of soil water retention characteristics. *Water Resources Research*, 24, 755–769.
- Carver, R. D. & Davidson, D. D. (1977). Dolos armor units used on rubble-mound breakwater trunks subjected to nonbreaking waves with no overtopping: Final report (Dept. of Defense, Dept. of the Army, Corps of Engineers, Waterways Experiment Station, Hydraulics Laboratory, Ed.).
- Casella, G. & George, E. I. (1992). Explaining the Gibbs Sampler. *The American Statistician*, 46, 167–174.
- Chan, K., Saltelli, A. & Tarantola, S. (1997). Sensitivity analysis of model output: variance-based methods make the difference (S. Andradóttir, K. J. Healy, D. H. Withers & B. L. Nelson, Eds.).
- Ching, J., Li, D.-Q. & Phoon, K.-K. (2016). Statistical characterization of multivariate geotechnical data. In K.-K. Phoon & J. V. Retief (Eds.), *Reliability of Geotechnical Structures in ISO2394* (pp. 89–126). CRC Press.
- Ching, J., Phoon, K.-K. & Wu, T.-J. (2016). Spatial correlation for transformation uncertainty and its applications. *Georisk: Assessment and Management of Risk for Engineered Systems and Geohazards*, 10, 294–311.
- Cho, S. E. (2014). Probabilistic stability analysis of rainfall-induced landslides considering spatial variability of permeability. *Engineering Geology*, 171, 11–20.
- Chowdhury, R. & Flentje, P. (2003). Role of slope reliability analysis in landslide risk management. *Bulletin of Engineering Geology and the Environment*, 62, 41–46.
- Christian, J. T. & Baecher, G. B. (1999). Point-Estimate Method as Numerical Quadrature. *Journal of Geotechnical and Geoenvironmental Engineering*, 125, 779–786.
- Christian, J. T., Ladd, C. C. & Baecher, G. B. (1994). Reliability Applied to Slope Stability Analysis. *Journal of Geotechnical Engineering*, 120, 2180–2207.
- Christiani, E. (1997). *Application of Reliability in Breakwater Design* (PhD thesis). Aalborg Universitet. Aalborg.

- Clifton, P. M. & Neuman, S. P. (1982). Effects of kriging and inverse modeling on conditional simulation of the Avra Valley Aquifer in southern Arizona. *Water Resources Research*, 18, 1215–1234.
- Cooley, J. W. & Tukey, J. W. (1965). An Algorithm for the Machine Calculation of Complex Fourier Series. *Mathematics of Computation*, 19, 297.
- Corbin, J. M. & Strauss, A. L. (2015). *Basics of qualitative research: Techniques and procedures for developing grounded theory*. Sage.
- Cornell, C. A. (1969). A Probability-Based Structural Code. *ACI Journal*, 66, 974–985.
- COST WG 1. (2019). *Performance indicators*. Retrieved July 3, 2019, from <https://www.tu1406.eu/working-groups/wg1-performance-indicators>
- Cukier, R. I., Fortuin, C. M., Shuler, K. E., Petschek, A. G. & Schaibly, J. H. (1973). Study of the sensitivity of coupled reaction systems to uncertainties in rate coefficients. I Theory. *The Journal of Chemical Physics*, 59, 3873–3878.
- Daemrich, K.-F., Mathias, H. J. & Zimmermann, C. (1996). Untersuchungen zur Bemessung von Deckwerken in Schiffahrtskanälen unter Wellenbelastung: Einfluss der Deckschichtdicke auf die Stabilität der Deckschicht. In H.-B. Horlacher (Ed.), *Wellen: Wirkungen am Ufer-Befestigungen; Wasserbaukolloquium '96 an der TU Dresden am 19. September 1996* (pp. 199–209).
- D'Agostino, R. B. & Stephens, M. A. (1986). *Goodness-of-Fit-Techniques* (1st ed., Vol. v.68). CRC Press.
- Dallal, G. E. & Wilkinson, L. (1986). An Analytic Approximation to the Distribution of Lilliefors's Test Statistic for Normality. *The American Statistician*, 40, 294.
- Darmois, G. (1936). Sur les lois de probabilités à estimation exhaustive. In L'Académie des Sciences (Ed.), *Comptes Rendus de l'Académie des Sciences* (pp. 1265–1266).
- Davis, M. W. (1987). Production of Conditional Simulations via the LU Decomposition of the Covariance Matrix. *Mathematical Geology*, 19, 91–98.
- de Rooij, G. H., Kasteel, R. T. A., Papritz, A. & Flüher, H. (2004). Joint Distributions of the Unsaturated Soil Hydraulic Parameters and their Effect on Other Variates. *Vadose Zone Journal*, 3, 947–955.
- Delignette-Muller, M. L. & Dutang, C. (2015). fitdistrplus: An R Package for Fitting Distributions. *Journal of Statistical Software*, 64, 1–34.
- Delignette-Muller, M. L., Dutang, C. & Siberchicot, A. (2017). Package 'fitdistrplus': Help to Fit of a Parametric Distribution to Non-Censored or Censored Data [Version 1.0-9].
- Der Kiureghian, A. & Ditlevsen, O. (2009). Aleatory or epistemic? Does it matter? *Structural Safety*, 31, 105–112.
- Der Kiureghian, A., Lin, H.-Z. & Hwang, S.-J. (1987). Second-Order Reliability Approximations. *Journal of Engineering Mechanics*, 113, 1208–1225.
- Der Kiureghian, A. & Thoft-Christensen, P. (Eds.). (1991). *Reliability and Optimization of Structural Systems '90: Lecture Notes in Engineering* (Vol. 61). Springer Berlin Heidelberg.
- Dithinde, M. (2007). *Characterisation of Model Uncertainty for Reliability-Based Design of Pile Foundations* (PhD thesis). University of Stellenbosch, Department of Civil Engineering, Faculty of Engineering. Stellenbosch.
- Dithinde, M., Phoon, K.-K., Ching, J., Zhang, L. & Retief, J. V. (2016). Statistical characterization of model uncertainty. In K.-K. Phoon & J. V. Retief (Eds.), *Reliability of Geotechnical Structures in ISO 2394* (pp. 127–158). CRC Press.
- Ditlevsen, O., Bjerager, P., Olesen, R. & Hasofer, A. M. (1988). Directional simulation in Gaussian processes. *Probabilistic Engineering Mechanics*, 3, 207–217.
- Ditlevsen, O. & Madsen, H. O. (2005). *Structural Reliability Methods* (H. Jun, Ed.). Tongji University Press.

- Dorer, H. (1986). Stabilitätsformeln für lose Deckschichten von Böschungs- und Sohlbefestigungen. *Mitteilungsblatt der Bundesanstalt für Wasserbau*, 58.
- Dornack, S. (2001). *Überströmbare Dämme - Beitrag zur Bemessung von Deckwerken aus Bruchsteinen*. DST (2006). Bericht 1794: Modellversuche zu schiffsinduzierten Wirkungen auf Ufer [unpublished] (E. für Schiffstechnik und Transportsysteme e.V., Ed.).
- DVWK (1997). *Maßnahmen zur naturnahen Gewässerstabilisierung* (Deutscher Verband für Wasserwirtschaft und Kulturbau e.V., Ed.).
- Ebtehaj, M. & Moradkhani, H. (2009). Parameter Uncertainty Estimation of Hydrologic Models Using Bootstrap Resampling. In S. Starrett (Ed.), *World Environmental & Water Resources Congress 2009* (pp. 1–10). American Society of Civil Engineers.
- Efron, B. (1982). *The Jackknife, the Bootstrap and Other Resampling Plans*. Society for Industrial and Applied Mathematics.
- Efron, B. & Tibshirani, R. (1993). *An introduction to the bootstrap* (Vol. 57). Chapman & Hall.
- English, L. P. (1999). *Improving data warehouse and business information quality: Methods for reducing costs and increasing profits*.
- Ewers, J., Sorgatz, J. & Montenegro, H. (2017). Laborversuche und gekoppelte Berechnungen zur Untersuchung von Porenwasserüberdrücken infolge schneller Wasserstandsabsenkungen. In Deutsche Gesellschaft für Geotechnik e.V. (Ed.), *Fachsektionstage Geotechnik der Deutschen Gesellschaft für Geotechnik*.
- Fenton, G. A. (1999a). Estimation for Stochastic Soil Models. *Journal of Geotechnical and Geoenvironmental Engineering*, 125, 470–485.
- Fenton, G. A. (1999b). Random Field Modeling of CPT Data. *Journal of Geotechnical and Geoenvironmental Engineering*, 125, 486–498.
- Fenton, G. A. & Griffiths, D. V. (Eds.). (2008). *Risk assessment in geotechnical engineering*. John Wiley & Sons.
- Fenton, G. A. & Vanmarcke, E. H. (1990). Simulation of Random Fields via Local Average Subdivision. *Journal of Engineering Mechanics*, 116, 1733–1749.
- Fermi, E. & Richtmyer, R. D. (1948). Note on census-taking in Monte Carlo calculations.
- Fiessler, B., Rackwitz, R. & Neumann, H.-J. (1979). Quadratic Limit States in Structural Reliability. *Journal of the Engineering Mechanics Division*, 105, 661–676.
- Fischer, N., Treiber, M. & Söhngen, B. (2014). Modeling and simulating traffic flow on inland waterways. In Permanent International Association of Navigation Congresses (Ed.), *Proceedings of PIANC World Congress 2014* (pp. 1–20).
- Fleischer, P. & Kayser, J. (2006). BAW-Gutachten. BAW-Grundsatzaufgabe. Bestandsaufnahme von Deckwerken. Aufgabenstellung und Struktur. 4. Teilbericht (report A39520410006.04 [unpublished]). *Bundesanstalt für Wasserbau*.
- Fleischer, P. & Kayser, J. (2009). Erfahrungen mit Deckwerken an Binnenwasserstraßen. In Hafentechnische Gesellschaft e.V. (Ed.), *Tagungsband HTG Kongress Lübeck, 09. September bis 12. September 2009 in Lübeck* (pp. 57–64).
- Font, J. B. (1968). The effect of storm duration on rubble mound breakwater stability. *Coastal Engineering Proceedings*, 1, 779–786.
- Font, J. B. (1970). Damage functions for a rubble-mound breakwater under the effect of swells. In American Society of Civil Engineers (Ed.), *Proceedings of 12th Conference on Coastal Engineering, Washington D.C., USA* (pp. 1567–1586).
- Fredlund, D. G., Rahardjo, H. & Fredlund, M. D. (2012). *Unsaturated Soil Mechanics in Engineering Practice*. John Wiley & Sons.
- Froehlich, D. C. (2012). Rock and Roll—It's Here to Stay: Sizing Loose Rock Riprap to Protect Stream Banks. In E. D. Loucks (Ed.), *World Environmental and Water Resources Congress 2012: Crossing Boundaries* (pp. 1603–1612). American Society of Civil Engineers.

- Froehlich, D. C. & Benson, C. (1996). Sizing Dumped Rock Riprap. *Journal of Hydraulic Engineering*, 122, 389–396.
- Fröhle, P. (2000). *Messung und statistische Analyse von Seegang als Eingangsgröße für den Entwurf und die Bemessung von Bauwerken des Küstenwasserbaus* (Vol. 2).
- Gates, E. T. & Herbich, J. B. (1977). Mathematical Model to Predict the Behavior of Deep-Draft Vessels in Restricted Waterways. *TAMU-SG-77-206 COE Report No. 200*.
- Geißler, K. (2019). Sicherheit, Robustheit, Duktilität, Ermüdungssicherheit und Dauerhaftigkeit der Tragwerke – eine Grundsatzdiskussion. *Stahlbau*, 88, 270–293.
- Geman, S. & Geman, D. (1984). Stochastic relaxation, gibbs distributions, and the bayesian restoration of images. *IEEE transactions on pattern analysis and machine intelligence, PAMI-6*, 721–741.
- Gersch, W. & Yonemoto, J. (1977). Parametric time series models for multivariate EEG analysis. *Computers and Biomedical Research*, 10, 113–125.
- Gesing, C. (2010). Hydraulische Belastungen am Ufer aus Schifffahrt und Abfluss. In Bundesanstalt für Wasserbau & Bundesanstalt für Gewässerkunde (Eds.), *Alternative technisch-biologische Ufersicherungen an Binnenwasserstraßen - Wirkungsweise, Belastbarkeit, Anwendungsmöglichkeiten* (pp. 7–14).
- Gier, F. (2017). *Zur Bemessung von verzahnten Setzsteindeckwerken gegen hydrodynamische Belastungen* (PhD thesis). RWTH Aachen. Aachen.
- Gläser, J. & Laudel, G. (2010). *Experteninterviews und qualitative Inhaltsanalyse als Instrumente rekonstruierender Untersuchungen*. VS Verlag für Sozialwissenschaften.
- Griffiths, D. V. & Fenton, G. A. (2007). *Probabilistic Methods in Geotechnical Engineering*. Springer-Verlag Wien.
- Griffiths, D. V., Huang, J. & Fenton, G. A. (2011). Probabilistic infinite slope analysis. *Computers and Geotechnics*, 38, 577–584.
- Hacking, I. (1975). *The Emergence of Probability*. Cambridge University Press.
- Hamby, D. M. (1994). A review of techniques for parameter sensitivity analysis of environmental models. *Environmental Monitoring and Assessment*, 32, 135–154.
- Hasofer, A. M. & Lind, N. C. (1974). Exact and Invariant Second-Moment Code Format. *Journal of the Engineering Mechanics Division*, 100, 111–121.
- Hastings, W. K. (1970). Monte Carlo Sampling Methods Using Markov Chains and Their Applications. *Biometrika*, 57, 97–109.
- Hedar, A. (1965). Design Of Rock-Fill Breakwaters. *American Society of Civil Engineers*.
- Heinrich, K. (2009). Geotechnisches Gutachten zur Beurteilung der Baugrund- und Gründungsverhältnisse sowie des Dammaufbaus (Baugrundgutachten): Dammnachsorge Los IV Wesel-Datteln-Kanal. Dammabschnitt 38 WDK-km 33,200 bis 33,400 Süd. *Baugrund Dresden Ingenieurgesellschaft mbH*.
- Herman, J. & Usher, W. (2017). SALib: An open-source Python library for Sensitivity Analysis. *The Journal of Open Source Software*, 2.
- Hicks, M. A. (2012). An Explanation of Characteristic Values of Soil Properties in Eurocode 7. In P. Arnold, G. A. Fenton & M. A. Hicks (Eds.), *Modern Geotechnical Design Codes of Practice* (pp. 36–45). IOS Press.
- Hiller, P. H., Aberle, J. & Lia, L. (2017). Displacements as failure origin of placed riprap on steep slopes. *Journal of Hydraulic Research*, 56, 141–155.
- Hiller, P. H., Lia, L. & Aberle, J. (2019). Field and model tests of riprap on steep slopes exposed to overtopping. *Journal of Applied Water Engineering and Research*, 7, 103–117.
- Hjulström, F. (1935). *Studies of the morphological activity of rivers as illustrated by the River Fyris* (Inaugural dissertation). Uppsala Universitet.

- Honer, A. (1994). Das explorative Interview: zur Rekonstruktion der Relevanzen von Expertinnen und anderen Leuten. *Schweizer Zeitschrift für Soziologie*, 20, 623–640.
- Hopf, C. (1978). Die Pseudo-Exploration - Überlegungen zur Technik qualitativer Interviews in der Sozialforschung. *Zeitschrift für Soziologie*, 7, 97–115.
- Hou, Y. H., Li, Y. J. & Liang, X. (2019). Mixed aleatory/epistemic uncertainty analysis and optimization for minimum EEDI hull form design. *Ocean Engineering*, 172, 308–315.
- Hubbard, D. W. (2010). *How to measure anything: Finding the value of 'intangibles' in business*. Wiley.
- Hudson, R. Y. (1959). Laboratory investigation of rubble-mound breakwaters. *Journal of the Waterways and Harbor Division, ASCE*, 85, 610–659.
- Hussaarts, M., Vrijling, J. K., van Gelder, P. H. A. J. M., de Looft, H. & Blonk, C. (1999). The probabilistic optimisation of revetment on the dikes along the Frisian coast. In Balkema Publishers (Ed.), *Proceedings Coastal Structures 1999, Santander, Spain* (pp. 325–330).
- IBS (2006). Bericht zu den Schiffsbeobachtungen am Dortmund-Ems-Kanal - Nordstrecke. Messungen vom 11.07.2006 bis 25.07.2006 (unveröffentlicht) (I. Schmid, Ed.).
- IBS (2007a). Bericht zu den Schiffsbeobachtungen am Silokanal. Messungen vom 30.05.2007 bis 05.06.2007 [unpublished] (I. Schmid, Ed.).
- IBS (2007b). Bericht zu den Schiffsbeobachtungen am Wesel–Datteln–Kanal in der Stauhaltung Dorsten. Messungen vom August 2007 [unpublished] (I. Schmid, Ed.).
- IBS (2008a). Bericht zu den weiteren Auswertungen der Schiffsbeobachtungen am WDK, Juni 2008. Messungen vom August 2007 [unpublished] (I. Schmid, Ed.).
- IBS (2008b). Kurzbericht zur Datenaufbereitung der Schiffsbeobachtungen am Wesel-Datteln-Kanal [unpublished] (I. Schmid, Ed.).
- IBS (2015). Bericht zu den Verkehrsbeobachtungen am Küstenkanal km 15,96 und km 46,90. Messungen vom Juni 2015 [unpublished] (I. Schmid, Ed.).
- IBS. (2016). Bericht zu den weiteren Auswertungen der Verkehrsbeobachtungen am Küstenkanal km 15,96 und km 46,90. Messungen vom Juni 2015 [unpublished] (I. Schmid, Ed.).
- Iribarren, R. (1949). A Formula for the Calculation of Rock-Fill Dikes: Translation from Revista de Obras Publicas. *The Bulletin of the Beach Erosion Board*, 3, 1–15.
- Iribarren, R. & Nogales, C. (1951). *The Bulletin of the Beach Erosion Board*, 5, 4–23.
- Iribarren, R. & Nogales, C. (1952). New confirmation of the formula for the calculation of rock fill dikes. In Council on Wave Research (Ed.), *Proceedings of the Third Conference on Coastal Engineering: Third International Conference on Coastal Engineering* (pp. 185–189).
- Izbash, S. V. (1935). Construction of Dams by Dumping Stones into Flowing Water: (English translation) (US Engineering Office & Scientific Research Institute of Hydrotechnics, Eds.).
- Izbash, S. V. & Khaldre, K. Y. (1970). *Hydraulics of river channel closure*. Butterworths.
- Jackson, R. A. (1968). Design of cover layers for rubble-mound breakwaters subjected to non-breaking waves.
- Jafarnejad, M., Pfister, M., Brühwiler, E. & Schleiss, A. J. (2017). Probabilistic failure analysis of riprap as riverbank protection under flood uncertainties. *Stochastic Environmental Research and Risk Assessment*, 31, 1839–1851.
- Jafarnejad, M., Pfister, M. & Schleiss, A. J. (2012). Failure risk analysis of riverbank ripraps with Monte Carlo simulation. In R. Murillo Muñoz (Ed.), *River flow 2012: Proceedings of the International Conference on Fluvial Hydraulics, San José, Costa Rica, 5-7 September 2012* (pp. 1325–1330). CRC Press.

- Jaksa, M. B. (1995). *The influence of spatial variability on the geotechnical design properties of a stiff, overconsolidated clay* (PhD thesis). University of Adelaide, Dept. of Civil and Environmental Engineering. Adelaide.
- JCSS (2006). *JCSS Probabilistic Model Code: Section 3.7: Soil Properties* (J. C. on Structural Safety, Ed.).
- Julien, P. Y. (2002). *River mechanics*. Cambridge University Press.
- Kahn, H. & Marshall, A. W. (1953). Methods of Reducing Sample Size in Monte Carlo Computations. *Journal of the Operations Research Society of America*, 1, 263–278.
- Kanning, W. (2007). Integrated Flood Risk Analysis and Management Methodologies Analysis and influence of uncertainties on the reliability of flood defence systems: FLOODSite. Report Number T07-07-03.
- Katz, R. W., Parlange, M. B. & Naveau, P. (2002). Statistics of extremes in hydrology. *Advances in Water Resources*, 25, 1287–1304.
- Kayser, J. (2003). BAW-Gutachten. Bestandsaufnahme vorhandener Deckwerke. Teil 2: Dortmund-Ems-Kanal, km 79,35 - 84,00 (report B3952.04.04.10006 [unpublished]). *Bundesanstalt für Wasserbau*.
- Kayser, J. (2006). BAW-Gutachten. BAW-Grundsatzaufgabe. Bestandsaufnahme von Deckwerken Untersuchungen am Main-Donau-Kanal, 5. Teilbericht (report A39520410006.05 [unpublished]). *Bundesanstalt für Wasserbau*.
- Kayser, J. (2007a). BAW-Gutachten. BAW-Grundsatzaufgabe. Bestandsaufnahme von Deckwerken. 8. Teilbericht. Untersuchungen am Wesel-Datteln-Kanal (report A39520410006.08 [unpublished]). *Bundesanstalt für Wasserbau*.
- Kayser, J. (2007b). BAW-Gutachten. Bestandsaufnahme von Deckwerken. Teilbericht Dortmund – Ems – Kanal, Lose 14 und 15 (report A39520410006.07 [unpublished]). *Bundesanstalt für Wasserbau*.
- Kayser, J. (2008). BAW-Gutachten. BAW Grundsatzaufgabe. Bestandsaufnahme von Deckwerken. 9. Teilbericht. Untersuchungen an der DEK-Nordstrecke (report A39520410006.09 [unpublished]). *Bundesanstalt für Wasserbau*.
- Kayser, J. (2015a). FuE-Abschlussbericht: Entwicklung des Zustands von Deckwerken bei Absenkung des technischen Standards (report A39520470004). *Bundesanstalt für Wasserbau*.
- Kayser, J. (2015b). Vermerk: Auswertung von Daten zum Unterhaltungsaufwand von Deckwerken zur weiteren Verwendung im Rahmen der Untersuchungen zu Ufersicherungen für Wasserstraßen mit geringem Verkehr [unpublished]. *Bundesanstalt für Wasserbau*.
- Kelle, U. & Kluge, S. (2010). *Vom Einzelfall zum Typus: Fallvergleich und Fallkontrastierung in der qualitativen Sozialforschung*. VS Verlag für Sozialwissenschaften.
- Klerk, W. J., van der Hammen, J. M., Wojciechowska, K. & Pot, R. (2018). A framework for assessing information quality in asset management of flood defences. In R. Caspeele, L. Taerwe & D. M. Frangopol (Eds.), *Life Cycle Analysis and Assessment in Civil Engineering: Towards an Integrated Vision: Proceedings of the Sixth International Symposium on Life-Cycle Civil Engineering (IALCCE 2018), 28-31 October 2018, Ghent, Belgium* (pp. 673–689). CRC Press.
- Köhler, H. J. (1985). Modellversuche für die Dimensionierung von Deckwerken an Wasserstraßen - Stabilität loser Steinschüttungen -. *Mitteilungsblatt der Bundesanstalt für Wasserbau*, 69–101.
- Köhler, H. J. (1989). Messung von Porenwasserüberdrücken im Untergrund. *Mitteilungsblatt der Bundesanstalt für Wasserbau*, 155–174.
- Köhler, H. J. (1993). The influence of hydraulic head and hydraulic gradient on the filtration process. In J. Brauns (Ed.), *Filters in geotechnical and hydraulic engineering* (pp. 225–240). Balkema.

- Köhler, H. J. (1997a). Boden und Wasser - Druck und Strömung. *Mitteilungsblatt der Bundesanstalt für Wasserbau*, 15–33.
- Köhler, H. J. (1997b). Porenwasserdruckausbreitung im Boden, Messverfahren und Berechnungsansätze. *Mitteilungsblatt der Bundesanstalt für Wasserbau*, 84–108.
- Kolmogorov, A. N. (1933). Sulla Determinazione Empirica di una Legge di Distribuzione. *Giornale dell'Istituto Italiano degli Attuari*, 4, 83–91.
- Koopman, B. O. (1936). On Distributions Admitting a Sufficient Statistic. *Transactions of the American Mathematical Society*, 39, 399–409.
- Kortenhaus, A. (2003). *Probabilistische Methoden für Nordseedeiche* (PhD thesis). Technische Universität Braunschweig, Fachbereich Bauingenieurwesen. Braunschweig.
- Kreyenschulte, M. (2020). *Wellen-Bauwerks-Interaktion bei mörtelvergossenen Schüttsteindeckwerken* [Institut für wasserbau und wasserwirtschaft]. RWTH Aachen. Aachen.
- Kuhnert, P. M., Martin, T. G. & Griffiths, S. P. (2010). A guide to eliciting and using expert knowledge in Bayesian ecological models. *Ecology letters*, 13, 900–914.
- Kysely, J. (2008). A Cautionary Note on the Use of Nonparametric Bootstrap for Estimating Uncertainties in Extreme-Value Models. *Journal of Applied Meteorology and Climatology*, 47, 3236–3251.
- Laboyrie, J. H. (1986). Recent small-scale model investigations with respect to the influence of ship-induced water motions on the stability of bank protections: Report M1115, part XVI (Delft Hydraulics Laboratory, Ed.).
- Lacasse, S. & Nadim, F. (1996). Uncertainties in Characterising Soil Properties (Plenary). In C. D. Shackelford, P. P. Nelson & M. J. S. Roth (Eds.), *Uncertainty in the geologic environment - From theory to practice: Proceedings of Uncertainty '96* (pp. 49–75). American Society of Civil Engineers.
- Laplace, P. S. (1774). Mémoire sur la Probabilité des Causes par les évènements. *Mémoires de Mathématique et de Physique*, 621–656.
- Latham, J.-P., Mannion, M. B., Poole, A. B., Bradbury, A. P. & Allsop, N. (1988). The influence of armourstone shape and rounding on the stability of breakwater armour layers (Queen Mary College, Ed.).
- Lebrun, R. (2013). *Contributions à la modélisation de la dépendance stochastique* (PhD thesis). Université Paris VII - Denis Diderot. Paris.
- Lee, D. W., Abt, S. R., Hinkle, N. E., Khattak, M. S., Nelson, J. D., Ruff, J. F., Shaikh, A. & Wittier, R. J. (1987). Development of riprap design criteria by riprap testing in flumes: Phase I. NU-REG/CR-4651, U.S. Nuclear Regulatory Commission, Washington, D.C., May, 111.
- Lesny, K. (2017, June 4–July 7). The Use of Databases to Analyze Model Uncertainties of Geotechnical Design Procedures. In J. Huang, G. A. Fenton, L. Zhang & D. V. Griffiths (Eds.), *Geo-Risk 2017: Reliability-Based Design and Code Developments* (pp. 660–669). American Society of Civil Engineers.
- Lesny, K., Akbas, S., Bogusz, W., Burlon, S., Vessia, G. & Zhang, L. (2017, June 4–July 7). Evaluation of the Uncertainties Related to the Geotechnical Design Method and Its Consideration in Reliability Based Design. In J. Huang, G. A. Fenton, L. Zhang & D. V. Griffiths (Eds.), *Geo-Risk 2017: Reliability-Based Design and Code Developments* (pp. 435–444). American Society of Civil Engineers.
- Lilliefors, H. W. (1967). On the Kolmogorov-Smirnov Test for Normality with Mean and Variance Unknown. *Journal of the American Statistical Association*, 62, 399.
- Linford, A. & Saunders, D. H. (1967). A hydraulic investigation of through and overflow rockfill dams (RR 888) (The British Hydromechanics Research Association, Ed.).
- Lloyd, D. K. & Lipow, M. (1962). *Reliability: Management, Methods, and Mathematics*.

- Low, B. K. & Tang, W. H. (1997). Efficient Reliability Evaluation Using Spreadsheet. *Journal of Engineering Mechanics*, 123, 749–752.
- Low, B. K. & Tang, W. H. (2004). Reliability analysis using object-oriented constrained optimization. *Structural Safety*, 26, 69–89.
- Lumb, P. (1966). The Variability of Natural Soils. *Canadian Geotechnical Journal*, 3, 74–97.
- Lumb, P. (1974). Application of Statistics in Soil Mechanics. In I. K. Lee (Ed.), *Soil Mechanics-New Horizons* (pp. 44–111). Newnes-Butterworths.
- Madsen, H. O. & Egeland, T. (1989). Structural Reliability: Models and Applications. *International Statistical Review / Revue Internationale de Statistique*, 57, 185–2–03.
- Madsen, O. S. (1978). Wave-induced pore pressures and effective stresses in a porous bed. *Géotechnique*, 28, 377–393.
- Mallants, D., Mohanty, B. P., Vervoort, A. & Feyen, J. (1997). Spatial analysis of saturated hydraulic conductivity in a soil with macropores. *Soil Technology*, 10, 115–131.
- Mara, T. A. & Tarantola, S. (2012). Variance-based sensitivity indices for models with dependent inputs. *Reliability Engineering & System Safety*, 107, 115–121.
- Marsili, F. (2018). *Bayesian approaches to the reliability assessment of existing structures* (PhD thesis). Universität Braunschweig, Department of Civil and Environmental Engineering. Braunschweig.
- Matheron, G. (1973). The intrinsic random functions and their applications. *Advances in Applied Probability*, 5, 439–468.
- May, R. & Escarameia, M. (1992). Channel protection: Turbulence downstream of structures: Technical Report (HR Wallingford, Ed.).
- Maynard, J. (1990). Velocities induced by commercial navigation: Technical Report HI-90-15 (Hydraulics Laboratory of the US Army Engineer Waterways Experiment Station, Ed.).
- Maynard, S. T. (2005). Wave height from planing and semi-planing small boats. *River Research and Applications*, 21, 1–17.
- McBride, M. F. & Burgman, M. A. (2012). What Is Expert Knowledge, How Is Such Knowledge Gathered, and How Do We Use It to Address Questions in Landscape Ecology? In A. H. Perera, C. A. Drew & C. J. Johnson (Eds.), *Expert Knowledge and Its Application in Landscape Ecology*. Springer Science+Business Media LLC.
- McGuire, M. P. & VandenBerge, D. R. (2017). Interpretation of shear strength uncertainty and reliability analyses of slopes. *Landslides*, 14, 2059–2072.
- McKay, M. D., Beckman, R. J. & Conover, W. J. (1979). A Comparison of Three Methods for Selecting Values of Input Variables in the Analysis of Output from a Computer Code. *Technometrics*, 21, 239–245.
- Melby, J. A. (1999). Damage Progression on Rubble-Mound Breakwater (American Society of Civil Engineers, Ed.).
- Melby, J. A. (2001). Damage development on stone armored breakwaters and revetments: ERDC / CHLCHETN-III-64 (US Army Engineer Research and Development Center, Ed.).
- Metropolis, N., Rosenbluth, A. W., Rosenbluth, M. N., Teller, A. H. & Teller, E. (1953). Equation of State Calculations by Fast Computing Machines. *The Journal of Chemical Physics*, 21, 1087–1092.
- Metropolis, N. & Ulam, S. (1949). The Monte Carlo Method. *Journal of the American Statistical Association*, 44, 335–341.
- Meuser, M. & Nagel, U. (1991). ExpertInneninterviews - vielfach erprobt, wenig bedacht: ein Beitrag zur qualitativen Methodendiskussion. In D. Garz & K. Kraimer (Eds.), *Qualitativ-empirische Sozialforschung: Konzepte, Methoden, Analysen* (pp. 441–471). VS Verlag für Sozialwissenschaften.

- Meyer-Peter, E. & Müller, R. (1948). Formulas for Bed-Load transport. In International Association for Hydro-Environment Engineering and Research (Ed.), *Proceedings of 2nd meeting of the International Association for Hydraulic Structures Research, 7th June 1948, Delft* (pp. 39–64).
- Meyer-Peter, E. & Müller, R. (1949). Eine Formel zur Berechnung des Geschiebetriebes. *Schweizerische Bauzeitung*, 67, 29–32.
- Mieg, H. & Näf, M. (2005). Experteninterviews in den Umwelt- und Planungswissenschaften. Eine Einführung und Anleitung [Skript]. *ETH Zürich, Institute of Human-Environment Systems*.
- Miles, M. B., Huberman, A. M. & Saldaña, J. (2014). *Qualitative data analysis: A methods sourcebook*. Sage Publ.
- Mol, A., Groeneveld, R. L. & Waanders, A. J. (1984). Safety and reliability of breakwaters. *Coastal Engineering Proceedings*, 1, 2451–2466.
- Möllmann, A. F. (2009). *Probabilistische Untersuchung von Hochwasserschutzdeichen mit analytischen Verfahren und der Finite-Elemente-Methode* (PhD thesis). Universität Stuttgart, Institut für Geotechnik. Stuttgart.
- Montenegro, H. (1995). Parameterbestimmung und Modellierung der Wasserbewegung in heterogenen Böden.
- Montenegro, H. (2016). FuE-Abschlussbericht: Infiltrationsdynamik in Erdbauwerken (report A39520310047) (Bundesanstalt für Wasserbau, Ed.).
- Montenegro, H., Köhler, H. J. & Holfelder, T. (2005). Inspection of excess pressure propagation in the zone of gas entrapment below the capillary fringe. In T. Schanz (Ed.), *Inspection of excess pressure propagation in the zone of gas entrapment below the capillary fringe: Unsaturated Soils: Numerical and Theoretical Approaches*. Springer Berlin Heidelberg.
- Montenegro, H., Stelzer, O. & Odenwald, B. (2014). Effect of Entrapped Gas Below the Phreatic Surface on Pressure Propagation and Soil Deformation. In E. Pardo-Igúzquiza, C. Guardiola-Albert, J. Heredia, L. Moreno-Merino, J. J. Durán & J. A. Vargas-Guzmán (Eds.), *Mathematics of Planet Earth* (pp. 425–429). Springer Berlin Heidelberg.
- Morris, M. D. (1991). Factorial Sampling Plans for Preliminary Computational Experiments. *Technometrics*, 33, 161–174.
- Nataf, A. (1962). Détermination des distributions de probabilités dont les marges sont données. In L'Académie des Sciences (Ed.), *Comptes Rendus de l'Académie des Sciences* (pp. 42–43).
- Nelsen, R. B. (2010). *An introduction to Copulas*. Springer New York.
- Newman, M. C., Ownby, D. R., Mézin, L. C. A., Powell, D. C., Christensen, T. R. L., Lerberg, S. B. & Anderson, B.-A. (2000). Applying species-sensitivity distributions in ecological risk assessment: Assumptions of distribution type and sufficient numbers of species. *Environmental Toxicology and Chemistry*, 19, 508–515.
- Nielsen, F. & Garcia, V. (2009). Statistical exponential families: A digest with flash cards. *Computer Research Repository*.
- Okusa, S. (1985). Wave-induced stresses in unsaturated submarine sediments. *Géotechnique*, 35, 517–532.
- Ouellet, Y. (1972). Effects of irregular wave trains on rubble-mound breakwaters. *Journal of the Waterways and Coastal Engineering Division, ASCE*, 98, 1–13.
- Oumeraci, H., Allsop, N., de Groot, M. T., Crouch, R. S. & Vrijling, J. K. (1999). MAST III / PROVERBS. Probabilistic Design Tools for Vertical Breakwaters. MAS3 - CT95 - 0041. Final Report. VOLUME I.
- Pandey, M. D., van Gelder, P. H. A. J. M. & Vrijling, J. K. (2003). Bootstrap simulations for evaluating the uncertainty associated with peaks-over-threshold estimates of extreme wind velocity. *Environmetrics*, 14, 27–43.

- Panenka, A., Nyobeu Fangue, F. M., Rabe, R., Schmidt-Bäumler, H. & Sorgatz, J. (2020). Reliability assessment of ageing infrastructures: An interdisciplinary methodology. *Structure and Infrastructure Engineering*, 16, 698–713.
- Parola, A. C. (1993). Stability of Riprap at Bridge Piers. *Journal of Hydraulic Engineering*, 119, 1080–1093.
- Peirson, W. L., Figlus, J., Pells, S. E. & Cox, R. J. (2008). Placed Rock as Protection against Erosion by Flow down Steep Slopes. *Journal of Hydraulic Engineering*, 134, 1370–1375.
- Pfadenhauer, M. (2009). Das Experteninterview. In R. Buber & H. H. Holzmüller (Eds.), *Qualitative Marktforschung: Konzepte - Methoden - Analysen* (pp. 449–461). Gabler Verlag / GWV Fachverlage GmbH Wiesbaden.
- Pham Quang, T., Vrijling, J. K., van Gelder, P. H. A. J. M. & Thu, T. M. (2010). Reliability-tools in geotechnical design, an approach for river dike analysis. *Proceeding of the International Symposium Hanoi Geoengineering 2010, Hanoi, Vietnam, 22-23 November 2010*.
- Phoon, K.-K. (2004, July 9). *Towards reliability-based design for geotechnical engineering: Special lecture for Korean Geotechnical Society*.
- Phoon, K.-K. (2020). The story of statistics in geotechnical engineering. *Georisk: Assessment and Management of Risk for Engineered Systems and Geohazards*, 14, 3–25.
- Phoon, K.-K. & Ching, J. (2015). *Risk and Reliability in Geotechnical Engineering*. Taylor and Francis.
- Phoon, K.-K., Ching, J. & Huang, H. (2012). Examination of Multivariate Dependency Structure in Soil Parameters. In A. Athanasopoulos-Zekkos, R. D. Hryciw & N. Yesiller (Eds.), *GeoCongress 2012 (Geotechnical Special Publication (GSP) 225): State of the Art and Practice in Geotechnical Engineering* (pp. 2952–2960). American Society of Civil Engineers.
- Phoon, K.-K., Ching, J. & Wang, Y. (2019). Managing Risk in Geotechnical Engineering – from Data to Digitalization. In J. Ching, D.-Q. Li & J. Zhang (Eds.), *Proceedings of the 7th International Symposium on Geotechnical Safety and Risk (ISGSR 2019)* (pp. 13–34).
- Phoon, K.-K. & Kulhawy, F. H. (1999a). Characterization of geotechnical variability. *Canadian Geotechnical Journal*, 36, 612–624.
- Phoon, K.-K. & Kulhawy, F. H. (1999b). Evaluation of geotechnical property variability. *Canadian Geotechnical Journal*, 36, 625–639.
- Phoon, K.-K., Prakoso, W. A., Wang, Y. & Ching, J. (2016). Uncertainty representation of geotechnical design parameters. In K.-K. Phoon & J. V. Retief (Eds.), *Reliability of Geotechnical Structures in ISO 2394* (pp. 49–87). CRC Press.
- Phoon, K.-K. & Retief, J. V. (2016). *Reliability of Geotechnical Structures in ISO2394*. CRC Press.
- Phoon, K.-K. & Tang, C. (2019). Characterisation of geotechnical model uncertainty. *Georisk: Assessment and Management of Risk for Engineered Systems and Geohazards*, 13, 101–130.
- PIANC (1987a). Report of Working Group I-4: Guidelines for the design and construction of flexible revements incorporating geotextiles for inland waterways (Permanent International Association of Navigation Congresses, Ed.).
- PIANC (1987b). Risk consideration when determining bank protection requirements (Permanent International Association of Navigation Congresses, Ed.).
- PIANC (1989). Risk analysis in breakwater design: Report of PIANC Working Group No. 12 of Permanent Technical Committee II. Analysis of rubble mound breakwaters. Sub-Group C (Permanent International Association of Navigation Congresses, Ed.).
- PIANC (1992a). Analysis of Rubble Mound Breakwaters: Uncertainty Related to Environmental Data and Estimated Extreme Events (Permanent International Association of Navigation Congresses, Ed.).

- PIANC (1992b). Report of Working Group II-21: Guidelines for the design and construction of flexible revetments incorporating geotextiles in marine environment (Permanent International Association of Navigation Congresses, Ed.).
- PIANC (2003). Breakwaters with Vertical and Inclined Concrete Walls: Report of Working Group No. 28 of the Maritime Navigation Commission (Permanent International Association of Navigation Congresses, Ed.).
- PIANC (2016). Criteria for the Selection of Breakwater Types and their Related Optimum Safety Levels (Permanent International Association of Navigation Congresses, Ed.).
- Pilarczyk, K. W. (1985). Stability of revetments under wave and current attack. *21st Congress, International Association of Hydraulic Research August 19–23, 1985, Melbourne, Australia*, 85.
- Pilarczyk, K. W. (1995). Simplified Unification of Stability Formulae for Revetments under Current and Wave Attack. In C. R. Thorne (Ed.), *River, coastal and shoreline protection: Erosion control using riprap and armourstone; papers presented at the International Riprap Workshop, held at Colorado State University, Fort Collins, Colorado in July, 1993* (pp. 53–76). Wiley.
- Pilarczyk, K. W. (2017). *Dikes and Revetments: Design, Maintenance and Safety Assessment*. CRC Press.
- Pilarczyk, K. W. & den Boer, K. (1983). *Stability and profile development of coarse materials and their application in coastal engineering: Paper presented at the International Conference on Coastal and Port Engineering in Developing Countries, Colombo, Sri Lanka, March 20–26, 1983* (D. H. Laboratory, Ed.; Vol. 293).
- Pitman, E. (1936). Sufficient statistics and intrinsic accuracy. *Mathematical Proceedings of the Cambridge Philosophical Society*, 32, 567–579.
- Pitt, J. D. & Ackers, P. (1983). Prototype Tests on Riprap under Random Wave Attack. In B. L. Edge (Ed.), *Proceedings of the 18th Coastal Engineering Conference, November 14 - 19, 1982, Cape Town, Republic of South Africa* (pp. 1820–1836). American Society of Civil Engineers.
- Prästings, A., Spross, J. & Larsson, S. (2019). Characteristic values of geotechnical parameters in Eurocode 7. *Proceedings of the Institution of Civil Engineers - Geotechnical Engineering*, 172, 301–311.
- Przedwojski, B., Blazejewski, R. & Pilarczyk, K. W. (1995). *River training techniques: Fundamentals, design and applications*. Balkema.
- Rackwitz, R. & Fiessler, B. (1978). Structural reliability under combined random load sequences. *Computers & Structures*, 9, 489–494.
- Raiffa, H. & Schlaifer, R. (1961). *Applied statistical decision theory*. Wiley.
- Raudkivi, A. J. (1998). *Loose boundary hydraulics* ([4. ed.]). Balkema.
- Rawls, W. J., Brakensiek, D. L. & Saxton, K. E. (1982). Estimation of soil properties. *Transactions of the American Society of Agricultural and Biological Engineers (ASAE)*, 25, 1316–1320.
- Robinson, K. M., Rice, C. E. & Kadavy, K. C. (1998). Design of rock chutes. *Transactions of the American Society of Agricultural Engineers (ASAE)*, 41, 621–626.
- Rosenblatt, M. (1952). Remarks on a Multivariate Transformation. *The Annals of Mathematical Statistics*, 23, 470–472.
- Rosenblueth, E. (1975). Point estimates for probability moments. *Proceedings of the National Academy of Sciences of the United States of America*, 72, 3812–3814.
- Rubinstein, R. Y. & Kroese, D. P. (2016). *Simulation and the Monte Carlo Method*. Wiley.
- Sachs, L. & Hedderich, J. (2009). *Angewandte Statistik: Methodensammlung mit R* (13., aktualisierte und erw. Aufl.). Springer.
- Saito, M. & Matsumoto, M. (2008). SIMD-Oriented Fast Mersenne Twister: A 128-bit Pseudorandom Number Generator. In A. Keller, S. Heinrich & H. Niederreiter (Eds.), *Monte Carlo and Quasi-Monte Carlo Methods 2006* (pp. 607–622). Springer-Verlag Berlin Heidelberg.

- Saltelli, A. (2002). Making best use of model evaluations to compute sensitivity indices. *Computer Physics Communications*, 142, 280–297.
- Saltelli, A. (2008). *Global sensitivity analysis: The primer*. Wiley.
- Saltelli, A., Aleksankinac, K., Becker, W., Fennell, P., Ferretti, F., Holst, N., Li, S. & Wu, Q. (2019). Why so many published sensitivity analyses are false: A systematic review of sensitivity analysis practices. *Environmental Modelling & Software*, 114, 29–39.
- Saltelli, A., Annoni, P., Azzini, I., Campolongo, F., Ratto, M. & Tarantola, S. (2010). Variance based sensitivity analysis of model output. Design and estimator for the total sensitivity index. *Computer Physics Communications*, 181, 259–270.
- Saltelli, A., Tarantola, S. & Chan, K. (1999). A Quantitative Model-Independent Method for Global Sensitivity Analysis of Model Output. *Technometrics*, 41, 39–56.
- Sánchez-Arcilla, A., Gomez Aguar, J., Egozcue, J. J., Ortego, M. I., Galiatsatou, P. & Prinos, P. (2010). Extremes from scarce data: The role of Bayesian and scaling techniques in reducing uncertainty. *Journal of Hydraulic Research*, 46, 224–234.
- Santoso, A. M., Phoon, K.-K. & Quek, S.-T. (2011). Effects of soil spatial variability on rainfall-induced landslides. *Computers & Structures*, 89, 893–900.
- Schaibly, J. H. & Shuler, K. E. (1973). Study of the sensitivity of coupled reaction systems to uncertainties in rate coefficients. II Applications. *The Journal of Chemical Physics*, 59, 3879–3888.
- Schiereck, G. J. (1998). Soil-Water-Structure Interactions. In K. W. Pilarczyk (Ed.), *Dikes and Retirements: Design, Maintenance and Safety Assessment*. CRC Press.
- Schijf, J. & Jansen, P. (1953). Communication No 1. In Permanent International Association of Navigation Congresses (Ed.), *Rapport XVIIIth International Navigation Congress: PIANC Roma, 1953 Section I Inland Navigation* (pp. 175–196).
- Schreier, M. (2011). Qualitative Stichprobenkonzepte. In G. Naderer & E. Balzer (Eds.), *Qualitative Marktforschung in Theorie und Praxis: Grundlagen - Methoden - Anwendungen* (pp. 241–256). Gabler Verlag / Springer Fachmedien Wiesbaden GmbH Wiesbaden.
- Schultze, E. (1972). Frequency distributions and correlations of soil properties. In P. Lumb (Ed.), *Statistics and Probability in Civil Engineering*. Hong Kong University Press; Oxford University Press.
- Schuppener, B. & Heibaum, M. (2012). The Safety Concept in German Geotechnical Design Codes. In P. Arnold, G. A. Fenton & M. A. Hicks (Eds.), *Modern Geotechnical Design Codes of Practice* (pp. 102–115). IOS Press.
- Schüttrumpf, H., Kortenhaus, A., Fröhle, P. & Peters, K. (2008). Analysis of uncertainties in coastal structure design by expert judgement: Chinese-German Joint Symposium on Hydraulic and Ocean Engineering. *Rheinisch-Westfälische Technische Hochschule Aachen, Lehrstuhl und Institut für Wasserbau und Wasserwirtschaft*.
- Schwarz, G. (1978). Estimating the dimension of a model. *The Annals of Statistics*, 6, 461–464.
- Sebastian-Coleman, L. (2012). *Measuring Data Quality for Ongoing Improvement: A Data Quality Assessment Framework*. Elsevier Science.
- Shields, A. (1936). *Anwendung der Ähnlichkeitsmechanik und der Turbulenzforschung auf die Geschiebewegung*.
- Siebertz, K., van Bebber, D. & Hochkirchen, T. (2017). *Statistische Versuchsplanung*. Springer Berlin Heidelberg.
- Singh, V. P. (1998). *Entropy-Based Parameter Estimation in Hydrology*. Springer.
- Skempton, A. W. (1954). The Pore-Pressure Coefficients A and B. *Géotechnique*, 4, 143–147.
- Sklar, A. (1959). Fonctions de repartition à n dimensions et leurs marges. *Publications de l'Institut de statistique de l'Université de Paris*, 8, 229–231.

- Smirnov, N. (1948). Table for Estimating the Goodness of Fit of Empirical Distributions. *The Annals of Mathematical Statistics*, 19, 279–281.
- Smith, G., Wallast, I. & van Gent, M. R. A. (2002). Rock Slope Stability with Shallow Foreshores. In J. M. Smith (Ed.), *Proceedings of the 28th International Conference Coastal Engineering 2002, Volume 2: Held on Cardiff, Wales, July 7 - 12, 2002*. American Society of Civil Engineers.
- Sobol, I. M. (1993). Sensitivity Estimates for Nonlinear Mathematical Models. *Mathematical Modeling and Computational Experiment*, 1, 407–414.
- Sobol, I. M. (2001). Global sensitivity indices for nonlinear mathematical models and their Monte Carlo estimates. *Mathematics and Computers in Simulation*, 55, 271–280.
- Sobol, I. M. & Kucherenko, S. (2009). Derivative based global sensitivity measures and their link with global sensitivity indices. *Mathematics and Computers in Simulation*, 79, 3009–3017.
- Söhngen, B., Kellermann, J. & Loy, G. (1992). Modeling Danube and Isar Rivers Morphological Evolution, Part I: Measurements and Formulation. In International Research and Training Center on Erosion and Sedimentation Beijing & International Association for Hydraulic Research (Eds.), *Sediment management: 5th International Symposium on River Sedimentation, Karlsruhe, 1992*.
- Söhngen, B., Pohl, M. & Gesing, C. (2010). Bemessung von losen Schüttsteinen gegen schiffsinduzierte Strömungen und Wellen. In Technische Universität Dresden, Fakultät Bauingenieurwesen, Institut für Wasserbau und Technische Hydrodynamik (Ed.), *Wasserbau und Umwelt - Anforderungen, Methoden, Lösungen* (pp. 137–149).
- Sorgatz, J. (2019). Zuverlässigkeitsbasierte Deckwerksbemessung (Bundesanstalt für Wasserbau, Ed.).
- Sorgatz, J. & Kayser, J. (2020). *Investigation of parameter uncertainties inherent to the geotechnical design of German bank revetments: International Probabilistic Workshop [accepted], conference postponed to Spring 2021*.
- Sorgatz, J., Kayser, J. & Schüttrumpf, H. (2018). Expert interviews in long-term damage analysis for bottom and bank revetments along German inland waterways. In R. Caspele, L. Taerwe & D. M. Frangopol (Eds.), *Life Cycle Analysis and Assessment in Civil Engineering: Towards an Integrated Vision: Proceedings of the Sixth International Symposium on Life-Cycle Civil Engineering (IALCCE 2018), 28-31 October 2018, Ghent, Belgium* (pp. 749–756). CRC Press.
- Sorgatz, J. & Soyeaux, R. (2019). BAW-Gutachten. Geotechnik am Küstenkanal. Baugrund und Deckwerk (report B3952.04.01.10313 [unpublished]). *Bundesanstalt für Wasserbau*.
- Soyeaux, R. (2009). BAW-Gutachten. Ausbau der Unteren Havel-Wasserstraße (UHW-km 32,610 - 54,250) - Ufersicherungen - (report A39530406303 [unpublished]) (Bundesanstalt für Wasserbau, Ed.).
- Stein, J. (2008). BAW-Gutachten. Bestandsaufnahme von Deckwerken. Teilbericht 6. DEK Los 2b (report B3952.04.04.10006 [unpublished]). *Bundesanstalt für Wasserbau*.
- Stephens, M. A. (1974). EDF Statistics for Goodness of Fit and Some Comparisons. *Journal of the American Statistical Association*, 69, 730–737.
- Stevens, M. A., Simons, D. B. & Richardson, E. V. (1984). Riprap Stability Analysis. *Transportation Research Record*, 950, 209–216.
- Teixeira, A. (2012). *Reliability and Cost Models of Axial Pile Foundations* (PhD thesis). Universidade do Minho. Minho.
- Terzaghi, K. (1943). *Theoretical soil mechanics*. J. Wiley and Sons Inc.
- Thompson, D. M. & Shuttler, R. M. (1975). Riprap design for wind-wave attack - A laboratory study in random waves: Wallingford report EX707 for CIRIA (HR Wallingford, Ed.).

- Travis, Q. B., Schmeeckle, M. W. & Sebert, D. M. (2011). Meta-Analysis of 301 Slope Failure Calculations. II: Database Analysis. *Journal of Geotechnical and Geoenvironmental Engineering*, 137, 471–482.
- Uliczka, K. (2018). FuE-Abschlussbericht. Schiffserzeugte langperiodische Belastung zur Bemessung der Deckschichten von Strombauwerken an Seeschiffahrtsstraßen (report B3955.02.04.70141 [unpublished]) (Bundesanstalt für Wasserbau, Ed.).
- Uzielli, M., Lacasse, S., Phoon, K.-K. & Nadim, F. (2006). Soil variability analysis for geotechnical practice. In K.-K. Phoon, D. Hight, S. Leroueil & T. Tan (Eds.), *Characterisation and Engineering Properties of Natural Soils* (pp. 1653–1752). Taylor & Francis.
- Uzielli, M., Vannucchi, G. & Phoon, K.-K. (2005). Random field characterisation of stress-normalised cone penetration testing parameters. *Géotechnique*, 55, 3–20.
- van Dantzig, D. (1956). Economic Decision Problems for Flood Prevention. *Econometrica*, 24, 276–287.
- van de Kreeke, J. (1969). Damage function of rubble-mound breakwaters. *Journal of the Waterways and Harbor Division, ASCE*, 95, 345–354.
- van der Krogt, M. G., Schweckendiek, T. & Kok, M. (2019). Uncertainty in spatial average undrained shear strength with a site-specific transformation model. *Georisk: Assessment and Management of Risk for Engineered Systems and Geohazards*, 13, 226–236.
- van der Meer, J. W. (1987). Stability of breakwater armour layers — design formulae. *Coastal Engineering*, 11, 219–239.
- van der Meer, J. W. (1988a). Deterministic and Probabilistic Design of Breakwater Armor Layers. *Journal of Waterway, Port, Coastal, and Ocean Engineering*, 114, 66–80.
- van der Meer, J. W. (1988b). *Rock Slopes and Gravel Beaches under Wave Attack* (PhD thesis). Delft University of Technology. Delft.
- van der Meer, J. W. & Pilarczyk, K. W. (1984). Stability of rubble mound slopes under random wave attack: Presented at 19th International Conference on Coastal Engineering, 3–7 September 1984, Houston (Delft Hydraulics Laboratory, Ed.).
- van Gelder, P. H. A. J. M. (2000). *Statistical methods for the risk-based design of civil structures* (PhD thesis). Delft University of Technology. Delft.
- van Gelder, P. H. A. J. . (2009). Reliability Analysis of Flood and Sea Defence Structures and Systems: FLOODSite. Report Number T07-08-01.
- van Gelder, P. H. A. J. M. & Mai, C. V. (2008). Distribution functions of extreme sea waves and river discharges. *Journal of Hydraulic Research*, 46, 280–291.
- van Gelder, P. H. A. J. M. & Vrijling, J. K. (1997). A comparative study of different parameter estimation methods for statistical distribution functions in civil engineering applications. In N. Shiraishi, M. Shinozuka & Y.-K. Wen (Eds.), *Safety and Reliability. Proceedings of ICOSSAR '97, the 7th International Conference on Structural Safety and Reliability, Kyoto, 24-28 November 1997* (pp. 665–668).
- van Gent, M. R. A. (2005). On the Stability of Rock Slopes. In C. Zimmermann, R. G. Dean, V. Penchev & H. J. Verhagen (Eds.), *Environmentally Friendly Coastal Protection: Proceedings of the NATO Advanced Research Workshop on Environmentally Friendly Coastal Protection Structures Varna, Bulgaria 25-27 May 2004* (pp. 73–92). Springer.
- van Gent, M. R. A., Smale, A. J. & Kuiper, C. (2003). Stability of Rock Slopes with Shallow Foreshores. In J. A. Melby (Ed.), *Coastal Structures 2003: Proceedings of the Conference, August 26 - 30, 2003, Portland, Oregon* (pp. 100–112). American Society of Civil Engineers.
- van Hijum, E. & Pilarczyk, K. W. (1982). Gravel beaches: Equilibrium profile and longshore transport of coarse material under regular and irregular wave attack (Delft Hydraulics Laboratory, Ed.).

- van Noortwijk, J. M., van der Weide, J. A. M., Kallen, M. J. & Pandey, M. D. (2007). Gamma processes and peaks-over-threshold distributions for time-dependent reliability. *Reliability Engineering & System Safety*, 92, 1651–1658.
- van Rijn, L. C. (1993). *Principles of sediment transport in rivers, estuaries and coastal seas*. Aqua Publications.
- Vanmarcke, E. H. (1977). Probabilistic Modeling of Soil Profiles. *Journal of the Geotechnical Engineering Division*, 103, 1227–1246.
- Vanmarcke, E. H. (2010). *Random fields: Analysis and synthesis*. World Scientific Publ.
- Vardon, P. J., Liu, K. & Hicks, M. A. (2016). Reduction of slope stability uncertainty based on hydraulic measurement via inverse analysis. *Georisk: Assessment and Management of Risk for Engineered Systems and Geohazards*, 10, 223–240.
- Veiga, A. K., Saraiva, A. M., Chapman, A. D., Morris, P. J., Gendreau, C., Schigel, D. & Robertson, T. J. (2017). A conceptual framework for quality assessment and management of biodiversity data. *PloS one*, 12.
- Verheij, H. J. & Bogaerts, M. P. (1989). Ship waves and stability of armour layers protecting slopes: Paper presented at the 9th International Harbour Congress (Delft Hydraulics Laboratory, Ed.).
- Voortman, H. G. (2003). *Risk-based design of large-scale flood defence systems* (PhD thesis). Delft University of Technology. Delft.
- Vrijling, J. K. (1993). Development in Probabilistic Design of Flood Defenses in the Netherlands. In B. C. Yen & Y.-K. Tung (Eds.), *Reliability and Uncertainty Analyses in Hydraulic Design* (pp. 133–178). American Society of Civil Engineers.
- Vrijling, J. K. (1999). MAST III/PROVERBS: Probabilistic design tools for vertical breakwaters: Vol. 2d: Probabilistic aspects.
- Vrijling, J. K. (2001). Probabilistic design of water defense systems in The Netherlands. *Reliability Engineering & System Safety*, 74, 337–344.
- Vrijling, J. K. & van Gelder, P. H. A. J. M. (1997). Probabilistic Design of Berm Breakwaters. In R. Cooke, M. Mendel & J. K. Vrijling (Eds.), *Engineering Probabilistic Design and Maintenance for Flood Protection* (pp. 181–198). Springer US.
- Vrijling, J. K. & van Gelder, P. . A. J. M. (1998). The effect of inherent uncertainty in time and space on the reliability of flood protection. *Safety and Reliability*, 451–456.
- Wang, H. (2000). *Theory of linear poroelasticity with applications to geomechanics and hydrogeology*. Princeton University Press.
- Weidema, B. P. (1998). Multi-user test of the data quality matrix for product life cycle inventory data. *The International Journal of Life Cycle Assessment*, 3, 259–265.
- Weidema, B. P. & Wesnæs, M. S. (1996). Data quality management for life cycle inventories – an example of using data quality indicators. *Journal of Cleaner Production*, 4, 167–174.
- Weißmann, R. (2014). *Probabilistische Bewertung der Zuverlässigkeit von Flussdeichen unter hydraulischen und geotechnischen Gesichtspunkten* (PhD thesis). Karlsruher Instituts für Technologie. Karlsruhe.
- Westrich, B., Siebel, R., Vermeer, P. A. & Zwegher, B. (2003). Neue naturnahe Bauweisen für überströmbare Dämme an dezentralen Hochwasserrückhaltebecken und Erprobung von Erkundungsmethoden zur Beurteilung der Sicherheit von Absperrdämmen: Schlussbericht zum BWPLUS Forschungsprojekt Stuttgart.
- Wichmann, B. A. & Hill, I. D. (1982). Algorithm AS 183: An Efficient and Portable Pseudo-Random Number Generator. *Applied Statistics*, 31, 188–190.
- Wolff, T. F., Demsky, E. C., Schauer, J. & Perry, E. (1996). Reliability assessment of dike and levee embankment. In C. D. Shackelford, P. P. Nelson & M. J. S. Roth (Eds.), *Uncertainty in the*

- geologic environment - From theory to practice: Proceedings of Uncertainty '96* (pp. 636–650). American Society of Civil Engineers.
- WSA Brandenburg (2018). Verkehrstagebuch Schleuse Brandenburg 2017.
- WSA Duisburg-Meiderich (2018). Verkehrstagebuch Schleuse Dorsten 2015.
- WSA Meppen (2018). Verkehrstagebuch Schleuse Doerpen 2015.
- WSA Rheine (2018). Verkehrstagebuch Schleuse Münster 2015.
- Xiao, F., Ligteringen, H., van Gulijk, C. & Ale, B. (2015). Comparison study on AIS data of ship traffic behavior. *Ocean Engineering*, 95, 84–93.
- Xu, C. & Gertner, G. Z. (2008). Uncertainty and sensitivity analysis for models with correlated parameters. *Reliability Engineering & System Safety*, 93, 1563–1573.
- Yamamoto, T., Koning, H. L., Sellmeijer, H. & van Hijum, E. (1978). On the response of a poro-elastic bed to water waves. *Journal of Fluid Mechanics*, 87, 193–206.
- Yuen, K.-V. & Mu, H.-Q. (2012). A novel probabilistic method for robust parametric identification and outlier detection. *Probabilistic Engineering Mechanics*, 30, 48–59.
- Zhang, J., Huang, H. W., Zhang, L. M., Zhu, H. H. & Shi, B. (2014). Probabilistic prediction of rainfall-induced slope failure using a mechanics-based model. *Engineering Geology*, 168, 129–140.
- Zhou, A., Li, C.-Q. & Huang, J. (2016). Failure analysis of an infinite unsaturated soil slope. *Proceedings of the Institution of Civil Engineers - Geotechnical Engineering*, 169, 410–420.
- Zimmermann, H.-J. (2012). *Fuzzy Set Theory and Its Applications*. Springer Netherlands.

STANDARDS, GUIDELINES AND LEGAL REGULATIONS

- BMVBS (2011). *Richtlinien für Regelquerschnitte von Binnenschifffahrtskanälen* (Bundesministerium für Verkehr, Bau und Stadtentwicklung, Ed.).
- Bundesministerium der Justiz (Ed.). (2011). *Binnenschifffahrtsstraßen-Ordnung (BinSchStrO)*.
- DIN 1054:2010-12 (2010). *Baugrund - Sicherheitsnachweise im Erd- und Grundbau - Ergänzende Regelungen zu DIN EN 1997-1* (Norm). Deutsches Institut für Normung e.V. Berlin, Beuth.
- DIN 4020:2010-12 (2010). *Geotechnische Untersuchungen für bautechnische Zwecke - Ergänzende Regelungen zu DIN EN 1997-2* (Deutsches Institut für Normung e.V., Ed.; Norm). Berlin.
- DIN EN 13383-1:2015-07 - Entwurf (2010). *Wasserbausteine – Teil 1: Anforderungen* (Norm). Deutsches Institut für Normung e.V. Berlin, Beuth.
- DIN EN 13383-2:2017-03-Entwurf (2010). *Wasserbausteine - Teil 2: Prüfverfahren* (Norm). Deutsches Institut für Normung e.V. Berlin, Beuth.
- DIN EN 1990:2010-12 (2010). *Eurocode: Grundlagen der Tragwerksplanung* (Norm). Deutsches Institut für Normung e.V. Berlin, Beuth.
- DIN EN 1997-1:2014-03 (2010). *Eurocode 7 - Entwurf, Berechnung und Bemessung in der Geotechnik - Teil 1: Allgemeine Regeln; Deutsche Fassung EN 1997-1:2004 + AC:2009 + A1:2013* (Norm). Deutsches Institut für Normung e.V. Berlin, Beuth.
- DNVGL-RP-C207:2017-05 (2017). *Statistical representation of soil data* (Norm). Det Norske Veritas. Norway.
- EAU (2012). *Empfehlungen des Arbeitsausschusses 'Ufereinfassungen' Häfen und Wasserstraßen* (Arbeitsausschuss 'Ufereinfassungen' der HTG e.V., Ed.). Ernst & Sohn.
- GBB (2010). *Grundlagen zur Bemessung von Böschungs- und Sohlensicherungen an Binnenwasserstraßen (GBB)* (Bundesanstalt für Wasserbau, Ed.; tech. rep.).
- ISO 2394:2015-03 (2015). *General principles on reliability for structures* (Norm).
- ISO/IEC 25012:2008-12. (2008). *Software-Engineering - Qualitätskriterien und Bewertung von Softwareprodukten (SQuaRE) - Modell der Datenqualität* (Norm).
- ISO/IEC 25024:2015-10 (2015). *System und Software-Engineering - Qualitätskriterien und Bewertung von System- und Softwareprodukten (SQuaRE) - Messung der Datenqualität* (Norm).
- JCSS (2001). *Probabilistic Model Code: PART I* (J. C. on Structural Safety, Ed.; tech. rep.).
- MAR (2008). *Anwendung von Regelbauweisen für Böschungs- und Sohlensicherungen an Binnenwasserstraßen* (Bundesanstalt für Wasserbau, Ed.).
- MSV (2015). *Merkblatt Schadensklassifizierung an Verkehrswasserbauwerken* (Bundesanstalt für Wasserbau, Ed.).
- MSV (2018). *Merkblatt Schadensklassifizierung an Verkehrswasserbauwerken* (Bundesanstalt für Wasserbau, Ed.).
- Rock Manual (2007). *The Rock Manual. The use of rock in hydraulic engineering*. CIRIA.
- TLW (2003). *Technische Lieferbedingungen für Wasserbausteine* (tech. rep.).
- US Army Corps of Engineers (2002). *Coastal Engineering Manual: EM 1110-2-1100*.
- US Department of Defense (1987). *MIL-HDBK-781, Military Handbook: Reliability test methods, plans, and environments for engineering development, qualification, and production*.
- USACE (1984a). *Shore Protection Manual: Volume I* (US Army Corps of Engineers, Ed.).
- USACE (1984b). *Shore Protection Manual: Volume II* (US Army Corps of Engineers, Ed.).

- USACE (1997). Design of Coastal Revetments, Seawalls, and Bulkheads (US Army Corps of Engineers, Ed.).
- USACE (1999). Engineering and Design: Risk-Based Analysis in Geotechnical Engineering for Support of Planning Studies: Technical Letter No. 1110-2-556 (Department of the Army, Ed.).
- WgV (2018). Handlungsempfehlung. Beurteilung von Ufersicherungen und Fahrrinnenquerschnitten von Wasserstraßen der Kategorie C hinsichtlich einer vergrößerten verkehrlichen Nutzung [unpublished draft] (Arbeitsgruppe ‘Wasserstraßen mit geringem Verkehr’, Ed.).

Appendices

APPENDICES

A	Model tests and resulting equations of revetment design	A1
A.1	Summary of common design equations	A1
A.1.1	Design against currents	A1
A.1.2	Design against waves	A5
A.2	Summary of experimental studies for breakwater and revetment stability	A8
A.3	Hydraulic design according to GBB (2010)	A17
A.3.1	Required stone diameter to resist currents	A17
A.3.2	Required stone diameter to resist wave attack	A18
A.3.3	Required stone diameter to resist different types of loads	A18
A.4	Geotechnical design according to GBB (2010)	A19
A.4.1	Required armour stone layer thickness to impede slope sliding	A19
A.4.2	Required armour stone layer thickness to impede liquefaction	A21
B	Supplementary material for theory of reliability assessment	B1
B.1	Mathematical definitions	B1
B.1.1	Random variables and events	B1
B.1.2	Probability functions	B1
B.1.3	Main descriptors of random variables	B2
B.1.4	Multiple random variables	B3
B.2	Standard distributions	B5
B.2.1	Gaussian distribution	B6
B.2.2	Lognormal distribution	B6
B.2.3	Poisson distribution	B7
B.2.4	Gamma distribution	B8
B.3	Beyond the Frequentist approach: Bayesian inference	B8
C	Additional information on field campaigns	C1
D	Documentation of expert interviews	D1
D.1	Interview guideline	D1
D.2	Questionnaire	D4
D.3	Interview excerpts	D6
D.4	Sub-categories summarising expert interviews	D12
E	Code documentation	E1
E.1	Models	E1
E.1.1	Hydraulic design	E1
E.1.2	Geotechnical design	E3
E.2	Addressing statistical uncertainty	E4
E.2.1	Bootstrapping	E4
E.2.2	Stability analysis	E6
E.3	Addressing transformation uncertainty	E9
E.3.1	Model factor	E9
E.4	Addressing spatial variability	E12
E.4.1	Infinite slope model	E12

E.4.2	Excess pore pressure model	E15
F	Statistical test results	F1
F.1	Hypothesis tests	F1
F.2	Correlation analysis	F8
G	Example	G1

A | MODEL TESTS AND RESULTING EQUATIONS OF REVETMENT DESIGN

A.1 Summary of common design equations

A.1.1 Design against currents

In contrast to waves, which mainly affect the zone of water level fluctuation and above, current attack affects the entire slope under water. In Table A.1 a number of common equations and their parameters required for revetment design against currents are summarised.

The design of bank revetments is commonly conducted with a modified formula of Izbash and Khaldre (1970). According to DVWK (1997), the formula of Izbash and Khaldre (1970) yields the most conservative design. For near-bed structures, the equations of Shields (1936) or a combination of Izbash/ Shields formulae are equally suitable depending on the limitations of each equation specifically. Using field and laboratory experiments, numerous authors have extended these two formulae.

The equation of Dorer (1986) is based on the formula introduced by Shields (1936). It assumes moderate turbulence and, thus, mainly applies to the river or canal bed.

The design equation of Pilarczyk (1995) is based on a combination of the Izbash/ Shields formula and features numerous empirical factors and coefficients whose specifications are, amongst others, outlined in Rock Manual (2007). The equation is suited for 'a preliminary assessment of armourstone and alternative protection elements (such as gabions) to resist current attack' (Rock Manual, 2007, p. 649).

May and Escarameia (1992) modify the Izbash and Khaldre (1970) equation to fully account for turbulence. It is thus particularly suitable for revetment close to gates, weirs, spillways, culverts. The extension results from experimental data and - as a result of the experimental set-up - is valid for flat beds and slopes not steeper than 1:2 (height:length). Additionally, the results were verified by measurements at the River Thames (Rock Manual, 2007).

The formula of Parola (1993) applies in particular to material of uniform particle size and to revetment areas near bridge piers where the flow velocity increases. According to DVWK (1997), the particle diameter of the uniform material corresponds to D_{80} , the armour stone diameter at 80 % mass throughput of the cumulative line. The calculated armour stone diameter exceeds the required armour stone diameter in track sections by a factor of four (DVWK, 1997).

Raudkivi (1998) requires the flow velocity near-bed u_b as input, which is obtained from the flow velocity of the canal or river v_0^* , however, does not cover ship-induced flow or turbulent flow near slopes. It is derived from the Izbash formula and is particularly suitable for unsteady flow conditions (DVWK, 1997).

Rock Manual (2007) recommends a combination of the Izbash/ Shields formulae. By introducing various correction factors, it is applicable to more turbulent flow conditions near the bank as well as near-bed flow conditions.

EGBB (2010) equations are valid for waterways with predominantly parallel banks and fairways confined both laterally and in depth. It originates from the Izbash and Khaldre (1970) formula. The introduction of $C_{B\ddot{o}}$ describes the increase of the required nominal stone diameter D_{n50} due to the slope inclination and the friction angle of the material. The second equation employs a reduced C_{Isb} as a response to turbulent flow resulting from the slope supply flow u_{max} .

Table A.1: Common parameters and their definition required for a design against currents.

D_i	mm	mean diameter of fraction i
D_m	mm	mean diameter of armour stones
D_{max}	mm	maximum diameter of armour stones
D_{50}	mm	mean diameter at 50 % mass throughput of the cumulative line
Fr^*	–	Froude number
g_0	9.81 m s^{-2}	gravity
ρ_w	kg m^{-3}	water density
ρ_s	kg m^{-3}	material density
ψ_{cr}	–	Shields parameter

Dorer (1986):

$$D_m = \frac{v^2}{Fr^* g_0 T_r^2} \quad Fr^* = \begin{cases} 0.030 \rightarrow \text{Meyer-Peter and Müller (1948), pier area} \\ 0.043 \rightarrow \text{Söhngen, Kellermann et al. (1992), Danube sediment} \end{cases} \quad (A.1)$$

$$T_r = \begin{cases} 0.70 \rightarrow \text{below weir apron} \\ 1.00 \rightarrow \text{steady open-canal flow} \end{cases}$$

where:

v ... flow velocity T_r ... Turbulence factor

GBB (2010):

$$D_{50} = C_{Isb} C_{B\ddot{o}} \frac{v_{max}^2}{g_0} \frac{1}{((\rho_s - \rho_w)/\rho_w)} \quad (A.2)$$

$$C_{B\ddot{o}} = 1/k \quad (A.3)$$

$$k = \cos \beta [1 - (\tan^2 \beta / \tan^2 \phi'_{hydr,D})]^{0.5} \quad (A.4)$$

$$D_{50} = 0.5 C_{B\ddot{o}} \frac{u_{max}^2}{g_0} \frac{1}{((\rho_s - \rho_w)/\rho_w)} \quad (A.5)$$

where:

$C_{B\ddot{o}}$... factor for consideration of the influence of the slope	u_{max}	... maximum supply flow velocity
C_{Isb}	... factor according to Izbash (≈ 0.7)	$\phi'_{hydr,D}$... repose angle of the armour layer material
v_{max}	... maximum flow velocity made up of return flow and flow at the shore		

Izbash and Khaldre (1970):

$$D_{50} > \frac{0.7v^2}{g_0} \quad (\text{A.6})$$

$$D_{50} > \frac{1.4v^2}{g_0} \quad (\text{A.7})$$

May and Escarameia (1992):

$$D_{n50} = c_T \frac{u_b^2}{2g_0((\rho_s - \rho_w)/\rho_w)} \quad (\text{A.8})$$

where:

c_T ... turbulence coefficient
 u_b ... near-bed flow velocity

Parola (1993):

$$D_E \approx D_{50} > \frac{v^2}{N_c g_0} \quad N_c = \begin{cases} 1.4 \rightarrow \text{for rounded piers} \\ 1.6 \rightarrow \text{for rounded piers and } v > 1 \text{ m s}^{-1} \\ 1.0 - 1.2 \rightarrow \text{for rectangular piers} \end{cases} \quad (\text{A.9})$$

where:

N_c ... stability factor

Pilarczyk (1995):

$$D = \frac{\Phi_{sc}}{((\rho_s - \rho_w)/\rho_w)} \frac{0.035}{\psi_{cr}} k_h k_{sl}^{-1} k_t^2 \frac{U^2}{2g_0} \quad (\text{A.10})$$

where:

Φ_{sc} ... stability correction factor
 k_{sl} ... slope reduction factor
 k_t ... turbulence amplification factor
 k_h ... velocity profile factor
 U ... depth-averaged current velocity

Raudkivi (1998):

$$D_{40} = \left(\frac{u_b}{4.92} \right)^2 \quad (\text{A.11})$$

$$y_0 = k/30.2 \quad (\text{A.12})$$

$$u_b = \frac{v_0^*}{\kappa} \ln(y_s/y_0) \quad (\text{A.13})$$

where:

- k ... equivalent uniform grain roughness
 κ ... Von Kármán constant (= 0.4)
 y_s ... height of measured flow velocity above bottom, recommendation $y_s = 0.1$ m
-

Rock Manual (2007):

$$\frac{U^2/2g_0}{((\rho_s - \rho_w)/\rho_w)D} = k_{sl}k_t^{-2}k_w^{-1}\Lambda_h\psi_{cr} \quad (\text{A.14})$$

where:

- k_{sl} ... slope reduction factor $k_{sl} \leq 1$
 Λ_h ... depth or velocity profile factor
 k_t ... turbulence amplification factor
 k_w ... wave-amplification factor
 U ... depth-averaged current velocity
-

Shields (1936):

$$\psi_{cr} = \frac{\tau_{cr}}{(\rho_r - \rho_w)g_0D} = \frac{u_{*cr}^2}{g_0D} = f(Re) \quad (\text{A.15})$$

$$\psi_{cr} = \frac{1}{C^2} \cdot \frac{U_{cr}}{((\rho_s - \rho_w)/\rho_w)D} \quad (\text{A.16})$$

where:

- τ_{cr} ... critical shear stress
 u_{*cr} ... critical value of the shear velocity,
commonly $u_* = \sqrt{\tau/\rho_w}$
 ρ_r ... apparent mass density of armour
stone pieces
 Re ... Reynolds number
 C ... Chézy friction coefficient
 U_{cr} ... depth-averaged critical velocity
-

A.1.2 Design against waves

Revetment design against waves has to encompass a design against primary waves (transversal stern wave height) and secondary waves. The presently employed equations for the revetment design against wave attack originate to a large extent from approaches developed for coastal engineering. A number of common equations and their parameters required for a revetment design against ship-induced waves is summarised in Table A.2. Literature provides a number of equations, which are commonly derived from supplementary investigations with respect to the work of Hudson (1959) and Iribarren and Nogales (1952).

The Hudson equation determines the unit weight of armour stones W_{50} required to resist wave attack. The stability factor K_D of the Hudson equation, which describes the allowable damage, depends in particular on the armour stone type and whether waves break or not. For design purposes K_D values which result in 0–5 % of displaced armour stones between crest and a level of one wave height below still water are recommended (Rock Manual, 2007). It is a rather generic equation. The uncertainty of the design results depends on the hydraulic structure to be designed (Rock Manual, 2007).

The equations of van der Meer (1988b) account for the wave breaker type. In contrast to the Hudson equation, which primarily addresses permeable structures, van der Meer (1988b) covers a variety of structures at deep-water conditions. Moreover, instead of targeting a damage level via site- and structure-specific stability coefficients, the stability of the structure is described via the damage level coefficient $S_d = A_e/D_{n50}^2$, which is a function of the eroded area in a cross-section A_e and the nominal armour stone diameter D_{n50} .

The influence of shallow shores on the wave height is included in a set of equations outlined by van Gent et al. (2003). The permeability of the structure is considered by the ratio of core to outer material ($D_{n50\text{-core}}/D_{n50}$). Based on the investigations of van Gent et al. (2003), the coefficient c_s and c_p in the formula of van der Meer (1988b) are adjusted to account for shallow water conditions (Rock Manual, 2007).

GBB (2010), Laboyrie (1986) and PIANC (1987b) present equations against ship-induced transversal stern waves. The equations are derived from the Hudson equation. They are modified to account for the conditions at inland waterways, i. e. by introducing stability factors B'_B and B_B^* based on field investigations (BAW, 2009).

Equations against secondary wave attack are given by GBB (2010), Pilarczyk (1985) and Verheij and Bogaerts (1989). The equation of Pilarczyk (1985) and Verheij and Bogaerts (1989) is based on the Hudson formula, whereas GBB (2010) uses the equation of van der Meer (1988b). In both equations the wave height is lowered by angle of wave attack β_W .

Table A.2: Common parameters and their definition required for a design against waves.

D_{50}	mm	mean diameter at 50 % mass throughput of the cumulative line
D_{n50}	m	nominal armour stone diameter
$m = \cot \beta$	- / °	slope inclination
H	m	design wave height
H_{stern}	m	stern wave height
H_{sec}	m	secondary wave height
K_D	-	stability coefficient, stability coefficient, i. e. depends on hydraulic structure, material and damage level
β_W	°	angle between the wave crest of the secondary diverging wave and the bank line, commonly 55°
ρ_w	kg m^{-3}	water density
ρ_s	kg m^{-3}	material density
ξ_m	-	surf similarity parameter

GBB (2010):

$$D_{50} \geq \frac{H_{\text{stern}}}{B'_B ((\rho_s - \rho_w)/\rho_w)} \quad (\text{A.17})$$

$$D_{50} \geq \frac{H_{\text{stern}} C_{\text{Bö}}}{B^*_B ((\rho_s - \rho_w)/\rho_w)} \quad (\text{A.18})$$

$$D_{n50} \geq \frac{H_{\text{sec}} (\cos \beta_W)^{1/2} \xi_m^{1/2}}{((\rho_s - \rho_w)/\rho_w) 2.25 (\cos \beta + \sin \beta)} \quad (\text{A.19})$$

where:

- B'_B ... stability factor, 1.5 - if the design case occurs frequently or if damage to the revetment should be completely avoided, 2.3 - if the design case occurs infrequently or when a limited amount of maintenance is acceptable
- B^*_B ... stability factor, ≈ 3 if the design case occurs infrequently or when a limited amount of maintenance is acceptable
- λ_s ... wave length of the secondary diverging wave

Hudson (1959):

$$W_{50} = \frac{\rho_r g_0 H^3}{K_D ((\rho_s - \rho_w)/\rho_w) \cot \beta} \quad (\text{A.20})$$

Laboyrie (1986) and PIANC (1987b):

$$D_{n50} \geq \frac{H}{1.5 (\cot \beta)^{1/3} ((\rho_s - \rho_w)/\rho_w)} \quad (\text{A.21})$$

van der Meer (1988b):

Plunging waves

$$\frac{H}{((\rho_s - \rho_w)/\rho_w)D_{n50}} = c_{pl} P^{0.18} \left(\frac{S_d}{\sqrt{N}} \right)^{0.2} \xi_m^{-0.5} \quad (\text{A.22})$$

$$\xi_m = \frac{\tan \beta}{\sqrt{(2\pi/g_0 \cdot H/T_m^2)}} \quad (\text{A.23})$$

Surging waves, $\xi_m \geq \xi_{cr}$

$$\frac{H}{((\rho_s - \rho_w)/\rho_w)D_{n50}} = c_{pl} P^{-0.13} \left(\frac{S_d}{\sqrt{N}} \right)^{0.2} \sqrt{\cot \beta} \xi_m^P \quad (\text{A.24})$$

where:

ξ_{cr} ... critical value of surf similarity parameter
 c_{pl} ... coefficient
 c_s ... coefficient

P ... permeability coefficient
 T_m ... mean wave period
 S_d ... damage level coefficient

van Gent et al. (2003):

$$\frac{H}{((\rho_s - \rho_w)/\rho_w)D_{n50}} = 1.75 \sqrt{\cot \beta} (1 + D_{n50\text{-core}}/D_{n50})^{\frac{2}{3}} \left(\frac{S_d}{\sqrt{N}} \right)^{0.2} \quad (\text{A.25})$$

Pilarczyk (1985) and Verheij and Bogaerts (1989):

$$D_{n50} \geq \frac{H_{\text{sec}} (\cos \beta_W)^{1/2}}{1.8 ((\rho_s - \rho_w)/\rho_w)} \quad (\text{A.26})$$

A.2 Summary of experimental studies for breakwater and revetment stability

Table A.3: Model tests and field investigations with regard to failure and design of revetments

Authors	Title	Experimental set-up	Definition of failure	Main results
Ahrens (1970)	The influence of breaker type on rip-rap stability	Investigation of the stability of dumped quarry stone riprap subjected to waves of different breaker types in a wave tank	'Failure, for these tests, was defined as having occurred when enough riprap stones were displaced so that the filter layer was exposed to wave action and core material was actually being removed through the filter layer.'	'It seems as if the physical characteristics of collapsing breakers have combined in an optimum way to yield low rip-rap stability.'
Thompson and Shuttler (1975)	Rip-rap design for wind-wave attack - A laboratory study in random waves	Scaled wave flume tests to investigate riprap stability at different slope inclinations and random waves	<ul style="list-style-type: none"> • 'No "damage" is the point at which erosion of the riprap shows a sharp increase with increasing wave height.' • 'Failure [...] occurred if the $D_{50}^R/2$ diameter of a hand held gauge could touch the filter layer [...] after a sequence of 500 waves, whether or not the filter material was eroded.' • Damage ΔN is the number of D_{50}^R sized spherical stones eroded from a $9 \cdot D_{50}^R$ area. 	<ul style="list-style-type: none"> • '[...] either a steady (but reducing) erosion led to failure or, at the other extreme, fell to a very low level where only a rare group of very large waves gave further damage.' • Damage was caused predominantly by the run-down of the waves pulling stones down the slope. [...] The small and medium stones were first removed to leave the partially exposed larger stones to be pulled down by the biggest waves. There was little healing [...]. • 'The very long preliminary tests [...] give no certainty of the riprap eroding to a totally stable or equilibrium state even with low damage rates. [...] the erosion rate may become small enough to be ignored in practice.'
Broderick (1983)	Riprap stability, a progress report	Scaled (1:10) wave tank tests with a loose armour stone revetment subjected to irregular wave attack	<ul style="list-style-type: none"> • Damage $D =$ Volume per unit length of the erosion zone • Dimensionless damage $D' = \frac{D}{\left(\frac{W_{50}}{W_r}\right)^{\frac{2}{3}}}$ • W_r ... unit weight of riprap, W_{50} ... medium armour stone size 	Description of a typical, S-shaped damage profile

Authors	Title	Experimental set-up	Definition of failure	Main results
Pilarczyk and den Boer, K. (1983)	Stability and profile development of coarse materials and their application in coastal engineering	Combination of large-scale flume tests (Ahrens, 1970) and own small-scale investigations under regular and irregular wave attack, various angles of wave approach, different material types	<ul style="list-style-type: none"> • dimensionless damage $S_2 = \frac{A_2}{D_{n50}^2}$ • A_2 ... eroded area of the profile, D_{n50} ... nominal armour stone diameter • Failure: $8 < S_2 < 17$ 	<ul style="list-style-type: none"> • 'The shape of the equilibrium profile is not influenced by the initial profile.' • Equations for the transport of gravel on coasts • Extension of the Hudson formula by a slope resistance factor
Pilarczyk (1985)	Stability of revetments under wave and current attack			
Pitt and Ackers (1983)	Prototype Tests on Riprap under Random Wave Attack	Damage description of rip-rap test panels on an offshore island and comparison to small-scale laboratory tests (1:17)	<ul style="list-style-type: none"> • Damage is the volume removed, expressed as an equivalent number of D_{50} - sized spherical stones for a $9 \cdot D_{50}$ width of panel considering only reductions in thickness • 'In the laboratory tests, these movements occurred in a fairly well-defined area about the still-water level. Positive movements (accretion of displaced stone) generally occurring in the region below the eroded area were ignored, since these are not of interest when considering the ability of the riprap layer to withstand damage [...].' 	<ul style="list-style-type: none"> • '[...] the clear conclusion is that using laboratory research results for rip-rap design, omitting any allowance for scale effects, does not result in an over-conservative design.' • 'This study has thus not confirmed [...] scale effects, namely that small scale model results tend to overestimate the size of rip-rap needed to provide protection against waves of a particular height.'
Köhler (1985)	Modellversuche für die Dimensionierung von Deckwerken an Wasserstraßen - Stabilität loser Steinschüttungen -	Full-scale model tests in a wave tank to investigate the stability of different revetment configurations subjected to wave attack	<ul style="list-style-type: none"> • Damage criterion according to Hudson (1959) • Failure: armour stone displacement $> 9 - 10\%$ 	<ul style="list-style-type: none"> • Armour stone displacement occurs mainly below still water level. • In the case of unstable armour stones, displacements progresses. • To ensure stability, a minimum covering layer thickness of $d = 1.5 \cdot D_{50}$ is required.

Authors	Title	Experimental set-up	Definition of failure	Main results
Blodgett and Mc-Conaughy (1986)	Rock Riprap for Protection of Stream Channels Near Highway Structures. Volume 2 - Evaluation of Riprap Design Procedures	Failure observations at 36 field sites designed according to 7 different design procedures	4 failure types: 1. particle erosion, 2. translational sliding, 3. modified slump and 4. slump	'Factors associated with riprap failure include stone size, bank side slope, size gradation, thickness, insufficient toe or endwall, failure of the bank material, overtopping during floods, and geomorphic changes in the channel. A review of field data and the design procedures suggests that estimates of hydraulic forces acting on the boundary based on flow velocity rather than shear stress are more reliable.'
Bezuijen, Klein Breteler and Bakker (1987) Bezuijen, Wouters et al. (1988) Bezuijen and Klein Breteler (1992)	Design criteria for placed block revetments and granular filters Block revetment design with physical and numerical models Oblique wave attack on block revetments	Large-scale flume tests to determine uplift forces that destabilize the revetment		Design criteria for block revetments and granular filters
Lee et al. (1987)	Development of riprap design criteria by riprap testing in flumes: Phase I. NUREG/CR-4651, U.S. Nuclear Regulatory Commission, Washington, D.C., May, 111.	Large- and small-scale flume tests to investigate failure due to overtopping	Failure criterion = filter layer or geotextile exposed	'In many cases, concentrated flows would scour a localized zone along the embankment. However, rock movement from up slope would subsequently fill and stabilize the scour area. When rock movement could no longer adequately replenish rock to the scour or failure zone, catastrophic failure was observed.'
Abt, Wittler et al. (1988)	Development of riprap design criteria by riprap testing in flumes: Phase II. NUREG/CR-4651, U.S. Nuclear Regulatory Commission, Washington, D.C., May, 113.			
Abt and Johnson (1991)	Riprap Design for Overtopping Flow			

Authors	Title	Experimental set-up	Definition of failure	Main results
Latham et al. (1988)	The influence of armour-stone shape and rounding on the stability of breakwater armour layers	Flume tests to investigate the influence of armour stone shape and surface texture with regard to the design equations by (van der Meer, 1988b; van der Meer and Pilarczyk, 1984)	Damage criterion according to Thompson and Shuttler (1975)	<ul style="list-style-type: none"> • ‘Armour consisting of a mixture of extremely tabular and elongate blocks [...] is significantly more stable than relatively equat [sic!] blocks when they are placed randomly in a double layer.’ • ‘Van der Meer’s equations may be written with an additional coefficient to include the armour shape effect.’
Verheij and Bogaerts (1989)	Ship waves and stability of armour layers protecting slopes	Small-scale and full-scale model tests in a towing channel and literature values for adapting the Hudson (1959) formula to account for ship-induced secondary waves	<ul style="list-style-type: none"> • Dimensionless damage $S_2 = \frac{A_2}{D_{n50}^2}$ (van der Meer and Pilarczyk, 1984) • A_2 ... eroded area of the profile, D_{n50} ... nominal armour stone diameter • Determination of the damaged area in relation to the water level: $\frac{Y'}{D_{50}} = \frac{(\beta+0.5) \cdot (H_i \cdot (\cos \beta)^{0.5})}{(\Delta D_{50})}$ • Y' ... Distance between water level and lower damage limit, β ... slope angle, H_i ... wave height, β ... angle of incidence of waves, Δ ...relative density of armour stones, D_{50} ... characteristic riprap diameter 	Formulation of design equations for bank revetments subjected to ship-induced loads based on the conclusion that ship-induced waves are similar to wind waves
Daemrich et al. (1996)	Untersuchungen zur Bemessung von Deckwerken in Schiffahrtskanälen unter Wellenbelastung	Scaled (1:4) wave flume tests with varying revetment installations loaded by regular waves of unfavorable period range	Failure criterion: filter layer or geotextile exposed	Limiting wave height as design criterion
Froehlich and Benson (1996)	Sizing Dumped Rock Riprap	Small-scale flume tests to investigate the stability of riprap of different geometry and revetment thickness against flow	Number of displaced rocks in relation to the overall number of rocks in %	Design equation against flow using a critical shear strength approach

Authors	Title	Experimental set-up	Definition of failure	Main results
Dornack (2001)	Überströmbare Dämme - Beitrag zur Bemessung von Deckwerken aus Bruchsteinen	Small-scale tests of riprap dikes subjected to overflowing	Failure is defined as the complete collapse of the structure	Design equations against overflowing
Westrich et al. (2003)	Neue naturnahe Bauweisen für überströmbare Dämme an dezentralen Hochwasserrückhaltebecken und Erprobung von Erkundungsmethoden	Large-scale flume model tests (1:1, 1:2) to investigate the stability of riprap against overflowing		Design equations for armour stone dikes subjected to flow and resulting hydrodynamic pressure fluctuations
Peirson et al. (2008)	Placed Rock as Protection against Erosion by Flow down Steep Slopes	Stability of placed and dumped rock against overtopping quantified by large scale flume tests	<p>‘Three damage definitions:</p> <ol style="list-style-type: none"> 1. Initial displacement of a single stone anywhere on the test surface q_{init} 2. Significant rock motion, defined as displacement of five rocks over a distance of more than 5 diameters q_{sig} 3. Armor failure, that is, exposure of the filter layer $q_{over,fail}$. 	Supplementation of design equations for placed rock revetments against overtopping
Froehlich (2012)	Rock and Roll—It’s Here to Stay: Sizing Loose Rock Riprap to Protect Stream Banks	38 on-site observations of riprap-lined stream channels		Verification of design equation against flow using a critical shear strength approach
Gier (2017)	Zur Bemessung von verzahnten Setzsteindeckwerken gegen hydrodynamische Belastungen	Large-scale flume tests to investigate the stability of different types of block revetment subjected to irregular waves		Development of a semi-empirical design formula

Authors	Title	Experimental set-up	Definition of failure	Main results
Hiller, Aberle et al. (2017)	Displacements as failure origin of placed riprap on steep slopes	Laboratory and field tests to investigate the stability and failure mechanisms of placed riprap as a consequence of overtopping	'For dumped riprap, failure is usually considered when the underlying filter layer is exposed to the flow due to the erosion of the riprap (e. g. Abt and Johnson (1991), Linford and Saunders (1967), Peirson et al. (2008) and Robinson et al. (1998)).'	<ul style="list-style-type: none"> • '[...] if a stone is eroded out of a placed riprap, the remaining stones can absorb the loss because the interlocking pattern allows for the formation of a bearing structure. Therefore, progressive erosion of the riprap layer should be considered as the critical condition [...] (Dornack, 2001; Hiller, Aberle et al., 2017).' • 'Erosion of the first stone did not necessarily cause failure and progressive erosion should be used as a failure criterion.'
Hiller, Lia et al. (2019)	Field and model tests of riprap on steep slopes exposed to overtopping			
Kreyenschulte (2020)	Wellen-Bauwerks-Interaktion bei mör-telvergossenen Schütt-steindeckwerken	Large-scale model tests to investigate the stability of mortar-grouted riprap ('crack formation in the toplayer' and 'erosion of an individual stone') against wave attack	'If the resistance of the revetment has been reduced as a result of deterioration or loading to such an extent that the design case cannot be absorbed without failure. [...] A damage usually does not occur without previous deterioration and often represents the consequence of the sum of previous deterioration.'; Investigations did not reach failure; deterioration was not investigated in detail.	Design equations for mortar-grouted riprap

Table A.4: Model tests and field investigations with regard to failure and design of breakwaters

Authors	Title	Experimental set-up	Definition of failure	Main results
Iribarren (1949)	A Formula for the Calculation of Rock-Fill Dikes	Summary of field observations and experience with rock fill dikes		New design formula
Iribarren and Nogales (1951)	Generalization of the Formula for the Calculation of Rock Fill Fikes and Verification of its Coefficients			
Iribarren and Nogales (1952)	New confirmation of the formula for the calculation of rock fill dikes			
Hudson (1959)	Laboratory investigation of rubble-mound breakwaters	Scaled model tests to investigate the stability of tetrapod and rock breakwaters against short-periodic wind waves	<ul style="list-style-type: none"> • Damage is described by percentage of displaced armour units $D = \frac{n}{n_{\text{surface}}}$ • n ... number of displaced armour stones, n_{surface} ... overall number of armour stones • $D < 1\% \rightarrow$ no damage • Stability number $N_S = \frac{\gamma_r^{\frac{1}{3}} \cdot H}{(S_r - 1) W_r^{\frac{1}{3}}}$ • γ_r ... unit weight of armour stones, H ... wave height, S_r ... specific gravity, W_r ... buoyant unit weight of armour stones 	Supplementation of the Iribarren and Nogales (1952) formula with an empirical factor that takes into account the slope inclination and stone shape. The experimentally determined damage coefficient K_D can be used to dimension breakwaters.
Font (1968)	The effect of storm duration on rubble mound breakwater stability	Small-scale and large-scale wave flume tests simulating a storm to investigate the stability of rock and tetrapod breakwaters		<ul style="list-style-type: none"> • ‘Uncovering of the filter layers in holes of diameter equal to two pieces ocured [sic!] for armor damage percentages between 10 % and 20 %. [...] total failure would follow for damage between 30 % and 40 %.’
Font (1970)	Damage functions for a rubble-mound breakwater under the effect of swells			<ul style="list-style-type: none"> • ‘[...] placing makes a big difference for the initial damage, but is less relevant for advanced damage, when the armor porosity and “dynamic” stability are essential.’

Authors	Title	Experimental set-up	Definition of failure	Main results
van de Kreeke (1969)	Damage Function of rubble-mound breakwaters	Small-scale wave flume tests on rubble-mound breakwaters subjected to oblique and perpendicular wave attack	<ul style="list-style-type: none"> • $D = \frac{n_{\text{displaced}}}{n_{\text{total}}}$ • $n_{\text{displaced}}$... number of displaced armour stones, n_{total} ... total number of armour stones in the 'attacked area' (sea water level \pm wave height) 	Damage curves for different breakwater slopes and directions of wave approach
Ouellet (1972)	Effects of irregular wave trains on rubble-mound breakwaters	Scaled wave flume tests with dolosses subjected to regular and irregular waves	<p>Two types of damage are identified:</p> <ul style="list-style-type: none"> • 'Stable damage – The number of units seen to rock and move a distance less than the overall size of the unit, expressed as a percentage of the total number of units in the attacked area. • Unstable damage - The number of units moved over a distance greater than the overall size of the units. In this case, the unit moved from one stable position to another by the waves or rolled down to the toe of the structure.' 	<ul style="list-style-type: none"> • '[...] damage is progressive and a certain period of destruction action is normally required before the structure ceases to provide adequate protection.' • 'Failure does not seem to occur from one maximum wave.'
van der Meer and Pilarczyk (1984)	Stability of rubble mound slopes under random wave attack	Large-scale wave flume tests to investigate stability and damage development of breakwaters of different slope inclination against wave attack	<ul style="list-style-type: none"> • $S_2 = \frac{A_2}{D_{n50}^2}$ • A_2 ... eroded area of the profile, D_{n50} ... nominal armour stone diameter • 3 damage levels: 1. start of damage, 2. intermediate damage, 3. failure = filter layer is exposed 	<ul style="list-style-type: none"> • 'The profile [of the slope] is influenced by the angle of wave attack.' • Design formula as a function of the wave number and wave breaker type (damage function)
van der Meer (1987)	Stability of breakwater armour layers – design formulae			
van der Meer (1988b)	Rock Slopes and Gravel Beaches under Wave Attack			

Authors	Title	Experimental set-up	Definition of failure	Main results
Smith et al. (2002)	Rock Slope Stability with Shallow Foreshores	Small-scale flume tests with breakwaters and different slope inclination of the foreshore (1:30 and 1:100) subjected to wave attack to investigate the stability against overtopping	<ul style="list-style-type: none"> • Damage is measured by the eroded area • $S_2 = \frac{A_2}{D^{n50}}$ (van der Meer and Pilarczyk, 1984) 	New stability formula based on Thompson and Shuttler (1975) and van der Meer (1988b), which accounts for the permeability of the structure
van Gent et al. (2003) van Gent (2005)	Stability of Rock Slopes with Shallow Foreshores On the Stability of Rock Slopes			
Uliczka (2018)	FuE-Abschlussbericht. Schiffserzeugte langperiodische Belastung zur Bemessung der Deckschichten von Strombauwerken an Seeschiffahrtsstraßen	Small-scale laboratory tests, field observations and expert surveys to assess ship-induced hydraulic loads and damage on jetties	<ul style="list-style-type: none"> • Failure as a result of the structure (design or construction): ochre formation or ineffectiveness of the filter, damage below the grout, exceedance of service life, structure geometry, jetty (field) geometry. • Failure due to hydraulic and external loading: ship-generated drawdown and swell, overflow current, ice drift. • Failure due to scour development. • No failure of the power structures due to the subsoil. 	<ul style="list-style-type: none"> • Description of damage development • Observation of ship-induced hydraulic loads

A.3 Hydraulic design according to GBB (2010)

The subsequent sections outline the design equations of GBB (2010) which are used throughout this thesis.

A.3.1 Required stone diameter to resist currents

The required mean armour stone diameter D_{50} when the flow is directed parallel to the embankment is determined as follows:

$$D_{50} \geq C_{\text{Isb}} C_{\text{Bö}} \frac{v_{\text{max}}^2}{g_0} \frac{1}{\frac{\rho_s - \rho_w}{\rho_w}} \quad (\text{A.27})$$

The maximum flow velocity v_{max} is the maximum of return current velocity v_{return} and the natural flow velocity at the shore. D_{50} is then obtained taking into account gravity g_0 , armour stone density ρ_s and water density ρ_w , which specify the resistance of the armour stones under water. Since eq. (A.27) relies on the formulation of Izbash and Khaldre (1970), the Izbash factor C_{Isb} is included assuming a value of 0.7. The slope characteristics are described by an empirical factor considering the slope inclination $C_{\text{Bö}}$ under consideration of the angle of repose of the armour stones $\phi'_{\text{D,hydr}}$ and the slope angle β .

$$C_{\text{Bö}} = \frac{1}{\cos \beta \left[1 - \frac{\tan^2 \beta}{\tan^2 \phi'_{\text{D,hydr}}} \right]^{0.5}} \quad (\text{A.28})$$

The armour stone diameter required to resist the largely turbulent slope supply flow u_{max} is determined with two different approaches. On the one hand, the same equation as for v_{return} is used:

$$D_{50} \geq 0.5 C_{\text{Bö}} \frac{u_{\text{max, B}}^2}{g_0} \frac{1}{\frac{\rho_s - \rho_w}{\rho_w}} \quad (\text{A.29})$$

However, due to the turbulent flow conditions, C_{Isb} is reduced to 0.5. A second approach is based on field observations (BAW, 2009) and accounts for flow separation caused by the shallow water depth close to the bank.

$$D_{50} \geq \left(\frac{u_{\text{max, B}}^2 C_{\text{Bö}}}{1.4 \frac{\rho_s - \rho_w}{\rho_w} g_0 H_{\text{stern}}^{\frac{1}{3}}} \right)^{\frac{3}{2}} \quad (\text{A.30})$$

A.3.2 Required stone diameter to resist wave attack

D_{50} required for the positional stability is, amongst others, a function of the design wave height H_{Bem} , which is the maximum of the transversal waves near the bank with and without superimposition of primary and secondary wave system. It is determined as follows:

$$D_{50} \geq \frac{H_{Bem}}{B'_B \left(\frac{\rho_s - \rho_w}{\rho_w} \right) m^{\frac{1}{3}}}. \quad (A.31)$$

Eq. (A.31) is based on the design formula of Hudson (1959) where the required armour stone diameter depends on breaker type and slope inclination m . An empirical factor considering revetment stability (stability coefficient) B'_B is derived from BAW (2009) and a measure for the admissible maintenance efforts. In particular for moderately inclined slopes, it overestimates the required D_{50} (GBB, 2010).

$$D_{50} \geq \frac{H_{stern} C_{B\ddot{o}}}{B_B^* \left(\frac{\rho_s - \rho_w}{\rho_w} \right)} \quad (A.32)$$

Eq. A.32 employs an empirical factor considering the frequency of occurrence B_B^* to describe the admissible maintenance efforts related to a specific design. If the design loads are observed regularly or if damage is to be avoided, $B_B^* \approx 2.0$, whereas for a less frequent occurrence of the design loads or when a limited amount of maintenance is tolerable, $B_B^* \approx 3.0$.

Eq. (A.31) and eq. (A.32) are also used to determine the armour stone diameter required to resist the transversal secondary wave height $H_{sec,trans}$. The results of eq. (A.31) and eq. (A.32) are equally weighted against

$$D_{n,50} \geq \frac{H_{sec} (\cos \beta_w)^{\frac{1}{2}} \zeta^{\frac{1}{2}}}{2.25 \cdot \left(\frac{\rho_s - \rho_w}{\rho_w} \right) (\cos \beta + \sin \beta)} \quad (A.33)$$

which defines the armour stone diameter required to resist the attack of the oblique secondary wave height H_{sec} . The wave height is reduced by the angle between wave crest of the secondary diverging wave and the axis of the ship or the bank line β_w . The similarity parameter ζ accounts for the wave length following the definition by Verheij and Bogaerts (1989). The nominal armour stone diameter $D_{n,50}$ is a function of shape factor SF and sieve diameter D of the armour stones:

$$D_{n,50} = \sqrt[3]{SF D} \quad (A.34)$$

A.3.3 Required stone diameter to resist different types of loads

As outlined in the previous two sections, there are multiple equations defining the required armour stone diameter. When a vessel passes a shore, a revetment is subjected to all types

load type		design equation	weights			
primary wave field	H_{stern}	GBB (2010) eq. (6-1)	mean	$D_{50, req, 1}$	max	
		GBB (2010) eq. (6-2)				
	u_{max}	GBB (2010) eq. (6-10)				
		GBB (2010) eq. (6-11)				
return current	v_{return}	GBB (2010) eq. (6-8)	$D_{50, req, 2}$			
secondary wave field	$H_{sec, div}$	GBB (2010) eq. (6-7)	mean	$D_{50, req, 3}$		
	$H_{sec, trans}$	GBB (2010) eq. (6-1)				max
		GBB (2010) eq. (6-2)				
$D_{50, req}$						

Figure A.1: Schematics to determine the required armour stone diameter weighting the following hydraulic loads: maximum stern wave height at the bank for an eccentric sailing line H_{stern} , slope supply flow u_{max} , return current velocity v_{return} , divergent secondary wave height $H_{sec,div}$ and transversal secondary wave height $H_{sec,trans}$; illustration based on GBB (2010, cf. p. 102).

of loads simultaneously. Thus, revetment design should account for all of the above introduced design equations according to the proportion of their impact. GBB (2010) employs a weighting concept that incorporates physical relations of the different load types. While different load types are treated as equally important, the competing design equations for the same load type are weighted. A graphical illustration of the weighing system is depicted in Figure A.1.

A.4 Geotechnical design according to GBB (2010)

A.4.1 Required armour stone layer thickness to impede slope sliding

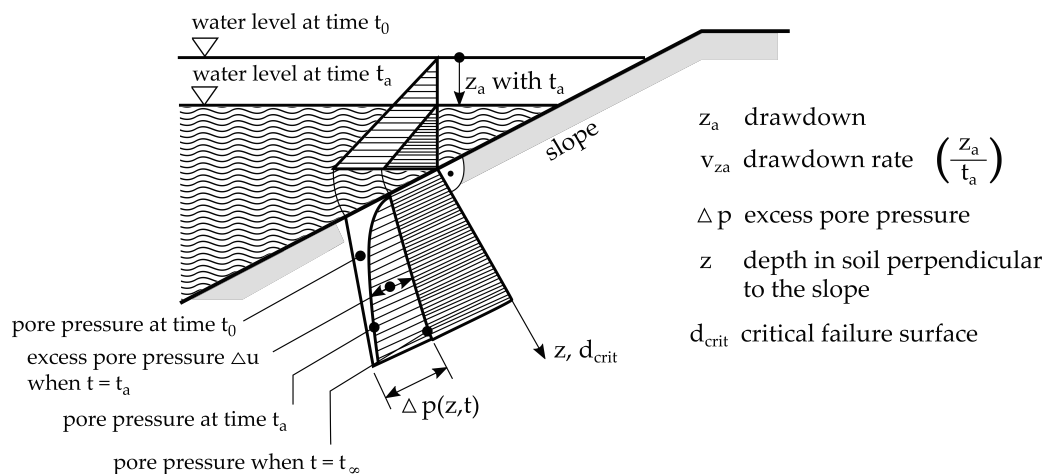


Figure A.2: Hydrostatic pore water pressure and excess pore pressure during rapid drawdown; illustration based on GBB (2010, cf. p. 20).

The drawdown and, thus, the development of excess pore pressure in the embankment is a time-dependent process. Based on the investigations of Köhler (1985), wave-induced drawdowns can be simplified by a uniformly decreasing water level characterised by a constant drawdown rate (change in water level z_a during the drawdown time t_a). It can be shown that the excess pore pressure attains a maximum at the end of the drawdown, which allows to assess the acting forces as a steady-state problem as shown in Figure A.2. A depth-depending excess pore pressure $\Delta p(z)$ may develop:

$$\Delta p(z) = \gamma_w z_a \left(1 - ae^{-bz}\right) \quad (\text{A.35})$$

The pore pressure parameter a is commonly defined as 1. The pore pressure parameter b is a function of z_a and the hydraulic conductivity k and defines the shape of the pore pressure profile, eq. (A.37). Amongst others, it accounts for a gas content between 85 % and 95 % in the pore fluid (Köhler, 1993, 1997b). It is obtained assuming a design drawdown time $t_a^* = 5$ s as given in eq. (A.36).

$$b^* = 0.166 \cdot k^{-0.327} \quad (\text{A.36})$$

$$b = b^* \sqrt{\frac{t_a^*}{t_a}} \quad (\text{A.37})$$

The excess pore pressure may cause the driving forces to exceed the resisting forces at the vertical slice of the infinite slope leading to a local sliding. The resisting forces are a function of buoyant unit weight of soil below the groundwater table γ'_B and effective friction angle of soil ϕ' . The difference of resisting and driving forces reaches a minimum at a critical depth of failure surface d_{crit} as follows:

$$d_{\text{crit}} = \frac{1}{b} \ln \left(\frac{\tan \phi' \gamma_w z_a b}{\cos \beta \gamma'_B (\tan \phi' - \tan \beta)} \right) \quad \phi' > \beta \quad (\text{A.38})$$

If $d_{\text{crit}} \leq 0$, the local slope stability is given without additional weight. If $d_{\text{crit}} > 0$, the equilibrium condition stated in eq. (A.39) is used to determine the required unit weight under buoyancy g' with the armour stone layer thickness d_D , the buoyant unit weight of the armour stones below the groundwater table γ'_D , the filter layer thickness d_F and the buoyant unit weight of the filter layer below the groundwater table γ'_F (see Figure A.3).

An effective cohesion c' reduces the required armour stone layer thickness. In case of $c' \geq \Delta p \tan \beta$, the slope safety against slope sliding is given without revetment. An additional toe support or a suspension of the armour stone layer can add a supporting additional stress from a revetment suspension τ_A or additional stress from a toe support τ_F , which leads to the reduction of the required armour stone layer thickness. However, for revetments with a toe blanket and/or a suspension, further failure mechanisms and, thus, additional design equations are to be considered. They can be found in GBB (2010).

$$g' = \gamma'_D d_D = \frac{\Delta p \tan \phi' - c' - \tau_F - \tau_A}{\cos \beta \tan \phi' - \sin \beta} - \left(\gamma'_F d_F + \gamma' d_{\text{crit}} \right) \quad (\text{A.39})$$

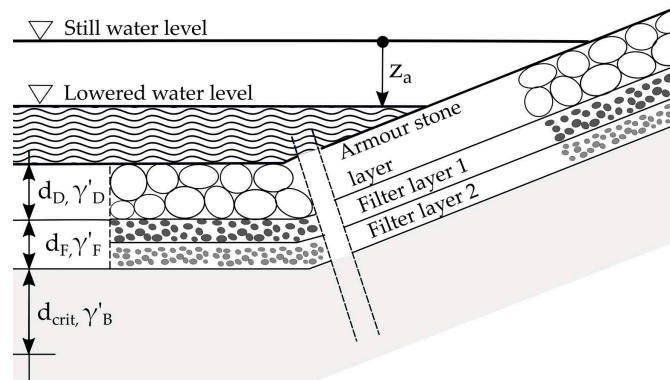


Figure A.3: Constructional elements considered in a revetment design.

A.4.2 Required armour stone layer thickness to impede liquefaction

Waves and drawdown generate flow in the permeable river bed, which may lead to considerable vertical hydraulic gradients at the river bed and the slope. This process is particularly amplified by a compressible pore fluid and soils of moderate to low hydraulic conductivity, moderate to large plasticity. The flow of pore water can lead to liquefaction of a near-surface layer of the river bed.

In case of a large toe support force, a revetment suspension or a very small slope inclination, the weight per unit area of the revetment resulting from the design against slope sliding failure may not satisfy the equilibrium equations of liquefaction. In non-cohesive soils ($c' = 0$), the excess pore pressures may cause soil liquefaction. The required g' is calculated from eq. (A.40), which is derived from the equations against hydraulic failure.

$$g' = \gamma'_D d_D \geq \frac{\Delta p}{\cos \beta} - (\gamma'_F d_F + \gamma'_B d_{critB}) \quad (A.40)$$

The critical depth of failure surface to prevent soil liquefaction d_{critB} at which the difference of the effective weight of soil particles and the excess pore pressures reaches a minimum is defined as follows:

$$d_{critB} = \frac{1}{b} \ln \left(\frac{\gamma_w z_a b}{\gamma'_B \cos \beta} \right) \quad (A.41)$$

B | SUPPLEMENTARY MATERIAL FOR THEORY OF RELIABILITY ASSESSMENT

B.1 Mathematical definitions

It is beyond the scope of this thesis to provide a full background on mathematical definitions and methods applied. This appendix supplies definitions of random variables, events and distribution functions to supplement the information on the probability theory outlined in Chapter 2. Notation and terminology in literature differs considerably. The notation this thesis applies is based on the work of Ang and Tang (2007).

B.1.1 Random variables and events

In contrast to a deterministic variable, a random variable X is defined by a range of possible values that are denoted by x . An event E encompasses a ‘subset of the sample space’ (Ang and Tang, 2007, p. 31), which is defined as the total of possible outcomes of a probabilistic problem. It relates X to x , e. g. $X = x$ or $X < x$ with $\bar{a} < x < \bar{b}$. Consequently, a random variable ‘can be considered as a mathematical function or rule that maps (or transforms) events in a sample space into the number system...’ (Ang and Tang, 2007, p. 81). Random variables can be discrete or continuous.

B.1.2 Probability functions

The values of a random variable are associated with a probability which relates the values or the range of values to the event. The probability measures are assigned by a predefined rule, the probability function. A random variable, either discrete or continuous, can then be described by its cumulative density function (cdf) as follows:

$$F_X \equiv P(X \leq x) \quad (\text{B.1})$$

The probability of a discrete variable may be expressed as probability mass function (pmf) according to eq. (B.2). As a continuous variable is only defined on an interval, a probability cannot be assigned to a specific value within the interval. Therefore, a probability density function as denoted in eq. (B.3) is defined. A probability density function can be interpreted as the likelihood that the random variable X takes a value x_i in the specified interval. Naturally, the function describing the probability of a random variable must satisfy the axioms of probability theory which can be reviewed in any basic literature on probability theory, e. g. Ang and Tang (2007).

$$F_X(x) = \sum_{\text{all } x_i \leq x} P(X = x_i) = \sum_{\text{all } x_i \leq x} p_X(x_i) \quad (\text{B.2})$$

$$P(\bar{a} < X \leq \bar{b}) = \int_{\bar{a}}^{\bar{b}} f_X(x) dx \quad (\text{B.3})$$

B.1.3 Main descriptors of random variables

Central values

Probability functions fully describe random variables. In practice, however, their exact form may not be known. Additional descriptors are required to describe the random variables.

The so called central values mean, mode and median are well known. The mean, also referred to as the expected value, is defined as weighted average of the probability or probability densities of a random variable. Eq. (B.4) and eq. (B.5) describe the mean of discrete and continuous variables.

$$E(X) = \sum_{\text{all } x_i} x_i p_X(x_i) \quad (\text{B.4})$$

$$E(X) = \int_{-\infty}^{\infty} x f_X(x) dx \quad (\text{B.5})$$

The mode, often denoted by \bar{x} , is the most likely value a random variable will take and hence, the maximum of its probability density or probability mass function. The median x_m is the value at 50% of the cdf. At that point, the probability of values smaller or greater than x is equal.

Dispersion

Commonly, engineers require information on minima and maxima of a variable. This question is closely related to how narrowly or widely the values deviate from a central value.

The variance describes the deviation in relation to the mean. It is the squared mean of the deviations weighted by their probability. Mathematically, the variance specifies the second central moment of a random variable. A definition for discrete variables is given in eq. (B.6), for continuous variables in eq. (B.7).

$$Var(X) = \sum (x_i - \mu_X)^2 p_X(x_i) \quad (\text{B.6})$$

$$Var(X) = \int_{-\infty}^{\infty} (x_i - \mu_X)^2 f_X(x) dx \quad (\text{B.7})$$

In practice, the standard deviation σ_X , the square root of the variance, as stated in eq. (B.8) and the coefficient of variance δ (cov) given in eq. (B.9), only valid for $\mu_X > 0$, may be easier to apply.

$$\sigma_X = \sqrt{\text{Var}(X)} \quad (\text{B.8})$$

$$\delta = \frac{\sigma_X}{\mu_X} \quad (\text{B.9})$$

Skewness

Symmetry and asymmetry of a probability distribution may be described by the skewness, which is the third central moment as defined in eq. (B.10) for discrete distributions and eq. (B.11) for continuous distributions. A negative measure of skewness characterises a left skewed, a positive measure of skewness a right skewed distribution - always in relation to the mean. The skewness coefficient θ_{skew} is a dimensionless measure as specified in eq. (B.12).

$$E(X - \mu_X)^3 = \sum_{\text{all } x_i} (x_i - \mu_X)^3 p_X(x_i) \quad (\text{B.10})$$

$$E(X - \mu_X)^3 = \int_{-\infty}^{\infty} (x_i - \mu_X)^3 f_X(x) dx \quad (\text{B.11})$$

$$\theta_{\text{skew}} = \frac{E(X - \mu_X)^3}{\sigma^3} \quad (\text{B.12})$$

Kurtosis

The kurtosis is the fourth central moment of a random variable. In physical space, it describes the degree of peakedness of a distribution. The peakedness of a discrete random variable is characterised by

$$E(X - \mu_X)^4 = \sum_{\text{all } x_i} (x_i - \mu_X)^4 p_X(x_i). \quad (\text{B.13})$$

The kurtosis of a continuous random variable may be determined by

$$E(X - \mu_X)^4 = \int_{-\infty}^{\infty} (x_i - \mu_X)^4 f_X(x) dx. \quad (\text{B.14})$$

B.1.4 Multiple random variables

When there is more than one variable of concern, a univariate probability function may be extended to a joint probability function; for discrete variables, the joint probability mass function (jpmf) and for continuous variables, the joint probability density function (jpdf). Geometrically, considering two variables, a jpdf may be understood as volume under a surface defined by the two variables and their range. The distribution of one variable under consideration of all values of the other variable is referred to as marginal distribution.

Eq. (B.15) and eq. (B.16) describe cdf and jpmf of two discrete variables; cdf and jpdf of two continuous distributions are defined in eq. (B.17) and eq. (B.18). The equations assume independent variables.

$$f_{x,y}(x, y) = \sum_{x_i \leq x} \sum_{y_i \leq y} p_{x,y}(x_i, y_i) \quad (\text{B.15})$$

$$p_{x,y} = p(x = x_i, y = y_i) \quad (\text{B.16})$$

$$f_{x,y}(x, y) = \int_{-\infty}^x \int_{-\infty}^y f_{x,y}(u, v) dv du \quad (\text{B.17})$$

$$f_{x,y}(x, y) = \frac{\partial^2 f_{x,y}(x, y)}{\partial x \partial y} \quad (\text{B.18})$$

Main descriptors or moments of multivariate distributions may be found by extending the equations outlined above, see e. g. Baecher and Christian (2003). The third moment of a multivariate distribution is of particular interest: The covariance indicates the correlation of multiple variables. Given the two random variables X_1 and X_2 , the covariance is denoted by eq. (B.19).

$$Cov(X_{1,2}) = E[(X_1 - \mu_{X_1})(X_2 - \mu_{X_2})] = E(X_1 X_2) - E(X_1)E(X_2) \quad (\text{B.19})$$

Normalised by the standard deviation, the correlation coefficient ρ is obtained as follows:

$$\rho = \frac{Cov(X_1, X_2)}{\sigma_{X_1} \sigma_{X_2}}. \quad (\text{B.20})$$

A covariance matrix C

$$C \equiv \begin{bmatrix} \sigma_{X_1}^2 & \sigma_{X_1, X_2} & \dots & \sigma_{X_1, X_n} \\ \sigma_{X_1, X_2} & \sigma_{X_2}^2 & \dots & \sigma_{X_2, X_n} \\ \vdots & \vdots & \ddots & \vdots \\ \sigma_{X_1, X_n} & \sigma_{X_2, X_n} & \dots & \sigma_{X_n}^2 \end{bmatrix} \quad (\text{B.21})$$

or a correlation matrix K

$$K \equiv \begin{bmatrix} 1 & \rho_{X_1, X_2} & \dots & \rho_{X_1, X_n} \\ \rho_{X_1, X_2} & 1 & \dots & \rho_{X_2, X_n} \\ \vdots & \vdots & \ddots & \vdots \\ \rho_{X_1, X_n} & \rho_{X_2, X_n} & \dots & 1 \end{bmatrix} \quad (\text{B.22})$$

summarise the covariance or correlation for more than two variables.

When the probability of X depends on X_2 and vice versa, the probability density must be expressed via a conditional probability function. The conditional probability mass function of X ,

which depends on X_2 , is given in eq. (B.23); the conditional probability density function for continuous variables is shown in eq. (B.24).

$$p_{X|X_2}(x_i, y_j) = y_j = \frac{p_{X, X_2}(x_i, y_j)}{p_{X_2}(y_j)} \quad p_{X_2}(y_i) \neq 0 \quad (\text{B.23})$$

$$f_{X|X_2}(x|y) = \frac{f_{X, X_2}(x, y)}{f_{X_2}(y)} \quad f_{X_2}(y) \neq 0 \quad (\text{B.24})$$

An efficient way to deal with dependent probability functions are copulas. In simplified terms, a copula summarises the dependence of multiple variables, while the values of these variables are described by their univariate, uniform marginal distributions. Copulas allow to connect the dependencies of multiple random variables with their marginal distributions. Mathematically, copulas are based on *Sklar's theorem* (Sklar, 1959), stating that every multivariate cumulative distribution can be described by their marginals and a copula function. A k -dimensional copula is denoted by eq. (B.25).

$$c : [0, 1]^k \rightarrow [0, 1] \quad (\text{B.25})$$

There are several copula families such as *Gaussian copulas*, *Archimedean copulas* and *Student t copulas* (Nelsen, 2010). The most common copula function is the *Gaussian copula* as introduced by eq. (B.26) with the correlation matrix K and the identity matrix I .

$$c_K^{\text{Gauss}} = \frac{1}{\sqrt{\det R}} \exp \left(-\frac{1}{2} \begin{pmatrix} \Phi^{-1}(u_1) \\ \vdots \\ \Phi^{-1}(u_i) \end{pmatrix}^T \cdot (K^{-1} - I) \cdot \begin{pmatrix} \Phi^{-1}(u_1) \\ \vdots \\ \Phi^{-1}(u_i) \end{pmatrix} \right) \quad (\text{B.26})$$

The Gaussian copula belongs to the class of elliptical copulas. It is characterised by asymptotically independent upper and lower tails, which refer to the probability of obtaining extreme high and low values at the same time. The dependence structure of a random vector described by linear correlation coefficients is best modelled with a Gaussian copula (Caniou, 2012).

B.2 Standard distributions

The following section provides a brief overview of common probability distributions focusing on the most popular distributions applicable in engineering. Not mentioned, yet also useful in engineering applications, are uniform distributions and extreme value distributions such as the Weibull, Fréchet and Gumbel distribution.

B.2.1 Gaussian distribution

The Gaussian distribution, also Normal distribution, is undoubtedly the best known probability function. The probability density function (pdf) is denoted by eq. (B.27). It is characterised by the parameters μ and σ , respectively mean and standard deviation. A common short notation is $\mathcal{N}(\mu, \sigma)$. An illustration of different Gaussian pdf and cdf is given in Figure B.1.

$$f_X(x) = \frac{1}{\sigma\sqrt{2\pi}} \exp \left[-\frac{1}{2} \left(\frac{x - \mu}{\sigma} \right)^2 \right] \quad -\infty < x < \infty \quad (\text{B.27})$$

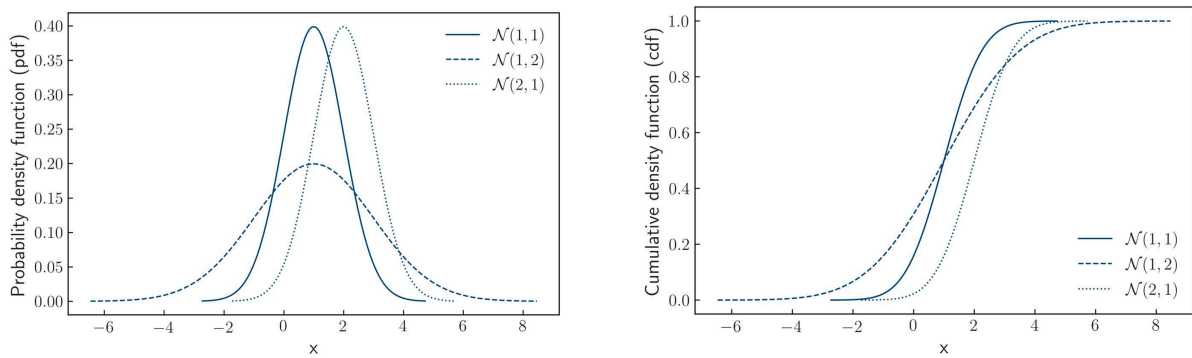


Figure B.1: Probability density function (pdf) and cumulative density function (cdf) of a Gaussian distribution.

B.2.2 Lognormal distribution

The Lognormal distribution is suitable for random variables whose values are greater/equal zero, such as the strength of soil or the height of waves. In theory, a distinction is made between two-parameters Lognormal and three-parameters Lognormal distributions. Three-parameters distributions are frequently used in hydrology. Especially for heavy skewed data, they may be a good approximate, see also Singh (1998).

The pdf of the two-parameters Lognormal distribution is given in eq. (B.28) with the parameters shape λ and scale ζ . The pdf of the three-parameters Lognormal distribution is given in eq. (B.29) with the additional shift parameter γ . The two-parameters distribution is a special case of the three-parameters distribution with $\gamma = 0$.

$$f_X(x) = \frac{1}{\sqrt{2\pi}(\zeta x)} \exp \left[-\frac{1}{2} \left(\frac{\ln x - \lambda}{\zeta} \right)^2 \right] \quad x \geq 0 \quad (\text{B.28})$$

$$f_X(x) = \frac{1}{\sqrt{2\pi}(\zeta(x - \gamma))} \exp \left[-\frac{1}{2} \left(\frac{\ln x - \gamma - \lambda}{\zeta} \right)^2 \right] \quad \gamma \leq x < \infty \quad (\text{B.29})$$

The parameter λ_{LG} corresponds to the mean of the distribution where $\lambda_{\text{LG}} = E(\ln X)$; ζ_{LG} characterises the standard deviation with $\zeta_{\text{LG}} = \sqrt{\text{Var}(\ln X)}$. γ_{LG} defines a lower bound of the distribution. Occasionally, this parameter set is referred to as native parameters. Eq. (B.30) and eq. (B.31) specify their deduction from μ and σ , parameters of the Gaussian distribution. Within this thesis, the Lognormal distribution is abbreviated by $\mathcal{LG}(\lambda_{\text{LG}}, \zeta_{\text{LG}}, \gamma_{\text{LG}})$. Figure B.2 illustrates pdf and cdf of three Lognormal distributions.

$$\lambda_{\text{LG}} = \ln(\mu - \gamma_{\text{LG}}) - \frac{\zeta_{\text{LG}}^2}{2} \quad (\text{B.30})$$

$$\zeta_{\text{LG}} = \sqrt{\ln\left(1 + \frac{\sigma^2}{(\mu - \gamma_{\text{LG}})^2}\right)} \quad (\text{B.31})$$

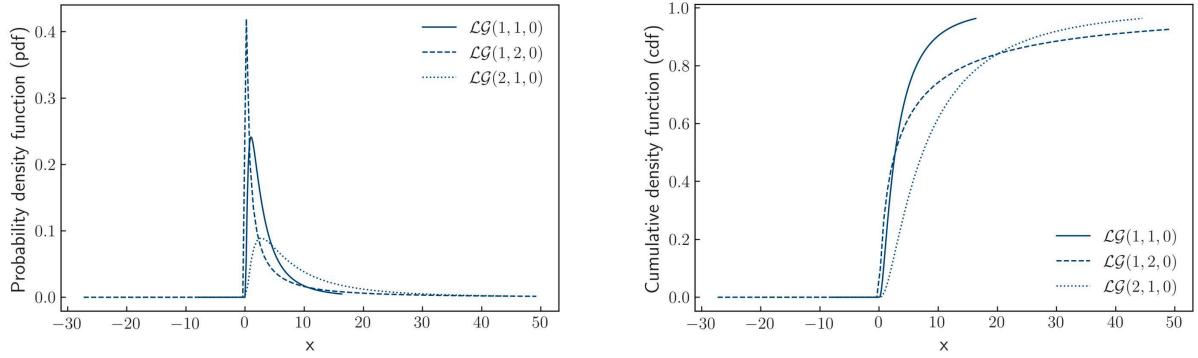


Figure B.2: Probability density function (pdf) and cumulative density function (cdf) of a Lognormal distribution.

B.2.3 Poisson distribution

Events that occur randomly and independently in a certain time interval or space can be best described by a Poisson distribution (see Figure B.3). The Poisson distribution represents counting processes and is closely related to Bernoulli sequences. Its pmf as stated in eq. (B.32) is specified for a time interval $[0, t]$. It is only valid for independent events and a discretisation of time or space which is proportional to the mean occurrence rate ν . However, the probability of two occurrences at the same time or space has to be negligibly small.

$$P(X_t = x) = \frac{(\nu t)^x}{x!} e^{-\nu t} \quad x = 0, 1, 2, \dots \quad (\text{B.32})$$

Due to the relation between the Poisson process and the Bernoulli process and thus, the Bernoulli distribution, it can be assumed that for large values of ν , $\mathcal{P}(\nu t)$ approximates $\mathcal{N}(\mu, \sigma)$. The parameters μ and σ are then obtained as follows:

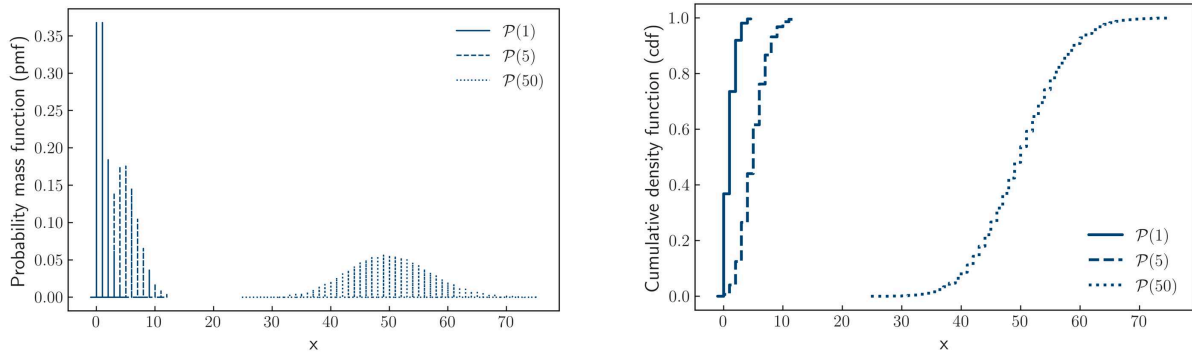


Figure B.3: Probability density function (pdf) and cumulative density function (cdf) of a Poisson distribution.

$$\mu = \nu_{\mathcal{P}} \quad (\text{B.33})$$

$$\sigma = \sqrt{\nu_{\mathcal{P}}}. \quad (\text{B.34})$$

B.2.4 Gamma distribution

The density functions of the Gamma distribution are shown in Figure B.4. The pdf is denoted by eq. (B.35) with the parameters ν , k and the gamma function $\Gamma(k_{\mathcal{G}})$ in eq. (B.36). In analogy to $\mathcal{LG}(\lambda_{\mathcal{LG}}, \zeta_{\mathcal{LG}}, \gamma_{\mathcal{LG}})$, there is also a shifted Gamma distribution with the shift parameter $\gamma_{\mathcal{G}}$ known. The short notation of the Gamma distribution is $\mathcal{G}(\nu_{\mathcal{G}}, k_{\mathcal{G}}, \gamma_{\mathcal{G}})$.

The distributions $\mathcal{G}(\nu_{\mathcal{G}}, k_{\mathcal{G}}, \gamma_{\mathcal{G}})$, $\mathcal{N}(\mu, \sigma)$, $\mathcal{P}(\nu_{\mathcal{P}})$ and $\mathcal{LG}(\lambda_{\mathcal{LG}}, \zeta_{\mathcal{LG}}, \gamma_{\mathcal{LG}})$ belong, when transformed to normal scale, to the exponential family of distributions introduced by Darmais (1936), Koopman (1936) and Pitman (1936). This class of distributions features specific algebraic properties allowing for some simplifications, for instance Bayesian Inference via conjugate priors, see also Nielsen and Garcia (2009).

$$f_X(x) = \frac{\nu(\nu k)^{k-1}}{\Gamma(k_{\mathcal{G}})} e^{-\nu x} \quad x \geq 0 \quad (\text{B.35})$$

$$f_X(x) = 0 \quad x < 0$$

$$\Gamma(k) = \int_0^{\infty} x^{k-1} e^{-x} dx \quad k > 1 \quad (\text{B.36})$$

B.3 Beyond the Frequentist approach: Bayesian inference

Bayesian statistics allow to deal with the vagueness associated with the statistical model by engaging different sources of information. Initial estimates, e. g. based on expert knowledge

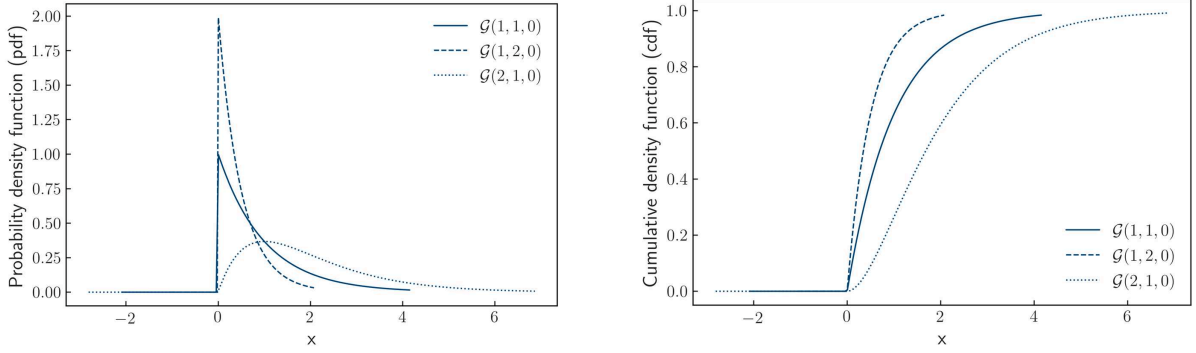


Figure B.4: Probability density function (pdf) and cumulative density function (cdf) of a Gamma distribution.

or previous investigations, can be supplemented by additional data from new measurements through Bayesian inference reducing the parameter uncertainty.

Bayesian statistics rely on a two-level hierarchical model. The second level represents the pdf (*hyperdistribution*) of the distribution parameters (*hyperparameters*), which specify the probability density function at the first level (Ang and Tang, 2007). Let us consider the observed wave loads denoted by X , whose probability function depends on a set of parameters ω , e. g. μ and σ . The prior pdf $f'_\omega(\omega)$ of these parameters is based on previous investigations or expert knowledge. Suppose that additional data x is gathered, for which the likelihood function $Lh(\omega|x')$ is known. The Bayes theorem (Bayes, 1763; Laplace, 1774) states that:

$$f''_\omega(\omega) = \frac{Lh(\omega|x')f'_\omega(\omega)}{\int_\omega Lh(\omega|x')f'_\omega(\omega)d\omega} \quad (\text{B.37})$$

with $f''_\omega(\omega)$ as the posterior pdf of X . $Lh(\omega|x')$, see eq. (B.38), is a measure for the goodness of fit of the pdf to the additional information. It characterises the likelihood of ω given the observations x . The maximum of the likelihood function describes the parameter combination that is most likely to describe the given data.

$$Lh(\omega|x') \propto \prod_{i=1}^n f_{X|\omega}(x_i|\omega) \quad (\text{B.38})$$

Up until a few years ago, computers were not easily accessible. Thus, approaches were developed that allow computing few posterior probability functions by closed-form analytical solutions. The most popular approach comprises the choice of a particular pdf of the prior pdf, given the form of the likelihood. These so-called conjugate priors are in the same pdf family as the posterior pdf, which means that prior and posterior have the same algebraic form, but with different values of the distribution parameters (Raiffa and Schlaifer, 1961).

Nowadays, numerical methods such as Markov Chain Monte Carlo (MCMC) simulations replace the conjugate priors since they impose fewer restrictions on the prior pdf. A Markov process is a special stochastic process that describes a state evolution based on limited knowledge from the past. This means that the transition probabilities from one state to the next are conditionally independent of each other. MCMC simulations employ different sampling algorithms such as Gibbs sampling (Casella and George, 1992; Geman and Geman, 1984) or the

Metropolis-Hastings sampling (Hastings, 1970; Metropolis, Rosenbluth et al., 1953) to specify the transition process (Rubinstein and Kroese, 2016).

C | ADDITIONAL INFORMATION ON FIELD CAMPAIGNS

Table C.1: Traffic regulations at the example canals.

	Permitted velocities		Permitted vessels		
	$T > 1.30 \text{ m}$	$T < 1.30 \text{ m}$	B	L	T
	km h^{-1}	km h^{-1}	m	m	m
DEK-2006	10	12	9.65	95.00	2.70
KuK-2015	8	10	9.65	100.00	2.50
SiK-2007	10	12	10.60	90.00	2.50
			11.40	110.00	2.80
WDK-2007	10	12	11.40	185.00	2.80
			11.45	135.00	2.80
			11.45	186.00	2.80

Table C.2: Description of field measurements: measurement set-up and devices based on measurement reports (IBS, 2006, 2007a,b, 2008a,b, 2015, 2016).

DEK-2006

- **Digital Radar Detection System:** A high-resolution **radar system** of the Furuno type 1403 was used to record vessel velocities and passing distances.
 - **Wave probes:** The recording of the vessel-induced water level fluctuations was carried out with pressure probes from Driesen und Kern. The pressure values were recorded with **5 Hz** and stored with reference to time and ambient temperature. **Two** pressure probes were used at **three** different depths. **One** barometric pressure transducer was positioned on land.
 - **Flow velocity probes:** **One** velocity probe from Nortek was used to measure the flow velocities. The probe recorded a three-dimensional velocity vector with a frequency of **8 Hz**.
-

KuK-2015

- **Vessel parameters:** The recording of vessel name, direction of travel, length, width, draught, passing distance and vessel velocity above ground was conducted from a truck. Each vessel passage was recorded as a **digital image sequence** which was used to determine the vessel's velocity. The passing distances were determined by means of a **distance laser**.
 - **Wave probes:** The recording of the vessel-induced water level fluctuations was carried out with pressure probes from Driesen und Kern. The pressure values, the time and the ambient temperature were recorded with a frequency of **5 Hz** on both bank sides. **Six** pressure probes were installed in pairs at **three** different depths.
-

SiK-2007

- **Digital Radar Detection System:** A high-resolution Furuno-type 1403 **radar system** was used to record vessel velocities and passing distances.
 - **Wave probes:** The recording of the vessel-induced water level fluctuations was carried out with pressure probes from Driesen und Kern. The pressure values were recorded with **2 Hz** and stored with reference to time and ambient temperature. A total of **six** pressure probes were installed in pairs at **three** different depths. **One** barometric pressure transducer was positioned on land. **Two** pressure probes were installed on the left bank and operated with a frequency of **12 Hz**.
 - **Flow velocity probes:** **Two** velocity probes from Nortek AS were used to determine flow velocities. The probes recorded a three-dimensional velocity vector with a frequency of **8 Hz**. The probes were installed on the left bank and in the fairway. It was not possible to install the probes with a defined orientation of the flow components in relation to the canal geometry.
-

WDK-2007

- **Digital Radar Detection System:** A high-resolution Furuno-type 1403 **radar system** was used to record vessel velocities and passing distances.
 - **Wave probes:** The recording of the vessel-induced water level fluctuations was carried out with pressure probes from Driesen und Kern. The pressure values, time and ambient temperature were recorded with a frequency of **4 Hz**. A total of **six** pressure probes were installed in pairs at **three** different depths. **Two** pressure probes were installed on the Northern shore operated with a frequency of **12 Hz**. **Two** barometric pressure transducers were used on land.
 - **Flow velocity probes:** **Five** flow velocity probes from Nortek AS were used to determine the flow velocities. The probes recorded a three-dimensional velocity vector with a frequency of **4 Hz**. Four probes were installed between the centre of the canal and the bottom of the Southern bank; one probe was installed halfway up the Southern bank.
-

D | DOCUMENTATION OF EXPERT INTERVIEWS

This appendix summarises key documents used and obtained from the expert interviews. The original documents were written as well as edited in German and translated into English afterwards.

D.1 Interview guideline

1. Introduction

- Brief personal introduction
- Brief introduction of the research project

'The research project deals, in simple terms, with the exploration and mathematical description of deterioration processes of bank protects (revetment) at German inland waterways. For this purpose, essential damage mechanisms in nature (known from theory) are to be identified and their significance for the occurrence of damage is to be classified. The term "damage" is to be defined in a uniform and practical way.'

Expert interview = first stage of a multi-stage interview procedure

- Explanation of the interview procedure (open interview, on-site inspection)
- Consent to the recording and use of data

Professional background of the interviewee

How long have you been with the WSV? Could you briefly outline your professional career? What were your previous jobs? How long have you been dealing with revetments?

2. Main part of the interview

Traffic

- Vessel traffic of an average week on the waterway (fleet, number of vessels, peak hours)
- Particular observations regarding the driving behaviour (speeding, encounters)
- Estimation of future traffic

Deterioration

- Observation of revetment deterioration on the waterway (methods, intervals, quantity)
- Documentation
- Chain of measures after observation of deterioration
- Sequence of revetment deterioration, description, (schematic/comparable?)
- Time of revetment deterioration (ad hoc → continuous deterioration), causes?
- Damage (quantity, quality) → questioning of questionnaire answers
 1. Displacement of single armour stones
 2. Cliff formation and demolition
 3. Scouring in the water change area
 4. Minor landslides
 5. Deeper landslides / damage to the subsoil / soil displacement
 6. Any other observed damage

Dealing with revetment changes / maintenance measures

- Procedure to deal with revetment deterioration (uniform?)
- Maintenance measures during the last years (minor repairs, major maintenance measures, new construction)
- Long-term revetment deterioration vs. immediate repair measures
- Quantity determination
- Repair measures (damage-related, equal share)
- Maintenance measure (additional armour stones) = indicator for 'damaged area' (damage class?)
- Proactive safeguard measures
- Documentation

Causes of damage

- Main cause of revetment deterioration vs. multiple causes:
 1. Ship-induced impacts
 - a) Waves (pressure fluctuations)
 - b) Ship-induced currents
 - c) Rapid ship-induced water-level decrease
 2. Ship collision / anchorage
 3. Vandalism
 4. Ice pressure
 5. Low quality installation
 6. Any other observed damage
- Questioning of questionnaire answers
- Initial damage
- Ageing process vs. damage as a result of overloading

Terminology of damage

- Definition of damage
- Time of intervention, need for action
- Limit states / risk assessment

Classification of damage

- Classification into damage classes (which, practicable, documentation)
- Scales of damage classification
- In-situ detectable damage classes (drawing, see Figure D.1)
- Tools and auxiliaries for applying a damage classification

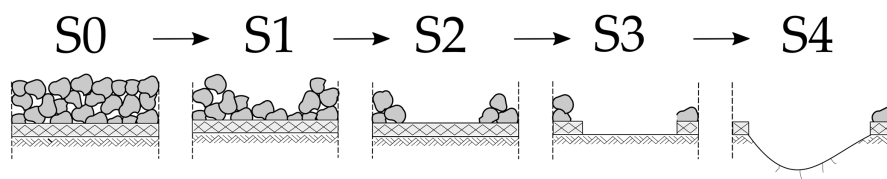


Figure D.1: Potential classification system of revetment damage (MSV, 2015).

- S0 – No change or max. armour layer thickness of $\frac{1}{2}$ of armour stone diameter is eroded.
 S1 – Armour layer thickness of one armour stone diameter is eroded.
 S2 – Filter / geotextile layer is exposed.
 S3 – Filter / geotextile layer is destroyed.
 S4 – Subsoil or seal eroded in decimetre range or more.

3. Site inspection

D.2 Questionnaire

Thank you for taking the time to answer this questionnaire. If you are unsure about any questions, you are welcome to note this on the questionnaire or contact me directly.

Field department, Local Office for Waterways and Shipping: _____

Waterway: _____ Year of construction: _____ Year of expansion: _____

Shipping:

Largest eligible vessel:

L: _____ m B: _____ m T: _____ m Type¹: _____

How many ships passed the waterway in the past year (estimate, if necessary)?

Cargo vessels: _____ Passenger vessels: _____ Leisure boats: _____

Waterway:

Above-ground canal sections: _____ Profile(s) (R-, T-, RT-, KRT-)²: _____

Please enter available information on the revetment construction in Table D.1. If required, you can also enter several construction types. Table D.1 is intended to show the characteristics of the waterway. Please tick the appropriate boxes (x).

Table D.1: Revetment construction.

Layer		Material / Construction (types)		
Amour stones	Armour stone class	_____	_____	_____
	Rock material	_____	_____	_____
Filter layer	Mineral filter	<input type="checkbox"/>	<input type="checkbox"/>	<input type="checkbox"/>
	Geotextile	<input type="checkbox"/>	<input type="checkbox"/>	<input type="checkbox"/>
	No filter	<input type="checkbox"/>	<input type="checkbox"/>	<input type="checkbox"/>
Toe support	Embedded toe	<input type="checkbox"/>	<input type="checkbox"/>	<input type="checkbox"/>
	Toe blanket	<input type="checkbox"/>	<input type="checkbox"/>	<input type="checkbox"/>
	Sheet pile wall	<input type="checkbox"/>	<input type="checkbox"/>	<input type="checkbox"/>
	No filter	<input type="checkbox"/>	<input type="checkbox"/>	<input type="checkbox"/>

¹MS - motor vessel (III), ES - Europaschiff (IV), GMS - large inland cargo vessel (Va), üGMS - extra-long motor cargo vessel (Va), 2SV - pushed barge unit with two lighters (Vb), Sp - leisure boat, FGS - passenger vessel, S - other

²R - rectangular profile, T - trapezoidal profile, RT - rectangular trapezoidal profile, KRT - combined rectangular trapezoidal profile

Damage patterns:

Which of the listed damage patterns can you observe on your waterway in the open track? How often does each of the damage patterns approximately occur? Please classify the damage patterns in Table D.2 using the provided symbols.

- (1) Displacement of single armour stones
- (2) Cliff formation and demolition
- (3) Scouring in the water change area
- (4) Minor landslides
- (5) Deeper landslides / damage to the subsoil / soil displacement
- (6) Any other observed damage: _____

Table D.2: Characteristic damage patterns and their occurrence.

Damage pattern	(1)	(2)	(3)	(4)	(5)	(6)
Occurrence ³						

Causes of damage:

In your opinion, which causes of damage are responsible for revetment damage in the open track? Please classify the damage patterns in Table D.3 using the provided symbols.

- (1) Ship-induced impacts
 - (1.1) Waves (pressure fluctuations)
 - (2.2) Ship-induced currents
 - (3.3) Rapid ship-induced water-level decrease
- (2) Ship collision / anchorage
- (3) Vandalism
- (4) Ice pressure
- (5) Low quality installation
- (6) Any other observed damage: _____

Table D.3: Characteristic causes of damage and their significance.

Causes of damage	(1)	(1.1) ⁴	(1.2)	(1.3)	(2)	(3)	(4)	(5)	(6)
Significance ⁵									

³occurs very often (++) , occurs (+) , occurs rarely (-) , does not occur (-)

⁴If no differentiation is possible, only complete (1).

⁵Main cause of damage (++) , causes damage (+) , may cause damage (-) , has no influence on damage (-)

D.3 Interview excerpts

Definition of damage

- ‘A: To me, damage is something what is not supposed to be. A deviation from the standard. B: Are you sure about that? May I get into this? Considering the term “damage” from the perspective of building inspection or dam inspection, you know, there are different categories. There’s impairment. There’s damage. To me, impairment is not damage. When you talk to people who are in structural inspection and dam inspection, when you use the term damage in dam inspection, it has different implications than in the construction inspection.’ (A1)
- ‘In the field of building inspection, damage is a deviation from the target. And then it always depends on the size of damage.’ (B2)
- ‘Well, if one armour stone is missing, that is no harm to me. Damage occurs when there is a hole where I can see the mineral filter. [...] But if I can see how the revetment is constructed, that’s where the damage starts.’ (C1)
- ‘So, the armour stones, the construction, is no longer there. Scouring. If several armour stones are missing. [...] Now, if I can only see single armour stones left, and I can already see the filter [or fleece] below.’ (D2)
- ‘Damage is when scour occurs, when the armour stones are displaced and whatever damage / defect is present. [...] Damage begins when there are four or five stones missing. [...] Well, there’s no damage, but that’s the beginning.’ (E2)
- ‘Change compared to the surrounding revetment structure in depth and width. For me, this is ultimately change through the displacement of armour stones, bank erosion, which is ultimately visually recognisable. So, if the revetment is not there, as you know it in its original state ...’ (F2)
- ‘To me, damage to the revetment is if the water is no longer slowed down by some kind of armour stones, but if it goes straight on to the sandy slope.’ (G1)
- ‘Damage to the revetment always occurs when the intended structure (armour stone revetment) is disturbed, scoured or slipped.’ (G1)
- ‘Impairment is when one armour stone is missing. I certainly do not pay attention to that. Damage is when I think that it is in need of repair. If there’s a hole in the embankment, I have to have it repaired or do it by myself.’ (H1)
- ‘Flaws in the revetment. If you see that it has collapsed somewhere ...’ (I2)

Classification of damage

- Use of **own damage classification**
- ‘Maybe you have to insert an intermediate stage. With S1, I assume that [...] we will not yet take action as a rule. S2 already shows too much damage.’ (A1)
- **Parallel classification** exists:
 1. S1: 0.1 t/m
 2. S2: 0.2 t/m
 3. S5: 0.5 t/m
- Definition of **own damage classification** according to **risk** depending on the location, A0 - no hazard present, A1 - slight hazard, observe areas, A2 - hazard potential present, A3 - acute hazard potential, immediate action necessary. (D2)

- Damage classes are used for guidance to determine the degree of urgency (E2)
- Damage classification is known, but only used for guidance (F2)

Damage development

- ‘Here it is a slowly but gradually increasing process. [...] But I rather believe that it is because the revetment is already damaged. If the armour stones are no longer stable, surge and waves hit them harder than if they were intact.’ (B2)
- ‘Of course, the armour stones to the left and right slide further and further. The hole gets bigger and bigger in the long run. [...] So, if there is damage, it will increase little by little. That fits. If it started with a 50 cm hole, we will have 2 m to 3 m later. And it’ll grow if we don’t do anything about it.’ (C1)
- ‘That doesn’t happen overnight. It is a long process. It’s getting worse and worse here. You absolutely have to do something about it now. Then it will be recorded, and then the worst areas will be in 2015, 2016 or now 2017 [reworked]. The revetment is not changing that fast. It’s not like everything changes from one day to the next. You have enough time.’ (D2)
- ‘Once the revetment is damaged, the damage progresses faster. The area to be potentially attacked has increased.’ (D2)
- ‘A: This means that at the beginning, you have a small damaged area, a kind of scour, and damage develops from there. Can you observe especially at this location that it progresses faster than elsewhere and then it slowly crumbles from top to bottom? B: That depends on the armour stone classes. With large armour stone classes, nothing happens. [...] Maybe if an angler comes... But the small ones, the ones that have just been installed in the canals, that can happen. The area where the boat pulls the water away, [...], that’s where the most energy is.’ (E2)
- ‘A: If individual stones have shifted, do you observe that the damage also continues to develop in this area, or does it remain rather constant? B: I would say it remains more or less the same. It remains the same, yes.’ (F2)
- ‘Damage moves quickly from S2 to S3; and from S3 to S4 it moves just as quickly. That’s a few weeks.’ (G1)
- ‘Yes, that would propagate in all directions. Widthways, down, up, and then eventually a cliff would develop.’ (H1)
- ‘A: And if you have initial damage, do you observe that it develops further? B: Selectively. [...] We go over the areas every year. It’s not exactly planned now, but we also have to deal with the equipment and people. Approximately, I would say we have 40 km, and we do an area of 7 km to 10 km each year where we go and repair damage. But sometimes, there are 20 damages in almost 10 km, and sometimes there are 80, but it is also possible that they are on 2 m.’ (I2)

Point of intervention

- ‘As a rule of thumb for the bottom, if the area of damage covers more than 50% of the protective layer, from an economic point of view, this is the very latest time that one goes for maintenance. [...] Especially when it comes to underwater construction, it is extremely difficult to ensure that the right quantity and that it [the protective layer] can be laid properly. Contrary to what the field the department says, the point of intervention is when the filter is exposed. No, I would say that the point of intervention is much earlier. When

isolated things are visible, perhaps at S1, when a layer of armour stones has been eroded. Earlier, he said two armour stone layers. One is nonsense.’ (A1)

- ‘If the filter layer is exposed, intervention is required.’ (A1)
- ‘If we have damage, they are immediately filled with hydraulic construction stones. As soon as we see that a row is missing, we will refill it, at the latest when the filter is exposed’, S2 (B2)
- starting from S2: repair, but not urgent (C1)
- S2 - Filter is visible, but depending on the hazard (D2)
- ‘When you see the filter material, then we are too late. I do not want to see that. [...] Well, I would already start here, at least at S2. And here [S3] the geotextile is destroyed. So, I would start at least here at S2, if not at S1.’ (E2)
- ‘Well, I would say from S2 on - I would leave this [everything below] as it is, if at all, from S2 on, ascending from S2 on to S4.’ (F2)
- ‘Within the framework of maintenance, there is a need for action if the entire layer of armour stones slips.’, **starting from S1** (G1)
- ‘I would leave S1 as an observation. But there, [S2] it would be urgent that I do something. If I see that there are some armour stones missing, I can just observe it, I don’t have to do anything, yet.’ (H1)
- ‘It depends on the area affected by damage. If there was damage at 50 m, maybe we’d do something there [S1], too.’ (H1)
- ‘When we see that there are no more armour stones on the slope. We need them against wave impact, because otherwise, the ground is eroded directly. At this point, we would already try to do something. Or at least observe and plan for it.’, S2 (I2)

Monitoring

- ‘We check the track every week. [...] We see if there is large damage, where we have to repair something. But we don’t look if something has changed, if there is one more armour stone displaced.’ (A1)
- Track checks every fortnight, once a week by ship or car in combination with other tasks, depth soundings as an important instrument for damage detection (B2)
- Track inspection by boat every fortnight (C1)
- ‘According to Administrative Regulation 1116 (VV-WSV 1116), we are obliged to conduct these inspection trips once a month. In addition, two night trips per year must be conducted. [...] When the colleagues are outside and there are changes, then they react.’ (D2)
- ‘Based on these damage patterns. The colleagues pass the waterway every day or at least three times a week and then, of course, see where such damage develops. At least once a month, the head of the department also visits the area and looks at critical locations.’ (E2)
- ‘This [damage] is documented monthly.’ (F2)
- Inspection takes place three times a year from the ship, every 14 days by car, once a year by depth sounding (G1)
- ‘I think we regularly check our revetments... Every six months, I would say, by looking at them. We try to pass the shore by boat as close as possible, then you lower the water level slightly and you can look below the initial water level.’, annual depth soundings (H1)
- ‘The one thing is, the colleagues that are on the waterway. Especially the skippers, foremen or so, who are on the water, anyway, come in here and say that they observed something. [...] We walk along the shore, if you are there anyway, then you walk this direction 100 m, that direction 100 m and you notice something. And if someone notices several things, somebody looks at them from the boat and from the shore in detail.’ (I2)

- ‘Well, there is no scheduled building inspection for river bank revetments, not yet.’ (I2)

Maintenance

- ‘The supervisor takes a look at it, tells you how many tons are used, then it’s loaded onto the ships, and the ships, they usually go there on their own, and the master always checks it, of course. And if he thinks that we have to bring some more at this or that place, then we do that too.’ (A1)
- ‘[...] there’s a shovel here, a shovel there. And it’s not every meter, but 200 m, 500 m, there are places like that. But you have to stay on the ball, otherwise it won’t work.’ (B2)
- ‘We have a look at it; if there is a hole somewhere, then we will react.’ (C1)
- ‘First of all, we take a close look at it. If the damage is acute, then there are armour stones dumped directly. We also had that last year on the sheet pile wall. There, we had strong scourings. There, we directly installed 1000 tons of hydraulic construction stones. [...] The maintenance works well in the last few years. They have all been put out to public tender. We make between 4,000 and 9,000 tons.’ (D2)
- ‘When the logging season is over, usually, inspection season starts [...] then you can put together a grab and push boat with a barge and say, go down the track and see where you can find holes or scours and fill them up again ...’ (E2)
- ‘We observe this [damage], and then we will, if it is in an area where we expect a great revision, repair it successively or, in areas where we notice that it is not necessary at all, we leave it to nature.’ (F2)
- ‘We conduct maintenance measures every year. We can easily recognise damage when armour stones have sunk again or slipped away or the edge of the slope has somehow broken away. Then, at some point, it [damage] will look like in the pictures here. And then we would say in a year or two. Depending on how much we get together then. We’ll put it out to tender and then refill again.’ (G1)
- ‘What we repair are mainly damages that are visible to us on the slope. When the damage is [...] only little below water level, we install new armour stones from the shore. If there is damage that’s deeper or wider, we have to think about whether we’ll get an installation device.’ (H1)
- ‘We only do maintenance up to a maximum of 50 tons.’ (H1)
- ‘Then it’s April, May, when we can say, now we can work with armour stones for four, six weeks and add armour stones ...’ (I2)

Time until maintenance measures are required

- ‘It doesn’t have to be done annually, when it comes up, maybe every four or five years, and that is always at certain points, not always at the same place. You could say that we have very specific areas, for example berths and areas resulting from nautical boundary conditions.’ (A1)
- ‘There’s really nothing there for 5 - 10 years, once they’re [the armour stones] lying there.’ (C1)
- ‘During the process of installation, we notice whether the armour stones roll on or whether they are stuck. If they cling to each other. If they lie properly, that’s fine. Otherwise, a layer thicker than 30 cm is installed so that a reasonable revetment is created. Considering the areas that we have built in the last few years, you can also see that the armour stones lie well. There is not much movement.’ (D2)

- ‘Well, you can say that if I notice that there is scour somewhere, you can already observe within one or two years that it will dissolve more and more. After five years, you must have done at least something [...].’ (E2)
 - ‘I believe years, two, three to five years, something like that. It always depends on the location.’ (F2)
 - Public tender and placement of new armour stones every two to three years (G1)
 - ‘They [armour stones] have been doing well for a few years. I would say that if we have normal winters, mild winters, they have been lying easily five to six years [...].’ [before intervention is required] (G1)
 - ‘It depends on the risk assessment. It is an empirical value; colleagues take a closer look at the areas where they say nothing has changed over 10 years. I don’t have to go there this year. The probability is just not very high that something will happen this year. But it is not itemised. It’s not written down. It’s just experience. And the depth sounding that we now get every year shows very clearly where the bottom is changing.’ (I2)
-

Required armour stone quantity

- Estimation of the amount of required armour stones from the boat - approx. 30 locations per year (A1).
 - ‘[...] it would be too much effort to measure it. [...] It is out of all proportion to the cost of the armour stones. [...] and if there are a hundred tons left, you keep them for next year’s maintenance.’ (B2)
 - ‘We measure the holes. Roughly the area required and the thickness of the armour stones, the location [...] And 50 tons more or less - this is not really important. We can store them for later. We go there, determine it by hand and measure the size of the damage with a tape measure. We have an approximate thickness of the layer, and then we determine the volume.’ (C1)
 - Determination of the required armour stone quantity from comparison of target and actual profile (D2)
 - ‘A: As a rule of thumb, you see the damage and then you fill the crane with stones. Roughly, square meters times density multiplied by the layer thickness. B: As the material is lying here at the field department, you can take more than you need. You only dump what you really need.’ (E2)
 - ‘It’s a rule of thumb. Of course, they have a look at the area, and then our colleagues learn. They then fill their deck container with armour stones. Yes, that is perhaps also a matter of experience, what kind of material is needed there.’ (F2)
 - ‘It depends on the feeling. When you see, like the years before, when you put out a public tender, you got there well. At the beginning, you quickly make the mistake of taking the tonnage that is too high. In the course of time, you realise that you don’t need that much to get a decent slope again. And if you’re lucky and get a good company, an excavator driver distributes the stones in a nice way. These are factors that all have to fit together.’ (G1)
 - ‘Experience. We have ordered an annual amount of 2000 to 2500 tons.’ (I2)
-

Documentation

- ‘No, this is clearly too much documentation effort. [...] Documenting would take longer than the actual work.’ (A1)

- Documentation of damage only internally and temporarily for work purposes, **no documentation** of installation measures (B2)
 - ‘We monitor those parts of the track which are badly damaged. Then we will make a technical report [...] Otherwise, we will repack the armour stones on the slope. We order the material we need and fill up the holes.’ (C1)
 - **Damage register** and **installation register**, shore monitoring for the zone of water level fluctuation is updated once or twice a year (D2)
 - ‘And then there are **damage pictures** and you document or photograph the damage.’ (E2)
 - ‘I record damage, also in terms of maps and locations, and where we have made the last repairs. [...] We have an Excel chart with waterway, kilometre range and what we have done there [...]. We document everything in **tables**, but also in **maps**.’ (F2)
 - Documentation is carried out using an Excel chart for larger measures carried out by the field department, **installation register** (G1)
 - ‘Whenever we pass the track and find damaged areas, they are **documented**. But we only indicate the damaged area and estimate the amount of material needed to repair the damage. Then, the damage is fixed with the material we already have on site.’ (H1)
 - ‘[...] a [standardised] building inspection of bank revetments, but the effort is **extraordinary**. [...]. In the field departments, there is basic knowledge available to say, this area is already damaged, I’ll have a look at it. I know there is damage, I am keeping an eye on it, I haven’t seen anything at this location, yet, and something has to be done in this area. That’s the area that’s going to be next.’ (I2)
-

D.4 Sub-categories summarising expert interviews

Table D.4: Matrix of sub-categories summarising the expert interviews.

Category	Waterway category A	Waterway category C
Observations on site	Waterways are in good condition. Damage beyond S1 is rarely or not observed at all.	Waterways are in good, few in a moderate condition. If the waterway is in good condition, damage is rarely observed. If the waterway is in moderate condition, damages are often in the range between S1 and S2. S3 damage can be observed occasionally.
Definition of damage	<ul style="list-style-type: none"> • Uniform understanding of damage: Visually identifiable alterations of the revetment due to armour stone displacement and cliff development. The filter layer or, in the absence of a filter layer, the soil is exposed. • Many of the damage patterns suggested in the questionnaire are rarely observed in nature. • Most frequently, armour stone displacements and cliff development are observed. • Following the current design standards, geotechnical failure is rarely observed. 	
Damage development	In general, initial damage develops into larger damage. A more significant deterioration process can be observed for initially damaged areas.	
Damage classification	<ul style="list-style-type: none"> • Different damage classifications are known in different field departments. In few cases, none of the existing damage classifications is familiar. • The damage classifications are rarely employed in everyday work routines. Occasionally, they serve as guidance to classify the severity of damage. • Two field departments developed their own damage classification, of which one not only accounts for observed damage, but also for potential risks. 	
Point of intervention	The desired intervention time is located slightly before S2. As a rule of thumb, maintenance measures are only conducted when the revetment is in damage class S2, not before. The measures are planned up to three quarters of a year in advance.	The point of intervention ranges between S2 and S3. In the case of moderate damaged revetments, small-scale measures are carried out at short notice.

Category	Waterway category A	Waterway category C
Monitoring	<ul style="list-style-type: none"> • Monitoring is conducted very differently in the various field departments. • There is no dedicated monitoring programme. • As a rule of thumb, the employees and the field engineers of the field departments control the condition of the waterway at regular intervals (at least once a month) and during their daily work. • Depth soundings are carried out annually. 	
Maintenance	<p>Maintenance is a regular process that contributes to retaining good standards of the waterway to date.</p> <ul style="list-style-type: none"> • Repairing usually consists of pulling the stones from bottom to top. • Measures up to approximately 50 t are conducted by the field departments. • The periods, in which maintenance tasks can be carried out, are limited to four to six weeks during the year due to other tasks and boundary conditions, e. g. water level, ecological boundary conditions, etc. • Sooner or later, a maintenance deficit will lead to additional expenditure. 	<p>Maintenance, if necessary, is damage control. In few cases, near-natural bank protection is permitted, e. g. vegetation is not removed.</p>
Time to maintenance	<p>Damage develops and progresses slowly. Accordingly, damage is observed for a long time before an intervention is necessary. The deterioration depends on hydraulic loads and traffic density at the respective waterway, which is captured well by the existing categorisation.</p> <p>Deterioration takes place within a period of five to six years. Subsequently, maintenance should be scheduled. In particular, the transition from S3 to S4 occurs quickly within a few days to weeks.</p>	<p>Damage develops gradually over a longer period of time. Areas in which maintenance has been conducted can be assumed stable for ten to twenty years.</p>
Required armour stone quantity	<ul style="list-style-type: none"> • The quantity of required repair material (tonnage of armour stones) is mainly determined on basis of experiences. The damaged areas are measured by eyesight. An actual measurement is classified as disproportional effort. • Armour stones are usually stored in the field departments. Installation takes place as required and with visual quality assurance. Therefore, it is usually difficult to determine the exact value of the installed quantity. • Every year or on demand, an order for new armour stones is placed via the Local Offices for Waterways and Shipping (WSA). Remaining armour stones are stored temporarily in the field departments and installed in case of damage in the following year. 	

Category	Waterway category A	Waterway category C
Documentation	<ul style="list-style-type: none">• Documentation takes place in a very different manner in different field departments.• In six out of nine field departments, documentation of damage is filed at least temporarily, i. e. as working directive for measures to be executed by the field department.• For all waterways, maintenance sites are documented, if maintenance measures comprise a certain tonnage, and thus, require a public tender.• Locally conducted measures are recorded in two out of nine field departments.• A documentation of damage location before and after maintenance measures is only kept in one out of nine field department. In addition, one out of nine field department keeps a damage and maintenance measures register.• There is currently no central repository of maintenance measures.• A standardised documentation of damage and maintenance measures is considered as disproportionate effort.	

E | CODE DOCUMENTATION

E.1 Models

E.1.1 Hydraulic design

```
def D50(H_Heck, vrueck, methode):  
    '''  
    Model to determine mean armour stone diameter D50 based on GBB (2010)  
    - random character of secondary waves are neglected  
    - stability factors B_B = 2.3 and B_H = 3.0  
    - mean armour stone density RHO_S = 2650 kg/m³  
  
    :H_Heck: probabilistic input variable, dtype = float  
    :vrueck: probabilistic input variable, dtype = float  
    :methode: with or without weighting system,  
    keywords "weight", "vrueck" or "Heck", dtype = str  
  
    :return: calculated mean armour stone diameter D50, rtype = float  
    '''  
  
    #-----#  
    # PART 1: PARAMETER DEFINITION  
    #-----#  
  
    # general  
    G = 9.81  
  
    # water density  
    RHO_W = 1000  
  
    # density and friction angle of armour stones  
    RHO_S = 2650  
    PHI_DH = 45 * 2 * math.pi / 360  
  
    # stability coefficient (GBB(6-1))  
    B_B = 2.3  
    # stability coefficient(GBB(6-2))  
    B_H = 3.0  
    # Izbash factor  
    C_isb = 0.7  
  
    # slope inclination  
    m = 3  
    beta = np.arctan(1 / m)  
  
    # secondary wave height  
    H_Sek = 0.09  
  
    # slope supply flow  
    u_max = 1.25  
  
    #-----#  
    # PART 2: START CALCULATIONS  
    #-----#
```



```

# GBB (6-8)
# slope effect
k_C = (math.cos(beta)*(1-((math.tan(beta)**2) /
                        (math.tan(PHI_DH)**2))))**(0.5))
C_B = 1/k_C

# design against primary waves
# GBB (6-1)
D50_reg = H_Heck / (B_B * ((RHO_S - RHO_W) / RHO_W) * m**(1/3))

# only for transversal stern wave
# GBB (6-2)
D50_Hudson = (H_Heck * C_B) / (B_H * ((RHO_S - RHO_W) / RHO_W))

# design against secondary waves
# GBB (6-1)
D50_reg_Sek = H_Sek / (B_B * ((RHO_S-RHO_W) / RHO_W) * m**(1/3))

# GBB (6-2)
D50_Hudson_Sek = (H_Sek * C_B) / (B_H * ((RHO_S - RHO_W) / RHO_W))

# armour stone size against flow
# only for canals where v_max = v_s
# GBB (6-8)
D50_Strom = (C_isb * C_B * (vrueck**2 / G) *
            (1 / ((RHO_S - RHO_W) / RHO_W)))

# armour stone size against return current velocity
# for canals without natural flow
# GBB (6-10)
D50_Wieder1 = (0.5 * C_B * (u_max**2 / G) * (1 /
            ((RHO_S - RHO_W) / RHO_W)))

# armour stone size against return current velocity
# for canals without natural flow
# GBB (6-11)
D50_Wieder2 = (((u_max**2 * C_B) / (((RHO_S - RHO_W) / RHO_W) * G *
            1.4 * H_Heck**(1/3))))**(3/2))

# determination of maximum armour stone size
max1 = (D50_reg + D50_Hudson + D50_Wieder1 + D50_Wieder2) * (1/4)
max2 = D50_Strom
max3 = (D50_Hudson_Sek + D50_reg_Sek)*(1/2)

# choice of weighing system
if methode == 'weight':
    if max1 > max2 and max1 > max3:
        D50 = max1
    elif max2 > max1 and max2 > max3:
        D50 = max2
    else:
        D50 = max3
    D50_max = D50 * 1000

if methode == 'vrueck':
    D50_max = D50_Strom * 1000
if methode == 'Heck':
    D50_max = (D50_reg + D50_Hudson) * 1000 * 0.5

return(D50_max)

```

E.1.2 Geotechnical design

```

import numpy as np
import math

def model_dD(phi_g, k, z_A, t_A, gamma_B):
    '''
    Model to determine required armour layer thickness based on GBB (2010)

    :phi_g: friction angle of soil, dtype = float
    :k: hydraulic conductivity of soil, dtype = float
    :z_A: drawdown height, dtype = float
    :t_A: drawdown time, dtype = float
    gamma_B: unit weight of soil, dtype = float

    :return: required armour layer thickness, rtype = float
    '''

    #-----#
    # PART 1: PARAMETER DEFINITION
    #-----#

    # d_dist = 0.6 # armour stone layer in-situ

    m = 3      # slope inclination
    G = 9.81   # gravity
    # h_w = 3.55 # still water level

    # pore pressure parameter
    GAMMA_W = 10.0 # unit weight water
    A = 1       # pore pressure parameter
    TAS = 5.0   # standard Koehler time

    # soil and armour stone characteristics
    c = 0 # cohesion
    RHO_S = 2650 # density armour stones

    # filter layer
    GAMMA_FF = 19 # unit weight filter layer
    d_F = 0.0 # layer thickness filter

    TAU_A = 0 # shear strength of toe and suspension
    TAU_F = 2

    #-----#
    # PART 2: START OF CALCULATION
    #-----#

    gamma = gamma_B
    beta = np.arctan(1 / m)

    # Gilt nur bei Kornfilter
    gamma_F = GAMMA_FF - GAMMA_W
    gamma_S = RHO_S * G / 1000
    gamma_D = (1.0 - n) * (gamma_S - GAMMA_W)

```

```

phi = phi_g * 2.0 * math.pi / 360

# Determination of pore pressure
# GBB (7-5)
bs = 0.166 * (k**(-0.327))

# GBB (7-4)
b = bs * ((TAS / t_A)**(1/2))

# critical depth (slope sliding)
# GBB (7-7)
d_krit = ((1.0 / b) * np.log((math.tan(phi) * GAMMA_W * z_A * b) /
                           (math.cos(beta) * gamma * (math.tan(phi) - math.tan
                           (beta))))))

# critical depth (liquefaction)
# GBB (7-12)
d_kritB = (1.0 / b) * np.log((GAMMA_W * z_A * b) / (gamma * math.cos(beta)))

# pore pressures at critical depth
# GBB (7-3)
u_abg = GAMMA_W * z_A * (1.0 - a * np.exp(-b * d_krit))

# GBB (7-3)
u_hyd = GAMMA_W * z_A * (1.0 - a * np.exp(-b * d_kritB))

# toe support
# GBB (7-14)
# tau_F = (((0.5*d_F**2 * gamma_F + (d_ist * d_F + 0.5 * d_ist ** 2.0) * gamma_D
           ) * np.tan(phi_D) * np.cos(beta)) / ((
           np.cos(beta) - np.sin(beta) * np.tan(
           phi_D)) * (h_w - z_A)))

# required unit weight against slope sliding
# GBB (7-9)
g_abg = ((u_abg * math.tan(phi) - c - TAU_F - TAU_A) /
         (math.cos(beta) * math.tan(phi) - math.sin(beta)) -
         (gamma_F * d_F + gamma * d_krit))

# required unit weight against liquefaction
# GBB (7-11)
g_hyd = (u_hyd / math.cos(beta)) - (gamma_F * d_F + gamma * d_kritB)

# required unit weight
g_D_erf = max(g_abg, g_hyd)

d_erf = g_D_erf / gamma_D
return(d_erf)

```

E.2 Addressing statistical uncertainty

E.2.1 Bootstrapping

```
import numpy as np
```

```

import scipy.stats as stats
import pandas as pd

def Bootstrap(parameter, log=False, norm=False):
    '''
    Bootstrapping with increasing number of samples

    :parameter: measurement data, dtype = np.array
    :log, norm: distribution type, dtype = bool
    :returns a number of characteristic values for the sampled distributions,
    rtype = pd.DataFrame
    '''

    results = {}
    no_samples = [10, 20, 50, 75, 100, 250, 500, 750, 1000, 1500, 2000]

    for samples in no_samples:
        mean = [] # mean of sample
        std = [] # standard deviation of sample
        mu = [] # distribution parameter
        sigma = [] # distribution parameter
        skewness = [] # skewness of fitted distribution
        kurtosis = [] # kurtosis of fitted distribution
        quantile_90 = [] # quantile of sample
        quantile_95 = [] # quantile of sample

        if log:
            for i in range(5000):
                sample = np.random.choice(parameter, size=samples, replace=False)
                mu_log = (np.log(sample)).mean()
                sigma_log = (np.log(sample)).std()
                skewness_log = stats.skew(sample, bias=False)
                kurtosis_log = stats.kurtosis(sample, fisher=True, bias=False)

                # scipy fit
                fitting_params_lognormal = stats.lognorm.fit(sample,
                                                              floc=0,
                                                              scale=mu_log)

                quantile_log_90 = np.quantile(sample, 0.9,
                                              interpolation='midpoint',
                                              overwrite_input=False)
                quantile_log_95 = np.quantile(sample, 0.95,
                                              interpolation='midpoint',
                                              overwrite_input=False)

                mean.append(np.exp(mu_log))
                std.append(sigma_log)
                skewness.append(skewness_log)
                kurtosis.append(kurtosis_log)
                quantile_90.append(quantile_log_90)
                quantile_95.append(quantile_log_95)
                sigma.append(fitting_params_lognormal[0])
                mu.append(fitting_params_lognormal[2])

        if norm:
            for i in range(5000):
                sample = np.random.choice(parameter, size=samples, replace=False)
                mu_norm = sample.mean()
                sigma_norm = sample.std()
                skewness_norm = stats.skew(sample, bias=False)
                kurtosis_norm = stats.kurtosis(sample, fisher=True, bias=False)

```

```

# scipy fit
fitting_params_normal = stats.norm.fit(sample, mean=mu_norm)
quantile_norm_90 = np.quantile(sample, 0.9,
                                interpolation='midpoint',
                                overwrite_input=False)
quantile_norm_95 = np.quantile(sample, 0.95,
                                interpolation='midpoint',
                                overwrite_input=False)

mean.append(mu_norm)
std.append(sigma_norm)
skewness.append(skewness_norm)
kurtosis.append(kurtosis_norm)
quantile_90.append(quantile_norm_90)
quantile_95.append(quantile_norm_95)
mu.append(fitting_params_normal[0])
sigma.append(fitting_params_normal[1])

results.update({'mean_' + str(samples): mean,
               'std_' + str(samples): std,
               'skewness_' + str(samples): skewness,
               'kurtosis_' + str(samples): kurtosis,
               'quantile90_' + str(samples): quantile_90,
               'quantile95_' + str(samples): quantile_95,
               'mu_dist_' + str(samples): mu,
               'sigma_dist_' + str(samples): sigma})

df = pd.DataFrame.from_dict(results)
return(df)

```

E.2.2 Stability analysis

```

import math
import numba
import numpy as np

@numba.jit(nopython=True)
def StabilityAnalysis(no_samples, shape_mean_Heck, shape_std_Heck,
                    scale_mean_Heck, scale_std_Heck, shape_mean_vrueck,
                    shape_std_vrueck, scale_mean_vrueck, scale_std_vrueck,
                    Heck, vrueck):
    """
    Stability analysis to determine D50 under uncertainty for different
    sample sizes

    :shape_mean_Heck, vrueck: mean of sigma for different sample sizes
    (HuHeck, vrueck), dtype = list
    :shape_std_Heck, vrueck: std of sigma for different sample sizes
    (HuHeck, vrueck), dtype = list
    :scale_mean_Heck, vrueck: mean of mu for different sample sizes
    (HuHeck, vrueck), dtype = list
    :scale_std_Heck, vrueck: std of mu for different sample sizes
    (HuHeck, vrueck), dtype = list
    :Heck, vrueck: parameter of uncertainty consideration, dtype=bool

    return:

```

```

:result, rtype = np.array
'''

# initialize result array
result = np.zeros((11, 5000, 5000), dtype = np.float64)

for it in range(0, len(no_samples)):
    if Heck:
        # sample distribution parameters
        mu_sample_Heck = np.random.normal(scale_mean_Heck[it],
                                          scale_std_Heck[it], 5000)

        sigma_sample_Heck = np.random.normal(shape_mean_Heck[it],
                                             shape_std_Heck[it], 5000)

    if vrueck:
        # sample distribution parameters
        mu_sample_vrueck = np.random.normal(scale_mean_vrueck[it],
                                             scale_std_vrueck[it], 5000)

        sigma_sample_vrueck = np.random.normal(shape_mean_vrueck[it],
                                                shape_std_vrueck[it], 5000)

# no of Monte-Carlo simulations for distribution parameters
for i in range(0, 5000):
    if Heck and not vrueck:
        if mu_sample_Heck[i] <= 0 or sigma_sample_Heck[i] <= 0:
            continue

        # no of MC simulations for wave height, without weighing
        c = sigma_sample_Heck[i] / mu_sample_Heck[i]
        std_log_Heck = np.sqrt(np.log(1 + c ** 2))
        mean_log_Heck = np.log(mu_sample_Heck[i]) - 0.5 * std_log_Heck ** 2
        sample_param = np.random.lognormal(np.log(mu_sample_Heck[i]),
                                           sigma_sample_Heck[i], 5000
                                           )

        num_2 = 0
        for j in sample_param:
            result[it][i][num_2] = D50(j, 0.9, methode='Heck')
            num_2 = num_2 + 1
    elif vrueck and not Heck:
        if mu_sample_vrueck[i] <= 0 or sigma_sample_vrueck[i] <= 0:
            continue

        # no of MC simulations for wave height, without weighing
        num_2 = 0
        sample_param = np.random.normal(mu_sample_vrueck[i],
                                       sigma_sample_vrueck[i],
                                       5000)

        for j in sample_param:
            result[it][i][num_2] = D50(0.4, j, methode='vrueck')
            num_2 = num_2 + 1
    elif vrueck and Heck:
        # no of MC simulations for wave height and vrueck,
        # weighing of GBB (2010) employed
        if mu_sample_Heck[i] <= 0 or sigma_sample_Heck[i] <= 0 or
           mu_sample_vrueck[i] <= 0
           or sigma_sample_vrueck[i]
           <= 0:

            continue # continue here

        c = sigma_sample_Heck[i] / mu_sample_Heck[i]
        std_log_Heck = np.sqrt(np.log(1 + c ** 2))
        mean_log_Heck = np.log(mu_sample_Heck[i]) - 0.5 * std_log_Heck ** 2
        sample_param_Heck = np.random.lognormal(mean_log_Heck, std_log_Heck,
                                                5000)

```

```

        sample_param_Heck = np.random.lognormal(np.log(mu_sample_Heck[i]),
                                                sigma_sample_Heck[i], 5000
                                                )
        sample_param_vrueck = np.random.normal(mu_sample_vrueck[i],
                                                sigma_sample_vrueck[i],
                                                5000)

        num_2 = 0
        for sample_Heck, sample_vrueck in zip(sample_param_Heck,
                                                sample_param_vrueck):
            result[it][i][num_2] = D50(sample_Heck, sample_vrueck, methode=
                                        'weight')

            num_2 = num_2 + 1

    return(result)

@numba.jit(nopython=True)
def ProbFailure(no_samples, shape_mean_Heck, shape_std_Heck,
                scale_mean_Heck, scale_std_Heck, shape_mean_vrueck,
                shape_std_vrueck, scale_mean_vrueck, scale_std_vrueck,
                Heck, vrueck, D50_mean):
    '''
    Determines the probability of failure for different sample sizes
    and, thus, distributions of different variability

    :no_samples: sample size, dtype = int
    :shape_mean_Heck, vrueck: mean of sigma for different sample sizes
    (HuHeck, vrueck), dtype = list
    :shape_std_Heck, vrueck: std of sigma for different sample sizes
    (HuHeck, vrueck), dtype = list
    :scale_mean_Heck, vrueck: mean of mu for different sample sizes
    (HuHeck, vrueck), dtype = list
    :scale_std_Heck, vrueck: std of mu for different sample sizes
    (HuHeck, vrueck), dtype = list
    :Heck, vrueck: parameter of uncertainty consideration, dtype = bool
    :D50_mean: mean armour stone diameter in mm, dtype = float

    return:
    :result, rtype = np.array
    '''

    # initialize result array
    result = np.zeros((11, 5000, 5000), dtype = np.float64)

    for it in range(0, len(no_samples)):
        if Heck:
            # sample distribution parameters
            mu_sample_Heck = np.random.normal(scale_mean_Heck[it],
                                              scale_std_Heck[it], 5000)

            sigma_sample_Heck = np.random.normal(shape_mean_Heck[it],
                                                 shape_std_Heck[it], 5000)

        if vrueck:
            # sample distribution parameters
            mu_sample_vrueck = np.random.normal(scale_mean_vrueck[it],
                                                scale_std_vrueck[it], 5000)

            sigma_sample_vrueck = np.random.normal(shape_mean_vrueck[it],
                                                  shape_std_vrueck[it], 5000)

        # no of Monte-Carlo simulations for distribution parameters
        for i in range(0, 5000):

```

```

sample_D50 = np.random.normal(D50_mean, 12, 5000)
if Heck and not vrueck:
    # no of MC simulations for wave height, without weighing
    sample_param = np.random.lognormal(np.log(mu_sample_Heck[i]),
                                       sigma_sample_Heck[i], 5000)

    num_2 = 0
    for j in sample_param:
        result[it][i][num_2] = D50(j, 0.9, methode='Heck') - sample_D50[
            num_2]

        num_2 = num_2 + 1
elif vrueck and not Heck:
    # no of MC simulations for wave height, without weighing
    num_2 = 0
    sample_param = np.random.normal(mu_sample_vrueck[i],
                                    sigma_sample_vrueck[i],
                                    5000)

    for j in sample_param:
        result[it][i][num_2] = D50(0.4, j, methode='vrueck') -
            sample_D50[num_2]

        num_2 = num_2 + 1
elif vrueck and Heck:
    # no of MC simulations for wave height and vrueck,
    # weighing of GBB (2010) employed
    sample_param_Heck = np.random.lognormal(np.log(mu_sample_Heck[i]),
                                             sigma_sample_Heck[i], 5000
                                             )

    sample_param_vrueck = np.random.normal(mu_sample_vrueck[i],
                                            sigma_sample_vrueck[i],
                                            5000)

    num_2 = 0
    for sample_Heck, sample_vrueck in zip(sample_param_Heck,
                                          sample_param_vrueck):
        result[it][i][num_2] = D50(sample_Heck, sample_vrueck, methode=
            'weight') -
            sample_D50[num_2]

        num_2 = num_2 + 1

return(result)

```

E.3 Addressing transformation uncertainty

E.3.1 Model factor

```

import numpy as np
import statsmodels.api as sm
import scipy.stats as stats
import pandas as pd

def modelfactor(whdb, bmf):
    """
    Determines model factor for different variables
    :df_whdb: measured data from wave height database, dtype = pd.DataFrame
    :df_bmf: calculated data from bmf-Tool, dtype = pd.DataFrame
    :name: name of dataset, dtype = str
    """

```



```

'''
# calculated values
param_bmf = ['H_uHeck', 'v_rueckBug', 'v_rueckHeck', 'u_max',
            'z_a,B', 'z_a,H', 't_a,B', 't_a,H']
# measured values
param_whdb = ['H_u,Heck', 'v_Rück,Ufer', 'v_Rück,Ufer', 'v_Wiederauffüllung',
            'z_a,Bug', 'z_a,Heck', 't_a,B', 'T_a,H']
# campaigns
name_w = ['DEK-2006', 'KuK-2015', 'SiK-2007', 'WDK-2007']

# check nan values
dicts = {}
for param_w, param_b, lab in zip(param_whdb, param_bmf):

    param = [] # regression parameter
    lower = [] # lower confidence interval of regression
    upper = [] # upper confidence interval of regression
    R2 = [] # coefficient of determination
    nobs = [] # number of observations

    for name, df_whdb, df_bmf in zip(name_w, whdb, bmf):
        if df_whdb[param_w].isna().sum() / len(df_whdb[param_w]) < 0.5:
            f1 = sm.OLS(np.array(df_whdb[param_w]), np.array(df_bmf[param_b]),
                        missing='drop')
            result1 = f1.fit()
            conf = result1.conf_int(0.05)
            param.append(result1.params[0])
            lower.append(conf[0, 0])
            upper.append(conf[0, 1])
            R2.append(result1.rsquared)
            nobs.append(result1.nobs)

        else:
            param.append(np.nan)
            lower.append(np.nan)
            upper.append(np.nan)
            R2.append(np.nan)
            nobs.append(np.nan)

    dicts.update({param_b + '_m': param,
                  param_b + '_lower': lower,
                  param_b + '_upper': upper,
                  param_b + '_R2': R2,
                  param_b + '_nobs': nobs})

results = pd.DataFrame.from_dict(dicts, orient='columns')
return(results)

def GeneralisedModelFactor(df_whdb, df_bmf):
'''
Regression of to determine model factor statistics
:df_whdb: measured data from wave height database for the different
waterways, dtype = list
:df_bmf: calculated data from bmf-Tool for the different
waterways, dtype = list
results: regression parameters a, b, xi and R2, rtype=pd.DataFrame
'''

param_bmf = ['H_uHeck', 'v_rueckBug', 'v_rueckHeck', 'u_max',

```

```

        'z_a,B', 'z_a,H', 't_a,B', 't_a,H']
param_whdb = ['H_u,Heck', 'v_Rück,Ufer', 'v_Rück,Ufer', 'v_Wiederauffüllung',
              'z_a,Bug', 'z_a,Heck', 't_a,B', 'T_a,H']
name_w = ['DEK-2006', 'KuK-2015', 'SiK-2007', 'WDK-2007']

dicts = {}

for param_w, param_b in zip(param_whdb, param_bmf):
    a = []
    b = []
    std = []
    R2 = []
    for canal_bmf, canal_whdb, name in zip(df_bmf, df_whdb, name_w):
        if canal_whdb[param_w].isna().sum() / len(canal_whdb[param_w]) < 0.5:
            X = sm.add_constant(np.log(np.array(canal_bmf[param_b])))
            model = sm.OLS(np.log(np.array(canal_whdb[param_w])), X, missing='drop')
            result = model.fit()
            N = result.nobs
            list(x_nan.reshape(len(x_nan)))
            list(x_nan.reshape(len(x_nan)))
            y_new = result.predict(sm.tools.add_constant(np.log(np.array(
                canal_bmf[param_b])))
            std_err = np.sqrt( (np.nansum(((y_new) - np.log(np.array(canal_whdb[
                param_w]))) **2) / N) )

            std.append(std_err)
            a.append(result.params[0])
            b.append(result.params[1])
            R2.append(result.rsquared)
        else:
            a.append(np.nan)
            b.append(np.nan)
            std.append(np.nan)
            R2.append(np.nan)
    Q = canal_whdb[param_w] / canal_bmf[param_b]
    dicts.update({param_b + '_a': a,
                  param_b + '_b': b,
                  param_b + '_std': std,
                  param_b + '_R2': R2})

results = pd.DataFrame.from_dict(dicts, orient='columns')
return(results)

def FactorStatistics(df):
    '''
    Calculates model factor statistics
    :df: regression parameters (a, b, xi), dtype = pd.DataFrame

    :results: mu and sigma of model factor, rtype = pd.DataFrame
    '''

    param_bmf = ['H_uHeck', 'v_rueckBug', 'v_rueckHeck', 'u_max',
                 'z_a,B', 'z_a,H', 't_a,B', 't_a,H']

    results = pd.DataFrame()

    for param_b in param_bmf:
        mu = np.exp(df[param_b + '_a'] + 0.5 * df[param_b + '_std'] ** 2)
        sigma = np.sqrt(mu ** 2 * (np.exp(df[param_b + '_std'] ** 2) - 1))
        results[param_b + '_mu'] = mu
        results[param_b + '_sigma'] = sigma

```

```

    results[param_b + '_b'] = df[param_b + '_b']
    return(results)

```

E.4 Addressing spatial variability

E.4.1 Infinite slope model

```

import math
import numpy as np
import pandas as pd
import RandomField as rf
import NumericalModel as NumModel

# %%
class InfiniteSlope():
    """
    class to evaluate several features of an infinite
    slope such as
    - slope stability and
    - dkrit

    :phi_mean: mean friction angle [°], dtype = float
    :k_mean: mean hydraulic conductivity [m/s], dtype = float
    :za: drawdown height in m, dtype = float
    :ta: drawdown time in s, dtype = float
    :gamma_b: unit weight under buoyancy in kN/m³, dtype = float
    :layer: layer thickness in m, dtype = float
    """

    def __init__(self, phi_mean, k_mean, za, ta, gamma_b, layer):

        # -----
        # PART 1.0: Initialize general parameter
        # -----

        self.k_mean = k_mean          # hydraulic conductivity
        self.phi_random = phi_mean * math.pi / 180    # friction angle in degree
        self.phi_mean = phi_mean      # friction angle in degree
        self.gamma_b = gamma_b        # unit weight under buoyancy
        self.gamma_s = 26.5           # unit weight armour stones
        self.beta = (18.43 * math.pi / 180)    # slope angle
        self.layer = layer            # layer thickness

        self.za = za                 # drawdown height
        self.ta = ta                 # drawdown time
        self.gamma_w = 10            # unit weight water

        self.depth = 5                # depth

    # -----
    def StabilityAnalysis(self, theta=1, phi_cov=0, k_cov=0,
                        method='cholesky', path='',
                        save=False, phi_r=False, k_r=False):
        """

```

```

Slope stability analysis following the notation of
Zhou, A., Li, C.-Q. and Huang, J. (2016)

:theta: correlation length of random variable in m, dtype = float
:phi_cov: coefficient of variance of friction angle, default=0,
dtype = float
:k_cov: coefficient of variance of hydraulic conductivity,
default=0, dtype = float
:method: method of random field generation, either 'cholesky' or
'eigenvalues', dtype = str
:path: file, the results are saved to, dtype = str
:save: save / not save, dtype = bool
:phi, k: variable to vary, dtype = bool
'''

# -----
# PART 1.1: Initialize parameter
# -----

# random field parameters
r_length = 5
r_nnode = 501
r_nfield = 500

y_i = 0.01          # size of one slice

# depth for infinite slope analysis
z = np.arange(y_i, (self.depth + y_i), y_i)

# Monte-Carlo parameter
no_mc = 10
d_GBB = np.zeros(no_mc)
G_min = np.zeros(no_mc)
u_G_min = np.zeros(no_mc)
df_collection = {}

# -----
# PART 1.2: Initialize random fields
# -----
field = rf.RandomField(length=r_length, npoint=r_nnode,
                       nfield=r_nfield, method=method)
field.IniRandomField(theta=theta)

# -----
# PART 1.3: Initialize numerical model
# -----
model = NumModel.Montenegro(k_mean=self.k_mean, ta=self.ta, za=self.za)

# -----
# PART 2.1: Begin infinite slope calculations
# -----
ov = self.gamma_b * z + (self.gamma_s - self.gamma_w) * 0.45 * self.layer

# shear stress
tau_1 = ov * math.sin(self.beta) * math.cos(self.beta)

# -----
# PART 2.2: Start Monte-Carlo for random parameters
# -----
for j in range(0, no_mc):
    if phi_r:

```

```

# create random field
phi = field.CreateRandomField(mean=self.phi_mean, cov=phi_cov)
self.phi_random = np.exp(phi[1:501, 0]) * math.pi / 180

if k_r:
    # create random field
    k = field.CreateRandomField(mean=self.k_mean, cov=k_cov)
    self.k_random = np.exp(k[:, 0])

    # run
    delta_u_mesh, z_u = model.RunModel(rfield=self.k_random,
                                       r_length=r_length,
                                       r_nnode=r_nnode,
                                       random=True)
else:
    delta_u_mesh, z_u = model.RunModel(random=False)

# demesh
delta_u = model.Demesh(z)

# shear strength
tau_2 = ((ov * math.cos(self.beta) ** 2 - delta_u)
         * np.tan(self.phi_random))

# -----
# PART 2.3: Minimum to determine critical depth
# -----
G = tau_2 - tau_1
index_d_GBB = np.argmin(G)
G_min[j] = np.min(G)
u_G_min[j] = delta_u[index_d_GBB]
d_GBB[j] = z[index_d_GBB]

# -----
# PART3: Post-processing
# -----
results = {'tau_1': tau_1,
          'tau_2': tau_2,
          'G': G,
          'z': z,
          'delta_u': delta_u}

if (j % 100 == 0):
    df_collection.update({'df' + str(j)}: results)

    if save:
        df = pd.DataFrame.from_dict(results, orient='columns')
        df.to_csv((path + '_' + str(j) + '.txt'))
        if k_r:
            np.save((path + '_k_random_' + str(j)), self.k_random,
                   allow_pickle=True)
        if phi_r:
            np.save((path + '_phi_random_' + str(j)),
                   self.phi_random,
                   allow_pickle=True)

np.save(path + '_d_krit', d_GBB, allow_pickle=True)
np.save(path + '_LimitState', G_min, allow_pickle=True)
np.save(path + '_u_G_min', u_G_min, allow_pickle=True)

return(df_collection, d_GBB, G_min)

```

E.4.2 Excess pore pressure model

```

import numpy as np
import RandomField as rf

#-----#
# Author: WaiChing Sun [steve.sun@u.northwestern.edu] #
# Purpose: solve one dimensional consolidation problem via mixed FEM #
# Last Update 3/6/2009 #
#-----#
# Hector Montenegro 16.03.2014
# Adjustment to consider transient p-boundary condition on top
#-----#
# Julia Sorgatz 25.09.2019
# Adjustment to work in Python and account for
# random hydraulic conductivity
#-----#

class Montenegro():
    ''' Determine excess pore pressure from drawdown
    :k: hydraulic conductivity [m/s], dtype = float
    :ta: drawdown time [s], dtype = float
    :za: drawdown height [m], dtype = float
    :depth: depth of numerical simulation [m], dtype = float
    '''

    def __init__(self, k_mean=5e-4, ta=5, za=0.6):

        #-----#
        # PART 1: ASSEMBLY PHASE
        #-----#

        # discretize time domain
        duration = ta
        self.dt = 1.e-1 * duration
        self.nstep = round(duration / self.dt)

        depth = 5

        self.nnode = 1001
        self.y = np.linspace(0, depth, self.nnode)

        # element data
        self.nelem = int((self.nnode-1) / 2)
        self.z=self.y[0:self.nnode:2]

        # hydrostatic assuming a water colum H above the topmost node
        self.H = self.y[self.nnode-1]
        self.WS = 5

        self.k_mean = k_mean

        self.Kf = 2.8e3 # [kPa]
        self.poro = 0.45 # [-]
        self.gamma = 10. # [kN/m³]

```

```

self.B_skemp = 0.01
# hydraulic conductivity
k_1 = np.full((int(self.nelem * 0.9), 1), k_mean)
k_2 = np.full((int(self.nelem * 0.1), 1), k_mean)
self.khydr = np.concatenate((k_1, k_2), axis=0)

# constrained modulus [kN/m2]
self.E = self.Kf / self.poro * (1 - self.B_skemp) / self.B_skemp

# drawdown
self.dh = -za      # head drop -> negative sign

def Map(self, rfield, r_length, r_nnode):
    '''Maps random variables on numerical model
    :rfield: random field
    :r_length: length of the generated random field
    :r_nnode: number of nodes in the random field

    :k_random: random variables mapped on the numerical elements,
    dtype = 1D-array
    '''

    z_random = np.linspace(0., r_length, r_nnode)
    k_random = np.interp(self.z, z_random, rfield)
    return(k_random[1:])

def RunModel(self, rfield=0, r_length=0, r_nnode=0, random=False):
    '''Runs numerical model
    :rfield: random field
    :r_length: length of the generated random field
    :r_nnode: number of nodes in the random field
    :random: integration of random fields, default=False, dtype = bool

    :output: excess pore pressures at the last time step, dtype = 1D-array
    :z: depths corresponding to the excess pore pressures, dtype = 1D-array
    '''

    if random:
        # -----
        # PART 1.2: Initialize random fields
        # -----

        self.khydr = self.Map(rfield, r_length, r_nnode)

    # initialize hydraulic results
    pprof = np.array([self.WS+self.H-self.y[0:self.nnode:2]]).reshape(self.nelem
+1)
    hpot = np.zeros([self.nelem+1, 1])      # initialize hydraulic head row-
vector [L]
    hgrad = np.zeros([self.nelem+1, 1])     # initialize hydraulic gradient row-
vector [-]
    topdisp = np.zeros([1, 1])

    # create element stiffness
    ke = np.zeros([3, 3, self.nelem])
    ge = np.zeros([3, 2, self.nelem])
    te = np.zeros([2, 2, self.nelem])
    phi_e = np.zeros([2, 2, self.nelem])

    for j in range(1, self.nelem+1):

```

```

ly = np.zeros(3)
ly[0] = self.y[j-1]
ly[2] = self.y[j+1]
le = abs(ly[2] - ly[0])

# solid stiffness
ke[:, :, (j-1)] = self.E / 3.0 / le * np.array([[7, -8, 1],
                                                [-8, 16, -8],
                                                [1, -8, 7]])

# coupling term
ge[:, :, (j-1)] = 1.0 / 6.0 * np.array([[5, 1],
                                         [-4, 4],
                                         [-1, -5]])

te[:, :, (j-1)] = (-le * self.poro / 6.0 / self.Kf *
                  np.array([[2, 1],
                             [1, 2]]))
                  - self.khydr[(j-1)] / self.gamma / le * self.dt *
                  np.array([[1, -1],
                             [-1, 1]]))

# fluid diffusion term 2
phi_e[:, :, (j-1)] = -le * self.poro / 6.0 / self.Kf * np.array([[2, 1],
                                                                    [1, 2]])

# assemble global matrice
K = np.zeros([self.nnode, self.nnode])
G = np.zeros([self.nnode, self.nelem+1])
T = np.zeros([self.nelem+1, self.nelem+1])
PHI = np.zeros([self.nelem+1, self.nelem+1])
# initialize p-boundary
Pbound = np.zeros([self.nnode + self.nelem - 1])

for j in range(1, self.nelem+1):
    K[(j*2-2):(j*2+1), (j*2-2):(j*2+1)] = (
        K[(j*2-2):(j*2+1), (j*2-2):(j*2+1)] + ke[:, :, (j-1)])

    G[(j*2-2):(j*2+1), (j-1):(j+1)] = (
        G[(j*2-2):(j*2+1), (j-1):(j+1)] + ge[:, :, (j-1)])

    T[(j-1):(j+1), (j-1):(j+1)] = (
        T[(j-1):(j+1), (j-1):(j+1)] + te[:, :, (j-1)])

    PHI[(j-1):(j+1), (j-1):(j+1)] = (
        PHI[(j-1):(j+1), (j-1):(j+1)] + phi_e[:, :, (j-1)])

K_1 = np.concatenate((K, G), axis=1)
K_2 = np.concatenate((np.transpose(G), T), axis=1)
K_eff = np.concatenate((K_1, K_2), axis=0)

# delete DOF of essential boundary conditions
# reduce degree of freedom for pressure bc on top
# column of global matrix corresp to bc node on top
Pbound = (K_eff[1:(self.nnode+self.nelem),
               self.nnode+self.nelem]).reshape(self.nnode+self.nelem-1, 1)

A = K_eff[1:(self.nnode+self.nelem), 1:(self.nnode+self.nelem)]
Ainv = np.linalg.inv(A)

```



```

F_ext = np.concatenate((np.transpose(G), PHI), axis=1)
B = F_ext[0:self.nelem, 1:(self.nnnode+self.nelem)]

# assemble initial global F
F = np.zeros([self.nnnode+self.nelem-1, 1])

#-----#
# PART 2: SOLVER
#-----#

# define solution space
d = np.zeros([(self.nnnode-1), self.nstep])
p = np.zeros([self.nelem, self.nstep])
#  $p(:,1) = -K_f/poro * sig / (K_f/poro + E) * ones(nelem,1)$ ;
curtime = np.zeros(self.nstep)

#  $F(nnnode-1,1) = sig$ ; % for (instantaneous) steady state b
# initialize time-dependent source term
f_t = np.zeros([self.nelem, self.nelem])
curtime[self.nstep-1] = self.dt
zero_pressure = np.zeros([1, self.nstep])

for i in range(0, self.nstep-1):
    curtime[i] = self.dt * i / (self.nstep)

    # update force
    f_t = np.dot(B, (np.concatenate((d[:, i], p[:, i]), axis=0)))
    F[(self.nnnode-1):(self.nnnode+self.nelem), 0] = f_t

    pbc = self.dh * self.gamma * (i+1) / (self.nstep-1)

    # load from rising head on top
    F[self.nnnode-2, 0] = -pbc

    # multiply known pressure-bcon Pbound and bring to the
    # right hand vector F
    F = F - Pbound * pbc
    zero_pressure[0, i+1] = pbc

    sol = np.dot(Ainv, F)
    d[:, i+1] = (sol[0: self.nnnode-1]).reshape(self.nnnode-1) # solid
                                                                displacement
    p[:, i+1] = (sol[(self.nnnode-1):(self.nnnode+self.nelem)]).reshape(self.
                                                                nelem) # excess pore
                                                                pressure
    F = np.zeros([self.nnnode+self.nelem-1, 1])

#-----#
# PART 3: POST PROCESSING
#-----#

disp = np.concatenate((np.zeros([1, self.nstep]), d), axis=0)
press = np.concatenate((p, zero_pressure), axis=0)

# pressure difference from init. condition = head drop on topmost node
# pressure nstep corresponds to time t0
pprof = pprof + press[0:, self.nstep-1] / self.gamma
pprof[self.nelem] = pprof[self.nelem] + self.dh # topmost node
hpot = pprof + self.z # head = pressure head + elevation

for j in range(0, self.nelem):

```

```
hgrad[j+1] = np.divide((hpot[j]-hpot[j+1]), (self.z[j+1] - self.z[j]))
# displacement at the topmost node at end of time step
topdisp[0, 0] = d[self.nnode-2, self.nstep-1]

self.output = press[:, self.nstep-1] - (self.dh * self.gamma)

return(self.output, self.z)

def Demesh(self, z_random):
    '''
    Calculates excess pore pressure for random field slices
    :z_random: z-coordinates of random field to map the excess pore
    pressures on, dtype = 1D-array
    '''

    yp= np.flip(self.output, axis=0)
    if np.diff(self.z)[0] < np.diff(z_random)[0]:
        interp_pp = np.interp(z_random, self.z, yp)
    else:
        interp_pp = yp[1:]
    return(interp_pp)
```

F | STATISTICAL TEST RESULTS

F.1 Hypothesis tests

Hypothesis tests are methods of statistical interference. In the context of a Goodness-of-Fit (GoF) test, a sample is compared to a theoretical distribution. A hypothesis test comprises two complementary statements regarding a distribution or a distribution parameter, the *null hypothesis* and the *alternative hypothesis*. The formulation of the hypothesis depends on the test and the distribution which is to be examined. The goodness-of-fit is frequently analysed with three hypotheses tests, namely the *Anderson-Darling-test* (AD) and the *Kolmogorov-Smirnov-test* (KS) for continuous data as well as the χ^2 -test for discrete or categorical data. Finally, the goodness-of-fit can be assessed by the *Akaike-Information-Criterion* (AIC) and *Bayesian-Information-Criterion* (BIC).

Often, when performing a hypothesis test by means of statistical software, the p-value is computed. The p-value describes the likelihood of the sample given the null hypothesis. The smaller the p-value, the less likely is the null hypothesis. Basic mathematics of the different tests may be revised in Sachs and Hedderich (2009).

The AD test, first proposed by Anderson and Darling (1952) and complemented by Stephens (1974), is commonly applied for normality tests but not confined to them. The critical values allow the acceptance or rejection of a hypothesis. They have to be established for each distribution individually and at specific significance levels α , yet, allowing a more precise decision on the goodness-of-fit. For a limited number of probability distributions, they can be reviewed in Stephens (1974).

In contrast, the KS test (Kolmogorov, 1933; Smirnov, 1948) is independent of the examined distribution. The test evaluates the distance between the empirical and the theoretical probability distribution. The null hypothesis is accepted if the determined maximum distance is smaller than a prescribed upper limit at a specific significance level α . For Gaussian distributions, the results of the KS test may be overly conservative (Dallal and Wilkinson, 1986; Lilliefors, 1967).

The χ^2 test compares the number of samples in empirical and theoretical distribution per category. The differences per category are added and result in the test parameter χ^2 . For large sample sizes, the test parameter is described by the χ^2 distribution. The goodness-of-fit, thus, can be assessed by the quantiles of the χ^2 distribution at a specific degree of freedom k and significance level α .

The AIC (Akaike, 1998) and the BIC (Schwarz, 1978) evaluate the goodness-of-fit comparatively, which means they compare different models fitted to the same data. Both methods determine the maximum of the log-likelihood function. Then, while the former adds a constant for the number of model parameters, the latter adds the product of the number of model parameters and the logarithm of the number of samples. Thereby, the BIC weights both, the number of parameters and the number of samples, more strongly than the AIC. The smaller the AIC or BIC, the more suitable is the model.

The following sections shows the tabulated results of the different hypothesis tests for four datasets and six parameters. The ranking sorts suitable distributions from *best fit* (1) to *not recommended* (3). Favourable distributions are coloured in grey. The implementation of Delignette-Muller and Dutang (2015) and Delignette-Muller, Dutang and Siberchicot (2017) is used in *RStudio* and substantiated by a manuel comparision of the threshold values; threshold values for the AD test may be reviewed in D'Agostino and Stephens (1986) and for the KS tests in Lilliefors (1967).

Although these hypothesis test may be an indicator for the suitability of a distribution, there are to be substantiated by visual tests as well. Often more than one distribution approximates a dataset in a sufficiently accurate manner. Then, Gaussian and Lognormal distributions are favoured in order to establish a user-friendly, functional model that is applicable to revetment design in practice.

Table F.1: Results of statistical hypothesis tests for DEK-2006 (H_{stern}).

	χ^2 test			AD test		KS test		BIC	
	χ^2	p-value	rank	AD	rank	KS	rank	BIC	rank
H_{stern}									
$\mathcal{N}(\mu, \sigma)$	25.916	1.745×10^{-2}	1	2.578	3	0.088	3	-367.456	1
$\mathcal{LG}(\lambda, \zeta, \gamma)$	352.003	0.000	3	42.717	3	0.302	3	-11.488	3
$\mathcal{G}(\nu, k, \gamma)$	126.817	0.000	2	23.054	3	0.221	3	-238.618	2

Table F.2: Results of statistical hypothesis tests for DEK-2006 (v_{return}).

	χ^2 test			AD test		KS test		BIC	
	χ^2	p-value	rank	AD	rank	KS	rank	BIC	rank
v_{return}									
$\mathcal{N}(\mu, \sigma)$	158.743	0.000	3	3.810	3	0.088	3	211.560	1
$\mathcal{LG}(\lambda, \zeta, \gamma)$	3873.824	0.000	1	57.515	3	0.352	3	695.266	3
$\mathcal{G}(\nu, k, \gamma)$	2601.889	0.000	1	42.168	3	0.290	3	420.667	2

Table F.3: Results of statistical hypothesis tests for DEK-2006 (u_{max}) using GBBSoft+ results.

	χ^2 test			AD test		KS test		BIC	
	χ^2	p-value	rank	AD	rank	KS	rank	BIC	rank
u_{max}									
$\mathcal{N}(\mu, \sigma)$	73.351	1.93×10^{-10}	3	4.735	3	0.112	2	485.441	2
$\mathcal{LG}(\lambda, \zeta, \gamma)$	57.543	1.44×10^{-7}	3	2.113	3	0.060	1	490.493	3
$\mathcal{G}(\nu, k, \gamma)$	52.512	1.10×10^{-6}	3	1.937	2	0.063	1	470.503	1

Table F.4: Results of statistical hypothesis tests for DEK-2006 ($t_{a,bow}$).

	χ^2 test			AD test		KS test		BIC	
	χ^2	p-value	rank	AD	rank	KS	rank	BIC	rank
$t_{a,bow}$									
$\mathcal{N}(\mu, \sigma)$	32.851	0.002	3	1.208	3	0.065	2	979.173	3
$\mathcal{LG}(\lambda, \zeta, \gamma)$	29.867	0.005	2	1.192	2	0.064	2	962.956	1
$\mathcal{G}(\nu, k, \gamma)$	28.624	0.007	1	0.960	3	0.056	2	963.975	2

Table F.5: Results of statistical hypothesis tests for DEK-2006 ($z_{a,bow}$).

	χ^2 test			AD test		KS test		BIC	
	χ^2	p-value	rank	AD	rank	KS	rank	BIC	rank
$z_{a,bow}$									
$\mathcal{N}(\mu, \sigma)$	7.613	8.679×10^{-1}	1	0.375	2	0.038	1	-479.359	1
$\mathcal{LG}(\lambda, \zeta, \gamma)$	284.382	0.000	3	36.824	3	0.249	3	-141.153	3
$\mathcal{G}(\nu, k, \gamma)$	98.809	2.821×10^{-15}	2	18.925	3	0.194	3	-352.186	2

Table F.6: Results of statistical hypothesis tests for DEK-2006 ($t_{a,stem}$).

	χ^2 test			AD test		KS test		BIC	
	χ^2	p-value	rank	AD	rank	KS	rank	BIC	rank
$t_{a,stem}$									
$\mathcal{N}(\mu, \sigma)$	29.889	4.885×10^{-3}	1	2.411	3	0.060	2	1913.141	1
$\mathcal{LG}(\lambda, \zeta, \gamma)$	108.711	0.000	3	16.401	3	0.157	3	2061.522	3
$\mathcal{G}(\nu, k, \gamma)$	68.127	1.772×10^{-9}	2	10.244	3	0.120	3	1993.426	2

Table F.7: Results of statistical hypothesis tests for DEK-2006 ($z_{a,stem}$).

	χ^2 test			AD test		KS test		BIC	
	χ^2	p-value	rank	AD	rank	KS	rank	BIC	rank
$z_{a,stem}$									
$\mathcal{N}(\mu, \sigma)$	19.429	1.104×10^{-1}	1	1.319	3	0.059	2	-424.842	1
$\mathcal{LG}(\lambda, \zeta, \gamma)$	354.913	0.000	3	42.515	3	0.293	3	-49.596	3
$\mathcal{G}(\nu, k, \gamma)$	129.820	0.000	2	23.198	3	0.215	3	-276.732	2

Table F.8: Results of statistical hypothesis tests for KuK-2015 (H_{stem}).

	χ^2 test			AD test		KS test		BIC	
	χ^2	p-value	rank	AD	rank	KS	rank	BIC	rank
H_{stem}									
$\mathcal{N}(\mu, \sigma)$	16.614	0.005	3	1.967	3	0.174	2	-55.904	3
$\mathcal{LG}(\lambda, \zeta, \gamma)$	7.964	0.158	1	0.357	2	0.092	1	-74.314	1
$\mathcal{G}(\nu, k, \gamma)$	9.293	0.098	2	0.641	1	0.116	1	-71.210	2

Table F.9: Results of statistical hypothesis tests for KuK-2015 (u_{max}) using GBBSOft+ results.

	χ^2 test			AD test		KS test		BIC	
	χ^2	p-value	rank	AD	rank	KS	rank	BIC	rank
u_{max}									
$\mathcal{N}(\mu, \sigma)$	16.618	5.00×10^{-3}	3	1.918	3	0.171	3	77.763	3
$\mathcal{LG}(\lambda, \zeta, \gamma)$	4.313	5.05×10^{-1}	1	0.350	1	0.078	1	62.691	1
$\mathcal{G}(\nu, k, \gamma)$	7.211	2.05×10^{-1}	3	0.666	3	0.109	2	64.918	2

Table F.10: Results of statistical hypothesis tests for KuK-2015 ($t_{a,bow}$).

	χ^2 test			AD test		KS test		BIC	
	χ^2	p-value	rank	AD	rank	KS	rank	BIC	rank
$t_{a,bow}$									
$\mathcal{N}(\mu, \sigma)$	5.774	0.217	3	0.933	3	0.130	1	289.234	3
$\mathcal{LG}(\lambda, \zeta, \gamma)$	4.003	0.406	1	0.457	2	0.092	1	283.898	1
$\mathcal{G}(\nu, k, \gamma)$	4.097	0.393	2	0.487	1	0.088	1	284.118	2

Table F.11: Results of statistical hypothesis tests for KuK-2015 ($z_{a,bow}$).

	χ^2 test			AD test		KS test		BIC	
	χ^2	p-value	rank	AD	rank	KS	rank	BIC	rank
$z_{a,bow}$									
$\mathcal{N}(\mu, \sigma)$	8.937	0.112	3	1.249	3	0.153	2	-82.567	3
$\mathcal{LG}(\lambda, \zeta, \gamma)$	3.944	0.558	1	0.276	2	0.098	1	-94.481	1
$\mathcal{G}(\nu, k, \gamma)$	4.497	0.480	2	0.442	1	0.120	1	-92.687	2

Table F.12: Results of statistical hypothesis tests for KuK-2015 ($t_{a,stem}$).

	χ^2 test			AD test		KS test		BIC	
	χ^2	p-value	rank	AD	rank	KS	rank	BIC	rank
$t_{a,stem}$									
$\mathcal{N}(\mu, \sigma)$	6.609	0.158	3	1.001	3	0.133	2	297.633	3
$\mathcal{LG}(\lambda, \zeta, \gamma)$	4.880	0.300	1	0.805	2	0.123	1	293.387	1
$\mathcal{G}(\nu, k, \gamma)$	5.241	0.263	2	0.847	3	0.126	1	294.348	2

Table F.13: Results of statistical hypothesis tests for KuK-2015 ($z_{a,stem}$).

	χ^2 test			AD test		KS test		BIC	
	χ^2	p-value	rank	AD	rank	KS	rank	BIC	rank
$z_{a,stem}$									
$\mathcal{N}(\mu, \sigma)$	17.319	0.004	3	1.984	3	0.171	2	-58.234	3
$\mathcal{LG}(\lambda, \zeta, \gamma)$	9.499	0.091	1	0.549	2	0.106	1	-74.815	1
$\mathcal{G}(\nu, k, \gamma)$	11.177	0.048	2	0.903	3	0.126	1	-70.821	2

Table F.14: Results of statistical hypothesis tests for SiK-2007 (H_{stern}).

	χ^2 test			AD test		KS test		BIC	
	χ^2	p-value	rank	AD	rank	KS	rank	BIC	rank
H_{stern}									
$\mathcal{N}(\mu, \sigma)$	27.650	2.545×10^{-4}	2	2.041	3	0.128	2	-194.650	2
$\mathcal{LG}(\lambda, \zeta, \gamma)$	40.282	1.112×10^{-6}	3	6.473	3	0.211	3	-143.071	3
$\mathcal{G}(\nu, k, \gamma)$	17.738	1.321×10^{-2}	1	2.086	3	0.140	3	-195.375	1

Table F.15: Results of statistical hypothesis tests for SiK-2007 (v_{return}).

	χ^2 test			AD test		KS test		BIC	
	χ^2	p-value	rank	AD	rank	KS	rank	BIC	rank
v_{return}									
$\mathcal{N}(\mu, \sigma)$	9.502	2.186×10^{-1}	1	0.472	2	0.063	1	-61.249	1
$\mathcal{LG}(\lambda, \zeta, \gamma)$	124.395	0.000	3	14.526	3	0.294	3	68.174	3
$\mathcal{G}(\nu, k, \gamma)$	44.160	1.990×10^{-7}	2	7.353	3	0.200	3	-16.719	2

Table F.16: Results of statistical hypothesis tests for SiK-2007 (u_{max}) using GBBSOFT+ results.

	χ^2 test			AD test		KS test		BIC	
	χ^2	p-value	rank	AD	rank	KS	rank	BIC	rank
u_{max}									
$\mathcal{N}(\mu, \sigma)$	54.084	4.68×10^{-8}	3	4.017	3	0.109	3	275.974	3
$\mathcal{LG}(\lambda, \zeta, \gamma)$	60.726	2.64×10^{-9}	3	2.790	3	0.090	2	249.528	2
$\mathcal{G}(\nu, k, \gamma)$	40.430	1.42×10^{-5}	3	1.049	2	0.074	1	223.716	1

Table F.17: Results of statistical hypothesis tests for SiK-2007 ($t_{a,bow}$).

	χ^2 test			AD test		KS test		BIC	
	χ^2	p-value	rank	AD	rank	KS	rank	BIC	rank
$t_{a,bow}$									
$\mathcal{N}(\mu, \sigma)$	22.046	0.005	3	2.175	3	0.110	2	363.736	3
$\mathcal{LG}(\lambda, \zeta, \gamma)$	11.241	0.188	1	0.774	2	0.078	1	340.632	1
$\mathcal{G}(\nu, k, \gamma)$	13.818	0.087	2	1.122	3	0.088	1	346.532	2

Table F.18: Results of statistical hypothesis tests for SiK-2007 ($z_{a,bow}$).

	χ^2 test			AD test		KS test		BIC	
	χ^2	p-value	rank	AD	rank	KS	rank	BIC	rank
$z_{a,bow}$									
$\mathcal{N}(\mu, \sigma)$	21.205	3.478×10^{-3}	2	2.360	3	0.146	3	-228.419	2
$\mathcal{LG}(\lambda, \zeta, \gamma)$	36.781	5.160×10^{-6}	3	6.094	3	0.200	3	-186.735	3
$\mathcal{G}(\nu, k, \gamma)$	15.996	2.515×10^{-2}	1	2.028	3	0.130	2	-235.305	1

Table F.19: Results of statistical hypothesis tests for SiK-2007 ($t_{a, \text{stern}}$).

	χ^2 test			AD test		KS test		BIC	
	χ^2	p-value	rank	AD	rank	KS	rank	BIC	rank
$t_{a, \text{stern}}$									
$\mathcal{N}(\mu, \sigma)$	11.809	0.160	3	0.982	3	0.093	2	596.126	3
$\mathcal{LG}(\lambda, \zeta, \gamma)$	8.470	0.389	1	0.476	2	0.065	1	583.437	1
$\mathcal{G}(\nu, k, \gamma)$	8.815	0.358	2	0.543	1	0.073	1	585.406	2

Table F.20: Results of statistical hypothesis tests for SiK-2007 ($z_{a, \text{stern}}$).

	χ^2 test			AD test		KS test		BIC	
	χ^2	p-value	rank	AD	rank	KS	rank	BIC	rank
$z_{a, \text{stern}}$									
$\mathcal{N}(\mu, \sigma)$	43.755	6.331×10^{-7}	3	2.400	3	0.127	2	-203.837	3
$\mathcal{LG}(\lambda, \zeta, \gamma)$	14.968	5.978×10^{-2}	1	0.533	2	0.067	1	-223.732	1
$\mathcal{G}(\nu, k, \gamma)$	22.012	4.893×10^{-3}	2	0.907	3	0.081	1	-220.555	2

Table F.21: Results of statistical hypothesis tests for WDK-2007 (H_{stern}).

	χ^2 test			AD test		KS test		BIC	
	χ^2	p-value	rank	AD	rank	KS	rank	BIC	rank
H_{stern}									
$\mathcal{N}(\mu, \sigma)$	88.468	1.914×10^{-12}	3	10.928	3	0.123	3	-837.544	3
$\mathcal{LG}(\lambda, \zeta, \gamma)$	24.476	5.744×10^{-2}	1	1.483	3	0.054	2	-958.967	1
$\mathcal{G}(\nu, k, \gamma)$	36.636	1.430×10^{-3}	2	3.367	3	0.078	3	-936.980	2

Table F.22: Results of statistical hypothesis tests for WDK-2007 (u_{max}) using GBBSoft+ results.

	χ^2 test			AD test		KS test		BIC	
	χ^2	p-value	rank	AD	rank	KS	rank	BIC	rank
u_{max}									
$\mathcal{N}(\mu, \sigma)$	30.115	1.74E-02	3	2.662	3	0.062	3	15.122	3
$\mathcal{LG}(\lambda, \zeta, \gamma)$	15.307	5.02E-01	2	0.658	2	0.039	2	-11.716	2
$\mathcal{G}(\nu, k, \gamma)$	11.727	7.63E-01	1	0.254	1	0.026	1	-20.195	1

Table F.23: Results of statistical hypothesis tests for WDK-2007 (v_{return}).

	χ^2 test			AD test		KS test		BIC	
	χ^2	p-value	rank	AD	rank	KS	rank	BIC	rank
v_{return}									
$\mathcal{N}(\mu, \sigma)$	18.183	0.253	1	0.240	2	0.023	1	-173.012	1
$\mathcal{LG}(\lambda, \zeta, \gamma)$	37.607	0.001	3	3.186	3	0.082	3	-130.595	3
$\mathcal{G}(\nu, k, \gamma)$	25.675	0.042	2	1.383	3	0.063	2	-158.708	2

Table F.24: Results of statistical hypothesis tests for WDK-2007 ($t_{a,bow}$).

	χ^2 test			AD test		KS test		BIC	
	χ^2	p-value	rank	AD	rank	KS	rank	BIC	rank
$t_{a,bow}$									
$\mathcal{N}(\mu, \sigma)$	28.197	0.008	3	4.117	3	0.074	3	2489.972	3
$\mathcal{LG}(\lambda, \zeta, \gamma)$	10.184	0.679	2	0.682	2	0.041	1	2431.220	1
$\mathcal{G}(\nu, k, \gamma)$	8.902	0.780	1	0.697	1	0.042	1	2432.757	2

Table F.25: Results of statistical hypothesis tests for WDK-2007 ($z_{a,bow}$).

	χ^2 test			AD test		KS test		BIC	
	χ^2	p-value	rank	AD	rank	KS	rank	BIC	rank
$z_{a,bow}$									
$\mathcal{N}(\mu, \sigma)$	19.768	0.181	1	0.483	2	0.030	1	-995.531	2
$\mathcal{LG}(\lambda, \zeta, \gamma)$	32.497	0.006	3	2.606	3	0.067	2	-972.593	3
$\mathcal{G}(\nu, k, \gamma)$	20.479	0.154	2	0.933	3	0.045	1	-995.909	1

Table F.26: Results of statistical hypothesis tests for WDK-2007 ($t_{a,stem}$).

	χ^2 test			AD test		KS test		BIC	
	χ^2	p-value	rank	AD	rank	KS	rank	BIC	rank
$t_{a,stem}$									
$\mathcal{N}(\mu, \sigma)$	83.031	7.722×10^{-12}	3	10.218	3	0.120	3	2930.381	3
$\mathcal{LG}(\lambda, \zeta, \gamma)$	29.073	1.022×10^{-2}	1	1.534	3	0.058	2	2804.260	1
$\mathcal{G}(\nu, k, \gamma)$	37.989	5.216×10^{-4}	2	3.155	3	0.076	3	2828.357	2

Table F.27: Results of statistical hypothesis tests for WDK-2007 ($z_{a,stem}$).

	χ^2 test			AD test		KS test		BIC	
	χ^2	p-value	rank	AD	rank	KS	rank	BIC	rank
$z_{a,stem}$									
$\mathcal{N}(\mu, \sigma)$	109.521	0.000	3	11.333	3	0.125	3	-849.224	3
$\mathcal{LG}(\lambda, \zeta, \gamma)$	36.836	2.212×10^{-3}	1	2.164	3	0.064	2	-967.845	1
$\mathcal{G}(\nu, k, \gamma)$	53.313	6.711×10^{-6}	2	4.273	3	0.085	3	-942.364	2

F.2 Correlation analysis

Table F.28: Results of correlation analyses. The correlation is described by the Pearson correlation coefficient ρ_P . A correlation is to be considered as moderate for $\rho_P > 0.4$, and as strong for $\rho_P > 0.6$ (Phoon and Ching, 2015).

	DEK-2006		KuK-2015		SiK-2007		WDK-2007	
	H_{stern}	v_{return}	H_{stern}	v_{return}	H_{stern}	v_{return}	H_{stern}	v_{return}
H_{stern}	1.00	0.68	1.00	0.79	1.00	0.71	1.00	0.58
v_{return}		1.00		1.00		1.00		1.00

G | EXAMPLE

In the following, the design approach proposed in Chapter 9 is demonstrated using two examples. To illustrate the independence of the design concept from the underlying design equations, a design is conducted according to PIANC (1987a) and GBB (2010). The following steps summarised in Figure G.1 are required for a probabilistic revetment design. First, a comprehensive description of the design object should be provided. Subsequently, collected data has to be analysed; outliers, distributions and correlations have to be determined. Finally, probabilistic and deterministic analyses are conducted, which yield the final revetment dimensions.

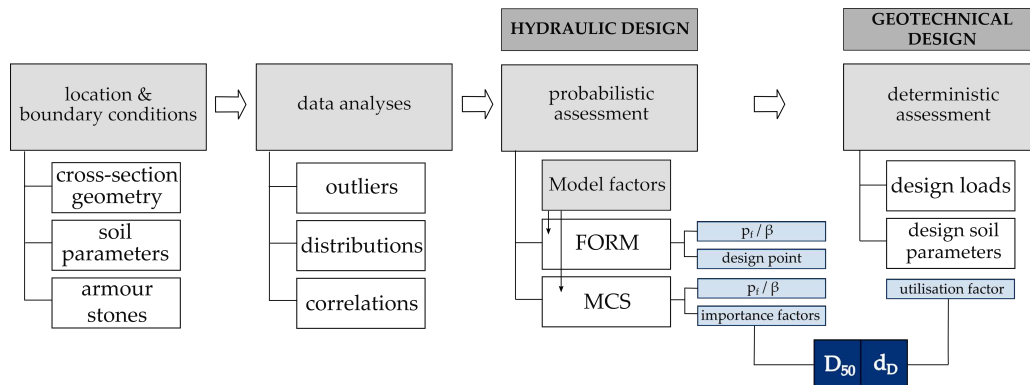


Figure G.1: Illustration of the workflow for an exemplary revetment design.

Hydraulic design: Input data

For the example, a detailed description of location, measurements and data analyses is omitted, since these information can be found in Chapter 3 and Chapter 6. Table G.1 summarises the data used for the presented example. Missing parameters such as u_{return} and u_{max} are calculated using the software *GBBSoft+*. This simplification is possible as the calculations primarily aim at demonstrating the proposed design concept.

When using calculated hydraulic loads, the limitations of the equations have to be complied to. In the case of GBB (2010), for example, vessel velocities, which appear to exceed the calculated critical vessel velocity, are observed in the measurement data. These values are a result of various assumptions regarding the cross-sectional area and vessel geometry, which leads to an underestimation of the critical vessel velocity. This, in turn, results in an overestimation of hydraulic loads. Thus, these vessel passages are not considered in further analyses.

As discussed in Chapter 6, hypothesis tests and several visual tests are used to verify the goodness-of-fit of a distribution. If, as in the example for u_{max} , calculated values are used as input, distributions have to be determined for these variables, too. A summary of the hypothesis tests, distribution parameters and correlation analysis is given in Appendix F. Furthermore, the workflow for distribution analyses outlined in Chapter 6 should be recalled. Figure G.3 shows two examples of goodness-of-fit plots for WDK-2007 and KuK-2015. As already discussed in previous chapters, the choice of distribution is not always obvious. In the following reliability

Table G.1: Summary of statistical measures describing the example datasets. The following parameters are used: vessel length L , vessel width B , vessel draught T , vessel velocity v_s , shore distance d_{shore} , stern wave height H_{stern} , return current velocity v_{return} and supply flow velocity u_{max} .

Measure	L	B	T	v_s	d_{shore}	$t_{a, bow}$	$t_{a, stern}$	$z_{a, bow}$	$z_{a, stern}$	H_{bow}	H_{stern}	H_{sec}	v_{return}	u_{max}
	m	m	m	m s^{-1}	m	s	s	m	m	m	m	m	m s^{-1}	m s^{-1}
KuK-2015														
(km 15.960, 09 June 2015 - 23 June 2015)														
count	47	47	46	46	47	47	47	47	47	47	47	47	-	-
mean	76.56	8.39	1.83	2.41	21.18	12.70	28.14	0.19	0.25	0.19	0.27	0.03	-	-
std	11.07	0.91	0.65	0.43	2.34	4.63	8.81	0.09	0.11	0.09	0.14	0.03	-	-
min	31.50	6.02	0.75	1.88	13.60	5.75	6.00	0.06	0.09	0.07	0.09	0.01	-	-
max	100.00	9.50	2.50	3.47	27.75	25.25	56.00	0.44	0.58	0.47	0.72	0.16	-	-
WDK-2007														
(km 33.450 - 33.800, 08 August 2007 - 22 August 2007)														
count	397	397	397	397	397	397	397	-	-	397	397	397	397	-
mean	84.82	8.88	2.25	2.83	26.71	16.30	27.90	-	-	0.23	0.23	0.06	0.71	-
std	19.76	1.18	0.56	0.40	3.55	5.49	9.56	-	-	0.07	0.08	0.02	0.19	-
min	39.00	5.05	0.55	2.06	14.60	3.50	8.75	-	-	0.06	0.07	0.02	0.14	-
max	181.00	11.48	2.83	4.16	38.15	45.25	77.00	-	-	0.49	0.65	0.21	1.38	-

analyses, a Lognormal distribution is used for H_{stern} and u_{max} ; v_{return} is approximated by a Gaussian distribution.

Hydraulic design: Reliability analysis using observed hydraulic loads

Table G.2 and Figure G.2 summarise the results of the reliability assessment. The underlying equations are derived from PIANC (1987a) and GBB (2010). In the case of PIANC (1987a), FORM analyses fail frequently in determining p_f indicated by high p_f values and the design points. MCS of PIANC (1987a) and GBB (2010) result in similar, yet diverging p_f .

Obviously, p_f decreases with increasing armour stone diameter. A design with GBB (2010) equations results in larger armour stones than a design with PIANC (1987a). Assuming a target reliability $p_f = 0.01$, KuK-2015 requires armour stones of class LMB_{5/40}, and WDK-2007 requires armour stones of class CP_{90/180} in accordance with GBB (2010). When complying to PIANC (1987a) standards, KuK-2015 requires armour stones of class CP_{90/180}, and WDK-2007 requires armour stones of class CP_{45/125}. These figures still consider stability coefficients, which are not replaced within these example in order to comply with the pre-defined design equations.

Figure G.2 shows the importance factors derived from the reliability analysis of the design case WDK-2007 - GBB (2010), CP_{90/250}. As in the analyses in the main part of the thesis, it can be concluded that H_{stern} and u_{max} have the strongest relevance for revetment design. Comparable results are obtained for PIANC (1987a). If the assumed armour stone diameter is strongly on the conservative side, its importance increases.

Probabilistic calculations with model factors would be performed in the same way. However, distributions of hydraulic loads which were calculated using vessel passages as input would have to be multiplied by the log-normally distributed model factor prior to reliability analysis.

Table G.2: Probability of failure and design points using MCS and FORM (Abdo-Rackwitz algorithm). FORM / MCS deviations are highlighted in grey. Calculations are conducted for the armour stone classes $CP_{45/125}$, $CP_{90/180}$, $CP_{90/250}$ and $LMB_{5/40}$. Blue shaded cells indicate the determined armour stone diameter as a result of a target reliability $p_f = 0.01$.

Equations	Armour stones	Method	MCS		FORM	FORM design point			
			number	p_f	p_f	H_{stern} m	v_{return} $m s^{-1}$	u_{max} $m s^{-1}$	$D_{50,pres}$ mm
GBB (2010)	KuK-2015	$CP_{45/125}$	2000	2.84×10^{-1}	2.56×10^{-1}	0.30	1.23	0.97	73.47
	KuK-2015	$CP_{90/180}$	8000	5.22×10^{-2}	4.25×10^{-2}	0.44	1.60	1.39	123.86
	KuK-2015	$CP_{90/250}$	15000	2.76×10^{-2}	1.74×10^{-2}	0.50	1.73	1.58	144.89
	KuK-2015	$LMB_{5/40}$	40000	1.00×10^{-2}	4.76×10^{-3}	0.60	1.90	1.87	174.26
	WDK-2007	$CP_{45/125}$	28000	1.45×10^{-2}	1.08×10^{-2}	0.43	1.03	1.29	67.18
	WDK-2007	$CP_{90/180}$	2113000	1.91×10^{-4}	1.45×10^{-4}	0.64	1.23	1.90	119.98
	WDK-2007	$CP_{90/250}$	10000000	3.97×10^{-5}	3.07×10^{-5}	0.70	1.28	2.11	140.56
	WDK-2007	$LMB_{5/40}$	10000000	6.00×10^{-6}	4.32×10^{-6}	0.78	1.35	2.39	171.49
PIANC (1987a)	KuK-2015	$CP_{45/125}$	10000	4.11×10^{-2}	3.89×10^{-6}	0.24	1.01	0.79	30.29
	KuK-2015	$CP_{90/180}$	56000	5.22×10^{-2}	2.00×10^{-22}	0.24	1.01	0.79	30.29
	KuK-2015	$CP_{90/250}$	94000	4.29×10^{-3}	9.70×10^{-24}	0.24	1.01	0.79	30.29
	KuK-2015	$LMB_{5/40}$	175000	2.29×10^{-3}	5.04×10^{-36}	0.24	1.01	0.79	30.29
	WDK-2007	$CP_{45/125}$	294000	1.36×10^{-3}	3.89×10^{-6}	0.21	0.71	0.69	30.29
	WDK-2007	$CP_{90/180}$	10000000	1.91×10^{-4}	2.00×10^{-22}	0.21	0.71	0.69	30.29
	WDK-2007	$CP_{90/250}$	10000000	8.00×10^{-7}	9.70×10^{-24}	0.21	0.71	0.69	30.29
	WDK-2007	$LMB_{5/40}$	10000000	0.00	5.04×10^{-36}	0.21	0.71	0.69	30.29

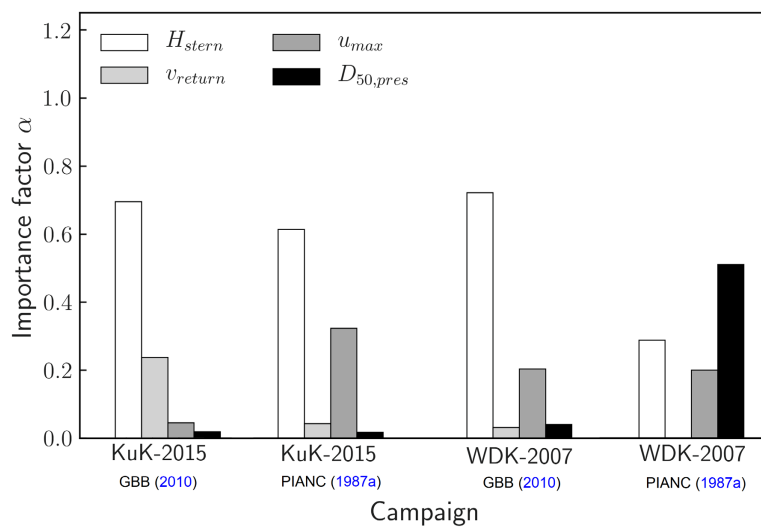
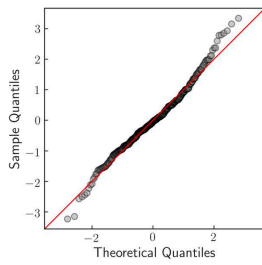
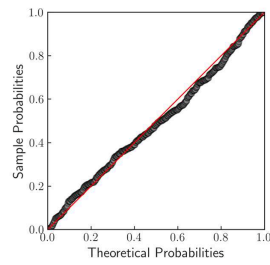


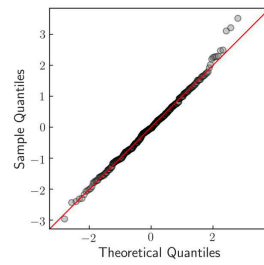
Figure G.2: Results of example reliability analyses: Importance factors for the design case $CP_{90/250}$.



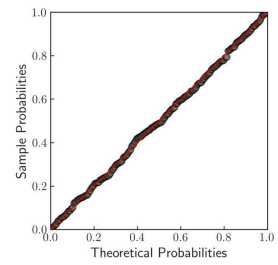
(a) Q-Q plot for the purpose of evaluating the distribution tail, Lognormal distribution, WDK-2007 (H_{stern}).



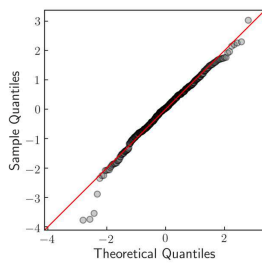
(b) P-P plot for the purpose of evaluating the distribution body, Lognormal distribution, WDK-2007 (H_{stern}).



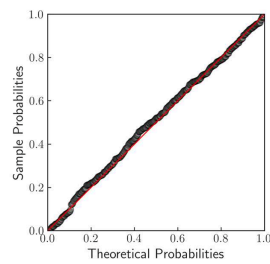
(c) Q-Q plot for the purpose of evaluating the distribution tail, Gaussian distribution, WDK-2007 (v_{return}).



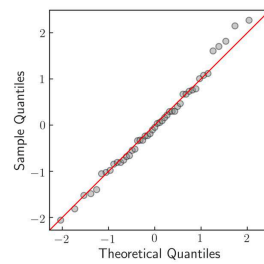
(d) P-P plot for the purpose of evaluating the distribution body, Gaussian distribution, WDK-2007 (v_{return}).



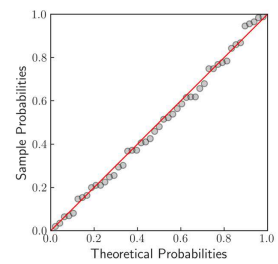
(e) Q-Q plot for the purpose of evaluating the distribution tail, Lognormal distribution, WDK-2007 (u_{max}).



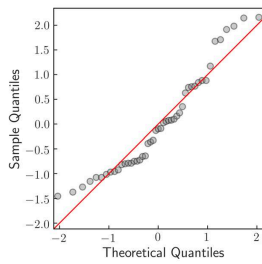
(f) P-P plot for the purpose of evaluating the distribution body, Lognormal distribution, WDK-2007 (u_{max}).



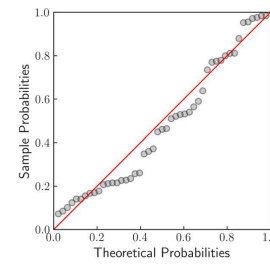
(g) Q-Q plot for the purpose of evaluating the distribution tail, Lognormal distribution, KuK-2015 (H_{stern}).



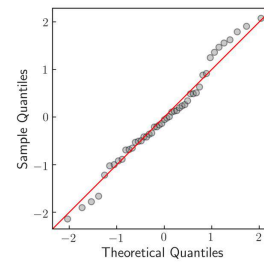
(h) P-P plot for the purpose of evaluating the distribution body, Lognormal distribution, KuK-2015 (H_{stern}).



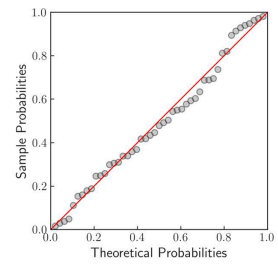
(i) Q-Q plot for the purpose of evaluating the distribution tail, Gaussian distribution, KuK-2015 (v_{return}).



(j) P-P plot for the purpose of evaluating the distribution body, Gaussian distribution, KuK-2015 (v_{return}).



(k) Q-Q plot for the purpose of evaluating the distribution tail, Lognormal distribution, KuK-2015 (u_{max}).



(l) P-P plot for the purpose of evaluating the distribution body, Lognormal distribution, KuK-2015 (u_{max}).

Figure G.3: Goodness-of-Fit plots to evaluate the fit of a distribution.

Hydraulic design: Deterministic calculations

The maxima of observed loads are used for deterministic dimensioning. The analyses result in the dimensions summarised in Table G.3. Considering the limited number of available measurements, the additive factors presented in Chapter 6 are applied to the deterministically determined armour stone diameter. Compared to the probabilistic analysis, in one case, a larger armour stone class is obtained. Compared with the probabilistic analysis, larger stone diameters are obtained. However, the results show that additive factors (or partial factors) may offer an alternative way to a fully probabilistic design approach. However, it must be noted that this approach will not lead to a comparable reliability level for revetments as soon as basic variables are changed.

Table G.3: Required armour stone diameter as a result of deterministic analyses. It is differentiated in required armour stone diameter to resist stern waves $D_{50,req}(H_{stern})$, required armour stone diameter to resist return current velocity $D_{50,req}(v_{return})$, required armour stone diameter to resist slope supply flow $D_{50,req}(u_{max})$, required armour stone diameter to resist secondary waves $D_{50,req}(H_{sec})$, maximum required armour stone diameter $D_{50, req}$ as a result of hydraulic loads and required armour stone diameter with additive factor $D_{50, factor}$.

	$D_{50,req}(H_{stern})$	$D_{50,req}(v_{return})$	$D_{50,req}(u_{max})$	$D_{50,req}(H_{sec})$	$D_{50, req}$	$D_{50, factor}$	Class
	mm	mm	mm	mm	mm	mm	–
GBB (2010)							
KuK-2015	147.08	88.69	133.23	16.34	133.23	159.23	LMB _{5/40}
WDK-2007	132.79	114.61	92.08	16.34	123.70	133.70	CP _{90/180}
PIANC (1987a)							
KuK-2015	77.62	51.27	57.63	30.29	77.62	103.62	CP _{90/180}
WDK-2007	70.07	35.43	70.02	30.29	70.07	80.07	CP _{90/180}

Geotechnical design: Input data

The geotechnical design is conducted deterministically in accordance with present standards using the design equations of Köhler (1985, 1989, 1993, 1997a,b). As an example, and since complete measurements of drawdown parameters are not available, load combinations of MAR (2008) are used for WDK-2007. In the case of KuK-2015, drawdown combinations have been measured in the field. Thus, the armour layer thickness is calculated for each of these 47 combinations in order to identify the worst case combination, which requires the thickest armour stone layer. For illustrative purposes, soil characteristics, geometry and revetment construction are derived from geotechnical reports in the vicinity of the location (Heinrich, 2009; Kayser, 2007a; Sorgatz and Soyeaux, 2019). Moreover, for WDK-2007, a toe support is assumed. This results in the design cases shown in Table G.4.

Geotechnical design: Stability analyses

Assuming an armour layer thickness of $d_{pres} = 0.60$ m, which is a result of additional requirements such as the protection against anchor drop and vessel impact, the stability analyses yield the results presented in Table G.5.

Table G.4: Combinations of loads and soil parameters investigated for the two example design cases.

Soil type	Effective friction angle ϕ'	Hydraulic conductivity k	Unit weight under buoyancy γ'_b	Draw-down time t_a	Draw-down height z_a	Unit weight armour stones γ_s	Slope inclination m
–	°	m s^{-1}	kN m^{-3}	s	m	kN m^{-3}	–
KuK-1 Silty sand	30.0	5.0×10^{-6}	9.5	measured	measured	26.50	3
WDK-1 Silty sand	32.5	2.75×10^{-5}	10.0	4.5	0.63	26.50	3
WDK-2 Silty sand	32.5	2.75×10^{-5}	10.0	27.6	0.83	26.50	3

Table G.5: Required layer thickness to ensure local slope stability.

Design case	$d_{D, \text{req}}$ in m	Degree of utilisation
KuK-1	0.209	0.349
WDK-1	0.600	1.000
WDK-2	0.600	1.000

Summary: The examples confirm the applicability of the probabilistic design approach as well as the extended deterministic design approach to revetment design. It is shown that the design concept works irrespectively of the underlying design equations. However, it should be noted that different equations can lead to different specifications and revetment dimensions.

The example calculations result in the following minimum requirements of revetment dimensions, where the armour layer thickness may have to be adapted in accordance with additional design specifications:

- ☑ KuK-2015: $\text{LMB}_{5/40} / \text{CP}_{90/180}$, $d_{D, \text{req}} = 0.21 \text{ m}$
- ☑ WDK-2007: $\text{CP}_{90/180} / \text{CP}_{45/125}$, $d_{D, \text{req}} = 0.60 \text{ m}$



Bundesministerium
für Digitales
und Verkehr

Bundesanstalt für Wasserbau (BAW)

Kußmaulstraße 17 · 76187 Karlsruhe

Tel. +49 (0) 721 9726-0

Fax +49 (0) 721 9726-4540

Wedeler Landstraße 157 · 22559 Hamburg

Tel. +49 (0) 40 81908-0

Fax +49 (0) 40 81908-373

www.baw.de